

## ABSTRACT

Title of Dissertation: SUBAQUEOUS SOILS OF CHESAPEAKE  
BAY: DISTRIBUTION, GENESIS, AND THE  
PEDOLOGICAL IMPACTS OF SEA-LEVEL  
ALTERNATIONS

Barret Morgan Wessel, Doctor of Philosophy,  
2020

Dissertation directed by: Professor Martin C. Rabenhorst, Department of  
Environmental Science and Technology

Soils and sediments make up a substantial portion of the resource base that supports human societies and other life on Earth, yet in the subaqueous environment our understanding of these materials pales in comparison to our understanding and management of upland soils. We must develop an understanding of how subaqueous soils/sediments are distributed, how they form and change over time, and how they will be impacted by rising sea-levels as a result of climate change if we are to wisely manage these resources. The goal of this study is to improve this understanding in Chesapeake Bay subestuaries. The Rhode River subestuary was first surveyed to identify rates of bathymetric change in these settings and to characterize the common material types found in these settings. Bathymetric change was evaluated using hydrographic surveys dating back to 1846, and though the river bottom does change slowly, it has been more or less stable during the years evaluated. Several types of morphologically distinct materials make up the soil profiles in Rhode River. Materials highest in organic matter are easy to identify in the

field, and commonly become ultra-acidic if disturbed. Also present were submerged upland soils, colored and structured like soils in the surrounding landscape. To better understand the impacts of submergence on these materials, a sampling campaign was conducted on shallow marine sediments, reclaimed land, and restored aquatic environments under both seawater and freshwater. This demonstrated that shallow marine sediments develop upland soil features and biogeochemical characteristics within 150 years of drainage, and that these characteristics do indeed persist in the subsoil two years after submergence. Topsoil changes more radically, releasing anomalous amounts of Fe while accumulating anomalous amounts of reduced S minerals, a process exacerbated by seawater flooding. Using these results, a soil-landscape conceptual model was developed and used to predict subaqueous soil distribution in the West River subestuary. These predictions were evaluated with a sampling campaign, and found to be significant. This model can now be used in other subestuaries to quickly and efficiently survey subaqueous soils, supporting the development of future land-use interpretations in these environments.

SUBAQUEOUS SOILS OF CHESAPEAKE BAY: DISTRIBUTION, GENESIS,  
AND THE PEDOLOGICAL IMPACTS OF SEA-LEVEL ALTERNATIONS

by

Barret Morgan Wessel

Dissertation submitted to the Faculty of the Graduate School of the  
University of Maryland, College Park, in partial fulfillment  
of the requirements for the degree of  
Doctor of Philosophy  
2020

Advisory Committee:

Professor Martin C. Rabenhorst, Chair  
Professor Sujay S. Kaushal  
Dr. J. Patrick Megonigal  
Professor Brian A. Needelman  
Professor Lance T. Yonkos

© Copyright by  
Barret Morgan Wessel  
2020

## Dedication

To Carl Sagan for inspiring me to become a scientist,  
To the mentors, colleagues, and students who have guided my journey,  
And to the friends and family without whose support I never could have finished.

## Acknowledgements

I am incredibly grateful for the advice, guidance, and direct assistance provided across a multitude of challenges over the past several years by my advisor Martin Rabenhorst and my committee members J. Pat Megonigal, Lance Yonkos, Brian Needelman, and Sujay Kaushal. Other substantial support came from my colleagues and mentors in Denmark including Erik Kristensen, Alexander Treusch, Kamilla Sjøgaard, and Søren Christensen, without whom I might still be lost in a freezing cold coastal lagoon.

A number of other scientists made more specific contributions to my development. When I review papers, I hope I do it like Philippe Hensel, who took time to help me through my tide data and imparted some scientific ethics while he was at it. Phil King and Rob Tunstead taught me much of what I know about soil survey. Del Fanning provided clarification on mineralogy and terminology, and helped me to realize the importance of acid sulfate soils. Ray Weil and Michael Williams gave me my first opportunities as a scientist, helping me get my foot in the door. Don Webster and Mutt Meritt helped me to think like an oyster, and to think of the oyster farmers as I went about my work. Hopefully they will benefit from it.

Additional help on the water and in the lab came from Jaclyn Fiola, David Vespe, Kristi Persing, Amanda Daly, Sarah Larkin, Sebastian Lecha, Tim Wilmot, Alice Murphy, Justin Lee, Leo Notto, and Evan Park. Some of the work was grueling, but you all helped keep it fun, and together we avoided any major disasters.

Thanks to my family and friends for supporting me and for putting up with me. The food, drinks, and companionship are much appreciated and helped to make

my time as a graduate student possible. Special thanks are due to Jaclyn for always being sure I stopped for meals. Many others helped me through this part of my life, and helped me to develop as a scientist, though the list would go on and on if I were to try to name everyone. Suffice it to say, thank you all.

Support for the work on Rhode River and West River was provided through the USDA Natural Resource Conservation Service award number 69-3B19-4-004, through contribution 22 from the Smithsonian's MarineGEO Network, and through the National Science Foundation Graduate Research Fellowship Program under grant number DGE 1322106. Additional support for West River work was provided by NIFA project number MD-ENST-18580. Support for research activities in Denmark was provided by the Fulbright Foundation / Danmark-Amerika Fondet (grant number DGE 1322106) and the Aage V. Jensen Nature Foundation (grant number 120925).

# Table of Contents

Dedication .....	ii
Acknowledgements .....	iii
Table of Contents .....	v
List of Tables .....	vii
List of Figures .....	viii
Chapter 1 : Introduction .....	1
1.1 Background .....	1
1.2 Objectives .....	3
Chapter 2 : Using historical hydrographic surveys to evaluate bathymetric stability in Rhode River subestuary, Maryland.....	5
2.1 Abstract .....	5
2.2 Introduction.....	5
2.2.1 Evaluation of historical data .....	9
2.3 Materials and methods .....	11
2.3.1 Study site.....	11
2.3.2 Hydrographic comparisons .....	11
2.4 Results and discussion .....	23
2.4.1 Evaluation of historical data .....	23
2.4.2 Hydrographic comparisons .....	26
2.4.3 Implications for erosion in the watershed.....	32
2.5 Conclusions.....	33
Chapter 3 : Identification of sulfidic materials in the Rhode River subestuary of Chesapeake Bay .....	35
3.1 Abstract .....	35
3.2 Introduction.....	36
3.2.1 Identification and classification of potential AS soil materials .....	39
3.2.2 Potential AS soil materials in the Rhode River region .....	47
3.3 Methods and materials .....	50
3.4 Results and discussion .....	52
3.4.1 SAS material types.....	52
3.4.2 Example profiles containing potential AS soil materials.....	69
3.5 Conclusions.....	76
Chapter 4 : Environmental consequences of polygenetic pedogenesis following the restoration of reclaimed land via flooding with fresh and marine water in Gyldensteen Strand, Denmark .....	79
4.1 Abstract .....	79
4.2 Introduction.....	80
4.3 Methods and materials .....	83
4.3.1 Study site.....	83
4.3.2 Soil survey field methods.....	85
4.3.3 Laboratory analyses .....	87
4.4 Results and discussion .....	92
4.4.1 Evaluation of select methods .....	92



4.4.2 Shoreface.....	112
4.4.3 Reclaimed land.....	132
4.4.4 Freshwater lake .....	136
4.4.5 Restored lagoon .....	141
4.5 Conclusions.....	146
Chapter 5 : Subaqueous soil-landscape model development and evaluation for Rhode and West Rivers, Maryland.....	148
5.1 Abstract .....	148
5.2 Introduction.....	148
5.3 Methods and materials .....	151
5.3.1 Study site.....	151
5.3.2 Rhode River subaqueous soil-landscape model.....	151
5.3.3 Model application and evaluation in West River.....	153
5.4 Results and discussion .....	156
5.4.1 Rhode River landforms and soils.....	156
5.4.2 SSLP conceptual model .....	163
5.4.3 Model application and evaluation in West River.....	175
5.4.4 Limitations .....	180
5.4.5 Future refinement.....	182
5.5 Conclusions.....	187
Chapter 6 : Conclusions .....	188
Appendices.....	191
Appendix A: Sea-level trends and variation from NOAA Tides and Currents ....	191
Appendix B: Rhode River pedons .....	193
Appendix C: Rhode River horizon data.....	197
Appendix D: Rhode River particle size analysis .....	243
Appendix E: Rhode River bulk density data.....	248
Appendix F: Gyldensteen Strand sample morphology .....	250
Appendix G: Gyldensteen Strand sample chemistry .....	259
Appendix H: West River pedon classifications .....	272
Appendix I: West River horizon data .....	274
Appendix J: West River particle size analyses .....	293
Appendix K: Proposed and tentative OSDs for Chesapeake Bay subestuaries ....	295
Appendix L: Blue carbon map.....	346
Bibliography .....	348

## List of Tables

Table 2-1. Plane of reference corrections applied to hydrographic surveys .....	21
Table 2-2. Categories of change and the area associated with each .....	30
Table 2-3. Bathymetric changes summarized .....	30
Table 2-4. Long-term changes calculated from 1846 survey points.....	31
Table 3-1. Soil materials and their common morphological properties.....	54
Table 3-2. Soil materials as sulfide-containing materials. ....	57
Table 3-3. Core A – Unconsolidated Holocene sandy materials with a buried A horizon. ....	61
Table 3-4. Core B – Fluid muds, buried surfaces, and Tertiary materials.....	63
Table 3-5. Core C – Fluid muds.....	74
Table 3-6. Core D – Sandy materials over Tertiary materials. ....	76
Table 4-1. Distribution of Gyldensteen Strand pedons.....	85
Table 4-2. Gyldensteen Strand modal morphological features.....	114
Table 4-3. Gyldensteen Strand average sampling depths .....	116
Table 5-1. The five point ordinal scale used to score observations .....	155
Table 5-2. Landforms delineated from Rhode River hydrographic survey data .....	159
Table 5-3. Rhode River landforms and associated soil taxonomic subgroups .....	161
Table 5-4. Proposed soil series for use in Chesapeake Bay subestuaries .....	168
Table 5-5. A proposed revision to the five point ordinal scale used to score observations .....	186

## List of Figures

Figure 2-1. Annapolis vs SERC Tide Gauge Bivariate Plot.....	15
Figure 2-2. An example polynomial model used to correct soundings .....	16
Figure 2-3. A comparison between the Baltimore and Annapolis tide gauges.....	19
Figure 2-4. Rhode River depicted in the 1846 hydrographic survey.....	22
Figure 2-5. Bathymetric changes in Rhode River occurring between surveys.....	29
Figure 3-1. Location of Rhode River with sampled pedon locations. ....	51
Figure 3-2. Moist aerobic incubation of selected materials. ....	58
Figure 4-1. Percent AVS by 3% H <sub>2</sub> O <sub>2</sub> color change reaction.....	93
Figure 4-2. Percent organic C by sample effervescence class .....	96
Figure 4-3. Percent CRS by sample effervescence class .....	99
Figure 4-4. Percent TRIS by sample effervescence class .....	100
Figure 4-5. Redox concentrations vs reactive ferric Fe .....	102
Figure 4-6. Fe vs matrix hue .....	105
Figure 4-7. Fe vs matrix value .....	106
Figure 4-8. Fe vs matrix chroma.....	108
Figure 4-9. Mean calculated practical salinity of porewater.....	111
Figure 4-10. Mean sample conductivity measured on 1:5 dilutions.....	116
Figure 4-11. The mean sample pH.....	117
Figure 4-12. The mean bulk density .....	117
Figure 4-13. The mean AVS content .....	118
Figure 4-14. The mean CRS content.....	120
Figure 4-15. The AVS/CRS ratio.....	121
Figure 4-16. The mean reactive ferric Fe.....	122
Figure 4-17. The mean reactive ferrous Fe.....	126
Figure 4-18. The mean relative contents of reactive Fe.....	127
Figure 4-19. Gyldensteen Strand Fe fractions .....	128
Figure 4-20. The mean degree of pyritization .....	129
Figure 4-21. The mean organic C content .....	130
Figure 4-22. The mean carbonate C content.....	131
Figure 4-23. A soil profile collected from the restored lagoon showing the three morphologically distinct layers.....	143
Figure 5-1. Landforms of Rhode River.....	158
Figure 5-2. Conceptual soil-landscape model.....	166
Figure 5-3. Soil map units for Rhode River.....	174
Figure 5-4. Bathymetric map and soil survey of West River .....	177
Figure 5-5. Histogram of scores from the 5 point scale.....	178
Figure 5-6. Results of resampling (bootstrapping) soil pedons .....	179

# Chapter 1: Introduction

## 1.1 Background

We map soils by considering the shape of a landscape and the factors that have shaped it over time, engaging our senses in the field and our skills in the lab. With an understanding of how these factors work in a landscape, a pedologist can predict what types of soils are found in different landscape positions. Various soils are suited to different uses and their identification facilitates more sustainable use by matching soils with optimal management activities (Jenny, 1941). Since the 1990s, soil scientists in the United States have been developing methods for mapping subaqueous soils (SAS) using bathymetric maps of estuaries and bays. Once mapped, the substrata in these landscapes can be evaluated regarding their suitability for aquaculture development, physical disturbance for dredging or construction, and myriad other uses (Rabenhorst and Stolt, 2012).

Many fundamental ecological phenomena at the land-sea interface -- both subtidal and intertidal -- reflect the physical and chemical characteristics of soils. Ecologically relevant characteristics include particle-size distribution, carbon and nutrient content, fluidity, and variation in these parameters both in space and with depth (Millar et al., 2015). Such information is needed to interpret the spatial distribution of organisms, to plan sampling campaigns, and to locate sites for activities including restoration of seagrass beds and oyster reefs. Presently, many sediment maps for estuaries such as Chesapeake Bay are relatively low-resolution,

two-dimensional maps that provide basic information on 1-2 variables (Demas and Rabenhorst, 2001). This approach to mapping has been the standard for subtidal sediments, and is the minimum required for TMON (Tennenbaum Marine Observatories Network) sites, such as the Rhode River site herein described. More advanced sediment mapping approaches have been developed for particular environments (Lisitzin and Kennett, 1996), but do not offer the generally standardized approaches to material characterization and classification that have been developed to survey soils. That said, soil survey methods have been recommended by the US Federal Geographic Data Committee for marine ecological mapping and classification where more information is required than traditional methods supply (FGDC-MCSDS 2012).

Here we propose a more detailed approach to mapping subtidal sediments that has been developed over the past two decades from terrestrial soil mapping techniques. The technique produces high resolution maps that include information on changes in substrate properties with depth, and incorporate a number of additional variables that are relevant to ecology, restoration, and management. This mapping approach is now a well-established technique that has been recognized by the USDA through official categories within US Soil Taxonomy for subaqueous soils (SAS) (Demas and Rabenhorst, 1999; Demas et al., 1996). Compared to the traditional approach, the soil classification approach provides 1) sediment characteristics presented to a greater depth (generally 2 m), rather than a bottom-type classification (such as mud bottom or rocky bottom), 2) a comprehensive classification scheme for shallow water sediments that facilitate comparisons across sites and 3) an established

framework for developing these data and classifications into land-use interpretations (i.e. land-management recommendations) to support shellfish restoration, estuarine protection, planning, and management. The approach has been used successfully to generate spatial maps of coastal lagoons and freshwater lakes (Erich et al., 2010), but has not yet been applied to estuaries.

### 1.2 Objectives

The overarching objective of this work is to advance the development of a unified framework for characterizing, classifying, and surveying the components of Earth's surface. At present, upland soils and aquatic sediments are considered to be different categories of materials by many who work within each of these historically distinct disciplines, but one might naturally ask what overarching category soils and sediments are subdivided from. The perspective taken here is that soils can form in sediments, and that it is useful to characterize, classify, and map sediments (even recent sediments) during soil survey efforts. By advancing soil survey into estuarine environments, this work in a small way advances us towards a unified understanding of the surface of the Earth.

Specific objectives of this work are:

- 1) To examine the validity of historical hydrographic surveys for use in soil survey, to evaluate bathymetric stability in Rhode River, and to provide guidance for coastal zone soil surveyors as they evaluate bathymetric stability in other locations.
- 2) To identify SAS materials in the Rhode River subestuary of Chesapeake Bay that are easily discerned from one another in the field (defined primarily by their field

morphological properties using common field and laboratory tests) and to establish if these morphologies exhibit strong relationships to three classes of sulfide-containing materials.

3) To investigate the presence and persistence of subaerial and subaqueous pedogenic features in a landscape with areas that have been subjected to varying hydrologic regimes relating to managed realignment of reclaimed land.

4) To develop and explain a conceptual soil-landscape model for western shore Chesapeake Bay subestuaries using the Rhode River subaqueous soil survey, and to apply and evaluate that model in West River.

## Chapter 2: Using historical hydrographic surveys to evaluate bathymetric stability in Rhode River subestuary, Maryland

### 2.1 Abstract

Cultural sedimentation, the infilling of floodplains and aquatic environments with sediment derived from human-accelerated erosion in uplands, has been credited with reshaping rivers and estuaries after the European colonization of North America. In most aquatic environments little or no work has been done to evaluate this assumption, and the historical period when the greatest geomorphic change took place is largely unknown. Because soil surveys are only useful for as long as geomorphology remains relatively stable, it is important to understand when cultural sedimentation took place and to what extent it altered or continues to alter subaqueous geomorphology (bathymetry). By using historical records including hydrographic surveys and long-maintained tide gauges, rates of bathymetric change were measured in the Rhode River subestuary of Chesapeake Bay. If cultural sedimentation had a substantial impact on the bathymetry of Rhode River, it must have occurred before 1846 (the earliest survey available), and changes since then have been largely within measurement errors of the survey methods used. The bathymetry of Rhode River has been relatively stable over the past 150 years.

### 2.2 Introduction

The physical structure of aquatic environments can be extremely dynamic, particularly in high-energy settings where sediment is continually transported



(Charlton, 2008; Wheeler et al., 2010), an observation which calls into question the long-term value of subaqueous soil surveys. Some subaqueous landforms such as washover fans and flood-tidal deltas are reshaped on timescales as short as a single storm event (Balduff, 2007; Demas, 1998), which can breach a barrier island and require soil surveys and other maps to be redrawn. It is therefore important to evaluate bathymetric stability through time so that we can better constrain the duration that maps of these landforms, and soil surveys that are generated using these maps, may remain valid. Further, by evaluating geomorphological changes in landforms it is possible to measure erosion and accretion rates (Sallenger et al., 1975), and therefore to date some features and materials in a landscape. These analyses may be possible to conduct along most of the US coastline thanks to the fact that over 16,400 hydrographic surveys have been conducted by the National Oceanic and Atmospheric Administration (NOAA) and its precursor agencies, and these have been made available online in recent years, eliminating time consuming searches and requests for data (Neumann, 2012). In landscapes where massive changes occurred before living memory, these and other archival resources offer a valuable tool for understanding the history of environmental change (Harris, 2001).

Soil science is a truly interdisciplinary field, which advances due to contributions both from practitioners in STEM fields and increasingly to contributions from those in the arts and the humanities (Brevik et al., 2015). Soil scientists have always utilized knowledge from other disciplines as they have conducted research and soil survey. A soil surveyor generally begins a project not by digging holes, but by collecting documentary evidence about the factors of soil

formation that are acting within a landscape to drive pedogenesis and create the soils that are found there (Jenny, 1941). In the United States, this nearly always includes United States Geological Survey quadrangle maps that provide topographic information and geologic maps that provide information about the parent materials present (Soil Science Division Staff, 2017).

Such reviews are not limited to these sources. Early ideas about erosion and the importance of soil management were derived from the archaeological record (Lowdermilk, 1948). Surveyors in urban environments utilize archival Sanborn Fire Insurance Maps to determine where hazardous chemicals were stored or produced (the Sanborn Map Company recorded these and other details relevant to insurance policies), which provides an indication of where soil contamination is more likely to have occurred due to spills of those chemicals (Kolodziej et al., 2004). When the soil survey expanded into tidal marshes in the 1970s, fence lines were used to determine the boundary between soft and hard tidal marsh map units, because farmers knew not to let their cattle graze the soft marsh or they could become stuck in the soft ground (Phillip King, NRCS State Soil Scientist DE/MD/DC, personal communication). In areas where traditional small rural farms still dominate the landscape, interviews with farmers have been used to create custom soil surveys that incorporate local knowledge (Barrera-Bassols et al., 2009). These are just a few examples of the great variety of historical and cultural resources that soil scientists have used to understand soils and landscapes (Trimble, 1998). Soil scientists are no strangers to archaeological, archival, or ethnographic data.

These three sources of data can be of particular value to studies of culturally accelerated sedimentation. Culturally accelerated sedimentation is the increase in sedimentation, often to deleterious levels in water bodies, that occurs after unsustainable land management practices cause massive increases in soil erosion within a watershed. In the early years of European colonization of North America, land was cleared of forests on the east coast and planted in row crops without any soil conservation practices. In some regions this caused areas to become unproductive within three years due to topsoil loss to erosion, at which point farmers abandoned the land and moved on (Otto, 1983; Trimble, 1969). In some parts of the United States, particularly on fairly level land between estuaries, previously cleared forests and soils slowly recovered before being cleared again, used for a few more seasons, and abandoned again in a cycle that repeated many times throughout history (Wolfanger, 1931). Eroded soil moved into valleys and waterways. It was so difficult for soil surveyors to map these deposits (because of widely varying textures) that early soil surveys simply refer to these areas as Meadow (Long et al., 1919) or Alluvial soils, occasionally attributing the material to erosion from the clearing of adjacent hillsides (Miller et al., 1941). Oral histories, abandoned structures, and archival records were all used to evaluate the impact of this process in the Georgia Piedmont, where over 3 meters of sediment filled streams from ~1890-1940. This caused the abandonment of mill dams and forced the reconstruction of bridges as they were overtopped by rising streambeds (Trimble, 1969).

In the Chesapeake Bay region, massive land clearing began around 1650. Jamestown was settled in 1607, and by 1700 the tidewater area of the Bay was widely

settled and new settlements were being constructed further inland across the fall line. Within 50 years of their establishment, most of the towns which had been established as shipping ports were adjacent to mud flats and were abandoned (Gottschalk, 1945). These mud flats formed largely as a result of culturally accelerated sedimentation. Few of these towns still exist. Stone mooring posts could be found two miles from the shore in Maryland by the 1940s, as archaeological remains of abandoned ports (Gottschalk, 1945). Potomac shipping was inhibited by mud banks as early as 1804, and the Port of Bladensburg permanently closed to tobacco ships around 1843 (Biddle, 1953). A lack of records inhibits estimation of sedimentation rates prior to the mid-1800s, though rates thereafter ranged from a meter of fill in the Anacostia River from 1891-1937 (~2 cm/yr) to five meters of fill in the Patapsco River at Baltimore from 1845-1924 (~6 cm/yr) (Gottschalk, 1945).

#### 2.1.1 Evaluation of historical data

Maps of various types are commonly used in historical research, and a four part test has been developed to evaluate their quality as a source of data. When deciding if features of a historical map are reliably presented, a researcher must evaluate 1) the purpose of the map when it was created, 2) the audience the map was intended for, 3) any bias likely to exist in the map, and 4) the cartographic accuracy of the map (Seasholes, 1988). Features of a map that are relevant to its purpose, such as the appearance of flammable chemical storage on a fire insurance map, are more likely to be precisely depicted than extraneous features such as trees drawn into a topographic map. Similarly, the intended audience for a map can highlight which features were carefully recorded. A navigation chart intended for mariners is likely to correctly

show known navigation hazards in a port, but may not correctly show wetlands along the shoreline even if they are drawn in (Shalowitz, 1964). Bias often results in omissions from historical documents and can be difficult to determine, as is the case with the dwellings and cemeteries of enslaved peoples, which were rarely recorded throughout much of US history even on otherwise detailed maps of plantations (Downer, 2015). Bias can also result in overly generous depictions of objects in maps, as can be the case when a map was produced by a developer attempting to sell homes in a new community, who may have included buildings not yet constructed (and sometimes never constructed) in maps used for marketing purposes (Seasholes, 1988). Cartographic accuracy can be evaluated as efforts are made to georeference historical maps. If no metadata are available for a map, no reliable cartographic coordinates appear on that map, and any locations of semi-permanent features don't correspond to one another, then the map lacks cartographic accuracy and should be used only with great caution (Uhl et al., 2018). Historical maps and other resources should not be rejected as valuable sources of information simply because of their age, but they should also not be accepted as invariably correct. Rather, they should be carefully evaluated and used to the extent that they can be deemed reliable (Seasholes, 1988).

Great care must be taken when using nautical charts, publically available digital elevation models, and publically available topobathymetric models when precise bathymetric data is needed because these resources may have utilized much older datasets than the year in which they were created. Navigation charts are not hydrographic surveys, they are amalgamations of those surveys. The citation years for

these products may suggest that the data with which they were created were obtained within the past several years, but in fact these often use the most recent hydrographic survey, which could be substantially older. For instance, the 2015 CoNED topobathymetric model of New Jersey and Delaware (OCM Partners, 2020) incorporates data from as early as 1888, which could introduce substantial error in landform delineation if bathymetric changes have occurred since then.

The objectives of this chapter are to examine the validity of historical hydrographic surveys for use in soil survey, to evaluate bathymetric stability in Rhode River, and to provide guidance for coastal zone soil surveyors as they evaluate bathymetric stability in other locations.

### 2.3 Materials and methods

#### 2.3.1 Study site

Rhode River is a microtidal brackish subestuary on the western shore of Chesapeake Bay, adjacent to the Smithsonian Environmental Research Center (SERC) in Anne Arundel County, Maryland. Including its larger tributaries, it consists of approximately 500 ha of open water fringed by tidal marshes, escarpments, developed uplands, and forested uplands. A recent publication contains a more complete description (Wessel and Rabenhorst, 2017).

#### 2.3.2 Hydrographic comparisons

Hydrographic comparisons were conducted by collecting historical and contemporary bathymetric datasets on the Rhode River estuary, correcting them to the same plane of reference, and importing them into a geographic information system

(GIS) for analysis. All historical hydrographic survey scans, descriptive reports, and downloadable data (where previously georeferenced) are publically available through the National Centers for Environmental Information of NOAA. This analysis includes contemporary bathymetric data collected as a part of this research during the summer of 2015, NOAA-georeferenced sounding data from a 1972 National Ocean Service (NOS) hydrographic survey (Austin and Baker, 1972) and a 1933 US Coast and Geodetic Survey (Bond and Sturmer, 1933a), a 1903 US Coast and Geodetic Survey (Flower, 1903), and an 1846 US Coast Survey (Lee et al., 1846). These data were used to generate digital elevation models (DEMs) using GIS interpolation tools (Bradley and Stolt, 2002). Map algebra was then used to produce maps of bathymetric differences (Hicks and Terry, 1997), and the ArcMap Cut Fill tool was used to generate volumes and average rates of bathymetric change.

Prior to comparisons, all datasets had to be corrected to the same plane of reference, or vertical datum. The plane of reference used in hydrographic surveys of the US east coast since 1878 has been mean low water (MLW), a tidal datum generally calculated from one or several tide gauges installed in a survey area (Sallenger et al., 1975). It is important to use a tide gauge or gauges located near the location of the survey, rather than predicted tide levels, when conducting water level corrections on soundings because wind and precipitation can cause observed water levels to deviate substantially from predicted tides (Smith, 1984). Correcting soundings to a tidal datum ensures that in one survey all depths are relative to the same plane of reference, but because long term relative sea-level rise (RSLR), seasonal variation, and interannual variation can all impact tidal datums, additional

corrections are necessary to compare surveys conducted at different times.

Interannual variation is caused by interaction between the atmosphere and the ocean; for example, El Niño/Southern Oscillation occurs irregularly every few years and drives changes in water temperature, salinity, ocean currents, atmospheric pressure, and wind that can all impact tides around the globe (Zervas, 2009). Seasonal variations have similar causes, but they are more predictable and the changes result from factors including greater energy input to coastal waters from solar radiation in the summer. Since 1928 most hydrographic surveys have used tide gauges that have been surveyed and connected to USGS benchmarks, allowing corrections to permanent planes of reference (Rude, 1928), but unfortunately it is often the case that gauges, benchmarks, and metadata necessary to conduct these comparisons for historical surveys have been lost. This situation can fortunately be overcome with a variety of corrections.

In recent decades, NOAA tide gauges have been more consistently maintained and surveyed than in the past. Modern NOAA tide gauges report multiple tidal datums relative to the National Tidal Datum Epoch 1983-2001 (NTDE), a vertical datum developed using 19 years of tide data, surveyed and adjustable to other vertical datums. This is now the standard datum and is evaluated every 20-25 years based on new tide data (Flick et al., 2013; Gill et al., 1998). Because the NTDE was calculated using 19 years of data from 1983-2001, it averages the impact of relative sea-level rise during those years, and therefore most precisely represents vertical datums at the midpoint, 1992 (Parker, 2003). Sea-levels today are slightly higher as a result of relative sea-level rise, but until the NTDE is updated the vertical datums that it



presents at a tide gauge best represent the midpoint of the period used to calculate it. A tide gauge maintained on Rhode River by SERC was installed in 1999, but had not been connected to the NTDE. Rather, the SERC tide gauge recorded data relative to the station datum (STND), the bottom of the tide gauge itself. Efforts were therefore undertaken to correlate the SERC tide gauge data with another reliable gauge in order to estimate NTDE at the SERC gauge.

The Annapolis, MD tide gauge (Station ID: 8575512) operated by NOAA has a well maintained record extending back to the 1930s, and it is located in a similar geomorphologic position on the same side of the Chesapeake Bay as the SERC tide gauge, 11 km away. The SERC dataset was adjusted by removing sections of data where the water level did not change throughout a day, indicating that the mechanism had jammed or frozen in place (checking historical weather records indicated that these errors did generally occur during deep winter freezes). Once these erroneous data were removed 130,401 paired hourly values between the two gauges from 1999-2015 (the extent of the SERC gauge data) were plotted in a bivariate analysis in order to relate the two gauges (Figure 2-1). The zero value for the Annapolis gauge is MLW connected to NTDE at that gauge, and the linear relationship between these datasets places MLW connected to NTDE at the SERC gauge at 1.77 m above the SERC gauge STND ( $r^2=0.98$ ). Where noted, corrections for RSLR, seasonal variation, and interannual variation were obtained for the Annapolis tide gauge from NOAA Tides and Currents.

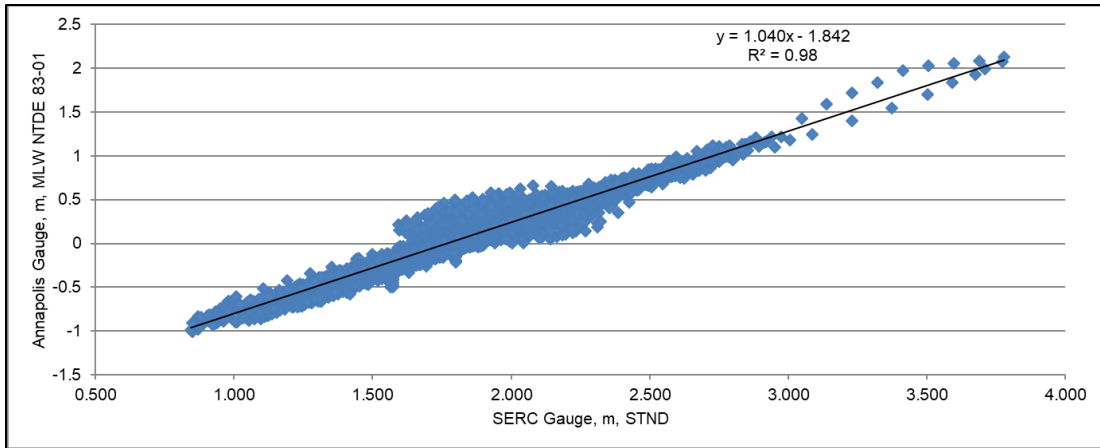


Figure 2-1. Annapolis vs SERC Tide Gauge Bivariate Plot. Equation shows best fit line relating the two tide gauges and is accompanied by a correlation coefficient of 0.98. The extreme points on the right are a result of Tropical Storm Isabel impacting the region on September 19, 2003 (MacGillis et al., 2003).

Having connected the SERC gauge to a vertical datum, a sonar survey of Rhode River was conducted in 2015 using a Garmin EchoMap 74sv echosounder/GPS sounding unit. Depths, times, and locations of soundings were simultaneously recorded on multiple boating transects through the estuary. The georeferenced bathymetry was then post-processed with data simultaneously obtained from the SERC tide gauge to account for tidal variations during data acquisition (Gibson and Gill, 1999; Hess, 2003) (Figure 2-2). Soundings were converted to depths relative to MLW at the SERC gauge, defined relative to the NTDE at the Annapolis gauge. These values were then joined with the Rhode River section of the NOAA Continually Updated Shoreline Product (CUSP), with its depth set to zero. Where High Island (a sunken island in Rhode River) once existed, the shoreline depth was set to 0.46 meters below MLW to represent the existing shoal surface. The High

Island shoreline depth was based on several measurements within the edge of the shoal in 2015, though it may be shallower in the center where it becomes hazardous to traverse by boat. In addition to the 23,096 data points in the 2015 survey, 480 corrected values were added from the 1972 NOS hydrographic survey. These values were incorporated to provide coverage for limited areas too shallow and choppy to safely survey in 2015. Kriging was used to generate a DEM map from these data in ArcMap.

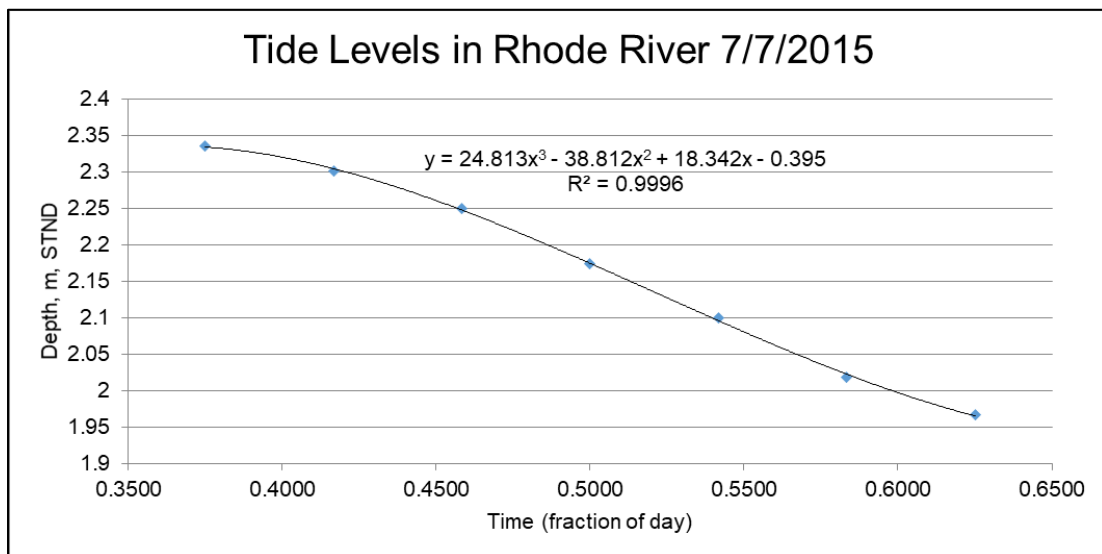


Figure 2-2. An example polynomial model used to correct soundings from a single day of surveying to a plane of reference. Best fit lines were generated for each day using several hours of tide data from the SERC gauge, extending at least an hour before and after the time of sounding collection.

The 1972 NOS hydrographic survey includes NOAA-georeferenced soundings and a descriptive report detailing its creation (Austin, 1972). Depths were reported relative to MLW, calculated from a tide gauge that was installed at Contees Wharf on Rhode River from April 21st to May 9th, 1972. Sea-level here is rising at a rate of 3.53 mm/yr, and 20 years have passed between 1972 and 1992 (the midpoint of NTDE 83-01, which will be used for all sea-level rise corrections in historical hydrographic surveys), resulting in a correction of 0.0706 m that was added to the 1972 depths (Table 2-1). Seasonal variation records show that sea-level is (on average) 0.021 m higher during this time of year, a value that must be subtracted from 1972 depths. Interannual variation shows that tides were on average 0.07 m higher in 1972, again a value that was subtracted from 1972 data., Kriging was used to create a DEM because soundings were dense and well distributed in Rhode River, so errors associated with the influence of the added shoreline points (at depth zero) were minimized because they could be excluded from interpolation calculations for all cells besides those very close to the shoreline (Childs, 2004). At lower sounding densities the shoreline points resulted in DEM depths which were far shallower than actual soundings near the shoreline because the zero depth of the shoreline outweighed the few soundings near the shore. In those cases, inverse distance weighted interpolation (IDW) provides a better approach because greater distances from points reduces their influence on calculated values in DEM cells (Childs, 2004).

The 1933 hydrographic survey points were available as a georeferenced file from NOAA and were also accompanied by a descriptive report (Bond, 1933). Accounting for the 59 years between this survey and 1992, a sea-level correction of

0.2083 m was added to the 1933 depths (Table 2-1). The survey was conducted from September to November, when seasonal variation records show that sea-level is on average 0.0537 m higher during this time of year, a value that must be subtracted from 1933 depths. Interannual variation shows that tides were on average 0.0023 m lower in 1933, again a value that was added to the 1933 soundings. Again, sounding density enabled kriging for DEM creation.

The 1903 survey was available as a scanned map which had to be georeferenced. The shoreline corresponded extremely well to most of the CUSP. Soundings were georeferenced, converted to meters, and corrected for sea-level rise and seasonal variation (Table 2-1). The 89 years between 1903 and 1992 corresponds to a 0.3142 m increase due to sea-level rise, which was added to the 1903 sounding depths. The survey was conducted in September when seasonal variation adds 0.109 m to the water depth, which was subtracted from the soundings. The survey precedes the Annapolis tide gauge record, so interannual variation was not accounted for using the Annapolis gauge directly. The Baltimore tide gauge record begins in 1902, so by comparing interannual variation between the Baltimore and Annapolis gauges in a manner similar to the method used in Figure 2-1, the relationship between the gauges (Figure 2-3) and the Baltimore interannual variation for 1903 was used to calculate a correction of 0.043 m higher than average for the Annapolis gauge, which was subtracted from the survey depths. Soundings were not well distributed throughout all of Rhode River, so a DEM was generated using IDW interpolation. This method was preferred for this survey because the depth soundings were generally far apart from one another and some areas of Rhode River were not sounded at all, and IDW

interpolation takes distance from data points into account as raster values are generated (Childs, 2004).

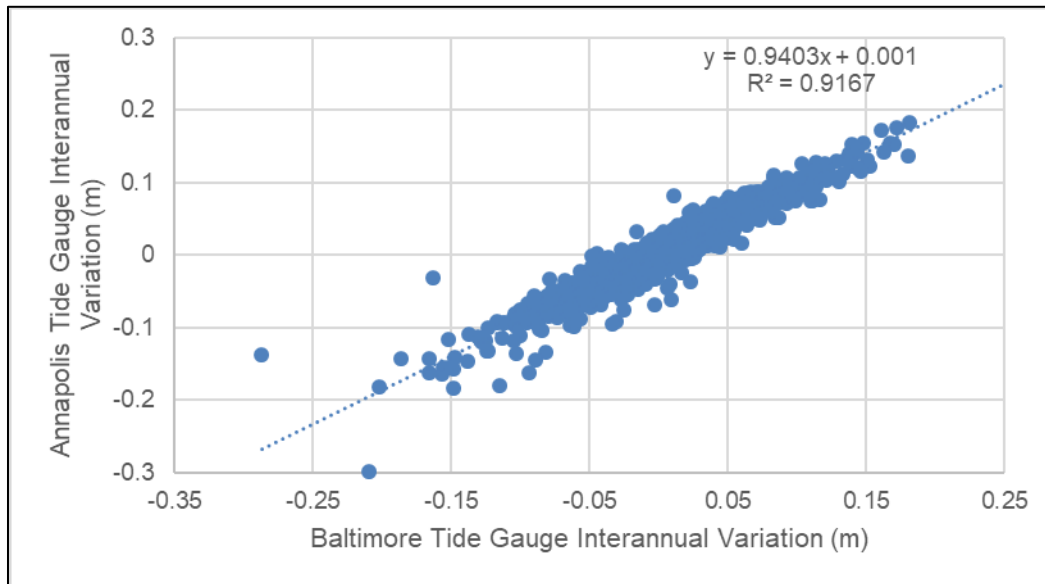


Figure 2-3. A comparison between the Baltimore and Annapolis tide gauges showing 1032 available monthly paired interannual variation values from 1928-2016. The Baltimore gauge record extends back to 1902, allowing an estimate of the interannual variation for the 1903 hydrographic survey of Rhode River.

The 1846 hydrographic survey was available as a scanned file created from the original paper sounding sheet (Figure 2-4). It was georeferenced in ArcMap, using stable reference points on the shoreline. Some areas of the surveyed shore differed from the CUSP so these were avoided when creating ground control points. Points were then created for the inked soundings, entering the depths as reported by the survey team. These data were then corrected for comparison to the NTDE 83-01 plane of reference by accounting for RSLR and seasonal variation (Table 2-1). Using

the 146 years between the survey and 1992, a correction of 0.5154 m was added to the 1846 depths for RSLR. Seasonal variation can be accounted for because the sounding sheet reports that the survey was conducted from August 14<sup>th</sup> to November 24<sup>th</sup>. The average seasonal variation for this period is 0.0608 m above MLW, so this value was subtracted from the 1846 soundings for a total correction of +0.4546 m. Like the 1903 survey, the interannual variation cannot be accounted for by using the Annapolis gauge record directly, nor can it be accounted for by using the Baltimore gauge record. Interannual variation at the Annapolis gauge (from 1928-2016) ranges from 30 cm below to 25 cm above average sea levels, though the values cluster relatively tightly around zero difference (mean = zero). The standard deviation of interannual variation at the Annapolis gauge was 0.058 m, so 95% of the reported values fall within the range (-0.116 cm, 0.116 cm), providing reasonable confidence that any error introduced by not accounting for interannual variation is less than about 13 cm. Large portions of Rhode River were not sounded during this survey, so no interpolation method could be used without introducing substantial error in the missing areas. Comparisons with the 1846 survey were done using the survey points themselves, and the corresponding depths at those locations on the DEMs created for the subsequent surveys.

Table 2-1. Plane of reference corrections applied to hydrographic surveys so that all depths are relative to NTDE 83-01 MLW. NOAA Tides and Currents plots from which corrections were taken are given in Appendix A. Values in meters.

	Sea-Level Rise	Seasonal Correction	Interannual Correction	Total Correction
2015	Corrected directly using current tide gauge			
1972	0.0706	-0.021	-0.07	-0.0204
1933	0.2083	-0.0537	0.0023	0.1569
1903	0.3142	-0.109	-0.043	0.1622
1846	0.5154	-0.0608	unknown	0.4546





Figure 2-4. Rhode River depicted in the 1846 hydrographic survey. Note the incomplete coverage of soundings, leaving many coves and one entire tributary unaccounted for. The dotted red lines are fathoms, 6 ft or 1.83 m, but represent interpolations of the survey team, not actual soundings. Subsequent surveys are of a higher quality.

## 2.4 Results and discussion

### 2.4.1 Evaluation of historical data

Hydrographic surveys vary in how well they meet the four tests used to evaluate historical maps. For all surveys conducted by NOS and its precursor agencies, the primary purposes were to provide data for national defense and commercial shipping. President Thomas Jefferson highlighted these national needs in his State of the Union Address (at that time, these were letters) to Congress in 1805, discussing the threat to US coasts and harbors and asking for warships to defend American ships and sailors from being harassed and impressed by the British Navy (Jefferson, 1805). In 1807, President Jefferson signed into law “An Act to Provide for Surveying the Coasts of the United States,” and on the same day requested additional gunships for the Navy. The survey was delayed until a theodolite and other scientific instruments could be imported from Europe (Gaye, 2007). It is therefore reasonable to conclude that trained professionals were using advanced instruments of the time in order to obtain positions and depth soundings as carefully as possible. The audience for these surveys would be naval commanders and commercial shippers, again highlighting the need to plot navigation hazards correctly. Deeper water areas, and shoreline features, may be less reliable than shallow water soundings, as they would represent less of a hazard to navigation.

Bias may exist in these soundings, particularly in how these data were collected. Prior to 1878 common hydrographic practice was to collect soundings on transects that ran along, rather than across, supposed contours. This method was observed to generate errors, and hydrographic survey manuals were changed in 1878

to clarify that sounding transects should be run across supposed contours, in order to better represent the highest and lowest points in the survey (Hydrographic Surveys Division, 1878; Sallenger et al., 1975). While the 1846 survey shows some transects running across contours, most of the survey transects do run directly up the channel, leaving the approaches to the shore largely unaccounted for.

Cartographic accuracy is particularly troubling for the 1846 survey. Because no Descriptive Report could be located, and the sounding sheet lacks these details, it is unknown what datum or projection was used to plot the map. Common projection options used at the time were the polyconic, Bonne, and equidistant polyconic projections (Sallenger et al., 1975). All of these contained errors and even with modern software a correction is not trivial, assuming the projection could be determined. The sounding sheet does have gridlines plotted, but contains several sets of lines, a common problem on these documents as efforts were made over subsequent years to plot corrected grids onto them (Shalowitz, 1964). The edges of the sounding sheet were damaged prior to when it was scanned, and no complete coordinates can be discerned on any of them (though several whole degrees can be read, minutes and seconds have been lost).

The plane of reference for older maps also raises issues of cartographic accuracy. Prior to 1856, soundings were generally corrected to the lowest water level observed during the survey period, which would be lower than MLW (Shalowitz, 1964). The 1846 survey does not denote a place of reference, so this could introduce an error into subsequent analyses. At the Annapolis gauge, MLW is 0.22 m higher than MLLW, which could be an estimate of this error if MLW was not used as the

plane of reference for the 1846 survey. This would mean that 0.22 m should have been added to the 1846 depths to correct them to MLW. The bottom of Rhode River would be 0.22 m lower than assumed in these comparisons, and sedimentation rates would be higher to account for that. Unless additional documents can be uncovered relating to the 1846 survey, this will remain unknown.

In 1856 MLW became the recommended plane of reference in the updated hydrographic manual (Bache, 1856). This plane was calculated using local tide gauges installed for one lunar month (except in the Pacific and other problem areas with larger and more irregular tides than the East Coast), or a few days of tide data would suffice for a reconnaissance survey. The need to consistently keep notes and produce reports was noted, and the stated justification for this was that inconsistent work was being done. Allowable error in 1856 was limited to tenths of a foot, though could grow to entire fathoms in deep water work, but should never exceed 5% of the water depth. Surveys produced prior to 1856, when these instructions first appeared, should therefore be used with caution. Even after 1856, shallow depths were often reported only to the nearest whole foot, which in many cases clearly violated the 5% error rule simply within measuring error.

Because it lacks important metadata, the 1846 map very poorly meets the test of cartographic accuracy. However, georeferencing this map using the shoreline revealed that the shape of the shoreline had changed very little and required virtually no “rubber-sheeting” to fit onto contemporary satellite photos. Thus, while using the gridlines to georeference shorelines and track shoreline change on maps of this era

may not always be possible, the positions of the soundings relative to stable shoreline features should be considered to be fairly reliable.

The 1903 survey was of a much higher quality. Edges of the sheet were intact with latitude and longitude and the shoreline was remarkably similar to the current shoreline. Soundings cover much more of the river in transects that cross bathymetric gradients, and the survey reports that mean low water was used as the plane of reference. The 1903 survey therefore meets the test of cartographic accuracy fairly well.

The more recent surveys that are accompanied by Descriptive Reports are much easier to work with, and have often already been professionally digitized and georeferenced by NOAA. That was the case with the 1933 and 1972 surveys used in this study.

#### 2.4.2 Hydrographic comparisons

A difference map showing depth changes between surveys appears in Figure 2-5, showing changes between each pair relative to MLW at the NTDE 83-01 datum. Displayed changes are best estimates of absolute changes in the elevation of the bottom, not changes in water depth. Due to the fact that soundings were reported in whole feet in most areas of the historical surveys considered, differences of less than 30 cm (~1 ft) are not considered to be significant because a 15 cm error is allowed within each survey. Table 2-2 lists the percentage of area for each comparison which exhibits the ranges of change displayed in Figure 2-5.

From 1846-1903 43.3% of the point comparisons of depth fall within the error of  $\pm 30$  cm (Figure 2-5, Table 2-2). There is a general decrease in bottom elevation of

8.4 cm (Table 2-3), but the 95% confidence interval for the point differences includes zero (Table 2-4). This means that with 95% confidence the mean change is between a loss of 18 cm and a gain of 1 cm, so we cannot conclude that any significant change has occurred in bottom elevation of Rhode River. Assuming that the 1846 survey was conducted relative to MLLW would alter these results by roughly 22 cm, but would still not show a massive signal of cultural sedimentation comparable with meters of deposition reported elsewhere. This may be due to the fact that Maryland experienced the greatest rates of culturally accelerated sedimentation prior to 1846, meaning that in 1846 there may have been a substantial amount of recently deposited cultural sediment in Rhode River, but that the rate of supply had diminished by then. If the mean change is correct and the bottom elevation decreased, this could correspond to tidal flushing and scour as the bathymetry returned to an equilibrium state, or autocompaction of materials deposited during periods of higher sedimentation (Massey et al., 2006). In Louisiana, current rates of autocompaction of surface sediments have been reported at rates of nearly half a centimeter a year (Prouhet, 2011). A few of the tributaries to Rhode River show sedimentation (Figure 2-5), but others show no significant change or decreases in bottom elevation, so no general trend can be stated.

From 1903-1933, the trend is clearer (Figure 2-5). The largest share of the bottom, 47.9%, shows no significant change, but 37.3% of the bottom shows 0.3-1 m of sedimentation (Table 2-2). The average change is 16 cm (comparable to 10 cm of sea-level rise over the same period), a sedimentation rate of 5.5 mm/yr between the surveys (Table 2-3). Comparing 1933 directly to 1846 also indicates sedimentation,

though at a lower rate of 1.1 mm/yr (Table 2-4). Soil conservation measures had yet to be adopted, so sediment may still have been transported in from the watershed. Sediment may also have been tidally transported in from elsewhere in Chesapeake Bay due to the fact that tidal flows pause briefly at tide reversal, sometimes allowing sediment that was carried in by flood tides to settle within an estuary at high tide (Bell et al., 2000; Dalrymple and Choi, 2003).

From 1933 to 1972, the sedimentation rate decreases from 5.5 to 1.9 mm/yr, dropping below the rate of sea-level rise (Table 2-3). No significant change was measured over 81.6% of the bottom (Table 2-2). However, by comparing 1972 with 1846 a small increase in sedimentation rate (1.1 to 1.3 mm/yr) is measured. The 95% confidence intervals of the point comparisons overlap, so sedimentation rates may not significantly differ between the two periods (Table 2-4).



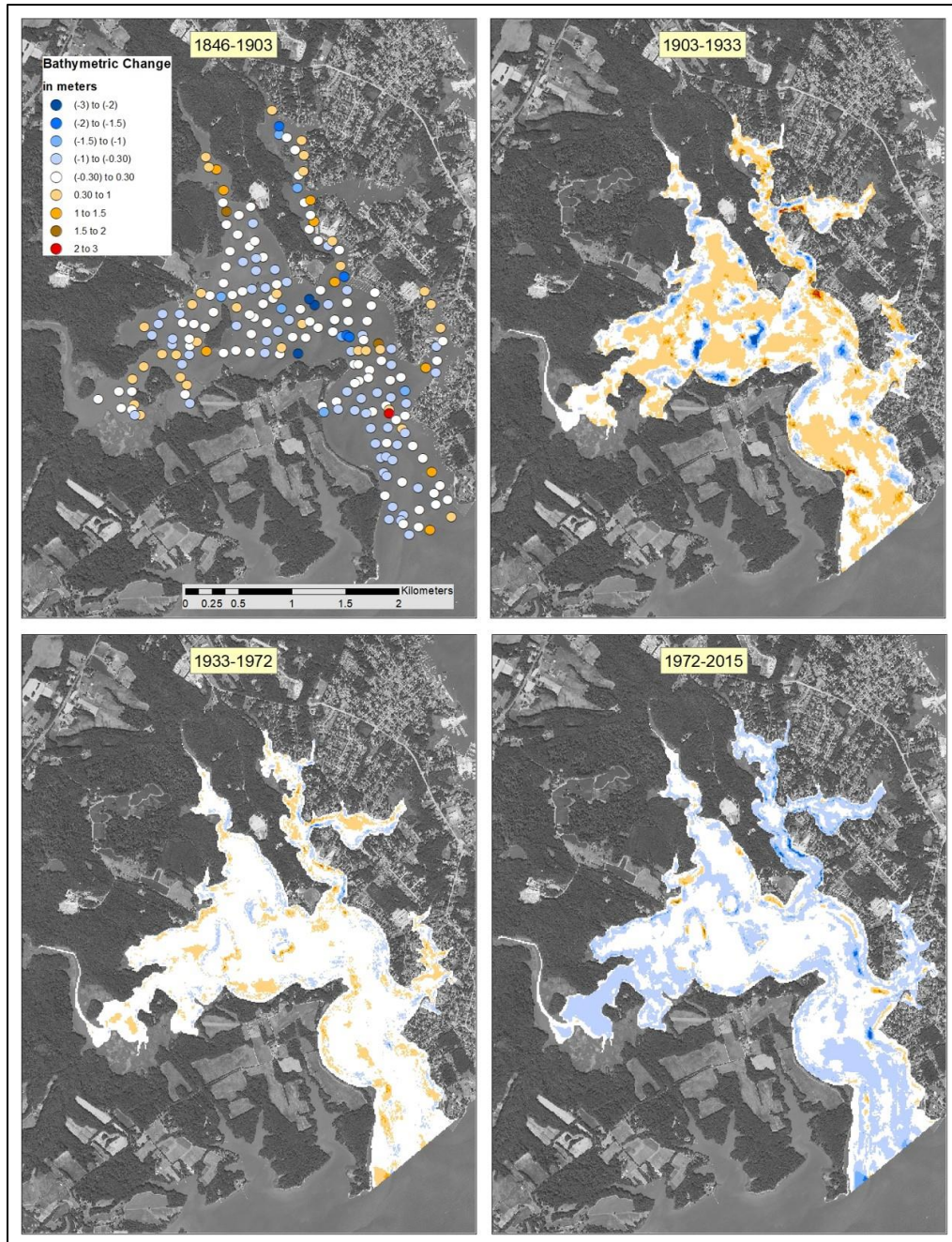


Figure 2-5. Bathymetric changes in Rhode River occurring between surveys, corrected to the NTDE 83-01 MLW. White areas indicate  $\pm 0.15$  m, within reasonable measurement error. Blue areas (negative change) show where the bottom has consolidated or scoured, and brown/red areas (positive change) show sedimentation.



Table 2-2. Categories of change and the area associated with each for each hydrographic comparison. Negative changes in bathymetry and mean rates correspond to erosion or consolidation of the bottom, while positive values correspond to sedimentation.

Magnitude of Bathymetric Change	Percentage of Survey Area			
	1846-1903	1903-1933	1933-1972	1972-2015
(-3) – (-2) m	1.5	0.2	0.0	0.1
(-2) – (-1.5) m	2.0	0.6	0.0	0.3
(-1.5) – (-1) m	3.4	1.8	0.2	1.7
(-1) – (-0.3) m	27.6	9.7	5.8	40.9
(-0.3) – 0.3 m	43.3	47.9	81.6	55.0
0.3 – 1 m	16.3	37.3	11.8	1.8
1 – 1.5 m	4.4	2.0	0.4	0.1
1.5 – 2 m	1.0	0.4	0.0	0.0
2 – 3 m	0.5	0.1	0.0	0.0

Table 2-3. Bathymetric changes summarized. Volume changes are net changes, sums of cut and fill areas. Sea-level changes between survey dates are shown for comparison to mean bathymetric change. Negative changes mean bottom loss or consolidation, positive changes mean sedimentation. Sea-level values are provided from NOAA estimates at the Annapolis tide gauge. Other values were calculated from DEM comparisons, except for the 1846-1903 values which are calculated from changes at the 1846 survey points relative to the 1903 DEM (therefore no volume measurement is provided).

Change	Surveys Compared			
	1846-1903	1903-1933	1933-1972	1972-2015
$\Delta$ Bathymetry ( $m^3$ )	-	$8.12 \times 10^5$	$3.56 \times 10^5$	$-1.43 \times 10^6$
$\Delta$ sea level (m)	0.20	0.10	0.14	0.15
Mean $\Delta$ bathymetry (m)	-0.084	0.16	0.072	-0.29
Mean rate (mm/yr)	-1.5	5.5	1.9	-6.8

Table 2-4. Long-term changes calculated from 1846 survey points and DEMs of subsequent surveys. Values are calculated using 203 survey points, precisely the same locations for each comparison. Rates given by this method are less reliable as they integrate progressively longer periods of time between comparisons.

Change	Surveys Compared			
	1846-1903	1846-1933	1846-1972	1846-2015
Years	57	87	126	169
Mean $\Delta$ bathymetry (m)	-0.084	0.092	0.16	-0.12
↳ 95% CI	(-0.18, 0.01)	(0.01, 0.17)	(0.07, 0.24)	(-0.21, -0.04)
Mean rate (mm/yr)	-1.5	1.1	1.3	-0.71

From 1972-2015, the trend reverses to a general decrease in the bottom elevation by a mean of 29 cm (Figure 2-5, Table 2-3). The change was widespread, covering 40.9% of the bottom. An additional 55.0% showed no significant change. The average rate was 6.8 mm/yr of surface loss, or 0.71 mm/yr on average since 1846. Overall, little change occurred, with the notable exception of High Island. Present in prior surveys (with depth set to zero) it has eroded to a wave-cut shoal since 1972. The 1972 survey was conducted just prior to Hurricane Agnes, and it is possible that some of the bathymetric decrease corresponds to scour by the storm, which was one of the most powerful storms ever recorded to impact the Chesapeake Bay. Additionally, tightening environmental regulations may have contributed to a decrease in sediment load in Rhode River since 1972, with counties enacting their own regulations regarding land disturbance and sediment control.

Regardless of the causes of the changes measured by comparing these surveys, they are relatively small and dispute claims that agricultural activity caused

massive infilling of aquatic environments in all settings leading up the implementation of soil conservation measures. The Soil Conservation Service (now NRCS) was founded in 1933 and it took several decades for counties to implement their own erosion controls, yet during these years Rhode River changed little due to sedimentation. Sedimentation rates did not exceed 5.5 mm/yr, a fraction of the reported values of 2-6 cm/yr from the Anacostia and Patapsco Rivers circa 1900.

#### 2.4.3 Implications for erosion in the watershed

Erosion rates in the watershed can be very roughly approximated by considering the greatest mean sedimentation rate of 5.5 mm/yr calculated for Rhode River for the period 1903-1933 (Table 2-3). Agricultural land use can be bounded between 1850 and today, likely extreme values. According to the 1850 Census, Anne Arundel County contained 222,228 ac (89932 ha) of improved farmland (DeBow, 1853). Anne Arundel County is 152291 ha in area, meaning that in 1850 a conservative estimate of cleared land would be 59%. The Rhode River watershed is 8764 ac (3547 ha) (Anne Arundel County Department of Public Works et al., 2016). If we assume that the 1850 Census results apply to this portion of the Rhode River watershed, 2093 ha were cultivated at the time. Today only 10.6% of the Rhode River watershed is in row crops or pasture (Anne Arundel County Department of Public Works et al., 2016), 376 ha (ignoring other land uses which produce minimal sediment, such as residential land). By assuming a reasonable bulk density for the majority of the soft sediment in Rhode River of 0.9 g/cm<sup>3</sup> upland erosion rates vary from 1.2 kg/m<sup>2</sup>/yr (5.2 tons/ac/yr) to 6.5 kg/m<sup>2</sup>/yr (28.9 tons/ac/yr).

The NRCS considers an erosion rate of 5 tons per acre per year to be the upper limit of acceptable erosion for cultivated land (though this number is not without its critics) (Schertz, 1983). Using either extreme of cultivated land in the Rhode River watershed, and the stated assumptions, upland erosion from 1903-1933 exceeded recommendations. Because Rhode River bottom elevation decreased from 1972-2015, this is assumed to have been corrected.

### 2.5 Conclusions

Historical hydrographic surveys were produced by trained professionals using some of the best scientific instruments available to them at the time, though surveys produced prior to the 1856 hydrographic manual may introduce substantial errors to analysis. Navigation channels and hazards are likely to be plotted correctly, though data coverage may be sparse and shoreline features may not have been plotted with the same care as the soundings. Still, these older maps are worth considering prior to conducting a soil survey, as they can indicate areas where islands have been lost. More recent surveys, particularly where data have been corrected and digitized by NOAA and Descriptive Reports are available, can be extremely useful in conducting an analysis of bathymetric change.

Rhode River has changed little over the last 169 years, with the bathymetric surface sometimes decreasing and sometimes increasing, though average rates of change never exceeding a cm a year. In all four survey comparisons the largest proportion of the bottom fell within the margin of measurement error for no change having been detected. Though the factors driving bathymetric change are myriad and complex, the bathymetry of Rhode River is remarkably stable through time.

Though Rhode River has changed, most of its landform features are generally stable over a period of decades or longer, suggesting that subaqueous soil surveys in Chesapeake Bay subestuaries and in similar settings will remain valid for the same period of time. Soil surveys have never been intended to be conducted once and used forever thereafter; they have always had to be updated as land uses change and as environments evolve. Like upland soil surveys, subaqueous soil surveys will need to be updated from time to time as subaqueous land uses are developed and data needs change.

## Chapter 3: Identification of sulfidic materials in the Rhode River subestuary of Chesapeake Bay<sup>1</sup>

### 3.1 Abstract

Sulfide-containing soil materials can undergo a process known as sulfuricization if disturbed, triggering the production of sulfuric acid through the oxidation of Fe sulfides and causing environmental degradation. Several systems exist to classify these types of materials based on the level of environmental hazard that they may pose. Hypersulfidic materials undergo extreme acidification, hyposulfidic materials may undergo acidification to a lesser extent or not at all, and monosulfidic materials contain a more reactive form of Fe sulfide. The definitions for these terms vary, so a brief review of how these materials are described and classified both globally and in the Rhode River region is provided. Testing for these materials is costly and time consuming, with current methods sometimes taking 16 weeks or longer to identify these materials. In subaqueous environments, where dredging and other marine construction activities may be delayed by requirements to obtain this

---

<sup>1</sup> This chapter has been published in an Elsevier journal, *Geoderma*. As author, I retain the right to include it in a thesis or dissertation, provided it is not published commercially. Permission is not required. The citation to the original source follows: Wessel, B. M., & Rabenhorst, M. C. (2017). Identification of sulfidic materials in the Rhode River subestuary of Chesapeake Bay. *Geoderma*, 308(Supplement C), 215-225. <https://doi.org/10.1016/j.geoderma.2017.07.025>

information, better methods for the field identification of these materials would be of use to subaqueous soil surveyors. In this study, subaqueous soil materials from the Rhode River estuary were sampled, described, and divided into six categories based on morphologic properties: fluid muds, unconsolidated Holocene sandy materials, organic materials, buried A horizons, Tertiary materials with Fe oxide concentrations, and Tertiary materials without Fe oxide concentrations. These materials were then evaluated and classified as different types of sulfide-containing materials using current methods. Buried A horizons, organic materials, and Tertiary materials without Fe oxide concentrations are the most likely to be hypersulfidic materials, and therefore of the greatest environmental concern. Fluid muds, unconsolidated Holocene sandy materials, and Tertiary materials with Fe oxide concentrations are less likely to consist of hypersulfidic materials, but may still be of environmental concern as hyposulfidic materials or monosulfidic materials. Subaqueous soil surveyors can use these findings to help understand the relative environmental hazards posed by similar subaqueous soil materials in similar settings.

### 3.2 Introduction

Acid sulfate (AS) soils are problematic soils that are able to undergo extreme acidification if disturbed (Fanning and Fanning, 1989); this kills plants or stunts their growth (Muhrizal et al., 2003), leaches heavy metals (Roos and Åström 2006), degrades infrastructure (Breitenbucher et al., 2009; Salmon et al., 2014), and contaminates waterways (Åström and Björklund 1995). These soils contain reduced sulfur compounds, often as pyrite but sometimes also as metastable Fe sulfides (e.g. mackinawite and greigite). If these soils are disturbed these minerals can oxidize and

produce sulfuric acid in a process known as sulfuricization, which is the root cause of the severe problems associated with these soils (Boman et al., 2008; Rickard, 2012). They have long been recognized and understood as environmental hazards (Pons, 1973), with early references to the problems associated with their disturbance extending back to the 1700s (Dent and Pons, 1995). The identification and classification of these soils is therefore important so that disturbance, and the subsequent problems that it entails, can be avoided or appropriately planned for.

This is a particularly pressing issue in the case of subaqueous soils (SAS). Shallow marine and freshwater sediments have only been recognized and mapped as SAS in the United States since 1999 (Rabenhorst and Stolt, 2012; Soil Survey Staff, 1999). Despite identifying pedogenesis in the subaqueous environment (Demas and Rabenhorst, 1999; Demas et al., 1996) and outlining the factors of SAS formation (Demas and Rabenhorst, 2001), the classification of these soils is still a matter of some controversy (Fanning and Rabenhorst, 2008; Rabenhorst et al., 2016b; Wessel et al., 2017b; Wessel et al., 2015), and the most appropriate analytical tests and technical terms to use for these soils and soil materials have yet to be agreed upon by the international community working in these environments (Kristensen and Rabenhorst, 2015). Several recent SAS studies have been conducted in the United States (Balduff, 2007; Erich and Drohan, 2012; Millar et al., 2015; Still and Stolt, 2015; Stolt et al., 2011), Australia (Creeper et al., 2015), and Italy (Antisari et al., 2016; Ferronato et al., 2016), and it has become clear that the international community can benefit from adopting standardized terms for describing the soil materials found in these environments in terms of their properties as AS soil



materials. In addition to the hazards associated with upland AS soils, some subaqueous AS soils can consume water column oxygen if disturbed, devastating populations of aquatic organisms (Holmer et al., 2003); additionally, understanding the environmental hazards of different SAS materials is also important in preventing dredged materials from producing acid drainage (Demas et al., 2004; Fanning and Burch, 2000; Koropchak et al., 2016). Unfortunately, despite several decades of research and development, there is no universally accepted method of identification or system of classification for “potential AS soil materials” (i.e. the bulk materials from different horizons in AS soils that are able to undergo acidification as a result of sulfur oxidation) (Wessel et al., 2016).

The goal of this study is to identify SAS materials in the Rhode River subestuary of Chesapeake Bay that are easily discerned from one another in the field (defined primarily by their field morphological properties using common field and laboratory tests) and to establish if these morphologies exhibit strong relationships to three classes of sulfide-containing materials. By classifying these common SAS materials as different types of sulfide-containing materials (i.e. hypersulfidic, hyposulfidic, and monosulfidic materials) the relative hazards associated with disturbing these types of materials can be understood. This will enable SAS surveyors in the field to better predict the environmental hazards that may be posed by disturbing these types of materials in similar settings. Further, because AS soils are handled differently in several different soil classification systems (and because these definitions have changed over time), a brief review will be provided on identifying and classifying AS soil materials globally and in the Rhode River region.

### 3.2.1 Identification and classification of potential AS soil materials

The first classification for these materials was adopted in the United States in 1975 and contains the single category “sulfidic materials.” These materials were defined as containing “0.75 percent or more sulfur (dry weight), mostly in the form of sulfides and that have less than three times as much carbonate ( $\text{CaCO}_3$  equivalent) as sulfur.” Alternatively, these can be identified by repeatedly moistening and air-drying a sample of material in the shade for about 2 months, and monitoring the pH drop. Sulfidic materials were those that became “extremely acid” under these conditions. As a field test, a sample could be boiled in concentrated  $\text{H}_2\text{O}_2$  to hasten the oxidation and pH change (Soil Survey Staff, 1975), a method no longer widely used in the United States due to interference from some clays (Fanning and Fanning, 1989). Definitions and methods have improved considerably since then, but *United States Soil Taxonomy* still only recognizes one type of sulfidic materials (Soil Survey Staff, 2014). In contrast, the *World reference base for soil resources* (WRB) recognizes “hypersulfidic materials” and “hyposulfidic materials” (Food and Agriculture Organization of the United Nations, 2015), and the *Australian Soil Classification* recognizes both of these as well as “monosulfidic materials” (Isbell and National Committee on Soil and Terrain, 2016).

Although the specific definitions of each of these types of materials varies by type and by classification system, all three of these soil classification systems recognize the importance of the “moist aerobic incubation” test for oxidized pH. In this test, enough field-moist soil is added to a sample container to cover the bottom to a depth of approximately 1 cm. Following the procedure of the 12th Edition of the

*Keys to Soil Taxonomy*, this is moistened to a paste and the pH is recorded before allowing the sample to air-dry over the following week. The sample is then moistened to a paste again and the pH recorded, and this process is repeated for up to 16 weeks, or longer if the pH is still dropping (Soil Survey Staff, 2014). The process fosters the growth of aerobic bacteria, including sulfur oxidizing bacteria that oxidize pyrite and other Fe sulfide minerals, producing sulfuric acid in the process (Arkesteyn, 1980; Fanning and Fanning, 1989). The process used in the WRB and the *Australian Soil Classification* is similar to that outlined in *Soil Taxonomy* but the sample moisture is maintained at field capacity and samples are not allowed to become air-dry, sample thickness is 2-10 mm, and the duration is at least 8 weeks. A similar yet simplified method of “chip-tray” incubation is increasingly being used in Australia because it offers time and space savings, allowing samples to be collected, incubated, and archived in one container (Creeper et al., 2012), though the method has yet to be adopted in the *Australian Soil Classification*. Soil materials can be classified as hypersulfidic materials or hyposulfidic materials based on the degree to which they acidify during moist aerobic incubation. The use of concentrated  $H_2O_2$  to force oxidation of sulfides and the associated pH change in a short amount of time (e.g. hours) is still in use in Australia (Ahern et al., 2004), but does not always correlate with the results from moist aerobic incubation (Fanning and Fanning, 1989).

In addition to acidification as a result of moist aerobic incubation, several definitions of the types of potential AS soil materials depend on measurements of soil S (as sulfide, which produces sulfuric acid upon oxidation) and measurements of the ability of a soil sample to neutralize or buffer acidity that may be produced in the soil.

The WRB and *Australian Soil Classification* relate these measurements through an “acid-base accounting” method that attempts to predict, based on stoichiometric relationships, whether a soil sample will produce excess acid or have the capacity to neutralize acid (Ahern et al., 2004). There are many methods available to make these measurements and to make an accounting of them (Ahern et al., 2004), but of particular relevance to this study are methods to measure acid volatile sulfide (AVS) and Cr reducible sulfur (CRS). These S fractions are measured sequentially in a distillation apparatus that produces  $\text{H}_2\text{S}$  gas from the S species in a sample, captures this gas as a precipitate in a gas trap, and subsequently measures the S concentration in the trap. Different fractions can be produced by heating or cooling the apparatus (cold Cr reducible sulfide, CCrS and hot Cr reducible sulfur, HCrS) (Boman et al., 2008), but the simplest fractionation is between AVS and CRS (this implies HCrS, bypassing and including the CCrS fraction). Diluted HCl (6 M) is added to samples to measure AVS and represents the metastable Fe sulfide fraction, probably a mixture of greigite and mackinawite, but also aqueous FeS and porewater bisulfide ( $\text{HS}^-$ ) (Rickard and Morse, 2005). The CRS fraction is resistant to acid treatment and requires 1 M  $\text{CrCl}_2$  to evolve  $\text{H}_2\text{S}$ . It is thought to represent pyrite and elemental S, with CCrS representing only pyrite while HCrS also represents elemental S (Boman et al., 2008).

Several field methods are also in use to better describe sulfide-containing soil materials. A “whiff” test can be done to rank the concentration of  $\text{H}_2\text{S}$  present in a soil on a scale from zero to three, with zero indicating no odor and three indicating that the “rotten egg” smell of  $\text{H}_2\text{S}$  can be smelled simply by walking through a site.

This rating does correlate with total S content (Darmody et al., 1977). The odor indicates ongoing sulfidization in the soil—sulfate reduction and the potential formation of metastable Fe sulfides and pyrite (Fanning and Fanning, 1989). In subaqueous settings, a whiff test result of one or greater is often taken as evidence that no Fe oxides remain in the soil material being examined. This is because  $\text{H}_2\text{S}$  will react with Fe oxides to form metastable Fe sulfides in a matter of minutes (Rabenhorst, 1990; Rabenhorst et al., 2010). The reaction is reliable enough and quick enough that porewater sulfide concentrations can be estimated based on the degree to which Fe oxides are transformed to Fe sulfides when they are inserted into the soil (Rabenhorst et al., 2016a; Rabenhorst et al., 2010). This is consistent with observations of sulfide-containing shallow marine sediments, which generally contain no reactive Fe oxides below the top few centimeters (Kristensen et al., 2003; Kristiansen et al., 2002); however, soils are not homogenous systems in chemical equilibria. Due to microsite variability and the preferential flow of  $\text{H}_2\text{S}$  along macropores, it is not out of the question to observe Fe oxides in a soil sample that scores higher than a zero on the whiff test. Still, a  $\text{H}_2\text{S}$  odor suggests that any remaining Fe oxides should be relatively occluded, and that the soil will have a high degree of pyritization because excess  $\text{H}_2\text{S}$  will react with metastable Fe sulfides to form pyrite (Leventhal and Taylor, 1990).

A modification of the whiff test, used to provide evidence for the presence of metastable Fe sulfides, is to add dilute (10%) HCl to a soil sample that has received a zero on the whiff test (either initially or because  $\text{H}_2\text{S}$  has been allowed to dissipate) to determine if  $\text{H}_2\text{S}$  will be produced (Fanning et al., 1993). This is easily done in the

field by taking a pinch of soil, adding it to a plastic bag, dropping the HCl on the sample, and allowing it to react for several seconds before taking a “whiff” from the bag. The theory behind this is that some of the sulfur in metastable Fe sulfides will react with the acid to form H<sub>2</sub>S, but it should be noted that if there is any porewater HS<sup>-</sup> present, this may also contribute to any odor produced by this test because it will also react with HCl to form H<sub>2</sub>S.

Looking at some literature values for the variables involved in this reaction, the two sources can be compared in a thought experiment. Literature values on the concentrations of metastable Fe sulfides and HS<sup>-</sup> in Chesapeake Bay sediments indicate that metastable Fe sulfides will generate many orders of magnitude more H<sub>2</sub>S than will be generated from HS<sup>-</sup> in most circumstances. Moderately fluid to highly fluid finely-textured marine surface sediments have an average bulk density of 0.13 g cm<sup>-3</sup> (Jespersen and Osher, 2007). Assuming the metastable Fe sulfide in our sample occurs as mackinawite (FeS), 0.2% by mass of a dry sample would be enough to color the soil black (Fanning and Rabenhorst, 1990). The black color would be one of the first clues that metastable Fe sulfides are present (Fanning et al., 1993). Chesapeake Bay sediment porewater has a range of HS<sup>-</sup> from 0.5 μM to 5.6 mM (MacCrehan and Shea, 1995). The human ability to detect H<sub>2</sub>S from a solution of water at ordinary temperatures begins at concentrations of 10 to 100 ng L<sup>-1</sup>, but the distinctive rotten egg smell is more evident at concentrations of 100 ng L<sup>-1</sup> or higher, with only a musty odor detected at lower levels (Pomeroy and Cruse, 1969). Based on these assumptions a sample containing just enough FeS to color it black, and no HS<sup>-</sup>, could produce a porewater concentration of 1.0 x 10<sup>8</sup> ng L<sup>-1</sup> with the addition of HCl;

this is six orders of magnitude greater than the detection threshold for the human nose. On the other hand, assuming that a sample contains no FeS and only HS<sup>-</sup>, the concentration range of 0.5 μM to 5.6 mM equates to a H<sub>2</sub>S concentration of 1.7 x 10<sup>4</sup> to 1.9 x 10<sup>8</sup> ng L<sup>-1</sup>, which is still more than enough to be detected by the human nose. The HCl-whiff test can therefore be a useful indicator of the presence of metastable Fe sulfides such as mackinawite, but it is subject to interference from HS<sup>-</sup>. That said, the concentration of H<sub>2</sub>S resulting from HS<sup>-</sup> is only comparable to that resulting from FeS at the highest observed concentrations of HS<sup>-</sup> in the Chesapeake Bay, and so it seems likely that a black-colored SAS sample that produces a positive result from the whiff test will do so predominately due to the presence of metastable Fe sulfides.

Further evidence for the presence of metastable Fe sulfides can come from the “peroxide color change” test. Immediately upon exposing a soil sample to the air, a few drops of 3% H<sub>2</sub>O<sub>2</sub> solution is added to a fresh surface on the soil material. An immediate (within 10 seconds) discernable color change from black to grey (an increase in value) is recorded as having reacted in SAS descriptions in the United States, and a lack of a color change is recorded as having not reacted. This is generally interpreted to be a result of the oxidation of metastable Fe sulfides (McVey et al., 2012).

One field test that has recently come into use to indicate the presence of pyrite in sulfide-containing materials is the rating of the exothermic reaction with 30% H<sub>2</sub>O<sub>2</sub> that occurs within 1-2 minutes of the addition of several drops to a spot on the soil material. This is similar to the “fizz test” for carbonates (Ahern et al., 2004). Reaction with 30% H<sub>2</sub>O<sub>2</sub> is rated by Effervescence Class (Schoeneberger et al., 2012) and has

been used in recent soil surveys in the US. If more than a few drops of 30%  $\text{H}_2\text{O}_2$  are added, enough to mix the soil into a slurry, a “runaway” reaction with pyritic soil can be produced. The reaction is distinctively slow at first and gradually builds in intensity as the mixture is heated by the exothermic nature of the reaction. The reaction rate increases with increasing temperature, feeding back into a runaway reaction. This is unlike the instantaneous reaction observed between  $\text{H}_2\text{O}_2$  and Mn oxides (Schoeneberger et al., 2012). It is also unlike the very slow reaction between  $\text{H}_2\text{O}_2$  and organic matter, which proceeds slowly and may take more than an hour to run its course (Robinson, 1927).

Taken together, these tests and observations can be used to classify potential AS soil materials as hypersulfidic materials, hyposulfidic materials, or monosulfidic materials.

#### 3.2.1.1 Hypersulfidic materials

Hypersulfidic materials fit the original concept of sulfidic materials, and the definition of sulfidic materials that currently appears in *The Keys to Soil Taxonomy* is treated as a definition of hypersulfidic materials for the purposes of this study. These are the AS soil materials of greatest environmental concern. Hypersulfidic materials must have an initial pH (1:1 in water) of greater than 3.5 that decreases by at least 0.5 pH units to a final pH of 4.0 or less over the course of the moist aerobic incubation. Alternatively, an acid-base accounting approach can be used. Materials with a pH greater than 3.5 (1:1 in water) that contain at least 0.75% S by mass, mostly as sulfide, and less than three times as much  $\text{CaCO}_3$  equivalent as S, are also considered sulfidic materials (Soil Survey Staff, 2014). The definitions in the WRB and



*Australian Soil Classification* are similar, but in both of these classification systems the initial pH of the sample must be greater than or equal to 4 (though with regard to significant figures, 4.0 is generally used in practice). The WRB also requires that the sample contain at least 0.01% inorganic sulfide S (dry mass); this is a substantially lower threshold than that used in the other taxonomic systems. The WRB describes hypersulfidic materials as being waterlogged or anaerobic at least seasonally, with Munsell hues of N, 5Y, 5GY, 5BG, or 5G. The value is commonly 2, 3 or 4, and the chroma 1.

#### 3.2.1.2 Hyposulfidic materials

Hyposulfidic materials are sulfidic materials in the sense that they contain unoxidized sulfides that are able to produce acidity, but the materials themselves will not undergo severe acidification. Both the WRB and the *Australian Soil Classification* define hyposulfidic materials as having an initial pH (1:1 in water) of greater than 4.0 that does not decrease to a final pH of 4.0 or less over the course of the moist aerobic incubation. The WRB further requires that hyposulfidic material contain at least 0.01% inorganic sulfidic S (dry mass). The *Australian Soil Classification* does not contain this requirement for inorganic sulfidic S, but does require a pH decrease during moist aerobic incubation of at least 0.5 pH units in order for soil materials to be classified as hyposulfidic materials. Morphologically, hyposulfidic materials may be indistinguishable from hypersulfidic materials.

### 3.2.1.3 Monosulfidic materials

Monosulfidic materials are recognized in the *Australian Soil Classification*, and are identified by their saturation with water, low bulk density (except for sands), a color change on exposure to air from black to lighter colors, and the presence of H<sub>2</sub>S (whiff test). Not all monosulfidic materials meet all of these criteria. They contain at least 0.01% AVS (Isbell and National Committee on Soil and Terrain, 2016). The use of 3% H<sub>2</sub>O<sub>2</sub> to accelerate the color change on exposure to air has become commonplace among AS soils professionals when describing these materials. The addition of 10% HCl to produce H<sub>2</sub>S is sometimes used as a field indicator for AVS.

### 3.2.2 Potential AS soil materials in the Rhode River region

The Chesapeake Bay and its subestuaries, including the Rhode River subestuary, formed as rising sea-levels following the last glaciation flooded the Susquehanna River valley in the Coastal Plain physiographic province (Nichols et al.,

1991). Practical salinity<sup>2</sup> (Sp) (Feistel et al., 2016; Lewis, 1980) in the Rhode River ranges from Sp = 0 to Sp = 20 and areas in the upper reaches grade into tidal freshwater wetlands (Jordan et al., 1983), though most of the estuary generally has a practical salinity of 8-16 (Cory and Dresler, 1980). The majority of the estuary is saline enough that sulfide-containing materials are expected to be common (Fanning et al., 2010). This estuary is predominantly underlain and surrounded by two Tertiary geologic formations—the Nanjemoy and the Aquia, as well as younger Holocene sediments, and traces of other formations in small areas (Cleaves et al., 1968). In addition to these geologic formations, a complex history of relative sea-level rise and fall has created submerged and buried marsh surfaces, and a variety of other paleosols, resulting in a number of polygenetic SAS.

The Nanjemoy and Aquia formations are glauconitic, green to gray clays and sands that are of Eocene and Paleocene age, respectively. Similar Tertiary marine sediments have also been described on the Virginia Coastal Plain (Orndorff et al.,

---

<sup>2</sup> Salinity is reported in Practical Salinity Units on the Practical Salinity Scale 1978 (PSS-78), as adopted by the Joint Panel on Oceanographic Tables and Standards of the United Nations Educational, Scientific and Cultural Organization (UNESCO) (Lewis, 1980). Many conductivity-based salinity meters incorrectly display “ppt” units for this value, though it has been correctly reported without units in international limnologic and oceanographic literature for over 30 years (Feistel et al., 2016). Because it is a water quality parameter, rather than a soil property, the convention has been adopted for this work.

2008). Many of the scour and lag deposits within the Rhode River still contain large amounts of glauconite, and the consolidated substratum commonly contains unoxidized sulfides. Unoxidized portions of these glauconitic Tertiary sediments in the Mid-Atlantic region invariably contain CRS (Rabenhorst and Valladares, 2005). Using scanning electron microscopy, this CRS has been shown to occur as microscopic pyrite in the Nanjemoy and the Aquia. Pyrite concentrations in these formations range from 6 to 8 g kg<sup>-1</sup>. This pyrite occurs in close association with glauconite and can be found filling fissures in glauconite grains, as well as in the matrix as framboids, crystal clusters, and euhedral octahedral crystals (Fanning et al., 1993; Rabenhorst and Fanning, 1989). These pyrite concentrations are comparable to concentrations in the unoxidized portions of similar formations in the Mid-Atlantic Coastal Plain. In the Matawan and Monmouth formations these have been reported as 1.1% to 1.9% CRS, and in the Magothy Formation as 0.5% to 1.8% CRS (Rabenhorst and Valladares, 2005). These CRS values equate to 20 to 36 g kg<sup>-1</sup> pyrite in the Matawan and Monmouth formations, and 9 to 34 g kg<sup>-1</sup> pyrite in the Magothy Formation. Unoxidized Tertiary marine sediments of the Virginia Coastal Plain have been reported to contain 1.0% to 2.5% total-S (Orndorff, 2001). Assuming that this represents pyrite, these values equate to 19 to 47 g kg<sup>-1</sup> pyrite. Samples in each of these studies have been shown to generate extreme acidity when allowed to oxidize. The Mid-Atlantic Coastal Plain, including the Rhode River, is therefore a landscape where potential AS soils and potential AS soil materials are of great concern.

### 3.3 Methods and materials

Subaqueous soil profiles were sampled and described throughout the Rhode River estuary through use of bucket augers, Macaulay peat augers, and a vibracorer (Lanesky et al., 1979; Rabenhorst and Stolt, 2012). A total of 151 horizons were sampled from 25 pedons. Site and pedon locations are shown in Figure 3-1. Auger samples were described in the field and subsequently frozen before being thawed for laboratory analyses; vibracores were stored frozen from a couple weeks to several months before being opened for description and laboratory analyses. Standard US Soil Survey field methods were used to describe and horizonate soils. Descriptions included field texture, Munsell color, whiff test, 3% H<sub>2</sub>O<sub>2</sub> test for color change, 30% H<sub>2</sub>O<sub>2</sub> test for pyrite, fluidity class, description of redoximorphic features, and description of mineral or organic coarse fragments (Schoeneberger et al., 2012). A subset of samples that were suspected to contain metastable Fe sulfides (due to black color and color change with 3% H<sub>2</sub>O<sub>2</sub>) were treated with 10% HCl using the modified whiff test to confirm that H<sub>2</sub>S would be produced (none of these samples rated above zero on the unmodified whiff test prior to testing with HCl). After horizons were described, portions were sampled for pH measurements using a HI 98103 meter and for moist aerobic incubation via the US *Soil Taxonomy* method (Soil Survey Staff, 2014). Moist aerobic incubations continued until pH readings stabilized, 13-16 weeks. The remainder of each sample was frozen before conducting particle size analysis using the pipette method (Hillel, 2004) and organic carbon measurement using a LECO CN628 instrument after acidifying the samples using sulfurous acid to remove carbonate carbon (Balduff, 2007; Piper, 1942). Soil textural classes were

assigned using the US Department of Agriculture (USDA) soil triangle and particle size definitions (Soil Survey Staff, 2014).

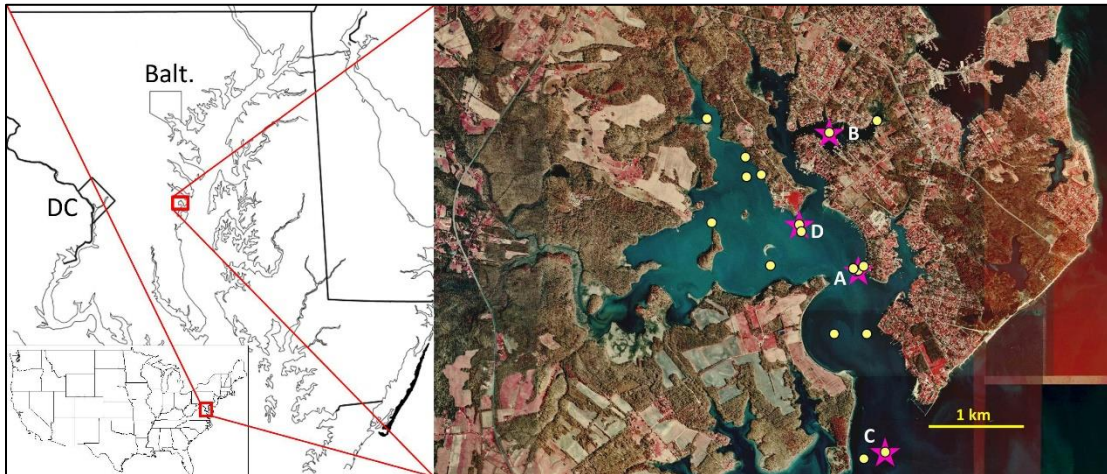


Figure 3-1. Location of Rhode River with sampled pedon locations. The Rhode River estuary is located on the western shore of the Chesapeake Bay in Maryland, USA. The red color indicates growing vegetation in the watershed (color IR image). The four starred pedons have been selected for more detailed explanation in section 3.4.2.

Subaqueous soil materials were classified in two ways. First, SAS materials were categorized into six distinct types based on properties observed in the field and recorded in descriptions: fluid muds, unconsolidated Holocene sandy materials, organic materials, buried A horizons, Tertiary materials with Fe oxide concentrations, and Tertiary materials without Fe oxide concentrations. These SAS material categories were developed for ease of field identification. The majority of SAS materials described in the Rhode River fall into one of these categories. Further, SAS materials were classified as hypersulfidic materials, hyposulfidic materials, and/or

monosulfidic materials, using the Australian definitions of these terms (though the minimum pH decrease of 0.5 units was waived for samples that indicated the presence of pyrite through reaction with 30% H<sub>2</sub>O<sub>2</sub>), based on their response to field tests and pH change during moist aerobic incubation. The relationship between soil material morphologic type and soil material as sulfide-containing material was then considered in order to aid soil surveyors in understanding the relative environmental hazards posed by these different types of materials as sulfide-containing materials.

### 3.4 Results and discussion

Each of the six SAS material types (fluid muds, unconsolidated Holocene sandy materials, organic materials, buried A horizons, Tertiary materials with Fe oxide concentrations, and Tertiary materials without Fe oxide concentrations) exhibited a range of morphological and chemical properties, including their propensity to undergo severe acidification during moist aerobic incubation. Descriptions and characterization data are available in Appendices B-E.

#### 3.4.1 SAS material types

##### 3.4.1.1 Fluid muds

Fluid muds are generally moderately to very fluid materials (in the past these have been described as having a high or very high n-value) with massive structure and textures of silty clay loam, clay loam, silty clay, clay, and rarely loam (loams tended to be located closer to eroding shorelines and may have received a slightly higher contribution of fluvial sand as a result) (Table 3-1). The properties and landscape positions of these materials were similar across these textures, and the

particle size distributions fit the definitions used by marine geologists, so the term “mud” is used in the technical sense to mean muds and modified muds as defined by the Folk classification (i.e. mud, sandy mud, slightly gravelly mud, and slightly gravelly sandy mud) (Folk, 1954). These texture classes are all less than 5% gravel and less than 50% sand. Extensive training in SAS texturing is not necessary for soil surveyors to be able to identify mud, whereas the field identification of more specific USDA soil textures within the muds may require special training (Balduff, 2007). Color is usually 10Y 2.5/1. Of a subset analyzed for organic carbon content, the range was 1.3-3.4%. These are mostly C horizons (and sometimes A horizons) found in deeper water, low energy environments and on landforms such as mainland coves, estuarine channels, and estuarine tidal creek channels (Schwartz, 1982) (Table 3-1). A and C horizons can sometimes be difficult to distinguish from one another in these SAS, though A horizons are usually more fluid and contain organic fragments or living macrofauna such as clams.



Table 3-1. Soil materials and their common morphological properties.

Si-silt/silty, C-clay, L-loam/loamy, S-sand/sandy, NF-nonfluid, SF-slightly fluid, MF-moderately fluid, VF-very fluid.

Material Type	Texture	Hue	Value	Chroma	Fluidity	Structure	Horizons	Landscape Units	% Organic Carbon
Fluid Mud	SiCL, CL, SiC, C, L	10Y, 5GY	2.5-3	0.5-1	MF-VF	Massive	Ase, Cse	Mainland Cove, Estuarine Channel, Estuarine Tidal Creek Channel	1.3-3.4
Holocene Sandy	S, LS, SL	5GY, N, 10Y, 5Y	2.5-5	1	NF-SF	Single Grain	Ase, Cg, Cse	Submerged Wave-Built Terrace, Submerged Wave-Cut Platform, Shoal	0.1-0.5
Organic	Muck, Mucky Peat	10YR, N	1-2	0-1	NF-VF	-	Oaseb, Oese	Submerged Tidal Marsh, Submerged Tidal Creek Platform, Submerged Tidal Creek Channel	41.5-48.9
Buried A	SL, L, LS, S	10Y, N	1-2.5	0-1	NF-MF	Massive, Single Grain	Aseb	Submerged Wave-Built Terrace, Submerged Wave-Cut Platform, Estuarine Tidal Creek Channel, Estuarine Channel, Submerged Tidal Marsh	2.3-3.6
Tertiary (-Fe conc.)	SCL, SL, S	10Y, 5GY	3-5	1-2	NF-SF	Massive	BCse, CB	Submerged Wave-Cut Platform, Estuarine Tidal Creek Platform	0.1-0.4
Tertiary (+Fe conc.)	SCL, SC, SL	10Y, 5GY, 10GY	3-5	1-2	NF-SF	Massive	Btse, Btsej, BCse	Submerged Wave-Cut Platform, Estuarine Tidal Creek Platform	0.1-0.4

Fifty two fluid muds were described (mostly as Cseg horizons), all of which showed some effervescence with 30%  $\text{H}_2\text{O}_2$ , indicating the presence of pyrite. Of these, only eight (15%) were shown to be hypersulfidic materials by moist aerobic incubation. Decrease in pH during moist aerobic incubation ranged from 0.6-4.6 pH units, with a median of 2.5 pH units (Table 3-2). Figure 3-2 shows a typical pH decrease in a hyposulfidic fluid mud. To determine the effect of shell fragments on these materials, they were further subdivided into two categories: fluid muds described with shell fragments (38 total), and fluid muds described without shell fragments (14 total). Fluid muds without shell fragments qualified as hypersulfidic materials in 21% of the samples tested, but fluid muds that contained shell fragments (observable in a hand sample) classified as hypersulfidic materials in only 13% of the samples tested (Table 3-2). This suggests that shell fragments may provide a greater neutralization potential to remove generated acidity, consistent with our understanding of acid-base accounting (Ahern et al., 2004). Shell fragments in SAS do react to changes in their pH environment, and mass losses of up to 24% shell in 29 days have been observed in Rhode Island coastal lagoons (Still and Stolt, 2015). Additional buffering is likely linked to the high clay content of these soils, reflected in their textures (Table 3-1). Thirty samples (58%) qualified as monosulfidic materials (Table 3-2). Metastable Fe sulfides were invariably present at the soil surface and occasionally extended to depths of nearly 2 meters into the soil (Table 3-4, Cse3 horizon and Table 3-5, Cse2 horizon), evidenced by immediate color change with the addition of 3%  $\text{H}_2\text{O}_2$ .

Table 3-2. Soil materials as sulfide-containing materials. Selected categories of soil materials and their occurrence as sulfidic materials. Percentages are percent of the Material Type samples that meet the requirements for that column. The 3 non-sulfidic Holocene sandy materials are included in Samples but not elsewhere.

Material Type	Samples	$\Delta$ pH range (median)	Hypersulfidic	Hypo-sulfidic	Mono-sulfidic	H <sub>2</sub> S Odor	30% H <sub>2</sub> O <sub>2</sub> Reaction	Hypersulfidic without shell	Hypersulfidic with shell
Fluid Mud	52	0.6-4.6 (2.5)	8 (15%)	44	30	0	52	3 (21%)	5 (13%)
Holocene Sandy	54	0.0-4.9 (2.2)	13 (25%)	38	19	2	49	8 (24%)	5 (23%)
Organic	9	0.9-4.6 (1.6)	4 (44%)	5	0	4	4	-	-
Buried A	9	1.0-5.0 (4.4)	6 (67%)	3	2	0	9	-	-
Tertiary (-Fe conc.)	7	0.0-3.9 (1.2)	2 (29%)	5	0	0	7	-	-
Tertiary (+Fe conc.)	20	0.0-3.8 (1.4)	2 (10%)	18	1	0	18	-	-

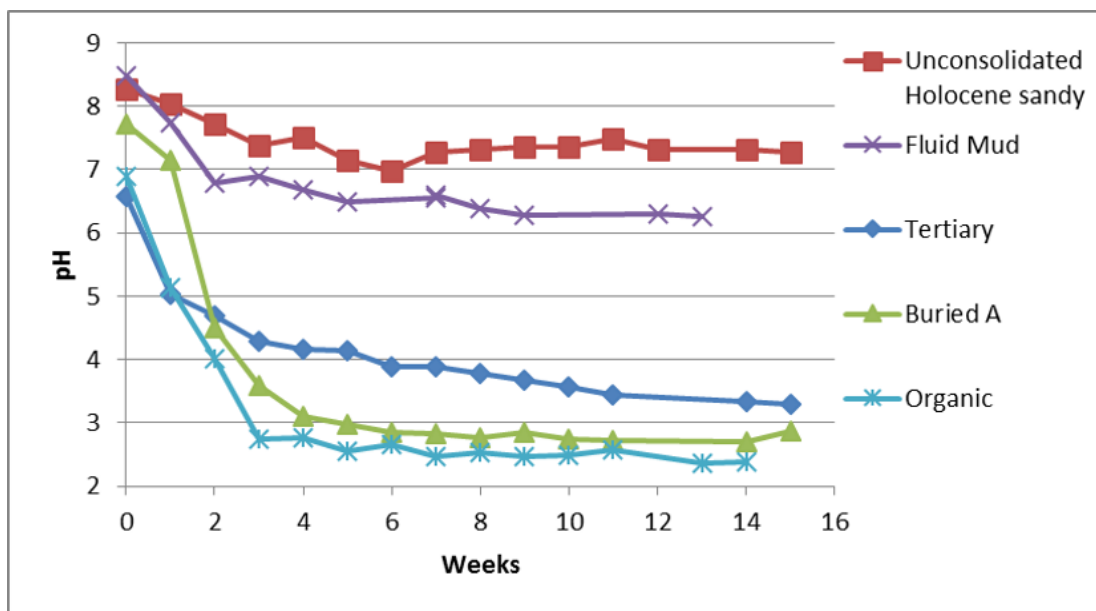


Figure 3-2. Moist aerobic incubation of selected materials. The fluid mud shows some drop in pH, but not below 4.0, and is an example of hyposulfidic material. The sandy material may not be sulfidic material, though a very small decrease in pH was seen (perhaps from the oxidation of organic matter). The selected Tertiary, buried A, and organic materials are all hypersulfidic materials. Note the early drop in pH in many samples, which is the result of the fast oxidation of monosulfide minerals.

#### 3.4.1.2 Unconsolidated Holocene sandy materials

Unconsolidated Holocene sandy materials are nonfluid or sometimes slightly fluid materials with single grained structure and textures ranging from gravelly coarse sand to fine sandy loam. Greater color variation was observed in these materials, from N 2.5 to higher value yellow hues (Table 3-1). Some pedons contained finely stratified materials with lenses or fine strata showing slight variations in texture and color over distances of several millimeters. Organic carbon contents are low, 0.1-0.5%. These materials usually constituted C or A horizons in shallower, higher energy environments such as shoals, submerged wave-built terraces, and the upper portions of submerged wave-cut platforms and estuarine tidal creek platforms (Schwartz, 1982) (Table 3-1).

Unconsolidated Holocene sandy materials accounted for 54 samples, 13 of which were hypersulfidic materials (24%). Nineteen (35%) of these materials were black and changed color on addition of 3%  $\text{H}_2\text{O}_2$  indicating these black horizons were monosulfidic materials. In the unconsolidated Holocene sandy materials, monosulfidic materials did not always occur at the surface, though they did occasionally extend to over a meter in depth. Some surface sands were light brown or gray colors instead of black, and these generally exhibited zero to little pH change. Considering all unconsolidated Holocene sandy materials, decreases in pH ranged from 0.0-4.9 pH units with a median of 2.2 pH units (Table 3-2).

There is no lower limit on the pH drop necessary to classify hyposulfidic materials using the WRB definition, so there is a risk of misinterpreting a small pH change as being caused by the oxidation of sulfides, when in fact it may be due to

organic matter decomposition. Decomposing organic matter can release organic acids (Hartley and Buchan, 1979) and ammonium (Weil and Brady, 2016), which can subsequently generate acidity by releasing protons during nitrification (Bolan et al., 1991; Rodriguez et al., 2008). It should be noted that this process can either raise or lower soil pH, with the outcome depending on nitrogen and cation content of the organic matter that is decomposing (Pocknee and Sumner, 1997). Most sandy materials, however, did show some effervescence with 30% H<sub>2</sub>O<sub>2</sub>, indicating the presence of sulfides (Table 3-2). Where such light-colored sandy materials did not indicate the presence of sulfides through odor, testing with H<sub>2</sub>O<sub>2</sub> (3% or 30%), or extreme acidification (generally to a pH less than or equal to 4.0) they were assumed to be non-sulfidic material; Figure 3-2 shows the pH decrease of one such sample that is typical of material that is difficult to identify as hyposulfidic material without S measurements. Some soil materials that did not effervesce when 30% H<sub>2</sub>O<sub>2</sub> was added were nonetheless shown to be hypersulfidic material (Table 3-3, Cseg3 horizon), emphasizing the importance of completing moist aerobic incubations.

Table 3-3. Core A – Unconsolidated Holocene sandy materials with a buried A horizon.

Fluventic Psammowassent ( <i>Soil Taxonomy</i> )			
Monohypersulfidic Subtidal Hydrosol ( <i>Australian Soil Classification</i> )			
1.1 m water depth, S <sub>p</sub> =14. Sampled 17 August 2015 from a submerged wave-built terrace with a bare sand bottom.			
Horizon	Depth (cm)	Description	Sulfidic Material
Aseg	0-24	Nonfluid fS, 5Y 4/1, contains a 10Y 2.5/0.5 krotovina, abrupt lower boundary. Very slightly effervescent with 30% H <sub>2</sub> O <sub>2</sub> .	Mono, Hypo
Cg	24-44	Nonfluid fS, 2.5Y 6/2, 15% clam shell fragments, clear lower boundary. No reaction with H <sub>2</sub> O <sub>2</sub> .	None
Cseg1	44-120	Nonfluid fS, 2.5Y 4/1, gradual lower boundary. Very slightly effervescent with 30% H <sub>2</sub> O <sub>2</sub> .	Hypo
Cseg2	120-153	Nonfluid fS, 10Y 4/1, clear lower boundary. Very slightly effervescent with 30% H <sub>2</sub> O <sub>2</sub> .	Hyper
Cseg3	153-212	Nonfluid LfS, 5GY 4/1, 3% plant fragments, abrupt lower boundary. No reaction with H <sub>2</sub> O <sub>2</sub> but pH dropped 8.0 to 3.6.	Hyper
Aseb	212-218	Nonfluid LfS, 10Y 3/1, 15% root fragments and trace shell fragments, abrupt lower boundary. Very slightly effervescent with 30% H <sub>2</sub> O <sub>2</sub> .	Hyper
C'seg	218-239	Nonfluid fS, 10Y 4/1, faint H <sub>2</sub> S odor. No reaction with H <sub>2</sub> O <sub>2</sub> .	Hyper



#### 3.4.1.3 Organic materials

Organic materials were usually mucks (Oa horizons) and sometimes mucky peats (Oe horizons). Buried O horizons were often overlain with fluid mud horizons (Table 3-4), but occasionally O horizons occurred as surface horizons along the edges of submerged tidal marshes. Organic materials were generally 10YR 2/1 and nonfluid to very fluid. Organic carbon contents ranged from 41.5-48.9%. Organic materials were found in landforms including submerged tidal marshes, estuarine tidal creek platforms, and estuarine tidal creek channels (Table 3-1).

Nine organic horizons were sampled, of which four were hypersulfidic materials (44%). Decrease in pH during moist aerobic incubation ranged from 0.9-4.6 pH units, with a median decrease of 1.6 pH units (Table 3-2). When these samples did undergo extreme acidification, it generally occurred within the first 2-3 weeks of moist aerobic incubation (Figure 3-2). None of these organic materials were considered monosulfidic materials, although any color change that would occur to indicate the presence of monosulfide minerals may be masked by the black colored organic materials that stain these horizons. Four of these horizons did contain odoriferous  $\text{H}_2\text{S}$ , indicating an excess in the porewater and a lack of labile and available (e.g. not occluded) Fe oxides, which would otherwise react to remove the  $\text{H}_2\text{S}$ . One of these four effervesced very slightly with 30%  $\text{H}_2\text{O}_2$ , as did three other organic samples that were scored as zero using the whiff test.

Table 3-4. Core B – Fluid muds, buried surfaces, and Tertiary materials.

Grossic Hydrowassent ( <i>Soil Taxonomy</i> )			
Monohyposulfidic Subtidal Hydrosol ( <i>Australian Soil Classification</i> )			
1.9 m water depth, S <sub>p</sub> =16. Sampled 19 August 2015 from an estuarine tidal creek channel with a bare mud bottom.			
Horizon	Depth (cm)	Description	Sulfidic Material
Ase1	0-27	Very fluid SiL, N 2.5, trace shell fragments, gradual lower boundary. Violently effervescent with 30% H <sub>2</sub> O <sub>2</sub> .	Mono, Hypo
Ase2	27-45	Very fluid SiCL, N 2.5, trace shell fragments, gradual lower boundary. Violently effervescent with 30% H <sub>2</sub> O <sub>2</sub> .	Mono, Hypo
Cse1	45-87	Moderately fluid SiC, 5GY 2.5/0.5, 3% shell fragments, gradual lower boundary. Violently effervescent with 30% H <sub>2</sub> O <sub>2</sub> .	Mono, Hypo
Cse2	87-142	Very fluid SiCL, 5GY 2.5/0.5, gradual lower boundary. Violently effervescent with 30% H <sub>2</sub> O <sub>2</sub> .	Mono, Hypo
Cse3	142-201	Moderately fluid SiC, 10Y 2.5/1, clear lower boundary. Violently effervescent with 30% H <sub>2</sub> O <sub>2</sub> .	Mono, Hypo
Oaseb	201-221	Nonfluid muck, 10YR 1/1, 5% root fragments, very abrupt lower boundary. Very slightly effervescent with 30% H <sub>2</sub> O <sub>2</sub> .	Hyper
2Cse	221-224	Nonfluid S, 5Y 3/0.5, 5% rounded quartz gravels, abrupt lower boundary. Very slightly effervescent with 30% H <sub>2</sub> O <sub>2</sub> .	Hyper
3Aseb	224-233	Nonfluid mucky SL, 10YR 1/1, clear lower boundary. Very slightly effervescent with 30% H <sub>2</sub> O <sub>2</sub> .	Hyper
3Cseg	233-257	Nonfluid S, 5GY 4/2, clear lower boundary. Violently effervescent with 30% H <sub>2</sub> O <sub>2</sub> .	Hypo
4Btseb	257-269	Nonfluid SCL, 5GY 4/2, contains 15% 10YR 3/4 iron concentrations and trace root fragments, gradual lower boundary. Violently effervescent with 30% H <sub>2</sub> O <sub>2</sub> .	Hypo
4Btseb	269-300	Nonfluid C, 5G 3/2, contains 7% 10YR 3/4 iron concentrations and 3% root fragments. Extremely violently effervescent with 30% H <sub>2</sub> O <sub>2</sub> .	Hypo
Note the 4Btse horizons were interpreted to be from paleosols formed within Tertiary materials, probably of the Nanjemoy formation, during a period of subaerial exposure.			

#### 3.4.1.4 Buried A horizons

Buried A horizons were sandy loams, loams, loamy sands, and sands. They were generally black in color, stained the hands, and often contained preserved roots or root channels (Table 3-3, Aseb horizon). Organic carbon content ranged from 2.3-3.6%, similar to the fluid muds. They were nonfluid to moderately fluid, contained massive or single grain structure, and were usually described as Aseb horizons. They were found on a variety of landforms including submerged wave-cut platforms, submerged wave-built terraces, estuarine tidal creek channels, estuarine channels, and submerged tidal marshes (Table 3-1).

All nine buried A horizons effervesced when 30%  $\text{H}_2\text{O}_2$  was added, indicating the presence of sulfide minerals (Table 3-2). Six of these were hypersulfidic materials (pH dropped below 4) and two of the remaining three buried A horizons changed color with 3%  $\text{H}_2\text{O}_2$  and were considered monosulfidic materials. Decrease in pH upon moist aerobic incubation ranged from 1.0-5.0 pH units, with a median value of 4.4 pH units (Table 3-2), making these materials the most concerning (from an acid sulfate perspective) of all material types considered. Like organic materials, acidification generally occurred within 2-3 weeks of moist aerobic incubation (Figure 3-2).

#### 3.4.1.5 Tertiary materials with and without Fe oxide concentrations

Tertiary materials were identified by an abundance of green glauconite, were generally nonfluid to slightly fluid, and commonly had textures of sandy clay loam, sandy loam, or sandy clay. Several Tertiary material horizons without Fe oxide concentrations were sands. Hues were commonly 10Y or 5GY, with values ranging

from 3-5 and chromas from 1-2. Tertiary materials with Fe oxides also sometimes had hues of 10GY. Organic carbon contents ranged from 0.1-0.4% in both types of Tertiary materials. Tertiary materials were commonly found on landforms including submerged wave-cut platforms and estuarine tidal creek platforms (Table 3-1). Nonfluid Tertiary materials were distinctively dense relative to other materials described in this study, and were more difficult to sample. Efforts at vibracoring in these materials were generally not successful (usually not more than 10 or 20 cm could be collected) so that bucket augering was typically needed.

Tertiary materials were divided into two classes based on the presence or absence of field-observable Fe oxide concentrations. These Fe oxides do not form in the subaqueous environment; they are inherited from soils formed in these materials when sea-level stands were lower. The Tertiary materials that were examined in this survey all began as marine sediment parent materials, evidenced by the glauconite pellets that they contain, which form exclusively in marine environments and have previously been described in the Mid-Atlantic region (Fanning et al., 2010; Fanning et al., 1989; Wagner, 1982). These materials were exposed by a drop in relative sea-level (Kraft and Belknap, 1986) before undergoing pedogenesis in a subaerial environment. This subaerial pedogenesis is evidenced by the presence of Fe concentrations, typically as soft masses (Table 3-4 and Table 3-6), which do not form in the subaqueous environment (Vepraskas and Craft, 2016). The landscape was subsequently re-submerged by a rise in relative sea-level (Fairbanks, 1989) that in some cases also eroded (truncated) the subaerial topsoil before burying the erosional surface under a layer of Holocene sediments, as evidenced by the commonly

observed contact between Holocene materials (unconsolidated sands and fluid muds) and buried B horizons (Table 3-4 and Table 3-6). Similar submerged and buried upland soils have previously been described in the coastal bays of Maryland (Balduff, 2007; Demas, 1998). All Tertiary horizons examined had undergone some oxidation, indicated by Fe oxides in some samples and by the green color in others, and were described as B, BC, or CB horizons based on the development of pedogenic features (such as color changes, Fe oxide and jarosite concentrations, and clay illuviation) that had occurred in them (Table 3-1). Unoxidized Tertiary materials in the subaerial environment are generally gray and contact the overlying B, BC, and CB horizons in an abrupt contact (Rabenhorst and Valladares, 2005). Such materials were observed in several locations throughout the Rhode River, but due to their firm consistence and depth in the profile, not enough could be collected to conduct analyses. Consistence was not measured because it requires intact peds, special tools, or an open soil pit (Schoeneberger et al., 2012), none of which was available at the time these materials were discovered. Because consistence measures the ability of soil material to resist deformation, and only a few scrapings of this material could be collected through use of a hand auger, we conclude that this soil material has a firm consistence. The small amounts recovered were enough to complete field tests and descriptions, which were consistent with previous descriptions of unoxidized Tertiary materials below the oxidized zone-unoxidized zone boundary (Rabenhorst and Valladares, 2005).

Tertiary materials nearly always reacted with 30%  $\text{H}_2\text{O}_2$ , though only one sample of the 27 examined reacted with 3%  $\text{H}_2\text{O}_2$  to qualify as monosulfidic material. This monosulfidic Tertiary horizon was moderately fluid and began at 19 cm, directly

below a scour-lag surface horizon of unconsolidated Holocene sandy material, suggesting that it had been influenced and perhaps partially reworked by wave action. The metastable Fe sulfides that it contains are therefore likely Holocene aged rather than inherited from the Tertiary parent material. In the Tertiary samples,  $\text{H}_2\text{O}_2$  reactions were generally more violent than those seen with the other types of materials considered. Tertiary materials that did not contain Fe oxide concentrations were more often hypersulfidic materials than those that did contain Fe oxide concentrations. Those with Fe oxides were at least partially oxidized at some point, though do contain unoxidized sulfides. While the presence of CRS has been reported in some subaerial soils above the boundary with the unoxidized zone, it is uncommon and the concentrations are lower than in the underlying material (Rabenhorst and Valladares, 2005).

It is more likely that all of the sulfides present in the Tertiary materials that were collected from above the oxidized zone-unoxidized zone boundary have formed since re-submergence. Sulfide formation since re-submergence would occur if  $\text{H}_2\text{S}$  diffused into this Tertiary material from overlying horizons and reacted with Fe oxides to form Fe sulfides, a process that occurs on a scale of minutes to hours when Fe oxides are inserted into soils in which sulfur reduction is taking place (Rabenhorst and Burch, 2006; Rabenhorst et al., 2010). Initially, metastable Fe sulfides may be formed, but over time they can react with additional  $\text{H}_2\text{S}$  to form pyrite (Rickard, 1997; Rickard and Luther, 1997). Tertiary materials that do not contain Fe oxide concentrations likely still have been oxidized at some point, because they do not occur below an abrupt boundary and they do not match the black or dark gray color

expected for completely unoxidized Tertiary materials (as they are observed in the upland environment) (Rabenhorst and Valladares, 2005). It may be that some Tertiary materials that do not contain Fe oxides once did contain them, and that they have all since reacted to form Fe sulfides. This would be consistent with the observation that Tertiary materials without Fe oxides were more commonly observed to be hypersulfidic materials than were Tertiary materials with Fe oxides.

Of the seven Tertiary materials without Fe oxide concentrations, 29% were hypersulfidic materials. In these seven samples, the decrease in pH on moist aerobic incubation ranged from 0.0 to 3.9 pH units, with a median value of 1.2 pH units. Tertiary materials of both types acidified slowly, taking approximately 6 weeks to classify as hypersulfidic materials (for those that did) and continuing to slowly acidify for several more weeks (Figure 3-2). Of the 20 Tertiary materials with Fe oxide concentrations, 10% were hypersulfidic materials. In these 20 samples, the decrease in pH on moist aerobic incubation ranged from 0.0 to 3.8 pH units, with a median value of 1.4 pH units (Table 3-2). Even some Tertiary materials that exhibited no change in pH during moist aerobic incubation did react with 30%  $\text{H}_2\text{O}_2$ , indicating the presence of pyrite. While Tertiary materials did not contain shell fragments, their high clay content and high initial pH (~8.0) (which indicates the influence of  $\text{CaCO}_3$ ) give them neutralization potential (as a result of carbonates reacting to neutralize formed acidity) and buffering capacity (as a result of the CEC of high base saturated clays and organic matter) to resist acidification. Thus, despite the indications of the presence of Fe sulfides from reaction with 30%  $\text{H}_2\text{O}_2$ , most Tertiary materials of both types were hyposulfidic materials (Table 3-2).

### 3.4.2 Example profiles containing potential AS soil materials

#### 3.4.2.1 Core A – Unconsolidated Holocene sandy materials with a buried A horizon

This pedon (Table 3-3) is classified as a Fluventic Psammowassent in *Soil Taxonomy*, a Monohypersulfidic Subtidal Hydrosol in the *Australian Soil Classification*, and an Orthofluvic Reductigleyic Subaquatic Gleysol (Hyposulfidic) in the WRB. The *Soil Taxonomy* name does not describe the AS soil materials in this pedon, the *Australian Soil Classification* name describes both monosulfidic materials and hypersulfidic materials by including the combined term “Monohypersulfidic,” and the WRB classification describes the hyposulfidic materials in the pedon. Note that the WRB overlooks the presence of hypersulfidic materials in this pedon because they occur below 100 cm in the profile and must occur above this threshold for a soil to receive “Hypersulfidic” in its name; on the other hand, the *Australian Soil Classification* uses a depth threshold of 150 cm, and the presence of hypersulfidic materials supersedes the presence of hyposulfidic materials in the soil name. Like most of the sandy materials examined, the horizons of this pedon showed little if any reaction with 30% H<sub>2</sub>O<sub>2</sub>. Only the buried A horizon and the horizons around it acidified enough during moist aerobic incubation to classify as hypersulfidic materials. This buried A horizon was easily identified by its dark color and the presence of preserved roots. The underlying horizon, C’seg, smelled of H<sub>2</sub>S, though it did not change color with the addition of 3% H<sub>2</sub>O<sub>2</sub>. This indicates that an excess of soluble H<sub>2</sub>S is present in this horizon, beyond what could be removed by reaction with reactive forms of Fe oxides or metastable Fe sulfides to form pyrite. The Cg horizon did not smell of H<sub>2</sub>S or react with either concentration of H<sub>2</sub>O<sub>2</sub>, and it did not



acidify during moist aerobic incubation. It is therefore one of only three horizons sampled that was not sulfidic material of any sort, and this is typical of what would be expected for very low-Fe materials that are unable to form Fe sulfides. All three such horizons were light yellow or brown and consisted of unconsolidated Holocene sandy materials.

It is possible that the excess accumulation of Fe sulfides in the several horizons above the buried A horizon, and the horizon immediately below, are due to the translocation of porewater sulfides and subsequent formation of Fe sulfide minerals as H<sub>2</sub>S diffused from the organic-rich buried A horizon. Sulfate reduction rates in this horizon would be enhanced by the high organic matter content (Berner, 1985; Westrich and Berner, 1984). Because this and other vibracore samples were generally stored frozen for up to several months before opening, it is possible that H<sub>2</sub>S was present throughout other areas of the profile and that it was able to escape during storage.

#### 3.4.2.2 Core B – Fluid muds, buried surfaces, and Tertiary materials

This pedon (Table 3-4) classifies as a Grossic Hydrowassent in *Soil Taxonomy*, a Monohyposulfidic Subtidal Hydrosol using the *Australian Soil Classification*, and an Orthofluvic Reductigleyic Subaquatic Gleysol (Clayic, Ochric, Limnic, Hyposulfidic) using the WRB. The *Soil Taxonomy* name does not describe AS soil materials in this pedon, the *Australian Soil Classification* name describes both monosulfidic materials and hyposulfidic materials by including the combined term “Monohyposulfidic,” and the WRB name describes hyposulfidic materials. Because samples were collected to a depth of 3 m at this site, it contains a number of

different materials below the fluid muds typically found in deeper water. The buried O and A horizons, as well as a thin layer of sand that separates them, are hypersulfidic materials. All horizons showed some pH drop upon moist aerobic incubation, with the majority of the change occurring in the first two weeks. Samples from the top 60 cm dropped from initial pH values of near 7.5 to final values near 5.0. Most samples through the deeper portion of the profile dropped from an initial pH of 8.0-8.5 to a final pH of 6.5-7.0. Such changes demonstrate the net production of some acidity in these samples, but not to an extent that would be likely to cause the dire environmental impacts associated with the exposure of hypersulfidic materials.

These fluid muds are also monosulfidic materials throughout (indicated by color change upon addition of 3%  $\text{H}_2\text{O}_2$ ), to a depth of 2 m. Despite their violently effervescent reactions with 30%  $\text{H}_2\text{O}_2$ , they either did not contain a sufficient concentration of sulfide minerals to acidify to a pH of 4.0 or lower, or they were buffered against this pH drop. Shell fragments were sparse in these horizons and missing entirely from several of them, suggesting that the clay may be playing a large role in buffering these materials. These fluid mud samples are thus hyposulfidic materials, which is unsurprising considering that only 15% of fluid muds examined were hypersulfidic materials. The buried Tertiary materials at the bottom of this core have been partially oxidized, demonstrated by the presence of Fe oxides and decomposed root fragments. These materials are Tertiary age marine sediments that were exposed in the subaerial environment at some point in their history, and at that point underwent oxidation and pedogenesis to create the redoximorphic features now present, before being submerged by further changes in relative sea-level. These

Tertiary samples reacted violently with 30%  $\text{H}_2\text{O}_2$ , and the bottom horizon (4Btseb) exhibited one of the strongest reactions seen in all of the materials examined, increasing to a point of steadily producing steam from a boiling slurry with no added source of heat. Though Fe oxides are present in this horizon, it seems likely that the concentration was once higher and some portion of the relict Fe has reacted with  $\text{H}_2\text{S}$  to form pyrite (Rabenhorst and Burch, 2006; Rabenhorst et al., 2010). Despite this indication of the presence of pyrite, these materials classify as hyposulfidic materials.

#### 3.4.2.3 Core C – Fluid muds

This pedon (Table 3-5) was collected from the mouth of the Rhode River estuary in 3-4 m of water. It classifies as a Grossic Hydrowassent in *Soil Taxonomy*, a Monohyposulfidic Subtidal Hydrosol in the *Australian Soil Classification*, and an Orthofluvic Reductigleyic Subaquatic Gleysol (Loamic, Ochric, Limnic, Hyposulfidic) using the WRB (though similar pedons would be described as Clayic instead of Loamic). The *Soil Taxonomy* name does not describe the AS soil materials in this pedon, the *Australian Soil Classification* name describes both monosulfidic materials and hyposulfidic materials, and the WRB classification describes the hyposulfidic materials in the pedon. Due to the relative homogeneity of the soil morphology, the pedon was divided into 15 sections, each 10 cm thick, for  $\text{H}_2\text{O}_2$  testing and moist aerobic incubation. No “hidden” horizons were discovered with this approach. Like most other fluid muds (85%), samples acidified but not enough to classify as hypersulfidic materials. Monosulfidic materials were identified throughout the profile, evidenced by color change from greenish black to lighter brown upon the addition of 3%  $\text{H}_2\text{O}_2$ . The strength of the effervescence from adding the 30%  $\text{H}_2\text{O}_2$

decreased slightly below 1 m, but all samples were at least strongly effervescent. The materials throughout this pedon are therefore considered to be hyposulfidic in addition to being monosulfidic.

Table 3-5. Core C – Fluid muds.

Grossic Hydrowassent ( <i>Soil Taxonomy</i> )			
Monohyposulfidic Subtidal Hydrosol ( <i>Australian Soil Classification</i> )			
3.9 m water depth, Salinity-16. Sampled 21 August 2015 from the estuarine channel at the mouth of the Rhode River with a bare muddy bottom.			
Horizon	Depth (cm)	Description	Sulfidic material
Ase	0-31	Very fluid SiCL, 5GY 2.5/1, trace shell fragments, diffuse lower boundary. Violently effervescent with 30% H <sub>2</sub> O <sub>2</sub> .	Mono, Hypo
Cse1	31-106	Very fluid SiCL, 5GY 2.5/0.5, trace shell fragments, diffuse lower boundary. Violently effervescent with 30% H <sub>2</sub> O <sub>2</sub> .	Mono, Hypo
Cse2	106-150	Very fluid SiC, 5GY 3/1, trace shell fragments. Strongly effervescent with 30% H <sub>2</sub> O <sub>2</sub> .	Mono, Hypo

#### 3.4.2.4 Core D – Sandy materials over Tertiary materials

This pedon (Table 3-6) classifies as an Aerice Fluviassent in *Soil Taxonomy* due to the presence of a slightly fluid horizon between 20 and 50 cm, though similar profiles are classified as Haplic Sulfiassents if nonfluid hypersulfidic horizons extend into this range. It is a Monohyposulfidic Subtidal Hydrosol in the *Australian Soil Classification* and classifies as a Subaquatic Reductic Gleysol (Hyposulfidic) in the WRB. The *Soil Taxonomy* name does not describe the AS soil materials in this pedon, the *Australian Soil Classification* name describes both monosulfidic materials and hyposulfidic materials, and the WRB classification describes the hyposulfidic materials in the pedon. These types of profiles are commonly seen in relatively shallow high-energy environments in the Rhode River estuary, on landforms that include mainland coves, estuarine channels, and estuarine tidal creek channels (Schwartz, 1982). The top consists of a layer of unconsolidated Holocene sandy scour-lag deposits, which are located directly above partially oxidized Tertiary

horizons. The Tertiary horizons in this pedon all contain Fe oxides, though this is not always the case in similar pedons. Density increases dramatically with depth in these samples and they are generally sampled to a point of refusal, from which no additional samples can be collected using hand tools. The sandy materials at the surface are often monosulfidic materials, though the Tertiary materials are not. In contrast to the behavior of many fluid mud profiles examined, successive Tertiary horizons generally demonstrated an increasing trend of effervescence with 30% H<sub>2</sub>O<sub>2</sub> with depth. In this pedon, Tertiary materials are strongly effervescent higher in the profile and violently effervescent at the bottom. Again, this reaction does not predict the presence of hypersulfidic materials, only the presence of sulfides. The grey colors in the 2BCseg horizon may have formed since submergence, evidenced by the brighter colors in the underlying 2BCse horizon. All horizons in this pedon classify as hyposulfidic materials.

Table 3-6. Core D – Sandy materials over Tertiary materials.

Aeric Fluviwasset ( <i>Soil Taxonomy</i> )			
Monohyposulfidic Subtidal Hydrosol ( <i>Australian Soil Classification</i> )			
1.4 m water depth, Salinity-16. Sampled 21 August 2015 from a submerged wave-cut platform with a bare sandy bottom.			
Horizon	Depth (cm)	Description	Sulfidic Material
Ase	0-25	Nonfluid S, 5GY 2.5/1, trace shell fossils, abrupt lower boundary defined by a 1 cm layer of clam shells. Slightly effervescent with 30% H <sub>2</sub> O <sub>2</sub> .	Mono, Hypo
2Btseg	25-58	Slightly fluid CL, 10Y 4/1, 3% root fragments lined with 10YR 3/3 iron concentrations, abrupt lower boundary. Strongly effervescent with 30% H <sub>2</sub> O <sub>2</sub> .	Hypo
2BCseg	58-70	Nonfluid SCL, 10GY 4/1, 30% 10YR 3/3 iron concentrations as soft masses, clear lower boundary. Violently effervescent with 30% H <sub>2</sub> O <sub>2</sub> .	Hypo
2BCse	70-78	Nonfluid SCL, 2.5Y 4/3, 45% 7.5YR 2.5/3 iron concentrations and 5% 10GY 4/1 depletions as soft masses. Violently effervescent with 30% H <sub>2</sub> O <sub>2</sub> .	Hypo

### 3.5 Conclusions

The three recognized types of AS soil materials are all present in the Rhode River subestuary. Conclusively distinguishing all of these materials from one another in the field using standard Soil Survey methods is therefore important in this and similar settings, but it is not possible at present. However, categorizing the materials in a given landscape into several types does offer some guidance when attempting to identify sulfidic materials. In the Rhode River estuary, organic horizons and buried A horizons are more commonly associated with hypersulfidic materials than are other types of materials. Mineral horizons adjacent to buried O and A horizons also appear more likely to be hypersulfidic materials. Tertiary materials, particularly those without Fe oxides, are also more commonly hypersulfidic materials. Other materials

cannot be ruled out as hypersulfidic materials until moist aerobic incubations are completed on them, though it is very unlikely that brown to yellow sands that exhibit no reaction with 30%  $\text{H}_2\text{O}_2$  are hypersulfidic materials. The presence of shell fragments or Fe oxides may indicate that a horizon is less likely to consist of hypersulfidic material.

Monosulfidic materials are present in nearly all surface horizons throughout the estuary, and may or may not also be hypersulfidic or hyposulfidic materials. Free  $\text{H}_2\text{S}$ , detected by odor, can generally only accumulate in a soil horizon if there is a lack of reactive Fe (such as Fe oxides) that would otherwise react to consume  $\text{H}_2\text{S}$  and generate Fe sulfides. Due to microsite heterogeneity, Fe oxides may still exist in these soil materials but remain unavailable to react with  $\text{H}_2\text{S}$ . The presence of  $\text{H}_2\text{S}$  provides no information about the concentration of Fe sulfides, it only indicates ongoing sulfur reduction and demonstrates that reactive Fe oxides are unlikely to remain in the horizon, if there ever were any. There seems to be little if any relationship between the reaction with 30%  $\text{H}_2\text{O}_2$  and hypersulfidic materials, because this test cannot account for neutralization potential (as is provided by carbonates) and buffering capacity (as is provided by high CEC clays and organic matter). Materials with low neutralization potential and buffering capacity may not contain enough sulfide-S to produce a noticeable reaction with 30%  $\text{H}_2\text{O}_2$ , but may yet acidify enough to classify as hypersulfidic materials, or alternatively they may not acidify at all. This, and the fact that there are additional sources of soil acidity (such as decomposing organic matter), makes it difficult to identify hyposulfidic materials without directly measuring their sulfur concentration. Sulfide-containing materials of



various sorts are nearly ubiquitous in these estuarine SAS, and their categorization by morphologic properties can be useful in predicting which soil materials are more likely to pose environmental hazards if disturbed, but the use of quick and simple field methods to classify these soil materials as types of sulfidic materials remains a challenge.

## Chapter 4: Environmental consequences of polygenetic pedogenesis following the restoration of reclaimed land via flooding with fresh and marine water in Gyldensteen Strand, Denmark

### 4.1 Abstract

The impacts of land reclamation via drainage are relatively well understood, but the impacts of inundation due to sea-level rise have only recently become a topic of scientific inquiry. In this study four landscapes were sampled and characterized in a Danish coastal environment: shallow marine sediments from a permanently submerged shoreface, soils from reclaimed land used for ~150 years for agriculture, submerged soils from a two year old constructed lake over reclaimed land, and submerged soils from a two year old restored coastal lagoon over reclaimed land. Land reclamation causes previously submerged land to undergo pedogenesis by forming soil structure, decreasing pH, accumulating organic matter in the surface, and forming soil colors as a result of mineralogical changes (among a variety of other changes). Land submergence reverses these processes, but increases the formation of reduced sulfur and iron in the soil surface beyond levels found in shallow marine sediments, likely due to the presence of organic carbon and more bioavailable forms of iron oxides accumulated during the period of land reclamation. Changes in the subsoil were minimal after two years, with upland soil structure and color well preserved. This suggests that land submergence by sea-level rise will not simply convert upland soils into shallow marine sediments, but will be accompanied by intense alterations of biogeochemical cycles that may continue for substantially

longer than several years as pedogenic carbon and minerals supply abundant reactants for redox reactions under the new environmental conditions. Some subsoil features may represent a lasting legacy of environmental history, persisting through geologic time.

#### 4.2 Introduction

The climate on Earth is warming and the seas are rising in most parts of the world, which forces coastal communities to plan adaptation strategies for reducing the consequences of these changes (Center for Naval Analysis, 2007; IPCC, 2014). One climate change adaptation strategy that has become increasingly common over the last few decades is managed realignment (Wolters et al., 2005). During managed realignment, areas of low-elevation land near coasts that are threatened by climate change are identified for preemptive restoration or conversion to a novel habitat such as a lake or engineered wetland (Stumpner et al., 2018). Such low-lying areas commonly consist of reclaimed land<sup>3</sup> used for agriculture in some parts of the world, which is created by artificially draining wetlands or shallow seafloors and protecting the area with dikes or levees (Martin-Anton et al., 2016). These lands are at increasing risk of catastrophic flooding due to sea-level rise and increasing storm

---

<sup>3</sup> The term reclaimed land is also used to refer to areas of landfill that create new subaerial land in bodies of water, as well as remediated mine land and other remediated land that had been drastically degraded. The term polder has been used to refer to areas of reclaimed land as defined here, but is not widely used in Denmark where this study was conducted.

intensity which can undermine, overtop, or breach dikes and levees. During managed realignment the ownership of the land changes or easements are put in place to regulate land use while accommodating this environmental change. New dikes may be built on the landward side of the realigned area, any artificial drainage in the landscape is disabled, and the outer dike is breached. This practice returns/surrenders land to the sea while allowing landowners to migrate away in a controlled manner and providing an enhanced buffer zone that better protects inland properties and infrastructure (Pethick, 2002).

Land reclamation has long been recognized to have major impacts on soil genesis, morphology, and classification (Pons and Vandermo, 1973). The newly exposed wetland or seafloor becomes irrigated with air as it dewateres, increasing the soil's redox potential (Megonigal and Rabenhorst, 2013) and allowing it to consolidate (Hillel, 2004). Once dewatered, sulfide minerals such as pyrite oxidize and generate sulfuric acid, mobilizing iron (Fe) and other metals. The level of Fe and manganese (Mn) oxide minerals increases in the soil matrix, and unless the generated acid can be neutralized or buffered by other soil constituents the pH can drop precipitously and result in the formation of jarosite, schwertmannite, and similar minerals (Fanning et al., 2010). Regardless of pH, soil structure forms and (when or once vegetated) terrestrially derived organic matter begins to accumulate in the formerly water-saturated aquatic profile (Lu et al., 2018). Once land reclamation has occurred, the materials in these landscapes have been converted from sediments or subaqueous soils (Demas and Rabenhorst, 2001; Kristensen and Rabenhorst, 2015) to

subaerial soils that meet even the most restrictive classic agricultural definitions of soil which are dependent on plant growth (Hartemink, 2016; Jenny, 1941).

The impacts of managed realignment on soil genesis, morphology, and classification are less well known. Because these projects are rare but now being considered and completed at an accelerating rate (Nunn et al., 2016), it is important to understand the environmental implications of this type of land conversion/restoration, which may further shed light on the impacts of sea-level rise as it occurs at an increasing rate along nearly every coastline in the world. Upon restoration of submergence (or submergence by natural processes), sediment diagenesis/subaqueous pedogenesis (again?) begins to act on these materials, under both fresh and saltwater conditions. In the Murray-Darling Basin in Australia, a severe drought exposed freshwater sediments from 2007 to 2009, during which time many of the processes associated with land reclamation (e.g. dewatering, sulfide oxidation, metal mobilization) occurred, forming sulfuric horizons as a result of the production of sulfuric acid by sulfide oxidation (Creeper et al., 2013), features which can persist in soils for decades or longer in upland environments (Wessel et al., 2017a). In the Murray-Darling Basin, the sulfuric horizons that formed during the drought persisted after two years of re-submergence; however, the uppermost part of these soils (~5 cm) did trend towards restored subaqueous pH, metal availability, and structure during the same time (Creeper et al., 2015). A study previously conducted in Gyldensteen Strand, Denmark (the same site as this study) found that bioturbation by benthic macrofauna returning after flooding with seawater affects transport conditions and destroys soil structure in the upper 5-10 cm (Valdemarsen et al., 2018). However,

there is a paucity of information about the impact of flooding on pedological features and soil chemistry deeper in these profiles.

The objective of this research was to investigate the presence and persistence of subaerial and subaqueous pedogenic features in a landscape with areas that have been subjected to varying hydrologic regimes relating to managed realignment of reclaimed land. We hypothesize that subaerial pedogenic features will persist within the upper meter of the substratum after submergence both by fresh- and seawater, though we expect that features indicative of sediment diagenesis/subaqueous pedogenesis will be found at the soil surface. Further, this study highlights the value of landscapes where managed realignment has been completed as experimental indicators of the likely impacts of sea-level changes.

#### 4.3 Methods and materials

##### 4.3.1 Study site

Gyldensteen Strand, a lagoon located on the northern coast of the Danish island of Fyn near the town of Bogense, has experienced a long history of intense anthropogenic alteration. It was a relatively undisturbed marine coastal lagoon until 1871, when it was diked off from the sea and drained for agricultural use during a period of massive land reclamation in Denmark (Pedersen, 2010). Due to subsidence of the drained land, a dependence on inefficient windmill pumps to drain the land, and occasional breaches of the dike, this site was only used for grazing and hay-making until 1960. At that time, modern pumps were installed and the land was finally dewatered to a point that intensive agricultural management could begin for

crop production (Stenak, 2005). Even so, yields were relatively low in comparison to other agricultural areas in Denmark.

In 2011 the site was purchased by the Aage V. Jensen Nature Foundation (Kristensen et al., 2016). An area of never-drained shoreface along the northern edge of the site allowed a comparison with pre-reclamation conditions in shallow marine sediments, underlying 22-26 salinity seawater (Sjøgaard et al., 2017). An adjacent area to the west of the site, drained during the same period of land reclamation and still used for agriculture, was sampled to evaluate pedogenesis in reclaimed land that has not yet been restored. The site purchased by the Foundation was divided in 2014 and restored in two ways; 142 hectares were separated by a dam and allowed to fill with meteoric water to form the freshwater lake Engsøen (though in dry years it retreats from its edges and the fringing freshwater marsh expands until it is submerged again in wet years), and 214 hectares were restored as the tidally influenced Gyldensteen Coastal Lagoon by breaching the dike to the sea and shutting off the water pumps. Both the lake and the lagoon were sampled to compare the impacts of these methods of managed realignment.

Thirty two pedons were sampled across these four areas (shoreface, reclaimed land, freshwater lake, and restored lagoon; Table 4-1) to determine the impact of this management history on these substrata. An existing sampling grid was used to select sample locations so that these data would complement a variety of ongoing field studies at Gyldensteen Strand by an interdisciplinary group from University of Southern Denmark; this sampling grid and other general site characteristics have been

described in several previous studies (Sjogaard et al., 2017; Sjogaard et al., 2018; Thorsen et al., 2019; Valdemarsen et al., 2018).

Table 4-1. Distribution of Gyldensteen Strand pedons (n=32) and the horizon samples that constituted them (n=207) collected at Gyldensteen Strand, by master horizon type and landscape unit. The three master horizon types used in this study allowed binning of samples into three morphologically distinct layers: A layer-surface and near-surface materials that exhibit evidence of alteration by plants and animals and the accumulation of organic matter and/or metastable Fe-sulfides; B layer-materials that show evidence of subaerial pedogenesis such as brown/red colors or soil structure; C layer-materials that show almost no evidence of recent alteration by pedogenic/diagenetic processes.

	Landscape Unit			
Master Horizon	Shoreface	Reclaimed Land	Freshwater Lake	Restored Lagoon
A	8	3	17	42
B	0	9	19	46
C	19	6	13	25
Pedons	5	2	7	18

#### 4.3.2 Soil survey field methods

Soils were collected and described in the field using selected US Soil Survey field methods (Schoeneberger et al., 2012). All soil profiles were collected using a stainless steel bucket auger with the exception of one vibracore sample collected from the shoreface landform. Munsell color (hue, value, and chroma), fluidity, soil



structure, redox features (concentrations and depletions), and the presence of fragments or inclusions (e.g. shells, roots) were described in the field. Reaction with both 3% and 30%  $\text{H}_2\text{O}_2$  was also recorded in the field to indicate the presence of sulfide minerals. The 3%  $\text{H}_2\text{O}_2$  test causes metastable Fe-sulfides to fade almost instantaneously, causing a sample to change from black to the underlying mineral grain color (usually grey or yellow) if sulfides are present in a sufficient quantity to color the soil matrix. The 30%  $\text{H}_2\text{O}_2$  test is used to indicate the presence of pyrite, manganese oxides, and organic matter, resulting in an exothermic effervescence that can be given an ordinal score. However, it can be difficult to distinguish which compound is causing the reaction in a particular sample (Duball et al., 2020; Wessel and Rabenhorst, 2017).

These data were used to horizonate the soil profiles into a total of 207 horizons, and horizons were named, sampled, and frozen until analyzed. Three distinct morphological groups of soil materials were identified throughout the sampled profiles and were classified by their master horizon type: A horizons, B horizons, and C horizons (Table 4-1). These were grouped into A, B, and C layers to simplify data presentation. Master horizons were assigned according to guidelines within US Soil Taxonomy (Soil Survey Staff, 1999); surface horizons were consistently interpreted as A horizons. Intact clods were collected from the auger wherever possible in order to minimize oxidation and chemical alteration of the interiors before laboratory analyses could be conducted.

#### 4.3.3 Laboratory analyses

Samples were thawed overnight under refrigeration for laboratory analyses the following morning. Chemical analyses included pH, moist aerobic incubation, extractable Fe fractionation, sulfur (S) fractionation, and measurement of organic and inorganic carbon (C) content. Physical analyses included bulk density via the cut-off syringe method (Hilton et al., 1986), which was used to convert Fe and S measurements to dry mass equivalents. For pH, Fe, and S measurements, great care was taken to sample the interior of clods in order to minimize any effects that might be introduced by chemical oxidation.

Soil electrical conductivity was measured on supernatants of 1:5 dilutions of field moist soil (v/v) according to the Soil Taxonomy method for subaqueous soils (Soil Survey Staff, 2014). Porewater salinity was calculated using the relationship

$$\text{Salinity} = (\text{conductivity} - 403.05) / 1582.6$$

from Dittmann et al. (2009), where conductivity is measured in  $\mu\text{S}/\text{cm}$ . Dilution was accounted for using sample bulk density and assuming complete saturation, so the porosity in the  $10 \text{ cm}^3$  of moist soil used corresponded to the initial porewater volume, diluted with the addition of  $40 \text{ cm}^3$  of distilled water to reach the final volume for measurement. Particle density was assumed to be  $2.65 \text{ g}/\text{cm}^3$ .

Soil pH was measured using a modification of the 1:1 water pH method (Soil Survey Staff, 2014). The published method calls for using dried soil, but because subaqueous soil samples may contain sulfide minerals that can generate acid upon drying (Fanning et al., 2002), the paste was prepared using field-moist soil in order to avoid this potential error. Moist aerobic incubations were conducted using the

oxidized pH method (Soil Survey Staff, 2014). Soil pH samples were retained after the 1:1 water pH was recorded and allowed to air dry at room temperature, and were remoistened to a paste approximately once weekly for 16 weeks. The pH of these pastes was occasionally recorded to monitor this process. The pH measured at the end of this process is the oxidized pH, which is a result of the oxidation of any sulfides present to create acid, and the reaction of this acid with any neutralization potential (from substances like calcium carbonate) or buffering capacity (from cation exchange on clay minerals) in the sample (Wessel and Rabenhorst, 2017). All pH values were measured using a HI 98103 meter, calibrated for each set of readings using pH 4.00 and 7.00 buffers, and checked in a pH 10.00 buffer.

Fe was extracted and measured using a sequential method to identify operationally-defined pools of reactive reduced ( $\text{Fe}^{2+}$ ) and oxidized ( $\text{Fe}^{3+}$ ) iron. This method is commonly used in the aquatic sciences to measure the poorly-crystalline pool of particulate Fe thought to be available to the sediment microbial community (Lovley and Phillips, 1987), though it does not extract Fe from more highly crystalline Fe minerals such as goethite (Claff et al., 2010). Soil subsamples of known mass (~0.5 g) were placed into centrifuge tubes with 5 mL of 0.5 M HCl and shaken for 30 minutes to extract iron. In addition to functioning as an extractant, the acid also stabilizes  $\text{Fe}^{2+}$  and slows its oxidation to  $\text{Fe}^{3+}$  at room temperature, allowing several hours to complete analyses while introducing minimal error (Shapiro, 1966). Tubes were centrifuged at 3000 rpm for 5 minutes to produce supernatant (Lovley and Phillips, 1987).  $\text{Fe}^{2+}$  content was determined by pipetting 40  $\mu\text{L}$  subsamples of the supernatant into cuvettes containing 2 mL of 0.02 % ferrozine to produce a colored

complex that was read at 562 nm (Stookey, 1970). The remainder of the supernatant was then treated with 0.2 mL of 1.5 M hydroxylamine to reduce any  $\text{Fe}^{3+}$  into  $\text{Fe}^{2+}$ . Subsamples of 40  $\mu\text{L}$  were again pipetted into cuvettes with ferrozine before being read at 562 nm to determine the total extracted Fe pool. The  $\text{Fe}^{3+}$  was then calculated as the difference between and  $\text{Fe}^{2+}$  measured before (i.e. only  $\text{Fe}^{2+}$ ) and after (i.e. total reactive Fe) reduction with hydroxylamine (Lovley and Phillips, 1987).

Less-bioavailable Fe was also measured using selected methods from a relatively common sequential extraction process (Jensen and Thamdrup, 1993). Water-washed samples were shaken at room temperature for 1 hour in a solution of 0.11 M sodium bicarbonate and 0.11 M sodium dithionite buffered to pH 7.0 to extract crystalline Fe. This bicarbonate-dithionite extractable Fe (BD-Fe) represents a portion of minerals such as goethite, but is less effective than the longer extractions at higher dithionite concentrations commonly used in soil science. It will also extract poorly crystalline Fe (overlapping with the 0.5 M HCl extraction), but not pyrite (Claff et al., 2010). Total Fe was measured on field-moist samples which were dried before being ignited at 520°C for two hours. The residue was then boiled for 10 minutes in 1 M HCl before the Fe concentration was measured spectrophotometrically (Jensen and Thamdrup, 1993).

Soil sulfur was fractionated into the acid volatile sulfide (AVS  $\sim \text{FeS} + \text{HS}^-$ ) and chromium reducible sulfur (CRS  $\sim \text{FeS}_2 + \text{S}^0$ ) pools (Rickard and Morse, 2005) using a two-step sequential distillation method (Fossing and Jørgensen, 1998). Soil subsamples of known mass ( $\sim 10$  g) were placed into centrifuge tubes with 10 mL of 1 M zinc acetate (ZnAc) before being vigorously mixed in order to fix the labile S

species present as ZnS, from which H<sub>2</sub>S can be evolved in a controlled manner (Wallmann et al., 1993). These were subsampled and ~4 g was transferred to the reaction flasks of a distillation apparatus. Fractions of S were then evolved as released H<sub>2</sub>S and captured in ZnAc bubbler traps, carried by N<sub>2</sub> gas. The AVS fraction is highly reactive relative to the CRS fraction, and evolves H<sub>2</sub>S from ZnS and FeS with the addition of 1 M HCl during the first step of the distillation. During the second step, 8 mL of 6 M HCl and 16 mL of 1 M Cr<sup>2+</sup> in 0.5 M HCl was added to the reaction flask, which was then brought to a boil. This evolves the remainder of the S (FeS<sub>2</sub> + S<sup>0</sup>) as released H<sub>2</sub>S, which was trapped in the second set of ZnAc bubbler traps. Cline's reagent was then used to pretreat subsamples of known volume from the bubbler traps before they were read at 670 nm on a spectrophotometer (Cline, 1969) to quantify the captured sulfide.

Some portion of Fe, here called refractory Fe, is substantially unavailable to microbial action. Refractory Fe was operationally defined as:

$$(\text{Total Fe}) - (\text{CRS-Fe}) - (\text{HCl-Fe}^{2+}) - (\text{BD-Fe}) = \text{Refractory Fe}$$

This is an imperfect approach because a sequential extraction process was not used for all Fe fractions. Total Fe (after combustion and boiling in 1 M HCl) is considered to be reasonably accurate measure of all Fe in a sample. CRS-Fe is calculated from CRS, assuming all measured S is FeS<sub>2</sub>. HCl-Fe<sup>2+</sup> is the 0.5 M HCl extraction, which includes reduced Fe in porewater and which may contain some Fe from FeS (this is why AVS-Fe is not subtracted as well). BD-Fe does not include porewater Fe because the samples were water washed to measure only particulate Fe, though it will include poorly crystalline Fe that would also have been measured as HCl-Fe<sup>3+</sup> (this is why

HCl-Fe<sup>3+</sup> is not subtracted as well). Refractory Fe includes crystalline Fe oxides that are relatively resistant to microbial reduction, as well as Fe sequestered in clays, other silicates, and carbonate minerals.

The extent to which bioavailable Fe is reduced or oxidized in materials where sulfides can accumulate is sometimes calculated as the degree of pyritization (DOP).

DOP was operationally defined as:

$$\text{DOP} = (\text{CRS-Fe} + \text{AVS-Fe}) / (\text{CRS-Fe} + \text{AVS-Fe} + \text{BD-Fe})$$

This definition varies slightly from more common operational definitions of DOP by including AVS-Fe, which was not prevalent in the black shales used to evaluate earlier DOP calculations (Leventhal and Taylor, 1990; Raiswell et al., 1988), with pyrite Fe. Berner (1970) included HCl extractable Fe in his formula for DOP as a measure of Fe which had not yet been pyritized, but he was working in reduced coastal sediments where Fe-oxide species found in soils would not be prevalent. In order to better capture the ratio of ‘Fe bound to reduced S’ to ‘Fe available to be bound to reduced S’, I have used BD-Fe as the measure of Fe available to be bound to reduced S.

Organic and inorganic C were determined using a Thermo Analytical elemental analyzer<sup>4</sup>. Soil subsamples were oven dried and ground using a mixer mill and grinding balls. Ground samples were further subsampled, with one subset being

---

<sup>4</sup> These measurements were conducted at the University of Southern Denmark using slightly different methods than those used to produce the C measurements in other chapters, where sulfurous acid was used to remove carbonate C.

acidified using 1 M HCl to remove inorganic C before measuring organic C on the elemental analyzer (Schlacher and Connolly, 2014). Another subset was run directly on the elemental analyzer to measure total C, and inorganic C was calculated as the difference between the pools.

#### 4.4 Results and discussion

##### 4.4.1 Evaluation of select methods

Most of the field methods used in this study are long established, but several (3% H<sub>2</sub>O<sub>2</sub> color change reaction, 30% H<sub>2</sub>O<sub>2</sub> effervescence reaction, reactive Fe<sup>3+</sup> extraction, conversion to salinity from electrical conductivity in 1:5 soil to water dilution by volume) were evaluated in light of the multidisciplinary marine/pedological nature of this study. The 3% H<sub>2</sub>O<sub>2</sub> color change reaction is thought to be an indicator of metastable Fe-sulfide minerals (AVS ~ FeS) (Duball et al., 2020), though threshold values are unknown. The lowest concentration to produce a positive color change reaction in this study was 0.0008 % AVS (dry mass), and the median value was 0.003 % AVS. The maximum concentration not to produce a color change reaction was also 0.003 % AVS (Figure 4-1). This demonstrates that while a sample content of slightly less than one thousandth of a % AVS can be sufficient to cause the color change reaction, a sample content of several thousandths of a % AVS will not necessarily result in a color change reaction. This may be because AVS includes porewater sulfide, which can be present in samples without metastable Fe sulfides. Despite the overlap between these groups they are significantly different ( $P < 0.0005$ ), though the positively skewed nature of the two sets of measurements

does violate the assumption of normally distributed data for the t-test. Nevertheless, Figure 4-1 clearly shows a relationship and validates the use of the 3%  $\text{H}_2\text{O}_2$  color change test to generally distinguish between groups based on AVS content.

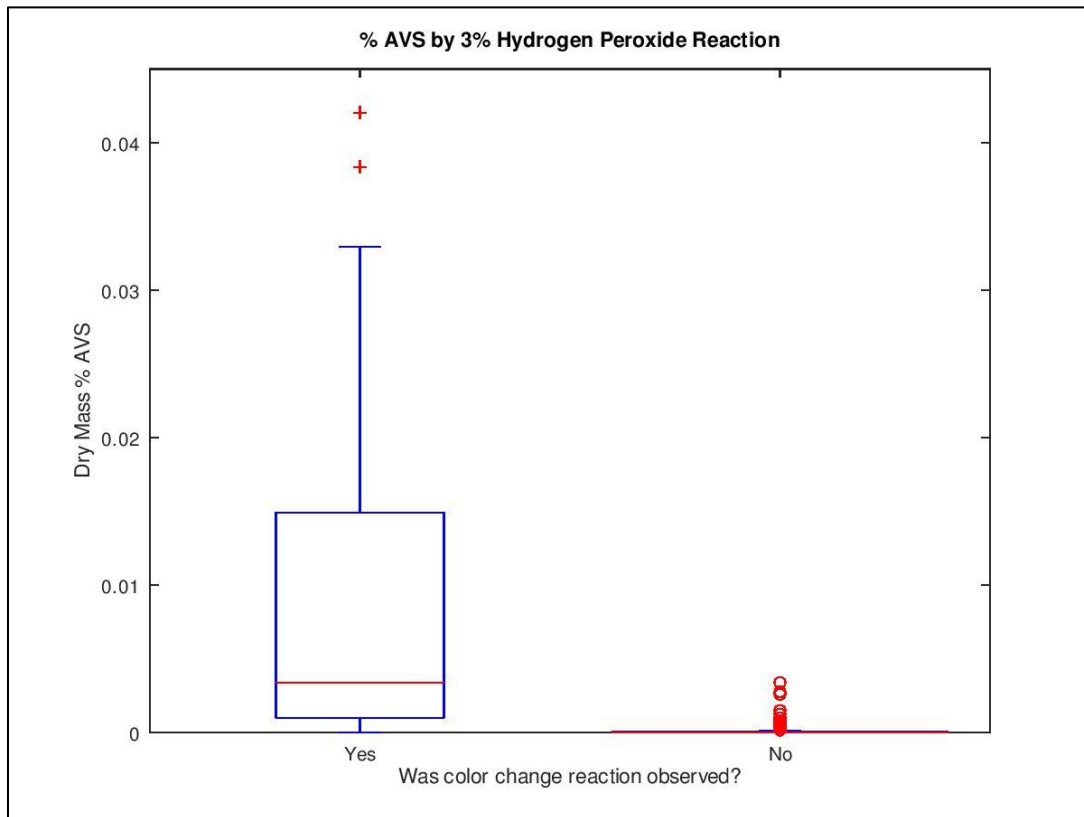


Figure 4-1. Percent AVS by 3%  $\text{H}_2\text{O}_2$  color change reaction (field test). N=69 (Yes color change), N=138 (No color change). Red line marks the median, box bounded by first and third quartile. Whiskers mark 1.5 times the interquartile range. Outliers marked 'o' if they are beyond 3 times the interquartile range, marked '+' if they lie 1.5-3 times beyond the interquartile range. The "No" group is plotted, but the median value is 0.00002 % AVS so the box is collapsed when compared to the "Yes" group. The % AVS in the group that showed the color change reaction was significantly



greater than the % AVS in the group without the color change (one-tailed t-test,  $P < 0.0005$ ), though the distributions of both groups were positively skewed.

The 30% H<sub>2</sub>O<sub>2</sub> effervescence reaction also lacks established threshold values. Organic matter will effervesce over the course of minutes to hours, Mn oxides will react violently and instantaneously as they catalyze the decomposition of the H<sub>2</sub>O<sub>2</sub>, and pyrite (CRS ~ FeS<sub>2</sub>) will react in a way that falls somewhere in between these extremes (Duball et al., 2020). Pyrite will react slowly over the course of several minutes, building up heat and accelerating the reaction. In high-pyrite samples this rapidly builds to a violently boiling effervescence (Wessel and Rabenhorst, 2017).

Effervescence classes after addition of 30% H<sub>2</sub>O<sub>2</sub> to Gyldensteen Strand samples varied from noneffervescent to violently effervescent, with most samples exhibiting slight effervescence. Noneffervescent samples had the lowest median organic C content and violently effervescent samples had the second lowest median organic C content. Many of the highest organic C samples were only slightly effervescent (Figure 4-2). This supports previous claims that the effervescence observed within a few minutes of adding 30% H<sub>2</sub>O<sub>2</sub> to a sample is not strongly related to the organic C content.

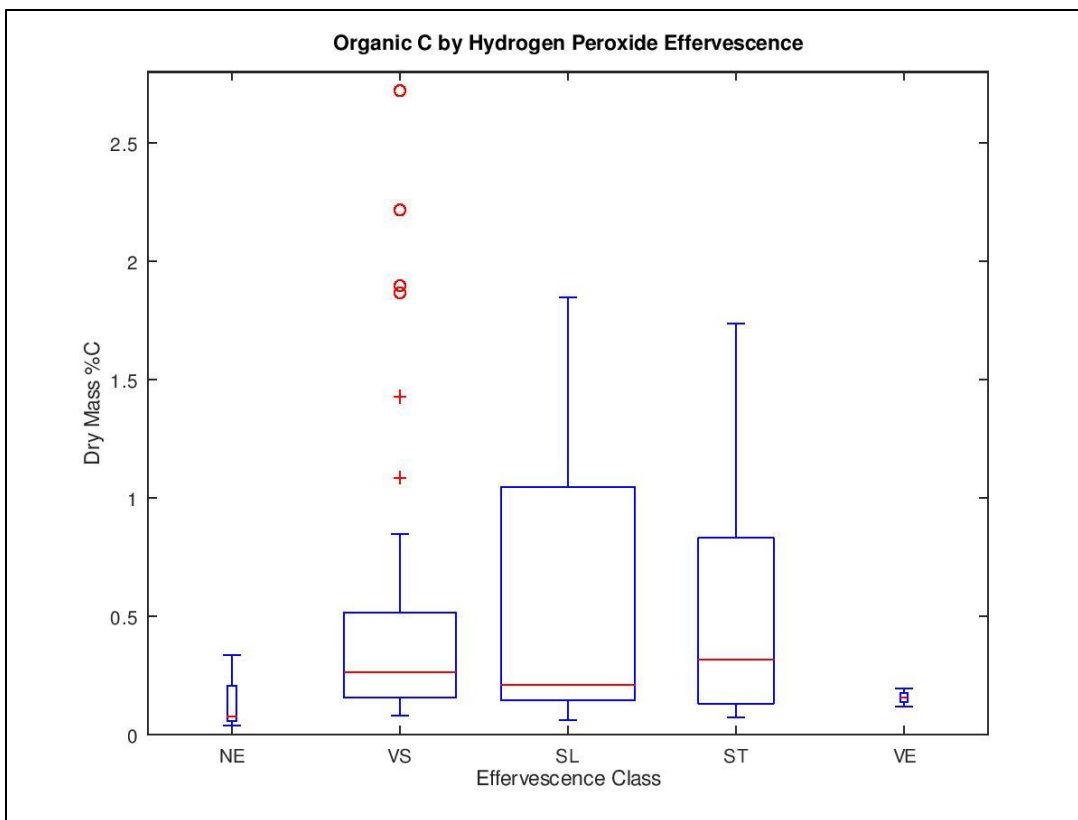


Figure 4-2. Percent organic C by sample effervescence class after addition of 30%  $\text{H}_2\text{O}_2$ . NE=Noneffervescent (no bubbles form), VS=Very Slight (few bubbles form), SL=Slight (numerous bubbles form), ST=Strong (bubbles form a low foam), VE=Violently Effervescent (bubbles rapidly form a thick foam). Box widths are proportional to sample number (N=103).

That said, when considering the relationship of the 30% H<sub>2</sub>O<sub>2</sub> test to CRS content (Figure 4-3) several of the highest % CRS outlier samples were noneffervescent, very slightly effervescent, or slightly effervescent. Many strongly effervescent samples contained a lower % CRS than those outliers. The several violently effervescent samples had among the lowest % CRS contents. The % CRS of the 75<sup>th</sup> percentile of slightly effervescent samples was lower than it was for very slightly effervescent samples (Figure 4-3). Similar patterns can be seen when considering total reduced inorganic sulfur (TRIS = CRS + AVS). There appears to be little difference between groups, and there are many outliers that defy their expected behavior. The interquartile ranges of the first four effervescence classes show considerable overlap (Figure 4-4).

This may be because nearly all of the sulfide levels in Gyldensteen Strand samples are below 0.1% S, a content that would be considered very low along the US east coast where the 30% H<sub>2</sub>O<sub>2</sub> test has been more widely used to indicate the presence of sulfidic materials. In this study, no moist aerobic incubation sample dropped by more than 1.0 pH units over 16 weeks of incubation (data not shown), so no soil materials would classify as sulfidic materials (Soil Survey Staff, 2014). Small amounts of acid may have been produced by sulfide oxidation, but if it was then it was neutralized by reactive carbonate minerals or buffered by the buffering capacity of the sample (i.e. cation exchange reactions on clays and organic matter) (Ahern et al., 2004). In Chesapeake Bay marshes and sediments pyrite-S contents average around 1.0% (Haering et al., 1989), more than ten times the CRS content in most of the highest-CRS outliers from Gyldensteen Strand, and several orders of magnitude

more than the majority of samples. In the deep (2 to 10 m below surface) unoxidized subsolum of upland environments of the US Mid-Atlantic region concentrations range from 0.5% CRS to 1.9% CRS (Rabenhorst and Valladares, 2005), again considerably higher than in Gyldensteen Strand. The 30% H<sub>2</sub>O<sub>2</sub> test should therefore not be used to infer the presence of pyrite at very low concentrations (< 0.1%), and the method still requires validation at higher pyrite/CRS concentrations. Future studies should also seek to evaluate the impact of Mn oxides on the test, which were not measured in this study.

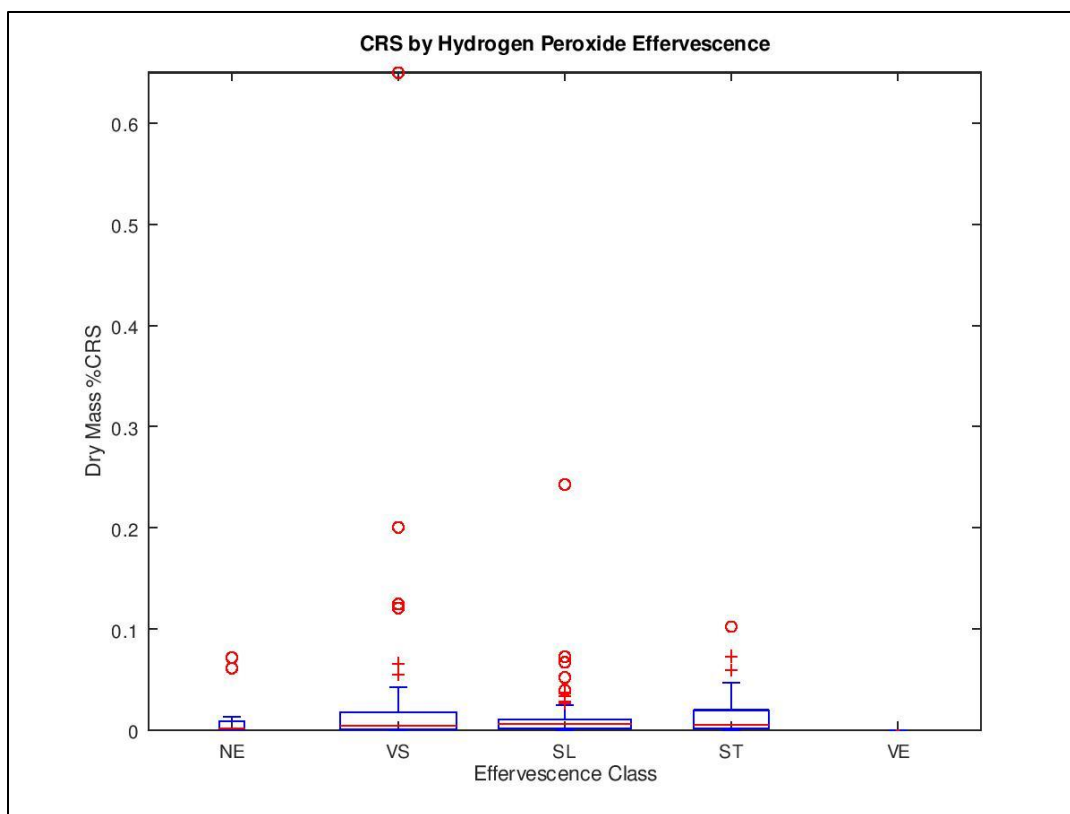


Figure 4-3. Percent CRS by sample effervescence class after addition of 30%  $\text{H}_2\text{O}_2$ .

NE=Noneffervescent (no bubbles form), VS=Very Slight (few bubbles form),

SL=Slight (numerous bubbles form), ST=Strong (bubbles form a low foam),

VE=Violently Effervescent (bubbles rapidly form a thick foam). N=207.

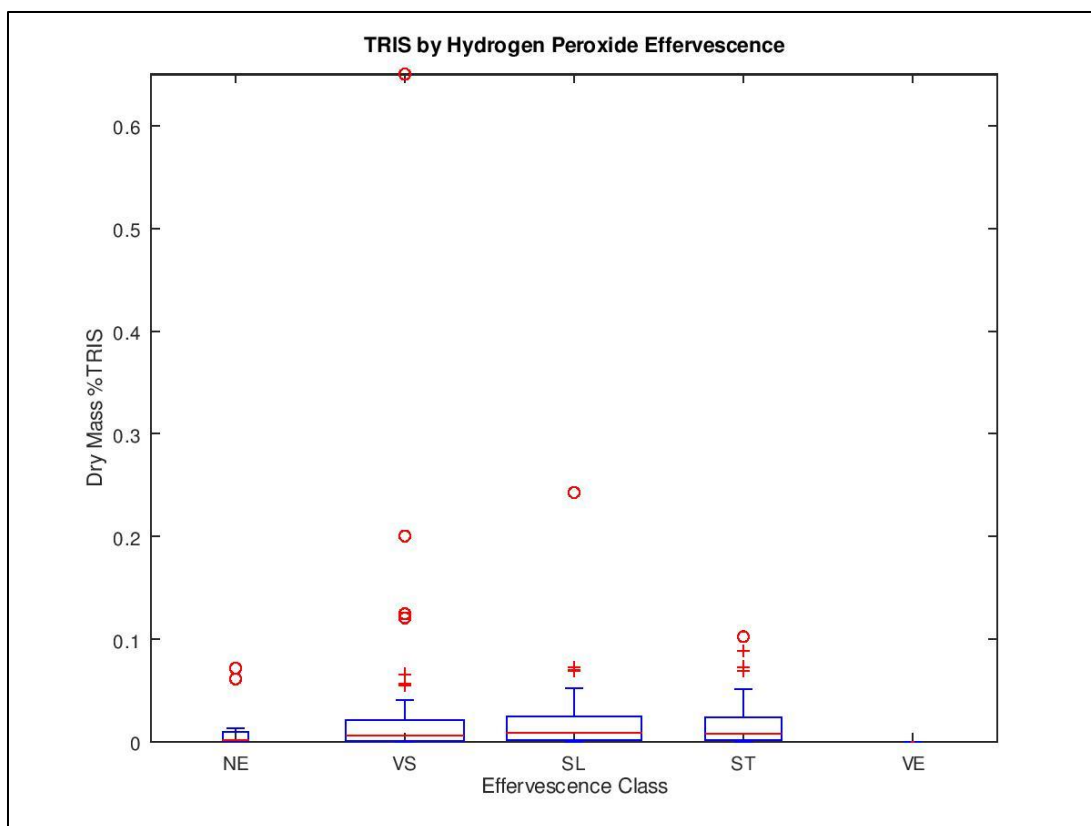


Figure 4-4. Percent TRIS by sample effervescence class after addition of 30%  $\text{H}_2\text{O}_2$ .

NE=Noneffervescent (no bubbles form), VS=Very Slight (few bubbles form),

SL=Slight (numerous bubbles form), ST=Strong (bubbles form a low foam),

VE=Violently Effervescent (bubbles rapidly form a thick foam). N=207.

Reactive (extractable)  $\text{Fe}^{3+}$  is a measure commonly used in the aquatic sciences, but generally not used in soil science. The forms of Fe in soils are often more stable/crystalline and require harsher extractions such as dithionite reduction to measure (Mack et al., 2018). Such extractions are sometimes used in the aquatic sciences for specific purposes (Jensen and Thamdrup, 1993), but the extraction used in this study was more analogous to an extraction of bioavailable Fe as might be used in a soil fertility study. The 0.5 M HCl extraction used here is stronger than a standard soil fertility extraction (e.g. Mehlich 3), and may therefore offer some proxy measurement of crystalline  $\text{Fe}^{3+}$ , even though it is not expected to bring all Fe into solution.

In morphological descriptions, percent redox concentrations (predominantly Fe oxides) were described in 96 samples, and ranged in abundance up to 35% (estimates by volume) of the soil matrix color. These morphological data were plotted against the extractable reactive  $\text{Fe}^{3+}$  (Figure 4-5), though little relationship can be seen. The correlation coefficient of 0.015 highlights the lack of a clear positive relationship between these variables. This may be because this approach ignores too many other variables, such as the matrix color and the color of the concentrations themselves. For instance, Fe and Mn concentrations were both observed, though they often co-occur and their composition varies; a red concentration is not necessarily composed completely of Fe minerals. Further, the 0.5 M HCL extraction will not dissolve substantial portions of crystalline Fe oxides such as goethite (important in causing the redder colors of reclaimed soils), though it may dissolve a greater portion of poorly crystalline Fe oxides such as ferrihydrite. Describing concentrations and



depletions is certainly useful to infer hydrologic history, but does not indicate the presence of reactive (extractable)  $\text{Fe}^{3+}$ .

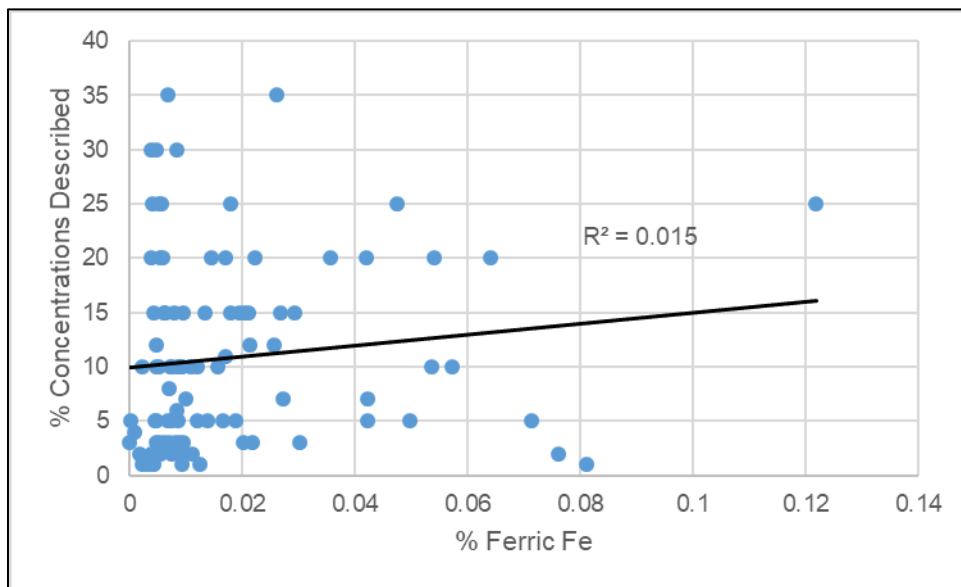


Figure 4-5. Redox concentrations vs reactive ferric Fe. Bivariate plot shows percent of morphological redox concentrations (predominantly Fe oxides, though several samples included Mn oxides) described in the field vs percent  $\text{Fe}^{3+}$  extracted using 0.5 M HCl (N=96). The weak relationship highlights that the presence of Fe and Mn oxide concentrations is not necessarily an indication of the presence of extractable reactive  $\text{Fe}^{3+}$  in the soil.

Matrix color may be expected to be of more use in indicating the presence of reactive  $\text{Fe}^{3+}$  in a sample; however, approaches to relate soil color to extractable Fe are fraught with possible sources of error. Fe oxide mineral color does not necessarily relate to the ease of Fe extraction, which depends on crystal size, crystallinity of the mineral, and the mineralogy itself. Lepidocrocite-Fe is relatively easy to extract (easier than goethite-Fe), but lepidocrocite may appear redder than goethite. Underlying mineral grain color also plays a role. If mineral grains possess a red color regardless of Fe oxide coating, then any Fe extracted from Fe oxide coatings won't necessarily relate to the color of the soil. Soil color is multifactorial, so relationships between color and any chemical measurement will always be imperfect.

The highest quantity of morphological redox concentrations observed was 35% (Figure 4-5), consistently missing at least 65% of the soil matrix. On the other hand, matrix color captures all of the matrix in many samples (those without described concentrations or depletions) and captures more of the matrix, or at least an intermediate color, where both concentrations and depletions are present. Samples with matrix colors having redder hues would be expected to release some  $\text{Fe}^{3+}$  to an extraction because the color is caused by coatings of Fe oxide minerals on grains of other minerals such as quartz and various clay minerals. Yellower hues and grayer colors would be expected to release less  $\text{Fe}^{3+}$  to an extraction because those Fe oxide grain coatings are thinner, or missing entirely. This trend can be seen, albeit weakly, in Figure 4-6 (top), which lists Munsell hues from reddest (left) to least red (right). The N hue is problematic because those are dark black samples (N 2.5) that by definition have no spectral hue component (chroma = 0), so these samples have been

omitted from evaluations of the relationship between hue and Fe content. From 7.5YR (the reddest) to 10Y (less red) the interquartile range limits (25<sup>th</sup> and 75<sup>th</sup> percentile) consistently show a downward trend in reactive Fe<sup>3+</sup> content. The single 5GY hue sample continues this trend as expected. BD extractable Fe shows a similar trend (Figure 4-6, bottom), particularly in the YR hues, which suggests that it would be worthwhile to include redder hues in future efforts to relate soil matrix color to operationally defined Fe fraction contents. Hue does seem to be an indicator of the presence of reactive Fe<sup>3+</sup> in these soils, though the precise provenance of reactive Fe<sup>3+</sup> remains unknown. It likely represents a mixed pool including adsorbed cations and some crystalline Fe.

Value, a measure of the lightness or darkness of a color, would not be expected to have a strong relationship with Fe<sup>3+</sup>. Fe minerals in soils can range from light pink (some hematite soils) to black (masked by Mn oxides). No linear relationship is expected, and Figure 4-7 demonstrates that variability in these data.

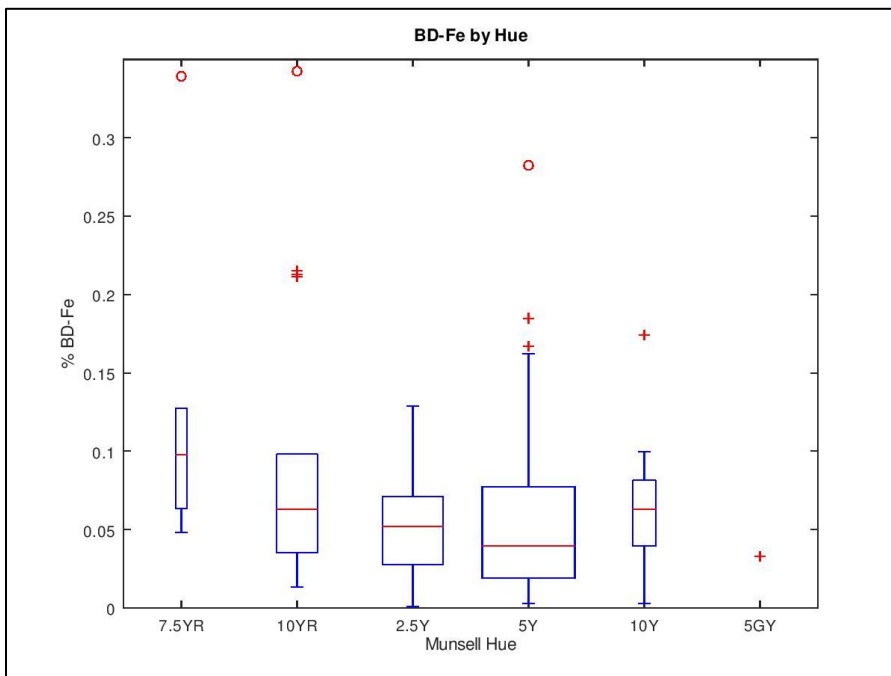
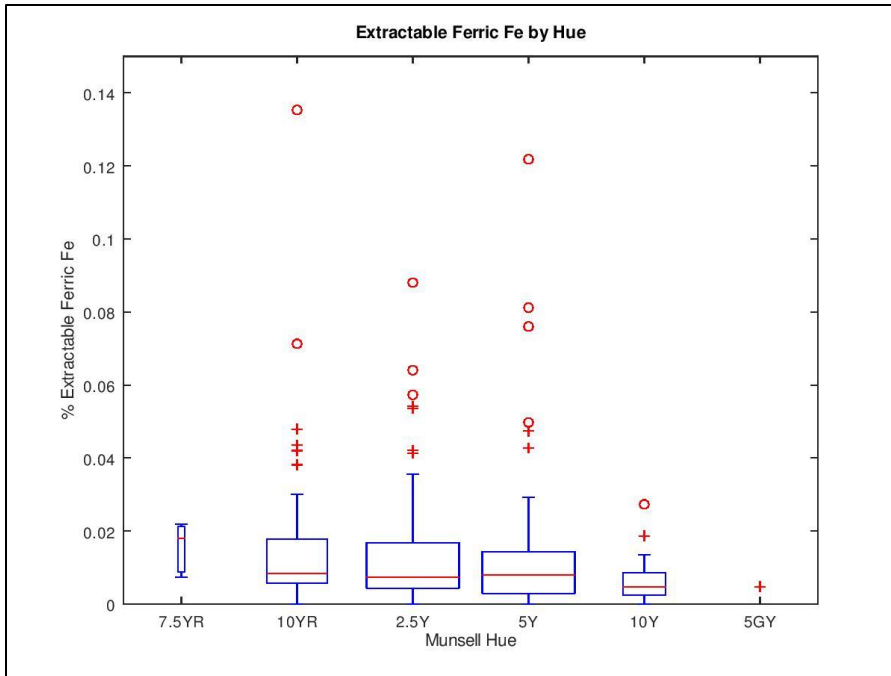


Figure 4-6. Fe vs matrix hue. Percent reactive (0.5 M HCl extractable)  $\text{Fe}^{3+}$  (top, N=202) and BD extractable Fe (bottom, N=102) listed by sample matrix Munsell hue, from reddest (left) to least red (right).

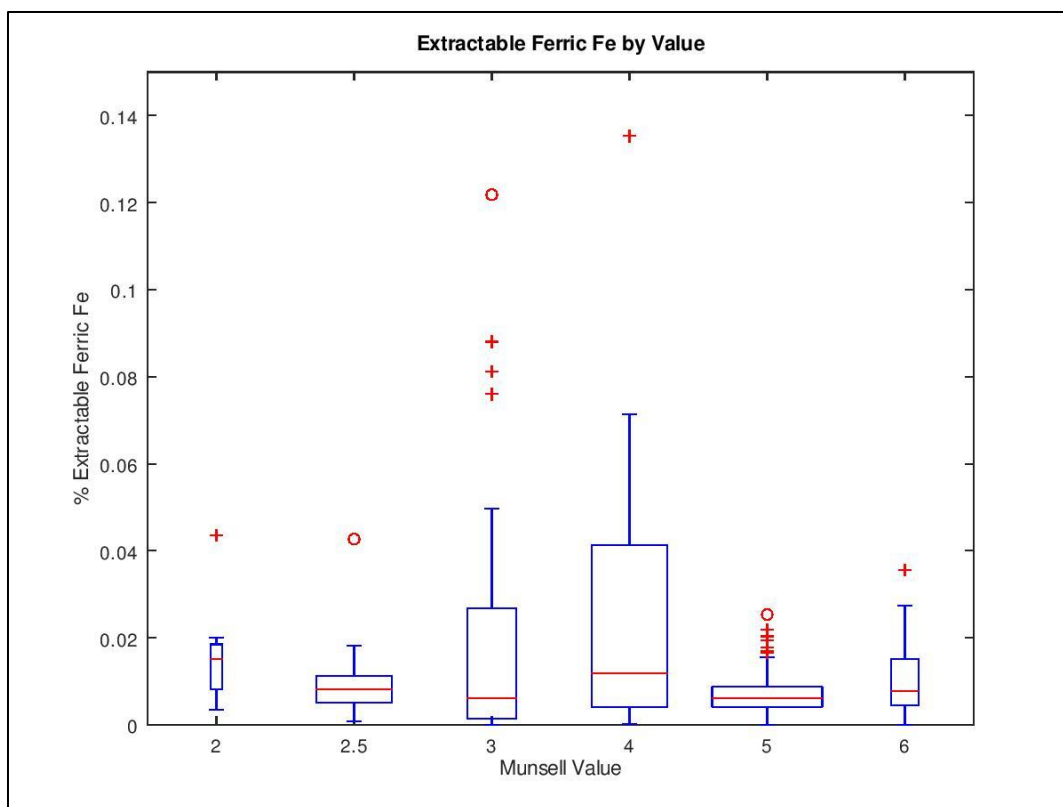


Figure 4-7. Fe vs matrix value. Percent reactive (0.5 M HCl extractable)  $\text{Fe}^{3+}$  listed by sample matrix Munsell value, from darkest (left) to lightest (right). N=207.

Chroma, like hue, has an expected relationship with the Fe in a soil. Chroma is a measure of the strength, intensity, or vividness of a color. It is sometimes thought of as the departure from a neutral version of the same color. The measurement of chroma is widely applied to identify wetland soils, which have remained wet enough for long enough under the right conditions that the Fe in Fe oxides has been reduced, stripping the minerals and colors from the soil matrix. A chroma of 2 or less is generally considered evidence of this stripping, though again this can be cofounded by very black colors, so regulations generally also require a value of 4 or greater to provide confidence that the colors have been caused by wetness. Soils with high chroma colors generally have them because they are oxidized and colored by oxides of Fe and other elements. This expected trend is generally seen in Figure 4-8 (top), which shows reactive  $\text{Fe}^{3+}$  contents generally increasing with increasing chroma. The trend is also seen with BD-Fe in Figure 4-8 (bottom).

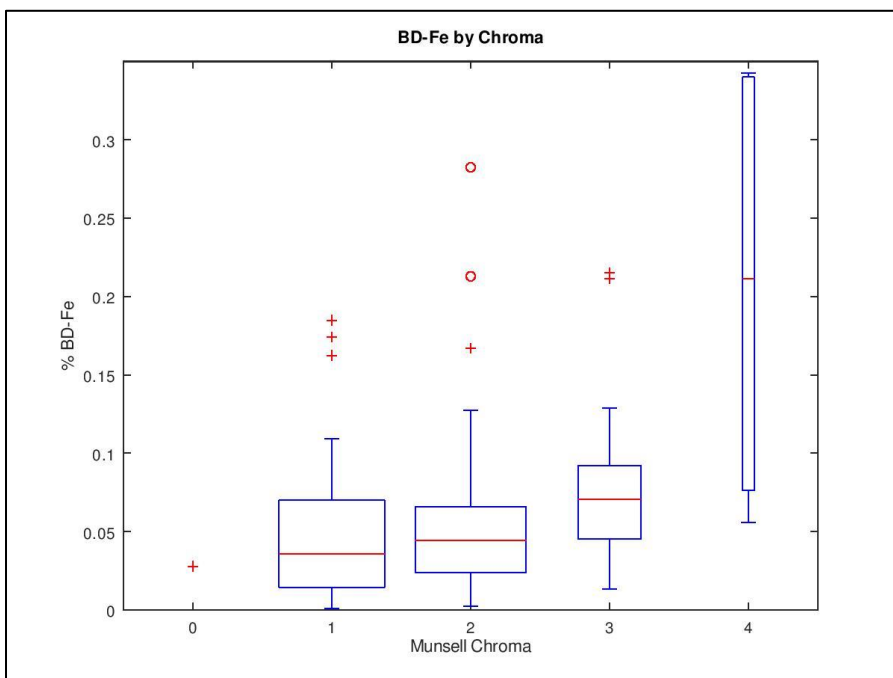
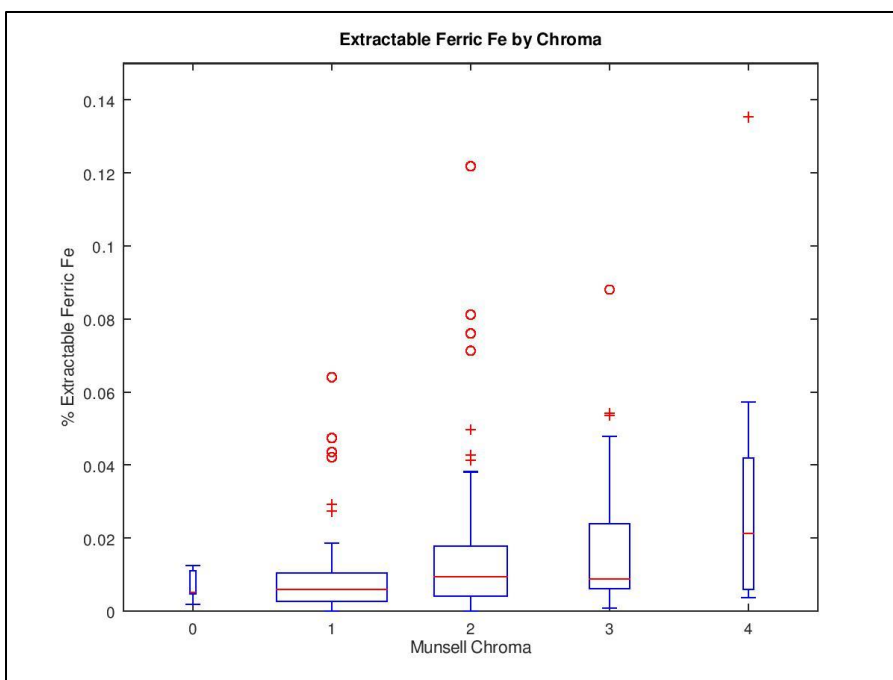


Figure 4-8. Fe vs matrix chroma. Percent reactive (0.5 M HCl extractable)  $\text{Fe}^{3+}$  (top, N=207) and BD-Fe (bottom, N=103) listed by sample matrix Munsell chroma, from least vivid (left) to most (right). The trend in reactive  $\text{Fe}^{3+}$  and BD-Fe content is as expected here, with higher chromas indicating the presence of more of each form.

Calculation of porewater salinity using the supernatant electrical conductivity of 1:5 dilutions of field moist soil (v/v) according to the Soil Taxonomy method for subaqueous soils (Soil Survey Staff, 2014) and sample bulk densities provided lower salinities than expected (Figure 4-9), particularly in the shoreface environment where overlying water salinity is known to range from 22-26 (Sjøgaard et al., 2017). Calculated mean salinity values were 11.8 in the shoreface A layer and 14.6 in the lagoon A layer. These are roughly half of the expected salinities in these materials, which should be similar to the salinity of the overlying water.

The difference in observed (calculated) and expected salinities may be due to several factors. Sample bulk density is probably altered by adding 10 cm<sup>3</sup> of moist sample to the centrifuge tubes used for the dilution; material is disturbed and added or removed as necessary to reach the desired volume. Samples with air-filled pore space, such as the agricultural soils (for which the calculated salinity means nothing) but also subaqueous soils that contain gas bubbles, result in a greater dilution than expected because they have less initial porewater. By assuming particle density of 2.65 g/cm<sup>3</sup>, porosity may be overestimated because organic matter (particularly in the A layer) and CaCO<sub>3</sub> have a lower particle density. By assigning an average expected salinity of 24, the equation of Dittmann et al. (2009) produces an electrical conductivity of 38,385 µS/cm, very close to the predicted value of ~36,000 µS/cm for the seas around Denmark (Tyler et al., 2017), validating the equation for seawater. However, porewater is not seawater, and contains a different mixture of ions in solution. Because electrical conductivity is dependent on ion activity and ion valency, different ionic solutions will produce different electrical conductivity/salinity



relationships (Simón and García, 1999). The measurement of electrical conductivity on the supernatant of 1:5 dilutions of field moist soil to distilled water (v/v) should therefore not be used to estimate overlying water salinity, unless these issues can be addressed.

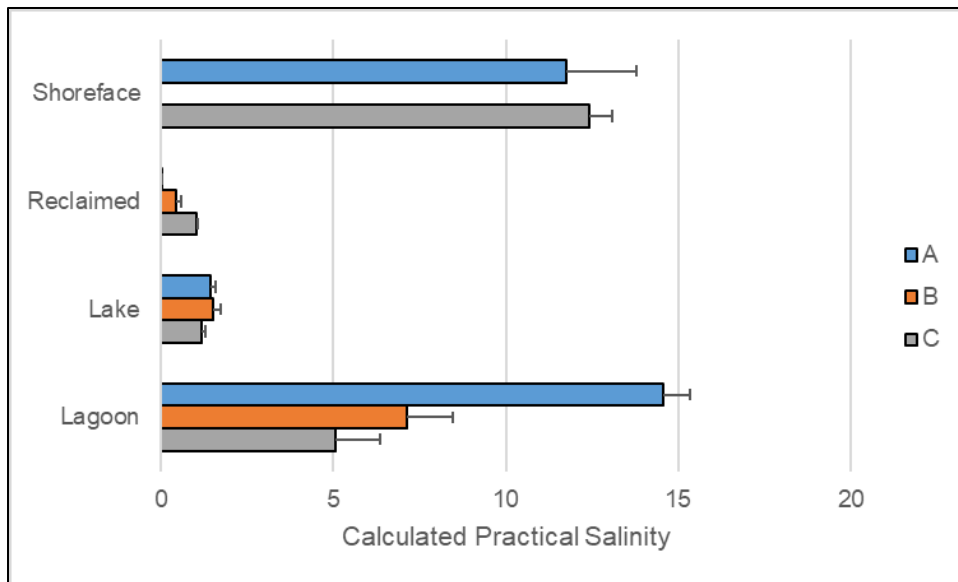


Figure 4-9. Mean calculated practical salinity of porewater in different layers (A, B, C) in the four landscape units sampled. Error bars show positive standard error.

Calculations assumed that all porosity was filled with porewater, so the reclaimed land values are erroneous. The shoreface A layer has roughly half the salinity of the overlying water, suggesting that this method may be unsuitable for estimating porewater salinity.

#### 4.4.2 Shoreface

The shoreface in this study was selected to present an example of materials unaltered by drainage and exposure to the atmosphere. Shoreface pedons were expected to consist of marine sediments formed via deposition and early diagenetic processes. Dominant colors were 5Y hue with chromas  $\leq 2$  (relatively grey). The A layer was much darker than the underlying C layer, with dominant values of 2.5 (black). Color values increased in the C layer to a dominant value of 5 (lighter grey). Both layers were dominantly nonfluid. The A layer was structureless (single grain), consisting primarily of loose sands with shell fragments. The C layer was dominantly structureless (massive), though was structureless (single grain) in some places (Table 4-2), indicating that these materials were not all deposited under the same environmental conditions (i.e. differences of flow regime, with coarser single grain materials deposited by faster moving water than the finer massive materials). The average lower depth of the shoreface A layer (identified primarily by color) was 16 cm and no B layer was described. The maximum sample depth was 172 cm (Table 4-3).

The shoreface is continuously flooded with seawater, and should therefore have been influenced by marine chemistry. The A and C layers have similar electrical conductivity (Figure 4-10), likely due to tidal pumping with seawater, resulting in a nearly uniform distribution of porewater salts in the profile. Unfortunately, the 1:5 (soil to water by volume) dilution used in the measurement of soil horizon conductivity presents issues when attempting to convert to porewater salinity. Nonetheless, the shoreface conductivity can be compared to the conductivity of the

reclaimed land or freshwater lake to see the substantial difference caused by the presence of seawater. The mean pH of the A layer was 7.7, and of the C layer was 8.2, close to the average global ocean surface pH of ~8.1 (Jiang et al., 2019) and the pH of upland soils containing more than a few percent  $\text{CaCO}_3$  (Rogovska et al., 2007). Bulk density varied little, with a mean near  $1.6 \text{ g/cm}^3$  in both layers (Figure 4-12).

Table 4-2. Gyldensteen Strand modal morphological features (multimodal where multiples appear) of landscape units and their master horizons. Hue  $\propto$  color wavelength, value  $\propto$  lightness, chroma  $\propto$  intensity, fluidity is measured by hand (moderately fluid samples can be squeezed through the fingers, leaving some in the palm; slightly fluid samples only allow some soil to pass between the fingers when squeezed), structure measures the occurrence of natural structural units (aggregates/peds) that dominate the sample volume. Structureless (single grain) materials were high in sand content (e.g. sands and loamy sands), structureless (massive) materials had higher contents of silt and/or clay. Descriptions and characterization data are given in Appendices F and G.

Landscape Unit	Layer	Hue	Value	Chroma	Fluidity	Structure	3% H <sub>2</sub> O <sub>2</sub> rxn	30% H <sub>2</sub> O <sub>2</sub> rxn	Other Common Features
Shoreface	A	5Y	2.5	1	Nonfluid	Structureless (single grain)	Yes	Very Slight	Weak H <sub>2</sub> S odor, shells
	C	5Y	5	2	Nonfluid	Structureless (massive)	No	Very Slight	Moderate H <sub>2</sub> S odor, shells, structureless (single grain)
Reclaimed Land	A	10YR	2	2	Nonfluid	Granular	No	Slight	Roots
	B	10YR	4, 5	3	Nonfluid	Subangular blocky	No	Slight	Fe and Mn concentrations, depletions
	C	2.5Y	5, 6	2	Slightly fluid	Structureless (massive)	No	Very Slight	Fe concentrations
Freshwater Lake	A	5Y	2.5	1	Nonfluid	Structureless (massive)	Yes	Strong	Roots, shells
	B	5Y	5	3	Nonfluid	Subangular blocky, structureless (massive)	No	Very Slight	Roots, shells, Fe concentrations, depletions
	C	2.5Y	5	1	Nonfluid	Structureless (single grain), structureless (massive)	No	Very Slight	Shells
Restored Lagoon	A	10Y	2.5	1	Moderately fluid	Structureless (massive)	Yes	Slight	Roots, shells, Fe concentrations
	B	2.5Y	5	3	Nonfluid	Subangular blocky	No	Slight	Roots, shells, Fe concentrations, depletions
	C	5Y	5	1	Nonfluid	Structureless (massive)	No	Slight, Very Slight	Shells, Fe concentrations

Table 4-3. Gyldensteen Strand average sampling depths (A, B layers) and maximum depth (C layer) in cm of zones of morphological alteration by landscape unit.

Layer	Landscape Unit			
	Shoreface	Reclaimed Land	Freshwater Lake	Restored Lagoon
A (mean)	16	25	41	39
B (mean)	n/a	148	135	122
C (max)	172	274	193	210

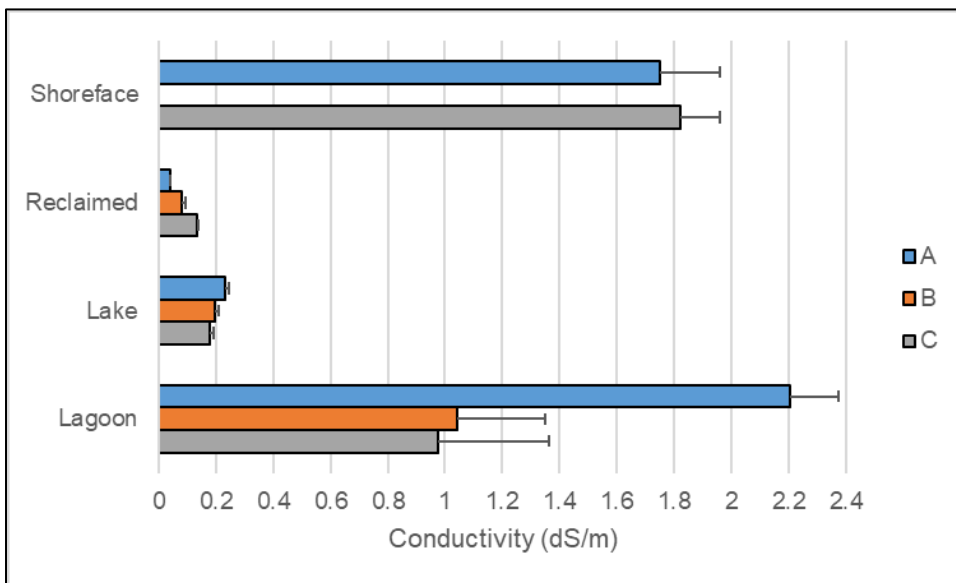


Figure 4-10. Mean sample conductivity measured on 1:5 dilutions of field moist soil to water (supernatants) of different layers (A, B, C) in the four landscape units sampled. Error bars show positive standard error. US Soil Taxonomy classifies soils as Frasiwassents (freshwater soils) if the measured conductivity using this method is below 0.2 dS/m in all horizons within 100 cm of the mineral soil surface. The lake soils are therefore borderline freshwater soils due to some horizons having higher conductivities. This criteria only applies to subaqueous soils, though the reclaimed land would meet that criteria if flooded with freshwater.

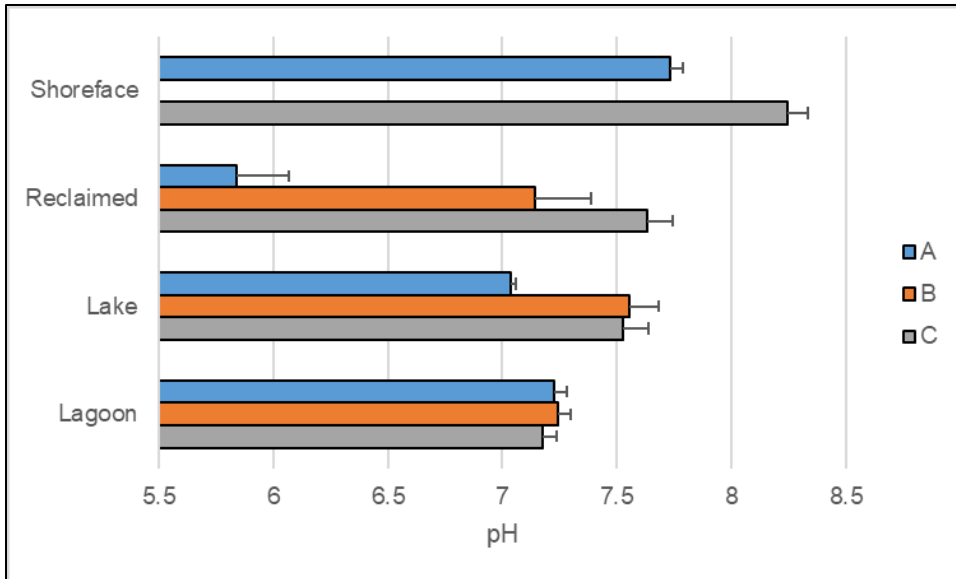


Figure 4-11. The mean sample pH of different layers (A, B, C) in the four landscape units sampled. Error bars show positive standard error.

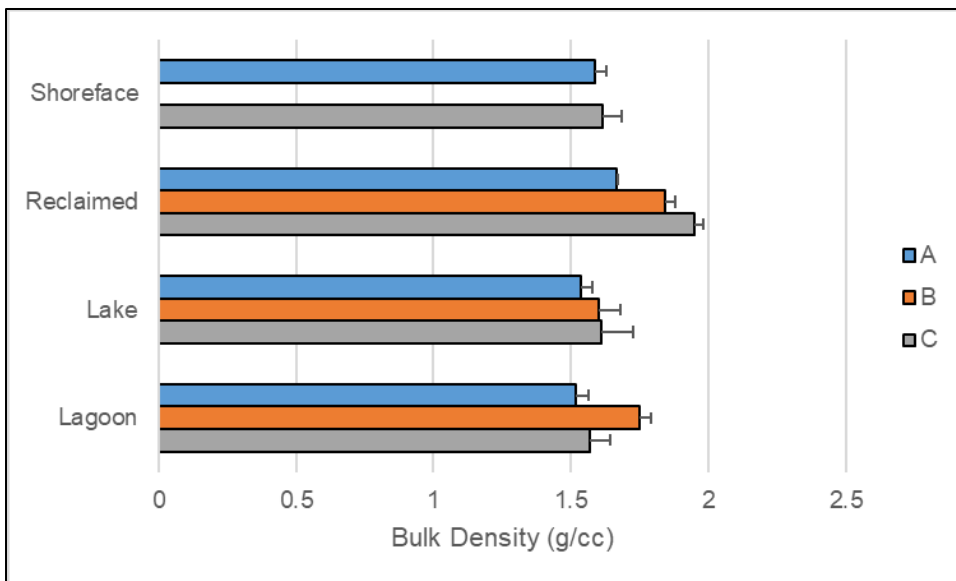


Figure 4-12. The mean bulk density of different layers (A, B, C) in the four landscape units sampled. Error bars show positive standard error.



The A layer changed color from black to grey upon addition of 3% H<sub>2</sub>O<sub>2</sub> (Table 4-2), evidence of recent diagenetic formation of metastable Fe-sulfides. Shoreface A horizons did have higher AVS contents (0.0009% AVS) than shoreface C horizons (0.0001% AVS) (Figure 4-13). This is consistent with the relationship between color change reaction and AVS content illustrated in Figure 4-1, and highlights that low AVS are sufficient to produce this reaction in structureless (single grain) materials. The H<sub>2</sub>S odor noted in many of the shoreface A and C horizons provides further evidence of active reduction of seawater sulfate (Table 4-2), a necessary process for the formation of metastable Fe-sulfides.

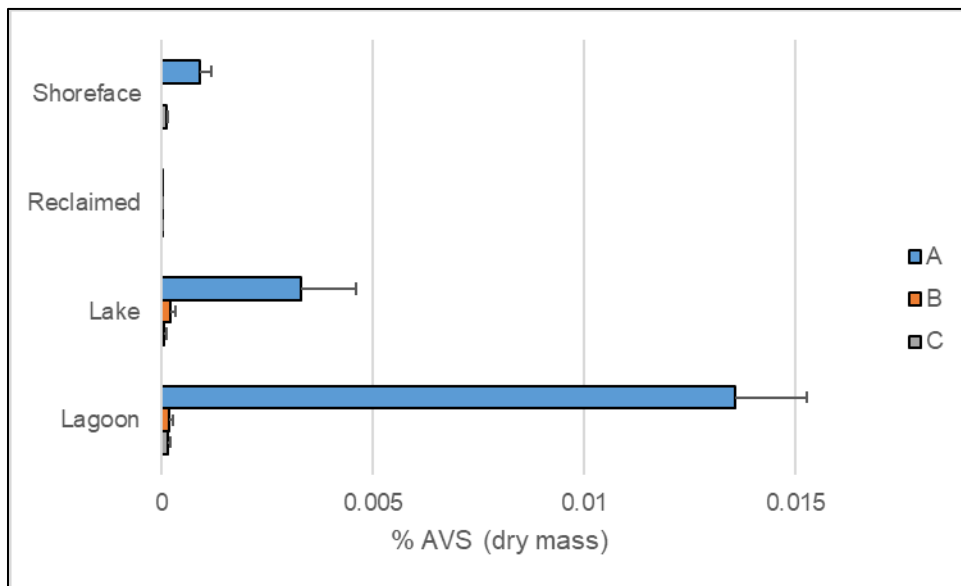


Figure 4-13. The mean AVS content of different layers (A, B, C) in the four landscape units sampled. The lower AVS content in the lake relative to the shoreface, both of which have been flooded for roughly the same period of time, suggests that sulfate (low in fresh water) is limiting the formation of AVS in the lake A layer. Error bars show positive standard error.

Though AVS can form quickly, CRS formation proceeds more slowly as AVS converts to CRS, primarily via continued reaction with  $H_2S$  (Leventhal and Taylor, 1990). This explains why AVS concentrations are generally low in subsurface layers (Figure 4-13). Not only is this the case in the shoreface pedons, but CRS has also accumulated to greater concentrations in the C layer than in the A layer (Figure 4-14). This is also reflected in the AVS/CRS ratio, which shows that CRS is dominant in both A and C layers, but that more AVS is present in the A layer (Figure 4-15). Seawater continually provides an excess of sulfate (evidenced by the high conductivity, Figure 4-10) for reduction, which can convert to  $H_2S$  as the S is reduced at some rate by microbial activity (evidenced by the  $H_2S$  odor, Table 4-2), so any AVS that forms in the C layer (or ends up there as a result of burial) does so under conditions that promote conversion to CRS. The CRS concentrations in the A layer may be lower simply because surface materials are younger in sedimentary environments, so CRS has had less time to accumulate there.

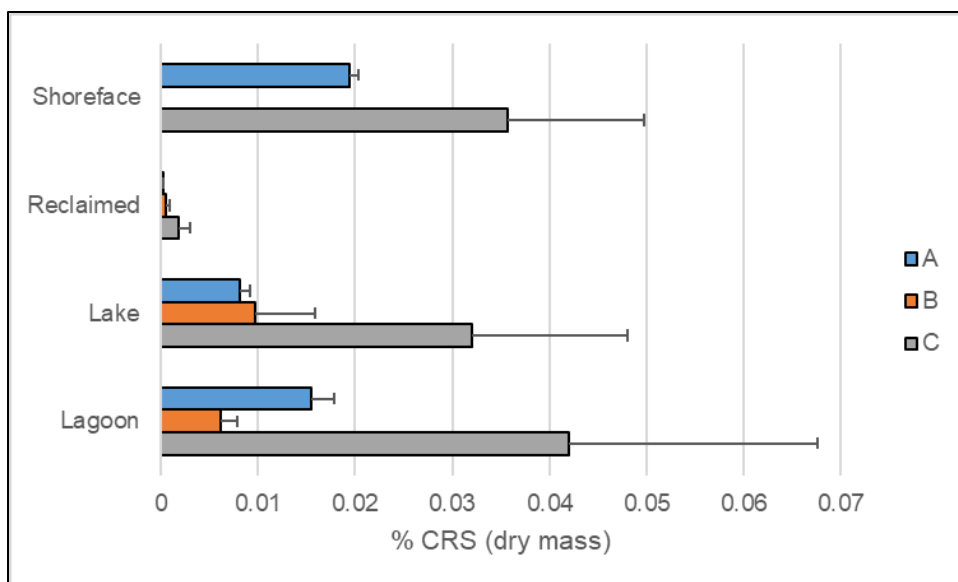


Figure 4-14. The mean CRS content of different layers (A, B, C) in the four landscape units sampled. Error bars show positive standard error. Like AVS in Figure 4-13, the difference between the lake and lagoon A layers is likely caused because the low sulfate concentration in freshwater is limiting CRS formation in the lake, while that limitation is not present in the lagoon.

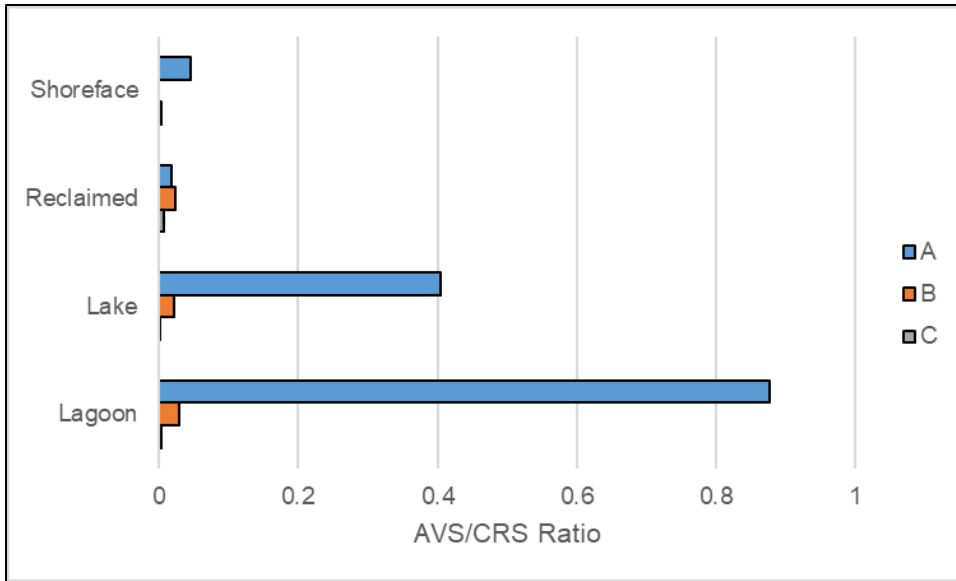


Figure 4-15. The AVS/CRS ratio of the mean AVS and CRS values for the three layers (A, B, C) in the four landscape units sampled. All values are below 1, indicating that the majority of S is in the CRS fraction in all cases. The high ratios in the lake and lagoon A layer are attributed to flooding of organic-rich topsoil, and the much higher ratio in the lagoon A layer likely shows the impact of abundant seawater sulfate on AVS accumulation in submerged topsoil.

Reactive  $\text{Fe}^{3+}$  concentrations are expected to be very low below the upper few cm in shallow marine sediments as a result of the microbial reduction of Fe (Kristensen et al., 2003; Kristiansen et al., 2002). The shoreface A layer and B layer contain 0.001% and 0.002 % reactive  $\text{Fe}^{3+}$ , respectively (Figure 4-16), consistent with expectations. Some  $\text{Fe}^{3+}$  will be generated from  $\text{Fe}^{2+}$  on an ongoing basis as a result of reaction with oxygenated seawater, but generally only along worm burrows (Kristensen et al., 2012) or in areas where groundwater is discharging (Williams et al., 2016). The only other source of  $\text{Fe}^{3+}$  will be as sediment additions to the surface, which are largely reduced and removed once buried if the forms of Fe oxides are available to microbial reduction.

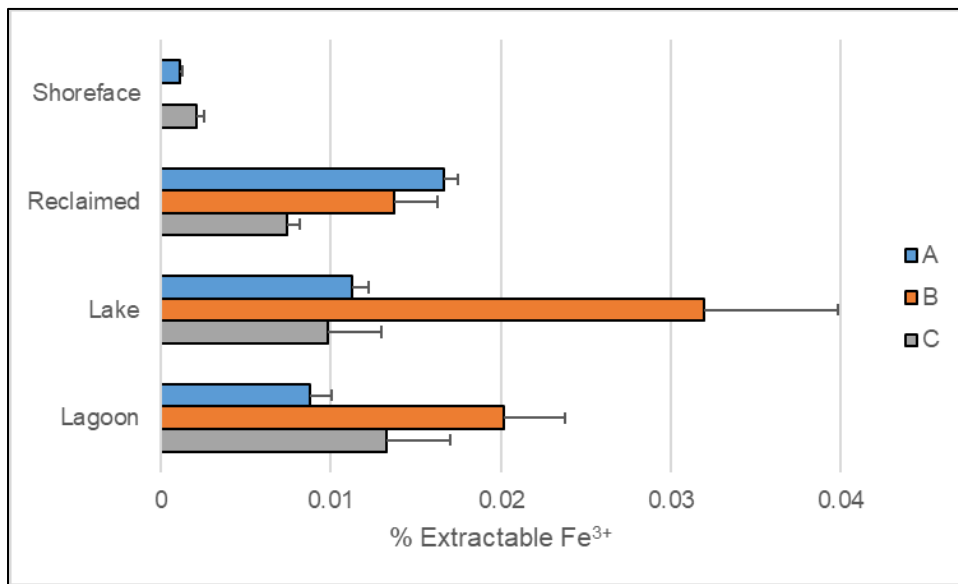


Figure 4-16. The mean reactive ferric Fe (0.5 M HCl extractable  $\text{Fe}^{3+}$ ) content of different layers (A, B, C) in the four landscape units sampled. Error bars show positive standard error.

In line with this process of burial and reduction,  $\text{Fe}^{2+}$  could be expected to occur at higher concentrations in the subsurface where it may be present in porewater; however, in the presence of porewater sulfide  $\text{Fe}^{2+}$  will react and precipitate as solid FeS/AVS (Rickard and Morse, 2005) and other minerals (Fanning et al., 1989). Mean reactive  $\text{Fe}^{2+}$  concentrations more than doubled from the shoreface A layer (0.0064%) to the C layer (0.016%) (Figure 4-17), somewhat surprising for an environment where porewater sulfide is expected due to the presence of abundant sulfate in seawater to be reduced via microbial activity. Shoreface C layer materials commonly exhibited an  $\text{H}_2\text{S}$  odor when freshly collected (Table 4-2) so there is no doubt that porewater sulfide was present in most, if not all, samples. The unexpected result of reactive  $\text{Fe}^{2+}$  in the presence of porewater sulfide may be due to several factors.

First, the somewhat poorly understood relationship between reactive Fe and carbonate/bicarbonate could mean that  $\text{Fe}^{2+}$  is present at the levels measured but in a form that is unavailable for reaction with porewater sulfide. When Fe is unavailable for plant uptake it can cause Fe chlorosis, which is commonly observed in plants grown on both carbonate-rich upland soils (Ferreira et al., 2019; Loeppert, 1986) and in seagrasses growing on carbonate-rich sediments (Anton et al., 2018; Duarte et al., 1995). This may be because the high pH and the high partial pressure of  $\text{CO}_2$  (particularly in wet soils) reduce the activity of  $\text{Fe}^{2+}$  through  $\text{OH}^-$  and bicarbonate, which may inhibit the reaction between  $\text{Fe}^{2+}$  and porewater sulfide. At the pH observed in these samples ( $>8.0$ , Figure 4-11), and under reducing conditions where sulfate reduction can occur, reactive  $\text{Fe}^{2+}$  should occur dominantly as  $\text{FeOH}^+$  (Hem and Cropper, 1962). Additionally, the abundant presence of bicarbonate in seawater

can favor the formation of  $\text{FeCO}_3$  (Hem, 1962), again a process that would reduce the activity of  $\text{Fe}^{2+}$  and potentially inhibit  $\text{FeS}$  formation. Some combination of ferrous carbonate/bicarbonate/hydroxide complexes may therefore have been present at a ferrous gel, extractable with the 30 minute 0.5 M  $\text{HCl}$  process used in this study, yet unavailable for precipitation as  $\text{FeS}$ .

Second, it is possible that some portion of the measured reactive  $\text{Fe}^{2+}$  was in fact occluded in a solid sulfide precipitate but was still solubilized by the 30 minute 0.5 M  $\text{HCl}$  extraction. Short extractions at this  $\text{HCl}$  concentration are not expected to extract most crystalline  $\text{Fe}$  species (Claff et al., 2010). However, in the shoreface environment where wave and tidal action may pump oxygenated seawater through the sediments, particularly coarsely textured sandy materials, redox alternations may cause an accumulation of short-range order or nano-particulate mineral phases that are susceptible to the extraction used here for reactive  $\text{Fe}$ . Thus, some portion of the  $\text{Fe}^{2+}$  extracted from the shoreface C layer may represent  $\text{AVS}$  or  $\text{CRS}$ , even though this would not ordinarily be expected.

Overall, there is more reactive  $\text{Fe}$  in the shoreface C layer than in the A layer. As the previous paragraphs highlight, this may be due to a combination of several factors that highlights a complex and poorly understood area of soil chemistry. Regardless, the reactive  $\text{Fe}$  fractions in both shoreface layers were dominated by  $\text{Fe}^{2+}$  (Figure 4-18), highlighting the reductive nature of the soil environment in shallow marine sediments. Despite this trend in reactive  $\text{Fe}$ , the majority of  $\text{Fe}$  in both layers of the shoreface is refractory  $\text{Fe}$  (Figure 4-19), either sequestered in grains of minerals that have not weathered under shoreface conditions, or otherwise in a

mineral form unavailable to microbial reduction. The DOP is higher in the A layer than in the C layer (Figure 4-20), reflecting the low BD-Fe content of the A layer (Figure 4-19).



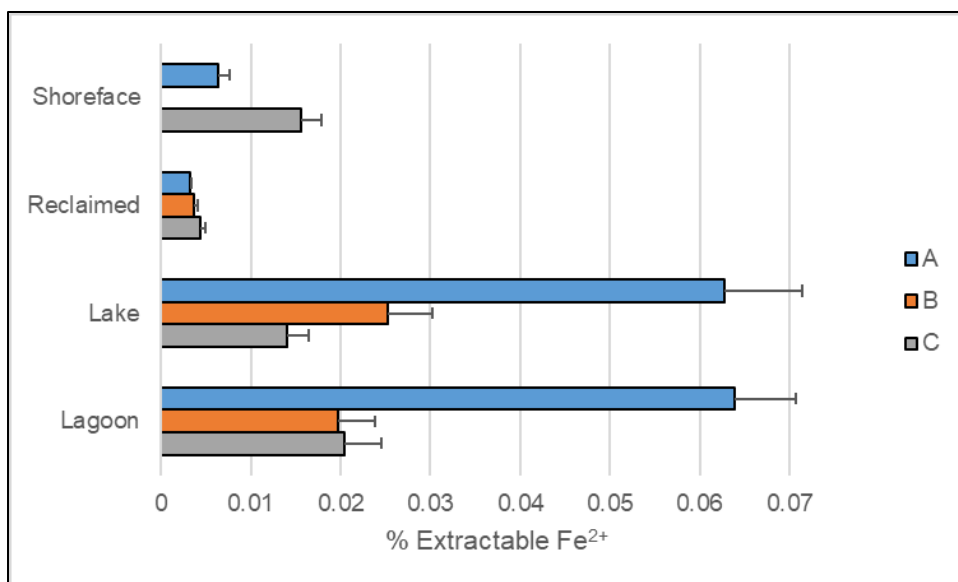


Figure 4-17. The mean reactive ferrous Fe (0.5 M HCl extractable Fe<sup>2+</sup>) content of different layers (A, B, C) in the four landscape units sampled. Error bars show positive standard error.

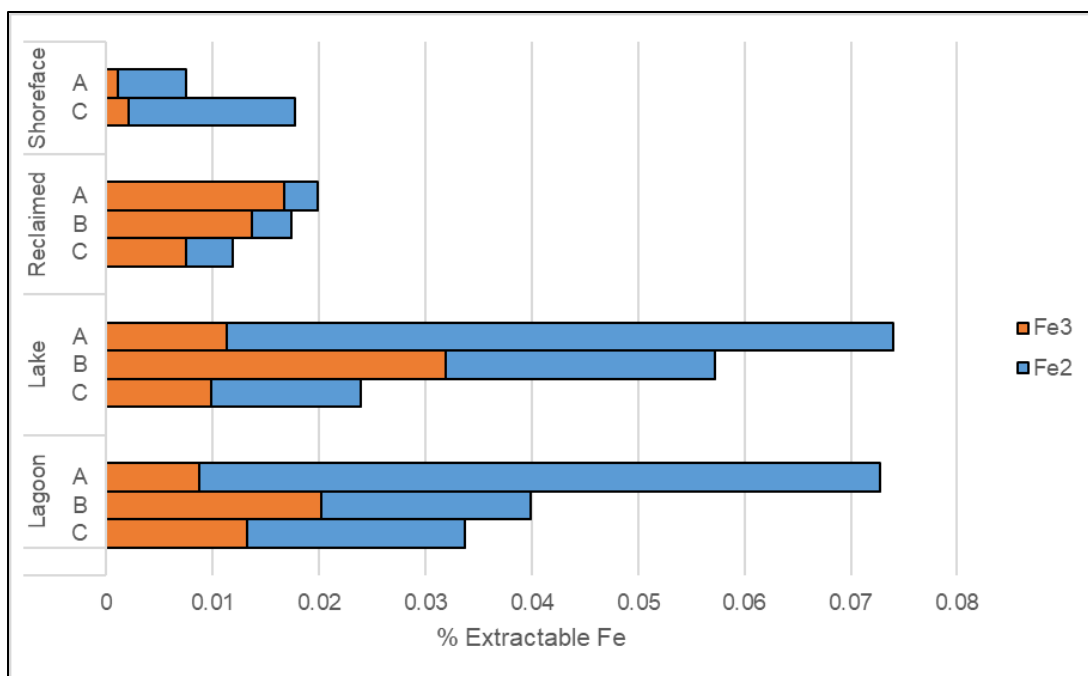


Figure 4-18. The mean relative contents of reactive Fe (0.5 M HCl extractable  $\text{Fe}^{3+}$  and  $\text{Fe}^{2+}$ ) in different layers (A, B, C) in the four landscape units sampled. Error bars show positive standard error.

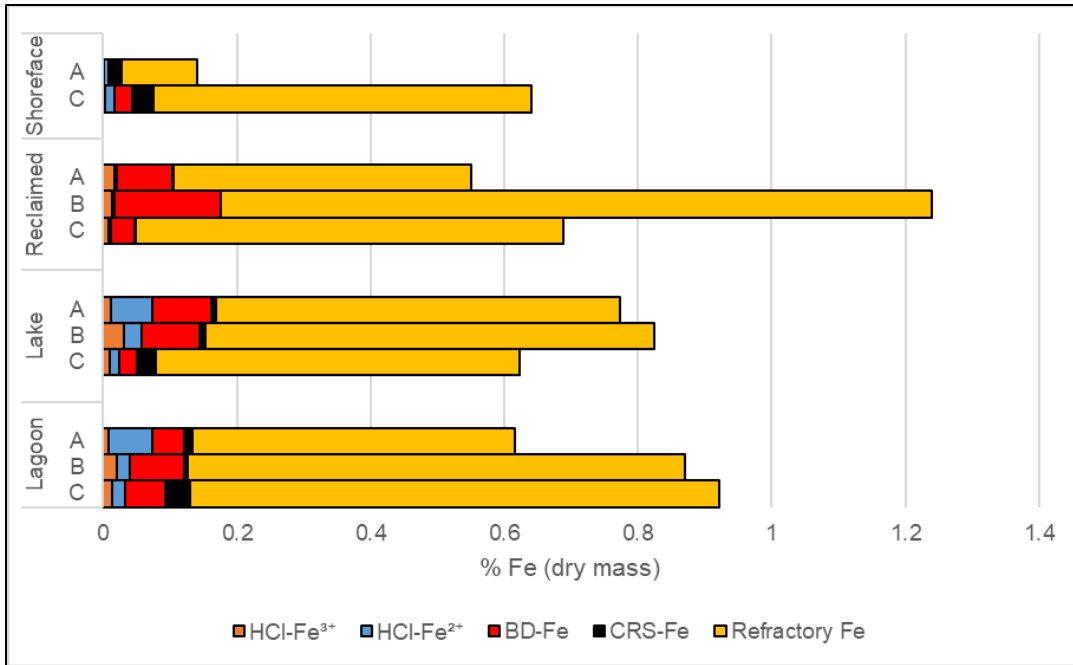


Figure 4-19. Gyldensteen Strand Fe fractions. The mean relative contents of reactive (0.5 M HCl extractable) Fe<sup>3+</sup> and Fe<sup>2+</sup> (from Figure 4-18), bicarbonate buffered dithionite extractable Fe (BD-Fe), CRS-Fe (assuming all CRS-S is in pyrite), and more refractory Fe in different layers (A, B, C) in the four landscape units sampled. Because a sequential extraction was not used, BD-Fe likely also represents some portion of HCl-Fe<sup>3+</sup>. In all settings, more refractory Fe is the majority of Fe.

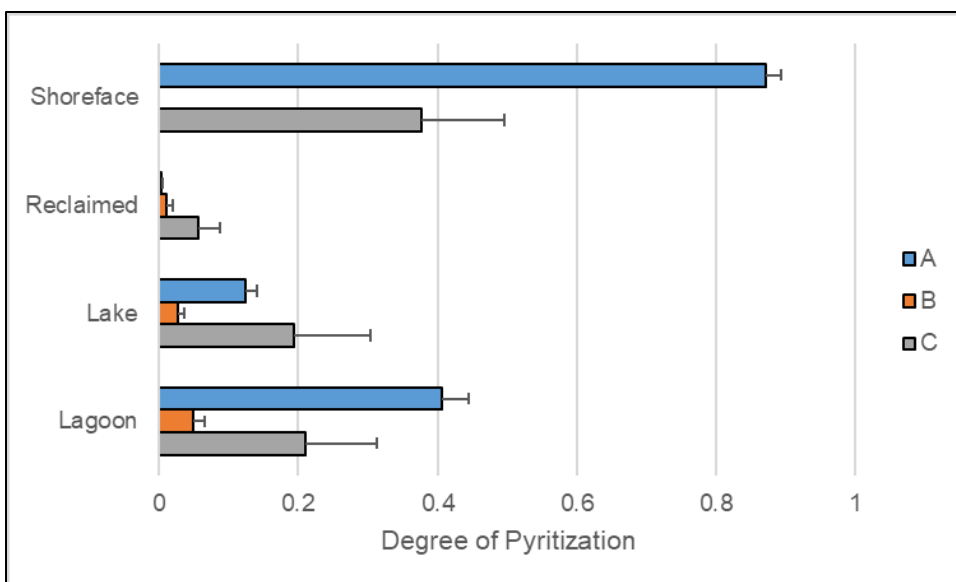


Figure 4-20. The mean degree of pyritization (DOP) of different layers (A, B, C) in the four landscape units sampled. DOP is operationally defined as  $(\% \text{CRS-Fe} + \% \text{AVS-Fe}) / (\% \text{CRS-Fe} + \% \text{AVS-Fe} + \% \text{BD-Fe})$ . Error bars show positive standard error.

Mean organic C content was 0.24% in the A layer and 0.48% in the C layer of the shoreface (Figure 4-21). Organic C often changes irregularly with depth in shallow marine sediments as a result of the burial of higher organic C surfaces by younger sediment lower in organic C (Demas and Rabenhorst, 1999). Organic C burial is an important process captured by several taxonomic groups in US Soil Taxonomy (Soil Survey Staff, 2014). This process has occurred in the shoreface, where several relatively high-C horizons in the C layer have resulted in the higher mean organic C content of that layer.

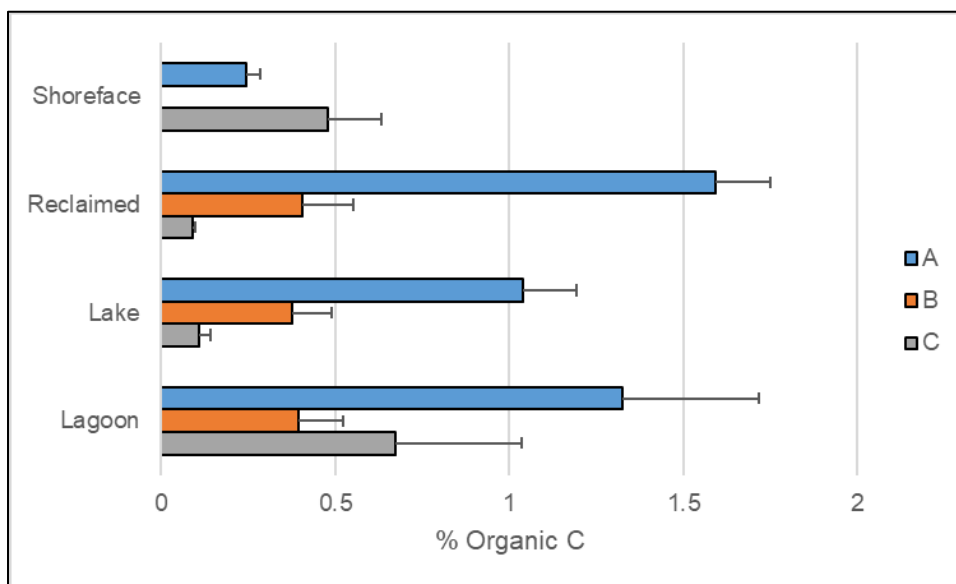


Figure 4-21. The mean organic C content of different layers (A, B, C) in the four landscape units sampled. Error bars show positive standard error.

In the shoreface, average carbonate C was low in the A horizons (0.26%) (Figure 4-22), possibly as a result of weathering in the high energy environment. Despite the alkaline pH, calcium carbonate fragments have been shown to dissolve at the sediment surface in marine environments (Still and Stolt, 2015), though once buried may become occluded and persist. To further complicate matters, the geology of the region consists of relatively young glacial deposits, which include calcium carbonate rocks including chalk and limestone (Nilsson and Gravesen, 2018), so the provenance of carbonate C is difficult to determine in this setting.

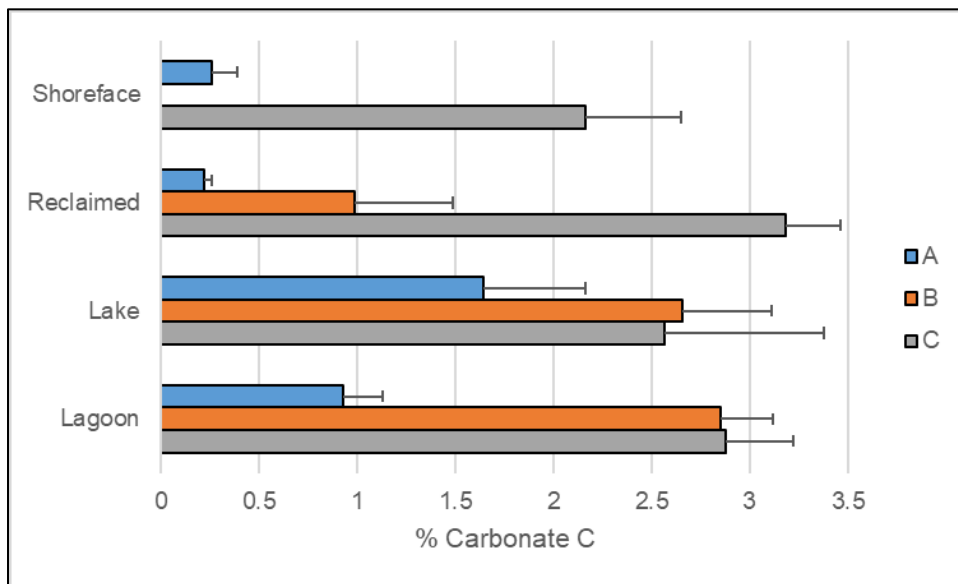


Figure 4-22. The mean carbonate C content of different layers (A, B, C) in the four landscape units sampled. Error bars show positive standard error.

Overall the shoreface is a structureless shallow marine sedimentary column. It is permanently saturated with seawater, giving it a high electrical conductivity and an alkaline pH. It has a black surface as a result of AVS, which has largely converted to CRS below the surface. Little reactive Fe is present throughout, and most of this is in the reduced form ( $\text{Fe}^{2+}$ ), possibly at a low activity due to the high pH and carbonate content. Substantial refractory Fe is present. Organic C and carbonate C are distributed irregularly throughout the profiles, reflecting the sedimentary nature of this environment.

#### 4.4.3 Reclaimed land

The area of reclaimed land should offer insight into what subaerial features and chemistry develop in drained shallow marine sediments (i.e. the shoreface) in this region over the course of ~150 years. The A layer has developed granular structure, many small crumb-like aggregates typical of subaerial topsoil. Its color is dominantly 10YR 2/2, very dark brown. It contains roots, and was planted with beets at the time of sample collection. A B layer has formed, marked by the development of subangular blocky structure, peds that are separated by cracks and pores in the soil and that come apart along their faces with relative ease. It has also developed a redder color, dominantly 10YR 4/3 and 5/3, brown. The B layer matrix is colored irregularly by red and black Fe and Mn oxide concentrations, and much lighter and less vivid depletions. The A and B layers were nonfluid. A change in color, fluidity, and structure marked the transition into the C layer. The C layer was 2.5Y 5/2 (greyish brown) and 6/2 (light brownish grey), the yellower hue and lower chroma corresponding to shoreface-like materials. Similarly, the C layer became slightly fluid

and structureless (massive) (Table 4-2) also typical of material that accumulated under water. The A layer extends on average to a depth of 25 cm (deeper than in the shoreface), and the B layer extends on average to 148 cm. The deepest sample was collected from 274 cm (Table 4-3).

The reclaimed land profile no longer reflects seawater inundation. Its electrical conductivity had dropped dramatically in all layers relative to the shoreface (Figure 4-10). The reclaimed land A layer average pH was 5.8, substantially lower than the shoreface pH (Figure 4-11). This is in line with expectations of upland soils in humid parts of the world as a result of precipitation and leaching (Jenny, 1941). Changes in pH were less pronounced in the B layer but were still lower than in shoreface materials (7.1), and rose in the C layer to an average of 7.6 (Figure 4-11). Bulk density increased slightly with depth (Figure 4-12), perhaps as a result of consolidation after dewatering and the use of heavy agricultural equipment.

No AVS was expected in reclaimed land soils (or any drained upland soils anywhere) because metastable Fe sulfides (~AVS) will spontaneously react with atmospheric oxygen over the course of several minutes to form sulfate from the sulfide present. As expected, no substantial AVS was measured in reclaimed land horizons (Figure 4-13).

In the reclaimed land unit, very little CRS was measured in A and B layers, with a small increase in the C layer (Figure 4-14). This is likely relict pyrite, formed via diagenesis in marine sediments as they accumulated and preserved below the seasonal high water table even in a dewatered landscape where pyrite higher in the profile has oxidized and been removed from A and B layers. Like AVS, CRS will



spontaneously react with oxygen, though the process is much slower in the case of pyrite and most of the oxidation that is observed in oxidizing CRS-containing materials is a result of acceleration of the oxidation process by chemoautotrophs (Arkesteyn, 1980; Fanning et al., 2017). The DOP does increase with depth though is very low overall (Figure 4-20), indicating oxidation of pyrite and formation of Fe oxide minerals as a result of subaerial pedogenesis, which may be limited somewhat in the reclaimed land C layer (where the mean DOP is greater than the mean DOP in flooded landscape B layers).

Mean reactive  $\text{Fe}^{3+}$  contents were highest in the A layer (0.017%) and decreased with depth through the B layer (0.014) and into the C layer (0.0074%) (Figure 4-16 and Figure 4-18). These contents were substantially higher than those in the shoreface, suggesting that reactive  $\text{Fe}^{3+}$  may have accumulated throughout the reclaimed land soil profile since reclamation. This is consistent with the greater BD-Fe contents seen in Figure 4-19. Some of this Fe may have come from the oxidation of Fe in AVS and CRS present at the time of land reclamation. Much of it may have come from more refractory forms like those present in the shoreface, previously sequestered in crystalline minerals. Mineral weathering is generally most intense at the soil surface as a result of alternating wet-dry cycles and organic acids produced by plants, which release Fe from silicate minerals and other sequestered forms, predominantly from the A layer where plant roots are most abundant (Certini et al., 2002). This would form reactive  $\text{Fe}^{3+}$ , providing Fe for the formation of more crystalline Fe oxides that are responsible for the soil color and the Fe oxide concentrations. Formation of reactive  $\text{Fe}^{3+}$  primarily in the A layer and to a lesser

extent in the B layer (and leaching down from the A layer) could explain the decrease of reactive  $\text{Fe}^{3+}$  content with depth seen in the reclaimed land.

Relatively little reactive  $\text{Fe}^{2+}$  was measured in reclaimed land horizons (mean  $<0.005\%$ ), though it did increase slightly with depth (Figure 4-17). Upland soils are generally wettest at the bottom of the profile due to groundwater saturation, so that is where anoxic conditions can be established and where Fe reduction is likely to occur. Similarly, areas of reclaimed land are generally pumped continuously to keep them dry and to prevent saltwater from intruding and reaching the surface (Zuur, 1952). Total reactive Fe content was low throughout reclaimed land layers and was similar to the shoreface layers, though it was highest at the surface and was predominately the  $\text{Fe}^{3+}$  form in all layers (Figure 4-18). The greatest BD-Fe accumulation was in the B layer, though a substantial amount seems to have formed in the A layer as well relative to the shoreface (Figure 4-19). The accumulation in the B layer may be due to leaching of soluble Fe and precipitation of crystalline Fe oxides.

Mean organic C contents in the reclaimed land A layer were 1.6% and decreased quickly through the B layer and C layer (Figure 4-21). Organic matter accumulation is a defining feature of A horizons (Soil Survey Staff, 2014), reflecting the signature left by the high primary productivity of subaerial environments. This relatively high organic C content also matches expectations based on the dark colored granular description of this layer (Table 4-2).

Carbonate C levels in the reclaimed land averaged 0.22% in A layer and increased with depth to 2.2% in the C layer (Figure 4-22). This shows the impact of weathering in a humid environment, the loss of carbonate C at the surface likely

being due to the addition of weak acids from precipitation and root exudates. In the C layer the mean pH remains above 7.5, and much carbonate C remains.

Reclaimed land is formed by the drainage of shallow marine sediments, superimposing subaerial soil features on sedimentary pedons while removing features unique to the subaqueous environment. Conductivity and pH decrease with the loss of seawater and the addition of precipitation and leaching. Reduced inorganic sulfur (AVS + CRS) is lost from most of the profile. Organic C accumulates in the surface, darkening it and helping to form granular structure and reactive Fe. The reactive Fe pool shifts from being dominantly  $\text{Fe}^{2+}$  to dominantly  $\text{Fe}^{3+}$ . Carbonate is weathered from the surface of the profile. Subsoil forms (a B layer) with subangular blocky structure, redder hues, and higher chromas. The soil consolidates and becomes nonfluid. Below the B layer, original sedimentary characteristics persist in the C layer including an alkaline pH, carbonate C, CRS, and yellower/greyer colors.

#### 4.4.4 Freshwater lake

Once flooded, reclaimed land was expected to lose some of its subaerial properties and to reacquire some subaqueous properties. Within two years of submergence the freshwater lake A layer had lost its granular structure, reverting to structureless (massive). It maintained a black color, though the hue became less red (5Y 2.5/1). Both roots and shells were present, and it remained nonfluid. The B layer maintained a higher chroma (5Y 5/3) and subangular blocky structure in many samples. Other samples were structureless (single grain), but maintained higher chroma colors, visible Fe oxide concentrations, and/or roots. The C layer was similar to the C layer in the shoreface and the reclaimed land, though a greater proportion of

samples were structureless (single grain) and nonfluid (Table 4-2). The A layer extended to a mean depth of 41 cm and the B layer to 135 cm, with the deepest sample being 193 cm (Table 4-3).

Restoration with freshwater results in some different environmental parameters than existed prior to land reclamation. Electrical conductivity was marginally fresh, with the mean of the A layer just exceeding the 0.2 dS/m threshold for classifying freshwater soils (0.23 dS/m). The underlying horizons did fall below that threshold (Figure 4-10). Mean pH in the A layer increased relative to the reclaimed land A layer, rising to 7.0 (Figure 4-11). This may be due to the constant saturation allowing shells to react and raise the pH.

The mean content of AVS increased substantially in the A layer, exceeding the mean in the A layer of the shoreface (Figure 4-13). The 3% H<sub>2</sub>O<sub>2</sub> reaction was also positive in most of the freshwater lake A horizons (Table 4-2). While commonly seen at the surface of subaqueous soils and sediments in marine and estuarine environments due to the high content of sulfate available for reduction and reaction with Fe to form metastable Fe sulfides (Fanning et al., 1993), this feature has only recently been reported in non-tidal (though still sometimes saline) soils of the western US (Duball et al., 2020). In this setting it may be due to the relatively high electrical conductivity of the samples, possibly indicating introductions of seawater and sulfate from sea spray or groundwater exchange. Nonetheless, comparing the A layer AVS in the lake to the shoreface (Figure 4-13) suggests that lower sulfate content is limiting Fe sulfide formation in the lake. A small AVS increase was also seen in the B layer, though was hardly detectable in the C layer. The Fe oxides in the B layer are highly

reactive with any  $\text{H}_2\text{S}$  that flows, forms, or diffuses into contact with them, spontaneously forming metastable Fe sulfides, which likely explains the slight increase in AVS seen in the B layer.

Mean CRS concentrations in all freshwater lake layers are much higher than in reclaimed land layers. The C layer has a mean CRS concentration comparable to that of the shoreface C layer (Figure 4-14), suggesting that the lake landscape may have experienced less leaching and weathering than the area of currently reclaimed land. The CRS in the A and B layers of the freshwater lake may represent recently formed pyrite as a result of sulfate reduction and reaction with Fe, which begins with  $\text{FeS}$  production but progresses to  $\text{FeS}_2$  (pyrite) production as long as there is an abundant supply of sulfide (Fanning and Fanning, 1989; Rickard, 1997). However, some of the CRS in the B layer may represent relict CRS preserved since before drainage, particularly if the freshwater lake landscape was less effectively drained. The most common 30%  $\text{H}_2\text{O}_2$  reaction in the freshwater lake A layer was strong, more reactive than any other landscape layers in this study, but neither CRS nor organic C seems to explain this (Figure 4-2 and Figure 4-3). The strong reaction may instead be due to Mn oxides. Mn can enter solution, move, and precipitate as Mn oxides relatively quickly in wet and flooded soils (Rabenhorst and Post, 2018), and might not be flushed out of the freshwater lake by tidal action. Mn oxides typically create a violent reaction with 30%  $\text{H}_2\text{O}_2$ , though perhaps this was mediated by the saturated state of the samples when the test was conducted, freshly collected below the lake bottom. Additional work would need to examine this possibility. The

AVS/CRS ratio is highest in the A layer (Figure 4-15), likely reflecting the role of topsoil organic C in driving sulfate reduction and the formation of AVS.

Mean reactive  $\text{Fe}^{3+}$  in the freshwater lake was lower in the A layer (0.011%) than in the restored land A layer, highest in the B layer (0.32%), and comparable in the C layer (0.0098%) to the content in the reclaimed land C layer (Figure 4-16). Mean reactive  $\text{Fe}^{2+}$  was highest in the A layer (0.63%) and decreased with depth in the in the B layer (0.025%) and C layer (0.014%) (Figure 4-17). Total reactive Fe is substantially higher in the A and B layers of the lake than in the reclaimed land, though the C layer is comparable to the shoreface C layer (Figure 4-18). This is likely a result of Fe moving between pools as a result of environmental changes. The shoreface initially had little reactive Fe and substantial refractory Fe, though the reclaimed land showed an accumulation of reactive Fe and BD-Fe in the A layer as a result of increased weathering of refractory Fe. Crystalline BD-Fe oxides accumulated in the A and B layers of the reclaimed land, indicated by the changes in color (redder hue, higher chroma) and accumulation of Fe oxide concentrations. After submergence and conversion to a freshwater lake, much of that crystalline Fe would be available for microbial reduction and mobilization. This may explain the substantial increase in reactive Fe in the freshwater lake relative to the reclaimed land. A portion of the oxidized Fe could be related to anaerobic microbial oxidation of Fe, linked to the reduction of other terminal electron acceptors besides diatomic O, such as nitrate (Straub et al., 1996). Some of this Fe may also have been derived directly from decomposing roots and other plant matter remaining from the period of

agricultural production on this land. The Fe may in turn help to explain the slightly high electrical conductivity of the A layer in the freshwater lake.

The mean organic C concentration of the freshwater lake decreased with depth, consistent with the pattern seen in the reclaimed land soil. The mean content in the A layer was 1.0%, somewhat less than in the reclaimed land A layer, though the freshwater lake B and C layer organic C contents were extremely close to those of the reclaimed land (Figure 4-21). This is likely a signature of the high organic C content that had accumulated in the A layer during its period of exposure and agricultural productivity. Once inundated, this organic C drives microbial growth, quickly establishing an anoxic soil environment and driving the reduction of even crystalline  $\text{Fe}^{3+}$  to  $\text{Fe}^{2+}$  (Lovley, 1993), which can then enter the water column. In fact, shortly after the freshwater lake was flooded, large accumulations of Fe oxide flocculate were observed at the soil surface, coloring the lake red. Consider the relative contributions of  $\text{Fe}^{3+}$  and  $\text{Fe}^{2+}$  to the total reactive Fe pool (Figure 4-18). In the A layer, where organic C is most abundant,  $\text{Fe}^{2+}$  dominates. In the B layer, where organic C is much less abundant and crystalline Fe is evident, the two redox species are nearly balanced. In the C layer, which has remained saturated,  $\text{Fe}^{2+}$  is again dominant. In the A and B layer there is more BD-Fe than reactive Fe (Figure 4-19). Possibly reflecting the mobilization and recrystallization of Fe oxides in the surface now that they can no longer be effectively leached through or flushed from the lake system. The DOP has increased in the A layer relative to the reclaimed land and remains high in the C layer, though the B layer has yet to change substantially (Figure 4-20).

Mean carbonate C is again somewhat irregularly distributed, evidenced by the relatively large standard errors on the measurements in the lake (Figure 4-22). Many relict shells remain throughout these profiles from before land reclamation.

Once restored as a freshwater lake, many subaqueous characteristics do return to reclaimed land within two years. Structure is lost from the surface layer, and it begins to accumulate AVS, and CRS begins to accumulate as well, although low salinity may result in low sulfate limiting sulfate reduction in this setting. DOP increases, but the B layer is insulated from short term changes over the two years since submergence. The pH increases (likely due to the abundant shells in this landscape), though under freshwater the electrical conductivity remains low. Organic C decomposes and drives an increase in the reactive Fe pool, largely as  $\text{Fe}^{2+}$ . Yet many other features are retained or changed. Subaerial structure and color remains in the B layer, more reactive Fe is generally available, and the surface still contains more organic C than was observed on the shoreface.

#### 4.4.5 Restored lagoon

The restored lagoon was expected to change in many of the same ways as the freshwater lake after submergence. Morphological changes proceeded in the lagoon as they did in the lake with few exceptions (Figure 4-23). Structure was lost in the A layer, though subaerial color and structure were retained in the B layer. Roots and shells were present, though some of the surface shells were recent biogenic additions. Some Fe concentrations were observed in the surface, generally along marine faunal burrows. The A layer did become moderately fluid (Table 4-2), having been reworked and ventilated by bioturbation or water movement, introducing oxygen and



accelerating organic matter decomposition (Valdemarsen et al., 2018). The mean A layer depth was 39 cm, the mean B layer depth was 122 cm, and the maximum sample depth was 210 cm (Table 4-3).



Figure 4-23. A soil profile collected from the restored lagoon showing the three morphologically distinct layers. At the surface (top of the photo) are black A horizons that have lost their structure and begun to accumulate metastable Fe sulfides (0-72 cm), below this are the consolidated red/brown B horizons that are nonfluid to slightly fluid (72-138 cm), and in the lower part of the profile are gray C horizons that are still slightly to moderately fluid (138-162 cm).

The lagoon seawater resulted in several chemical differences. Electrical conductivity increased in all layers relative to the restored land and freshwater lake. It was substantially higher in the surface, 2.2 dS/m compared to 1.0 dS/m in the B layer and 0.97 dS/m in the C layer (Figure 4-10), caused by seawater moving through the landscape. The pH value was 7.2 throughout the A, B, and C layers (Figure 4-11), almost certainly due to inundation with alkaline seawater and the dissolution of the abundant shells throughout the layers. Bulk density was slightly higher in the B layer than in the A or C layers (Figure 4-12), perhaps a legacy of compaction followed by reworking of the surface by waves and organisms.

The mean AVS content in the A layer of the restored lagoon was several times greater than it was in the freshwater lake (0.014%), though the B and C layer and contents were similar to those in the freshwater lake (Figure 4-13). Again, this increase corresponded to color changes in response to the 3%  $\text{H}_2\text{O}_2$  reaction in the A layer (Table 4-2). The substantial difference in the lagoon AVS content is likely caused by the abundance of sulfate in seawater, which may be limiting in the freshwater lake.

Similarly, CRS is higher in the A and B layers of the lagoon than in reclaimed land, indicating that it is forming again. It is also much higher in the C layer (Figure 4-14), though this is likely relict pyrite preserved through land reclamation by being below the water table. Like AVS, the higher CRS content in the lagoon A layer than in the freshwater lake A layer is likely caused by the abundant sulfate in seawater. The AVS/CRS ratio in the lagoon A layer is the highest observed in all settings in this study (Figure 4-15), indicating that the organic-rich A layer of topsoil drives

anomalous AVS accumulations when submerged by seawater. The DOP has also increased, though substantial reactive Fe remains to transform to pyrite, so the DOP has not yet reached the level of the shoreface A layer (Figure 4-20). Like the lake, the B layer seems to be somewhat buffered or insulated against these changes in the two years since submergence, though the DOP is higher there than in the lake, possibly reflecting faster changes under the lagoon restoration method.

Reactive Fe follows the same patterns in the lagoon as it does in the freshwater lake. It has increased overall, is dominantly  $\text{Fe}^{2+}$  in the A layer, is split nearly evenly between redox species in the B layer, and is dominantly  $\text{Fe}^{2+}$  in the C layer (Figure 4-18). The B layer contains more BD-Fe than the A or C layers (Figure 4-19), showing the legacy of accumulation during the period of land reclamation, and perhaps the impact of reduction and flushing in the A layer, which has less BD-Fe (compared to the lake A layer, which had roughly the same amount of BD-Fe as the lake B layer).

Organic C mean concentration in the lagoon follows nearly the same pattern as in the freshwater lake, though it is much higher in the C layer (0.67%) (Figure 4-21). Like the shoreface just outside of the lagoon, this carbon likely represents buried marine surfaces with higher organic C contents, again reflecting the sedimentary provenance of these materials. Carbonate C is lower in the A layer (0.92%) than in the underlying layers (2.8% and 2.9%) (Figure 4-22), possibly indicating the marine dissolution of surface shells since the tides have returned.

Overall, the restored lagoon is very similar to the restored lake. Both have lost soil structure in the A layer and begun to accumulate AVS and CRS, though at a

much greater rate in the lagoon. Iron dynamics are similar in both cases, with much more reactive Fe being present than in the shoreface. The B layers remain somewhat unaltered, retaining subaerial soil structure and color. Organic C remains high in the surface.

#### 4.5 Conclusions

Land reclamation, and its subsequent restoration, leaves an indelible mark on the landscapes where these processes occur. Once drained, shallow marine sediments consolidate, form soil structure, accumulate organic C in the surface, and accumulate crystalline and reactive Fe throughout the profile. Soil chemistry is driven by climate rather than water column attributes, with precipitation driving changes in pH and electrical conductivity. Subaerial A and B horizons form as a result of these processes, within 150 years at Gyldensteen Strand. Below the depth of drainage and alteration, marine sedimentary characteristics can persist, though leaching processes can influence even this zone by removing salts. Accumulations of marine materials such as shells can counterbalance this, maintaining alkaline pH even in B horizons. Buried sedimentary organic C in saturated C horizons may persist for centuries or longer, unaffected by environmental changes in the overlying material.

After flooding with either fresh or salt water, A horizons acquire marine sedimentary characteristics with the loss of subaerial characteristics within two years (Figure 4-23), including the obliteration of soil structure, the release of reactive Fe, and the accumulation of both AVS and CRS. However, these processes now operate at much greater rates than before due to the abundant organic C left in these horizons. After two years of submergence, B horizons maintain much of the morphologic and

chemical characteristics that they acquired during their subaerial formation (structure and color), so continued observation is warranted to determine the longer term consequences of chemical and physical changes in these materials even after subaerial A horizons appear to have acquired subaqueous/sedimentary characteristics. The B horizons, substantially altered by subaerial exposure, can be expected to continue to serve as sinks for CRS and sources of reactive Fe for many years to come, processes which will become widespread along the coastlines of the world as they are inundated by rising seas.

These processes will continue to play out on a large scale, so it is vitally important to environmental management that we continue to improve our understanding of the impacts of sea-level rise. We recommend that sediment/subaqueous soil surveyors conduct the 3%  $\text{H}_2\text{O}_2$  color change test even in freshwater environments, where metastable Fe sulfides have in the past been assumed not to occur. Where possible, survey measurements should include AVS, CRS, and reactive Fe speciation. The 30%  $\text{H}_2\text{O}_2$  test, while useful in the identification of high-S sulfidic materials, requires greater testing and validation in low-S settings, and as it relates to the presence of Mn oxides in saturated samples.

## Chapter 5: Subaqueous soil-landscape model development and evaluation for Rhode and West Rivers, Maryland

### 5.1 Abstract

Rhode River and West River, subestuaries on the western shore of Chesapeake Bay, contain a diverse array of subaqueous soils that range from submerged paleosols to finely-textured fluid soils. A subaqueous soil survey was completed for the Rhode River subestuary by collecting bathymetric data, delineating landforms, and sampling soils across this submerged landscape. Soil map units were developed by correlating soil properties and taxonomic classification with landscape position. Together with supporting information about the dominant factors of soil formation in this landscape, these data were used to develop a conceptual subaqueous soil-landscape model of soil genesis that explains soil mapping distribution in western shore Chesapeake Bay subestuaries. This model was used to develop a draft soil map for West River, which was then sampled along transects. Transect samples were classified and these data were resampled via a bootstrapping method to determine if the predictions of the West River soil survey were significantly different from random predictions. Significant information was provided by the survey, and suggestions for future refinement of the statistical method are discussed.

### 5.2 Introduction

Above the water's edge, soil survey and mapping efforts over the last century have yielded a high quality spatial database available for nearly the entire U.S. that

includes a host of soil properties and accompanying guidance on best uses, limitations, and potential hazards (Soil Survey Staff, 2016). One of the key tools facilitating the mapping of over 2 billion acres in the US has been the soil-landscape paradigm (SLP), which recognizes that soils change systematically and predictably across the landscape (Hudson, 1992). Operating under the SLP, conceptual models have been developed to explain the covariance of soils and landforms in landscapes around the world (Hudson, 1990). Thus, as you understand what governs the changes and distribution of soils in one area, based on landform analysis, you can then predict the distribution of various soils (and soil properties) in similar areas. This approach has been used for much of the past century to rapidly produce maps of terrestrial soils as 3-D natural bodies, by developing conceptual models that relate soil properties to the factors and processes of soil formation (Jenny, 1941; Simonson, 1959).

In using the SLP to conduct a soil resource inventory, landforms are identified and strategically sampled, avoiding the cost and time constraints of exhaustive grid type sampling, and producing useful information in a small fraction of the time (Indorante et al., 1996). The way that a pedologist develops an SLP is sample by sample, moving across gradients in the landscape, and to similar landforms in the landscape, making and testing predictions as they go. Each of these predictions and tests functions as a hypothesis and an experiment. It would be nigh impossible to plot the entire process, which occurs over hundreds of samples and several years as a pedologist investigates a landscape (Daniels, 1988). It can be difficult to articulate the details of an SLP in prose, so they are rarely intensively recorded in the literature, and are instead only partially recorded within the soil survey products that SLPs enable



the creation of (e.g. Soil Taxonomy, soil block diagrams, and soil surveys). An SLP is tacit knowledge, difficult to transfer between individuals orally or in text.

Unfortunately, the result is that SLPs are often lost when the pedologists that developed and used them leave the workforce (Hudson, 1992). Tacit knowledge is not highly valued by many scientists, particularly when evaluating the tacit knowledge of a discipline outside of their own. The claim that SLPs are tacit knowledge is unsatisfying to many, so pedologists have a responsibility to better explain what they do and what it means (Bicki and Tandarich, 1989). Here we attempt to clearly explain how and why we think the soils change the way they do across a landscape.

Application of the SLP approach to subaqueous soil survey in estuarine settings was evaluated in coastal lagoons (Barrier Island systems) of the Mid-Atlantic region and southern New England by following an analogous “subaqueous soil-landscape paradigm” (SSLP) (Bradley and Stolt, 2002; Demas and Rabenhorst, 1999). This approach utilized an understanding of bathymetry, sediment dynamics, benthic ecology, and early diagenetic processes to develop conceptual models that relate the properties of soil/sediment columns to geomorphic units (i.e. landforms) and to produce maps that describe both surficial and underlying horizons. Much like traditional soil surveys, these subaqueous inventories also have been interpreted to produce guidance for best uses, limitations, and potential hazards (Rabenhorst and Stolt, 2012). These relatively low cost products have been used to better manage marine resources by appropriately positioning shellfish aquaculture plots, submerged aquatic vegetation (SAV) restorations, and other projects related to subaqueous land management (Erich et al., 2010). Given the value of the Chesapeake Bay resource and

especially efforts to revive shellfisheries and benthic ecosystem function, the need for subaqueous soil information in Chesapeake Bay is critical to coastal zone management (Turenne, 2014).

### 5.3 Methods and materials

#### 5.3.1 Study site

Rhode and West Rivers, adjacent subestuaries on the western shore of Chesapeake Bay, have been previously described (Cory and Dresler, 1980; Jordan et al., 1983; Jordan et al., 1986; Wessel and Rabenhorst, 2017), as have some of their tidal marshes (Bernal et al., 2017; Pastore et al., 2017). The development of an SSLP conceptual model in these subestuaries of Chesapeake Bay will have immediate implications for the development of subaqueous soil surveys in other western shore estuaries of Chesapeake Bay (South River, Severn River, Magothy River, Patapsco River, Back River, Middle River, Gunpowder River, and Bush River).

#### 5.3.2 Rhode River subaqueous soil-landscape model

During 2015-16, a subaqueous soil survey project was undertaken in the Rhode River estuary with the goal of developing and compiling an SSLP conceptual model relating subaqueous soil series to particular subaqueous landforms. Landforms were first delineated in ArcMap by generating a contour map and a DEM using bathymetric survey point data. Four criteria were used to differentiate subaqueous landforms: 1) proximity of a landform to other subaqueous and subaerial landforms (e.g. escarpments, tidal marshes), 2) the water depth where a landform occurs, 3) the three dimensional shape of a landform, and 4) the slope and fetch (length of open

water that wind can blow over to generate waves) of the landform. Landform names were assigned using a combination of pedological (U.S. Department of Agriculture, 2019) and geological (Neuendorf et al., 2011) terms.

Soil sampling transects were then selected so that they would cross contours, ensuring sample collection along a gradient from high to low points in the estuary. Soil profiles were sampled at 81 locations using a vibracore for unconsolidated materials (Lanesky et al., 1979), a Macaulay auger for fluid and organic soils (Bakken and Stolt, 2018), and a bucket auger for nonfluid consolidated materials (Rabenhorst and Stolt, 2012). Soil profiles were horizonated and described using standard soil survey field methods including color, texture, structure, odor, fluidity, and reactions to adding 3% and 30% H<sub>2</sub>O<sub>2</sub>. Special features such as redoximorphic concentrations and depletions, coarse fragments, and krotovina were also described where encountered (Schoeneberger et al., 2012). Soil horizons were grouped into five material types and ranked by their relative risk as sulfidic materials based on moist aerobic incubation oxidized-pH tests (Wessel and Rabenhorst, 2017).

Profiles were then classified using the Keys to Soil Taxonomy (Soil Survey Staff, 2014), and the soils identified were correlated with their associated landforms and relevant factors and processes of soil formation (Demas and Rabenhorst, 2001; Jenny, 1941; Simonson, 1959) to complete a soil survey of Rhode River and to develop an SSLP conceptual model, including new soil series. This included consideration of the geology (Glaser, 2002) and the soils surveyed in the surrounding uplands (Soil Survey Staff, 2016).

### 5.3.3 Model application and evaluation in West River

The SSLP conceptual model developed in Rhode River was then used to develop a draft soil survey of West River. The most recent National Ocean Service hydrographic survey (Bond and Sturmer, 1933b) was used to generate a contour map and DEM in ArcMap. Geomorphic analysis was then conducted and major subaqueous landforms were identified, delineated, and named using the same terminology as in Rhode River. After landforms were identified, the relationships between soil series and subaqueous landforms observed in Rhode River were utilized to infer the presence and distribution of soils expected to be found in conjunction with identified landforms in the West River (Hudson, 1992). From this a draft soils map (a hypothesis ready for testing) was compiled for the West River estuary before making any field visits to West River.

Before initiation of field investigations in West River, six sampling transects were identified that crossed geomorphic landforms normal to the maximum topographic gradient. Field observation points were selected along these transects in the center of each soil map unit segment crossed, which resulted in 42 sampling points. At each sampling point, using appropriate methodologies (Macaulay sampler, vibracorer, or bucket auger), the subaqueous soil profile was examined. Soils were horizonated and described to a depth of one to two meters (or to refusal depth if shallower) using the same methods and terminology as in Rhode River (Schoeneberger et al., 2012). Profiles were classified according to US Soil Taxonomy (Soil Survey Staff, 2014).

The degree to which the Rhode River SSLP conceptual model accurately predicted the distribution of soils across subaqueous landscapes and landforms in West River was evaluated by comparing the soils observed at each sampling point with the dominant (i.e. modal) soil predicted in the corresponding soil map unit by the SSLP conceptual model. For each observation (soil profile) a five point ordinal scale (Table 5-1) was used with the following decreasing order of fit: 5) the observed soil matched the predicted soil series; 4) the observed soil was similar to the predicted soil series; 3) the observed soil fell within the same soil taxonomic subgroup as the predicted soil; 2) the observed soil is formed from the same parent materials (organic, Holocene mineral, or Tertiary mineral) as the predicted soil; 1) the observed soil shares no noteworthy properties with the predicted soil. The term “similar” is technical, meaning “Soils having properties that are slightly outside the defined taxonomic limits but that do not adversely impact major land uses” (Soil Science Division Staff, 2017). Accordingly, values from 1-5 were assigned to each of the 42 observations. Higher numbers indicated a better fit to the predicted modal soil in the corresponding soil map unit of the draft, or hypothesis, soil survey. These observation scores were then summed to generate an observed map score for the draft soil survey.

Table 5-1. The five point ordinal scale used to score observations (soil profiles) relative to the modal series for each soil map unit.

Point Score	Criteria
5	Observed soil matches predicted series
4	Observed soil is similar to the predicted series (i.e., shares most interpretive properties)
3	Observed soil matches the taxonomic subgroup of the predicted series
2	Observed soil is formed in the same parent materials as predicted series (Holocene mineral, Tertiary mineral, organic)
1	Observed soil shares no noteworthy properties with the predicted series and is formed in different parent materials

The significance of this map score was then statistically evaluated using a modified bootstrapping, or data resampling, method. This method was used to test the null hypothesis:

$H_0$ : The distribution of observed soils in the West River landscape generates a map score that is not significantly different from a map score generated from a random selection of observed soils distributed randomly across this landscape.

A similarity matrix was developed using the observed soil descriptions, the predicted modal soil series in the soil map units, and the five point ordinal scale used to generate the observed map score. Location data of the observed soil descriptions were masked during this process to reduce any investigator bias and each observed soil description was given a 1-5 point value for every possible predicted soil series (this similarity matrix was also used to generate the observed map score once location data were unmasked, again to reduce bias). The 42 observations were resampled via bootstrapping using the GNU Octave scientific programming language (Eaton et al., 2018), randomly assigning a randomly chosen observed soil to one of the 42 sampling

points, and assigning each pairing the corresponding 1-5 point value from the similarity matrix. These 42 values were then summed to generate a single random map score. This process was iterated to generate a total of 10,000 random map scores. The 95<sup>th</sup> percentile of these was then selected as a significance threshold, commonly used in related statistical tests to distinguish signal from noise via data resampling (Overland and Preisendorfer, 1982). This threshold and the observed map score were then used to test the null hypothesis.

#### 5.4 Results and discussion

##### 5.4.1 Rhode River landforms and soils

The bathymetric maps of Rhode River generated from hydrographic survey data revealed a surprisingly complex subaqueous landscape consisting of deep channels and coves that are commonly fringed by submerged wave-cut platforms or submerged wave-built terraces along the main stem of Rhode River. There were several sunken islands or shoals, and submerged saddles connecting these to the shore in some places. In the upper reaches of the tidal creek channels, which are also fringed by platforms and terraces, the channel bottom rises gradually and grades gently into submerged tidal marshes before becoming shallow enough to support emergent vegetation, marking the transition to the surrounding tidal marshes (Figure 5-1). Ten different landform types were identified (Table 5-2).

The soil survey of Rhode River demonstrates that classified soil profiles do vary by landform (Table 5-3), with some landforms having much more consistent soil-landscape relationships than others. Estuarine channel pedons were 69% Grossic

Hydrowassents, estuarine tidal creek channel pedons were 61% Grossic Hydrowassents, cove pedons were 100% Grossic Hydrowassents. Shoals and submerged wave-cut platform pedons were 50%, and submerged saddles were 100%, Typic Fluviwassents. Submerged tidal marsh pedons were 100% Sapric Sulfiwassists. Submerged wave-built terraces and estuarine tidal creek platforms are composed of a greater diversity of soil taxa at the subgroup level, in part due to the difficulty delineating these landforms primarily on bathymetric data. Another likely source of error is the swimming areas and the construction of bulkheads, which destroys the natural interface between the subaqueous and upland environment (Jackson et al., 2002). The boundary between the submerged wave-cut platform and the submerged wave-built terrace does not occur reliably at a particular depth or slope threshold, and should be moved in a revised soil survey to accommodate observed pedons as well as is possible. Estuarine tidal creek platforms are smaller features, typically only a few tens of meters wide (Figure 5-1), and could only be broken apart into platform and terrace components in a more detailed survey. It might therefore be prudent to delineate these as complexes (i.e. dominated by two or more dissimilar soils) in initial surveys, and updating them to consociations (i.e. dominated by a single soil series and similar soils) as more detailed field sampling is conducted.



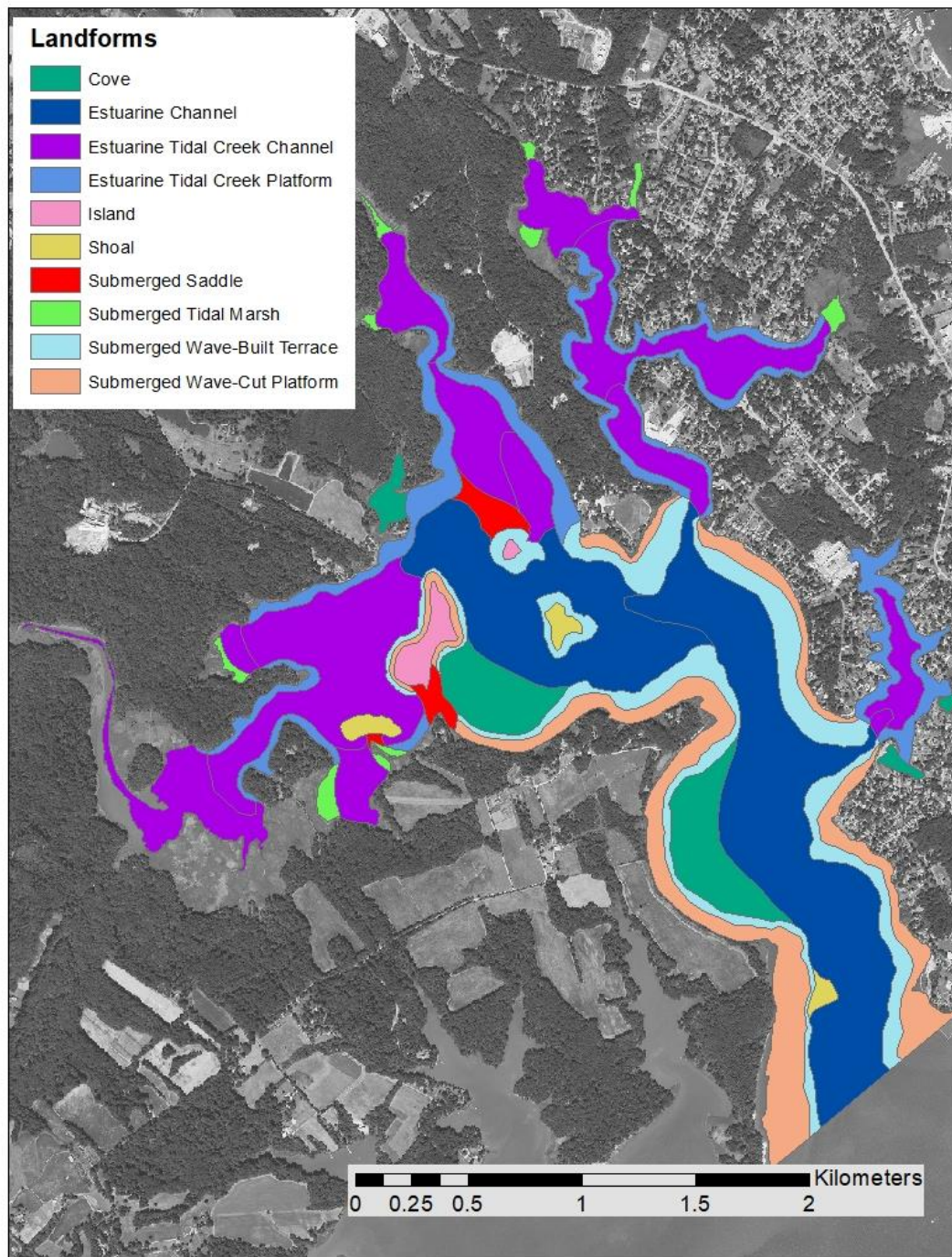


Figure 5-1. Landforms of Rhode River, delineated from bathymetric contours. All except islands are subaqueous. Tidal marshes with emergent vegetation are not included in these units.

Table 5-2. Landforms delineated from Rhode River hydrographic survey data. Key characteristics compiled from (Neuendorf et al., 2011) and (Stolt et al., 2005). New terms that are composites/modifications of existing terms are marked (\*). Note that the use and definitions of geomorphic terms vary widely across and even within disciplines.

<b>Landform</b>	<b>Key characteristics</b>	<b>Identification issues</b>
Estuarine channel*	Deep, central, and elongated portion of the subestuary where most of the current flows	Difficult to distinguish from estuarine tidal creek channel due to dependence on relative sizes
Estuarine tidal creek channel*	Deep, central, and elongated portion of a relatively small and narrow tributary of a larger subestuary	Difficult to distinguish from estuarine channel due to dependence on relative sizes
Estuarine tidal creek platform*	Nearly level and relatively shallow submerged bench along the edge of the relatively small and narrow tributary of a larger subestuary	Hydrographic data may be sparse in small tidal creeks
Island	Subaerial land surrounded on all sides by water	Can be difficult to distinguish from a shoal if it is becoming one
Cove	Sheltered embayment opening into a larger body of water	Often grades imperceptibly into estuarine channel, especially when opening is unrestricted
Shoal	Feature that rises from the basin floor of a body of water, may occasionally be exposed, and is composed of or covered with unconsolidated sediment	Vary in nature from submerged islands to temporary sandbars
Submerged saddle*	Ridge that rises at the ends to form a concave feature along one axis, commonly connects islands to the shore	Ridge is easy to identify, but edges are difficult to distinguish from other landforms
Submerged tidal marsh*	Shallow areas adjacent to tidal marshes that don't support emergent vegetation but still contain organic soil material	Is not always present along tidal marshes, and grades imperceptibly into estuarine tidal creek channels
Submerged wave-cut platform	Erosional feature, gently sloping bench extending from the shore, commonly adjacent to eroding cliffs	Often grades imperceptibly into submerged wave-built terrace
Submerged wave-built terrace	Depositional feature, extension of wave-cut platform that commonly maintains the same gentle slope before sloping steeply into deeper water	May extend beyond the steep slope into deeper water

Table 5-3. Rhode River landforms and associated soil taxonomic subgroups. Numbers of samples are reported as well as the percentage of pedons collected from those landform map units to classify as the named US Soil Taxonomy subgroup. A (.) indicates that no pedons of that subgroup were observed in that landform map unit. Proposed soil series were developed for shaded subgroups (three for Grossic Hydrowassents, one each for the other subgroups). Data used for classification are given in Appendices H-J.

Subgroup		Aeric Fluviowassent	Aeric Haplowassent	Fluventic Psammowassent	Fluventic Sulfowassent	Grossic Hydrowassent	Haplic Sulfowassent	Sapric Haplowassent	Sapric Sulfowassent	Sulfic Fluviowassent	Sulfic Hydrowassent	Sulfic Psammowassent	Thapto-Histic Sulfowassent	Typic Fluviowassent	Typic Haplowassent	Typic Hydrowassent	Typic Sulfowassent	Upland Soil
Landform	Estuarine channel	.	.	1 (8%)	1 (8%)	9 (69%)	.	.	.	.	.	1 (8%)	.	.	1 (8%)	.	.	.
	Estuarine tidal creek channel	.	.	.	3 (17%)	11 (61%)	1 (6%)	.	.	.	.	2 (11%)	.	.	.	.	.	1 (6%)
	Estuarine tidal creek platform	2 (22%)	1 (11%)	.	.	.	1 (11%)	.	.	.	.	.	1 (11%)	1 (11%)	2 (22%)	1 (11%)	.	.
	Island	.	.	.	.	.	.	.	.	.	.	.	.	.	.	.	.	2 (100%)
	Cove	.	.	.	.	5 (100%)	.	.	.	.	.	.	.	.	.	.	.	.
	Shoal	.	.	.	.	1 (25%)	.	.	.	1 (25%)	.	.	.	.	2 (50%)	.	.	.
	Submerged saddle	.	.	.	.	.	.	.	.	.	.	.	.	.	2 (100%)	.	.	.
	Submerged tidal marsh	.	.	.	.	.	.	.	.	3 (100%)	.	.	.	.	.	.	.	.
	Submerged wave-cut platform	1 (7%)	1 (7%)	1 (7%)	.	.	.	1 (7%)	1 (7%)	1 (7%)	.	.	1 (7%)	.	7 (50%)	.	.	.
	Submerged wave-built terrace	1 (9%)	.	1 (9%)	.	2 (18%)	1 (9%)	.	.	1 (9%)	.	.	1 (9%)	.	3 (27%)	.	1 (9%)	.
Sampled Pedons		4	2	3	4	28	3	1	5	2	3	3	3	1	17	1	1	2

#### 5.4.2 SSLP conceptual model

Based on the geological maps of the region and soil surveys of surrounding areas, several different parent materials are expected in similar western shore subestuaries of Chesapeake Bay, primarily recent Quaternary Period (Holocene) sediments and older Tertiary Period (Paleocene or Eocene Epoch) materials of the Nanjemoy Formation, Marlboro Clay, and Aquia and Brightseat Formations (Glaser, 2002). Holocene sediments consist of unconsolidated mineral materials of a variety of textures ranging from silts and clays deposited in deeper areas, to sands and coarse fragments deposited in shallow areas regularly reworked at the soil surface by wave action. Holocene organic soil materials are anticipated near Transquaking (Typic Sulfihemists) and Mispillion (Terrestrial Sulfihemists) soils that are mapped in some of the tidal marshes surrounding western shore subestuaries (Soil Survey Staff, 2016). Natural oyster bars once covered large portions of the bottom of western shore subestuaries (Smith et al., 1997), but only scattered shells and shell fragments were observed throughout most of this study—if robust shell reefs were in fact once present they have been completely destroyed, not simply buried by Holocene sediments.

The Nanjemoy and Aquia formations are rich in green glauconite sand (Figure 5-2a) and date back to the Eocene (34-56 mya) and Paleocene (56-66 mya) epochs, respectively (Cohen et al., 2013). These formations formed as marine deposits in water as deep as 300 ft. The Aquia is a regressive sequence, with accommodation space (the distance between the soil surface and the water surface) decreasing as it accumulated, and the upper portion thought to have formed in a very shallow shoal

environment. The Nanjemoy probably formed in deeper littoral environments, perhaps near the foreshore on the continental shelf (Glaser, 1971). The Brightseat formation underlies the Aquia and is very similar, though generally contains more clay. The Brightseat and Aquia formations are difficult to distinguish and are not mapped separately (Glaser, 2002). The Nanjemoy and Aquia are separated by the Marlboro Clay, a much finer unit dominated by clays and silts. It ranges from silvery-grey to light pink and sometimes red, and is a distinctive marker bed in the stratigraphy of the region. The clay mineralogy is largely kaolinite and illite, with enough smectite to make it of concern to engineers in the region. The silt fraction consists mostly of well-aggregated clay, and decreases in proportion to clay in the more weathered portions of the formation (Scott, 2005). Where sand occurs in the Marlboro Clay, it is due to glauconitic infilling of burrows in the upper part of the formation by material from the Nanjemoy. The Marlboro Clay may have formed in a very shallow environment as a tidal flat deposit (Glaser, 1971).

Much of the glauconite in these formations is thought to have formed from fecal pellets of marine organisms, the morphology of which is still evident in thin sections of nearby outcrops (Fanning et al., 1989; Wagner, 1982; Wessel et al., 2017a). Glauconite grains in the Aquia formation appear lobate and intact and are therefore thought to be formed in place from fecal pellets, though glauconite grains in the Nanjemoy formation are rounded and more highly weathered, containing higher proportions of goethite, and are therefore thought to have been heavily reworked or transported from elsewhere (Teifke, 1973). During their periods of submergence by seawater, the marine sediments of the Aquia, Marlboro Clay, and Nanjemoy

formations also accumulated pyrite. This iron sulfide mineral forms when anaerobic processes produce hydrogen sulfide from the reduction of sulfate, which then reacts with iron oxides in the accumulating surface of the seafloor to form pyrite (Figure 5-2a) (Fanning et al., 2010; Rabenhorst and Fanning, 1989).

After this period of glauconite and pyrite accumulation, additional sedimentation deposited thick (e.g. tens of meters) deposits of Miocene and possibly Quaternary materials in marine and coastal environments above the Nanjemoy formation (Figure 5-2b) (Glaser, 1971). Sea-levels subsequently fell (Hansen et al., 2013) and exposed these materials, as well as much of the continental shelf, to the atmosphere. These materials dewatered, consolidated, and eroded to form dissected landscapes. To some depth, the glauconitic Tertiary materials underwent sulfurization and other pedogenic processes, forming brownish colors (from Fe oxides coating mineral grains), as well as iron oxide and jarosite concentrations in B and BC horizons deep in the solum (perhaps to a depth of 5-10 m or even more). The surface was vegetated and formed terrestrial A horizons. Below the vadose zone, an unoxidized zone remained that still contained pyrite (Figure 5-2c). This resembles the soils of the surrounding landscape, including Annapolis and Donlonton series. It is unknown when exactly these features formed, other than after their exposure to the atmosphere and prior to the significant increase in sea-levels beginning at the end of the last glaciation roughly 10,000 years ago (Rabenhorst and Valladares, 2005).



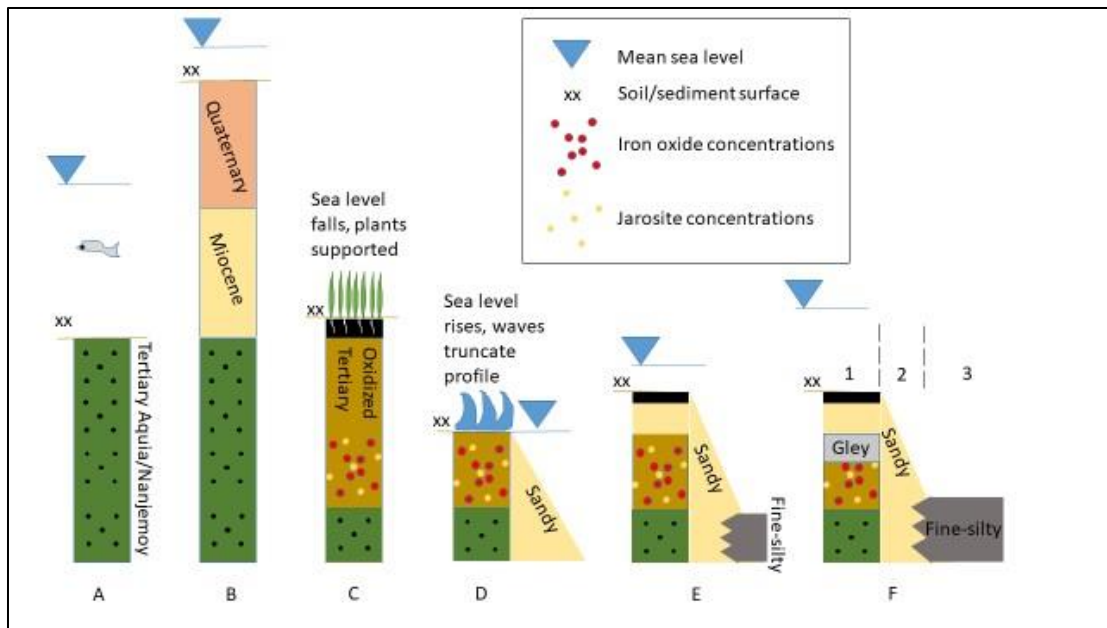


Figure 5-2. Conceptual soil-landscape model. A) Glauconite (green) and pyrite (black dots) accumulate as Tertiary marine deposits. B) Miocene and possibly Quaternary deposits continue to accumulate. C) Sea-levels drop and erosion exposes the Tertiary deposits (Nanjemoy or Aquia). Oxidation of the pyrite-containing Tertiary sediments and the forms soils containing Fe oxide and jarosite accumulations in the lower (BC) horizons. An organic rich A horizon develops at the surface (upper black horizon). Unoxidized zone containing pyrite is preserved below vadose zone. D) Sea-levels rise, waves truncate the profile forming a submerged wave-cut platform. Coarse materials accumulate adjacent as a submerged wave-built terrace. E) Sea-level continues to rise, truncated soil is buried by Holocene sediments, subaqueous A horizon forms, the wave-built terrace grows, and clays and silts accumulate in deeper water. F) Fe oxides in the upper paleosol are reduced (Gley zone), fine and fine-silty soils form deposits in deeper-water. F1, 2, and 3 correspond to extant submerged wave-cut platforms, submerged wave-built terraces, and coves or estuarine channels.

As sea-levels rose after the end of the most recent glaciation, the advancing shoreline truncated these soils through wave action (Kraft, 1971). This created wave-cut platforms, shoals, and submerged saddles. These are consolidated paleosol surfaces that are often adjacent to eroding cliffs (platforms) or that mark eroded islands (shoals) and isthmuses (saddles) (Figure 5-1). These landforms are dominantly the weathered lower sola (e.g. BC horizons) of older soils and landscapes that were once exposed above water. At these sites, shallow water is actively cutting and winnowing the surface (Figure 5-2d). This can be seen in action by wading out along some shorelines in Chesapeake Bay, where exposed red paleosols are eroding at the soil surface just a few meters from the shore. This has formed Coarse-loamy, glauconitic, nonacid, mesic Typic Fluviassents, described by the proposed Rhode River soil series (Table 5-4, Appendix K). Other soils present in these settings are Aeric Fluviassents, which preserve high chroma colors in their profiles, such as the reds and pinks of the Marlboro Clay. Adjacent to submerged wave-cut platforms, coarse material commonly settles out of the deeper water to form submerged wave-built terraces (Figure 5-1) that generally consist of sandy and unconsolidated Holocene materials (Figure 5-2d). These are commonly Glauconitic, mesic Fluventic Psammowassents, described by the proposed Dutchman Point soil series (Table 5-4, Appendix K).

Table 5-4. Proposed soil series for use in Chesapeake Bay subestuaries . While some of these soils are morphologically similar to existing subaqueous soil series, those series have been developed for fresh or marine water, leaving a need for the development of subaqueous soil series to use in brackish water environments (Dahl, 1956). Proposed and tentative Official Soil Series Descriptions (OSDs) with descriptions of modal pedons are in Appendix K<sup>5</sup>.

---

<sup>5</sup> The Sellman, Contees Wharf, and Muddy Creek series are listed as having mixed mineralogy in this table, though there is ongoing debate on this due to the presence of glauconite in the clay fraction of these soils (perhaps eroded from the Nanjemoy/Aquia formations) and to the presence of fecal pellets, though these fecal pellets do not necessarily correspond to the glauconite pellets required by the definition of the glauconitic mineralogy class (Soil Survey Staff, 2016). The OSDs in Appendix K may therefore differ, as this is an evolving topic.

Series Name and Family Classification	Series Criteria
Rhode River Coarse-loamy, glauconitic, nonacid, mesic Typic Fluviwassents	Lithological discontinuity with Tertiary materials (Aquia, Marlboro Clay, Nanjemoy) within upper 50 cm
Dutchman Point Glauconitic, mesic Fluventic Psammowassents	Nonfluid or slightly fluid Holocene sands or loamy sands throughout upper 100 cm
Sand Point Sandy, glauconitic, mesic Sulfic Fluviwassents	Sandy textures overlying lithological discontinuity with finer textured Holocene mineral materials below within upper 100 cm
Contees Wharf Fine-silty, mixed, nonacid, mesic Grossic Hydrowassents	Moderately to very fluid Holocene mineral material through upper 200 cm Upper 100 cm generate acid upon oxidation but do not classify as sulfidic materials
Sellman Fine, mixed, nonacid, mesic Grossic Hydrowassents	Moderately to very fluid Holocene mineral material through upper 200 cm Upper 100 cm generate acid upon oxidation but do not classify as sulfidic materials
Fox Creek Euic, mesic Sapric Sulfiwassists	Organic soil materials, generally covered with 0-39 cm of Holocene mineral materials
Muddy Creek Fine-silty, mixed, mesic, Grossic Hydrowassents	Moderately to very fluid Holocene mineral materials in upper 100 cm Contain buried organic horizons between 100-200 cm

As the sea-level continued to rise, submerged wave-cut platforms were buried by a mantle of sands eroded from the advancing shoreline. Metastable iron sulfide accumulated in and darkened the upper horizons of this material, and in some cases, growth of SAV may also have contributed to higher OC near the surface, both of which contribute to formation of subaqueous A horizons (Figure 5-2e). Channels that had been cut down into the landscape while it was above sea-level filled in, some with unconsolidated sands and others with accumulating organic soils as tidal marshes developed and grew upward and inland with the rising sea. This explains inclusions of Holocene mineral and organic materials in submerged wave-cut platforms. Submerged wave-built terraces continued to grow via sand transport and deposition as sea-level increased. In deeper estuarine channels and estuarine tidal creek channels, silts and clays accumulated. Where these interface with the submerged wave-built terraces, profiles develop with a sandy mantle over finer materials (Figure 5-2e). In some cases, this mantle is tens of cm thick and extends into the estuarine channel, which is why some estuarine channel soils did not classify as Grossic Hydrowassents (Table 5-3). These are sometimes seen as Sandy, glauconitic, mesic Sulfic Fluviwassents, described by the proposed Sand Point soil series (Table 5-4, Appendix K).

As sea-levels rose further, the cutting action of the waves along the shore continued this process while the older submerged wave-cut platform was further submerged and buried. This makes it very difficult to delineate the submerged wave-cut platform from the submerged wave-built terrace using bathymetric data alone, because the platform is present at some depth along much of the terrace. Together,

these two landforms form a shallow shelf that runs along the outer edge of the Rhode River (Figure 5-1). Paleochannels from the previously dissected landscape that fill in are also indistinguishable from the surface and can hide inclusions of organic soils under the thin sandy scour-lag deposits that are present on these landforms.

Fortunately the orientation of the shoreline seems to provide some clue as to where these two landforms can be delineated. Where there is a long fetch for winds to raise waves, deeper and sandier soils dominate the feature, seen in Sp and Dp map units on the eastern shore of Rhode River (Figure 5-3). Where there is a somewhat sheltered cove, much of the shelf seen in the bathymetry will represent soils with a shallower contact with buried Tertiary materials. This is seen the Rr map unit that runs along much of the western shore of Rhode River (Figure 5-3).

As sea-levels rose further, reaching today's level, silts and clays continued to settle out in the wide areas of the estuarine channels, mainland coves, and estuarine tidal creek channels (Figure 5-1 and Figure 5-2f). The soils here tend to be Fine, glauconitic, nonacid, mesic Grossic Hydrowassents, though some samples do classify as Sulfic Hydrowassents (Wessel and Rabenhorst, 2017). The Grossic Hydrowassents do contain reduced sulfide minerals, though their pH does not decrease enough (over the course of moist aerobic incubation) in the upper part to meet the definition of sulfidic materials (Soil Survey Staff, 2014). The proposed Sellman soil series describes the Fine Grossic Hydrowassents (Table 5-4, Figure 5-3, Appendix K). Higher in the estuary, in the estuarine tidal creek channels, these transition to Coarse-loamy Grossic Hydrowassents, though most of the intervening area seems to be dominated by Fine-silty, glauconitic, mesic Grossic Hydrowassents. These Fine-silty

Grossic Hydrowassents are described by the proposed Contees Wharf soil series (Table 5-4, Figure 5-3, Appendix K). This is likely due to the closer shorelines and shallower water, allowing a greater rate of sand transport into these soils as the shorelines erode.

At the highest points of the estuary, where the shorelines are mapped as Mispillion and Transquaking series (organic tidal marsh soils), submerged tidal marshes are found. These contain Euic, mesic Sapric Sulfiwassists, which sometimes contain a lithological discontinuity with submerged paleosols. These Wassists are sometimes covered with up to about 20 cm of Holocene mineral soil, and are occasionally preserved on submerged wave-cut platforms as well. They are described by the proposed Fox Creek soil series (Table 5-4, Figure 5-3, Appendix K). These organic subaqueous soils only make up a small portion of the subaqueous landscape but are the most likely materials to contain high enough concentrations of sulfide minerals to generate extreme acidity if disturbed and allowed to oxidize (Wessel and Rabenhorst, 2017). Between these submerged marshes and the Contees Wharf soils are Fine-silty, glauconitic, mesic, Grossic Hydrowassents with buried organic horizons occurring between 100 and 200 cm in the profile. The proposed Muddy Creek soil series describes these soils (Table 5-4, Figure 5-3, Appendix K).

The overall process of sea-level drop → emergence → dewatering → formation of pedogenic features → preservation of those features after submergence, is consistent with observations in the restored lagoon and artificial lake discussed in Chapter 4. There, pedogenic features including colors and structure were developed within ~150 years after the landscape was drained, and persisted in the subsoil after

two years of submergence (Chapter 3). In Rhode River, these features formed circa 15,000 years ago when the Wisconsin Glacial Episode caused sea-levels to fall and expose the continental shelf (or perhaps far earlier, during a prior glacial episode) (Edwards and Merrill, 1977); and have persisted on submerged wave-cut platforms following about 500-1000 years of submergence (based on depths of 2-3 m and current rates of sea-level rise).

With the SSLP conceptual model and soil series, the landform survey was revised to produce a soil survey giving the best estimates of the modal soils present in map units of Rhode River (Figure 5-3). Appendix L provides an example interpretive map for blue carbon accounting that can be produced from these data, one of many possible products.



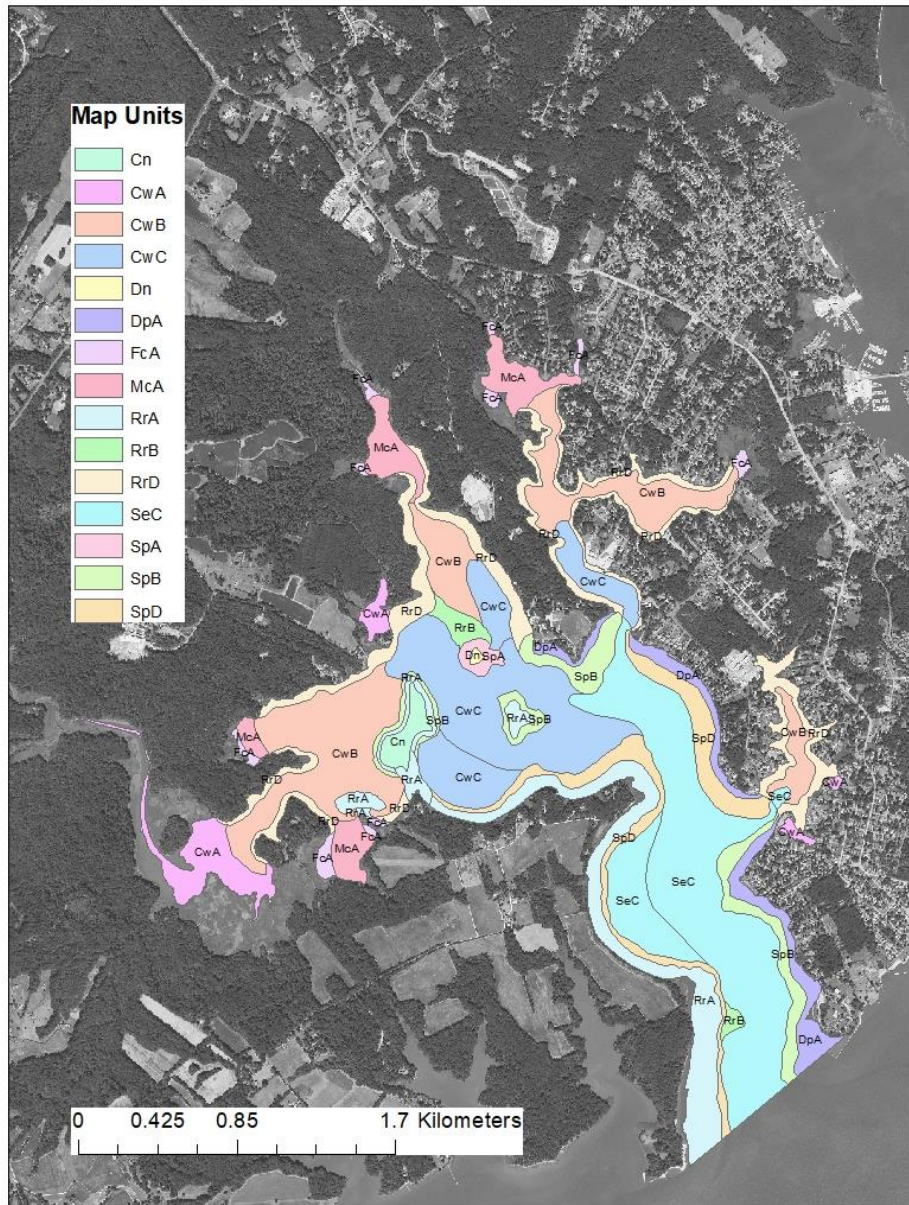


Figure 5-3. Soil map units for Rhode River. The first two letters in each map unit name denote the modal soil series for that unit. Rr-Rhode River, Dp-Dutchman Point, Sp-Sand Point, Cw-Contees Wharf, Se-Sellman, Fc-Fox Creek, Mc-Muddy Creek. The third letter in these map units corresponds to depth phase. A=0-1 m, B=1-2.5 m, C=2.5-4.5 m, D=0.3 m. The subaqueous soil map created in 2015-16 that includes 16 distinct soil map units (in 57 delineations).

#### 5.4.3 Model application and evaluation in West River

By using the SSLP conceptual model, geologic map, and the 1933 hydrographic survey (which was used to generate a bathymetric map of West River) a soil survey was prepared that included map units tied to identified landforms, and that predicted the distribution of soils in West River. Transects were selected to evaluate these predictions (Figure 5-4). A total of 42 pedons were collected and scored using the 5 point scale (Table 5-1).

The distribution of those scores is not normal (Figure 5-5) but is illustrative of the utility of the scoring system. Exact matches to the predicted soil series were rare, though similar soils that shared most interpretive properties with the predicted soil series were the most common result. This is not surprising, considering the taxonomic variability observed in Rhode River (Table 5-3) and previous studies that have indicated that even well-defined map units often show substantial variability in soil families and higher taxa present (Hudson, 1990; Young et al., 1997). Several pedons matched at the subgroup level, but based on their profile characteristics they were deemed to be similar soils to their corresponding map units during the development of the similarity matrix, and they were given scores of four rather than three. Scores of two were assigned where parent material was of the same category, such as Holocene mineral, but varied greatly in texture or fluidity from the predicted properties. Scores of one were assigned where parent materials did not match predictions, such as where Holocene material was discovered on submerged wave-cut platforms where Tertiary materials were expected. Notably, though some organic horizons were observed in some pedons, no organic soils were observed in West

River; the Fox Creek series was absent. Map units mapped as submerged tidal marshes did contain thin organic horizons and organic fragments (wood, roots, leaves), and did tend to classify as sulfidic materials. That said, they are of a different character to the submerged tidal marshes observed in Rhode River, where the pedons were at times dominated by organic soil materials.

Despite the rarity of exact matches to the predicted soil series, an evaluation of these results using bootstrapping does enable evaluation of the SSLP conceptual model. These data were resampled 10,000 times, scoring the pedons based on a random assignments to map units in West River, generating a random map score each time (Figure 5-6). The 95<sup>th</sup> percentile of these random map scores, a pre-selected significance threshold, was 103. The observed map score, based on the real locations where the pedons were sampled, was 124 (out of a possible 210). The observed score exceeds the significance threshold, so the null hypothesis that our observed score would not differ significantly from a random distribution of these pedons across West River can be rejected. Therefore, the SSLP conceptual model, while not perfect, does convey a significant amount of information relating to the distribution of soils in western shore subestuaries of Chesapeake Bay.



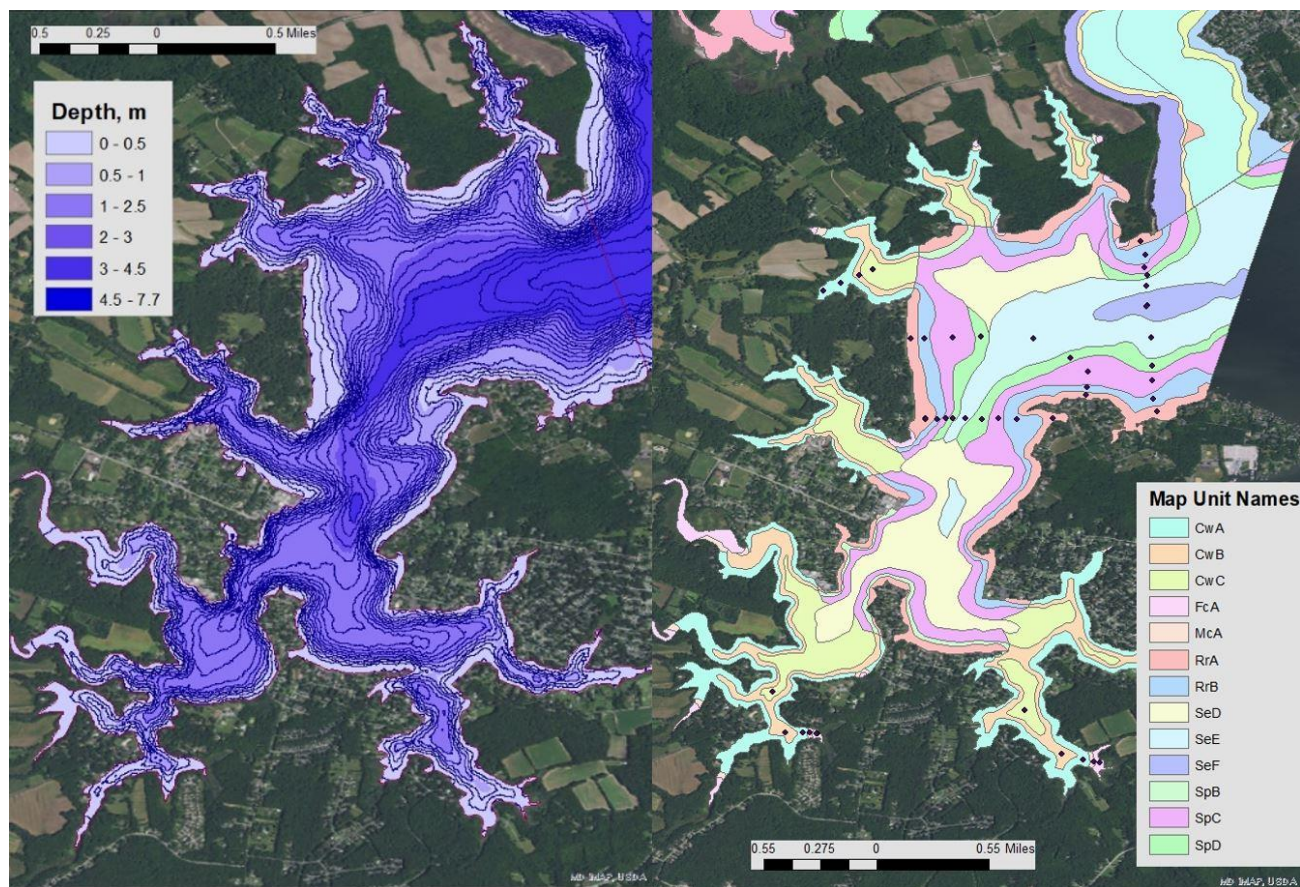


Figure 5-4. Bathymetric map and soil survey of West River with sampling points on six transects crossing map units (right). Depth phases were added to provide more sampling points along transects. A=0-0.5 m, B=0.5-1 m, C=1-2 m, D=2-3 m, E=3-4 m, F=4-5 m.

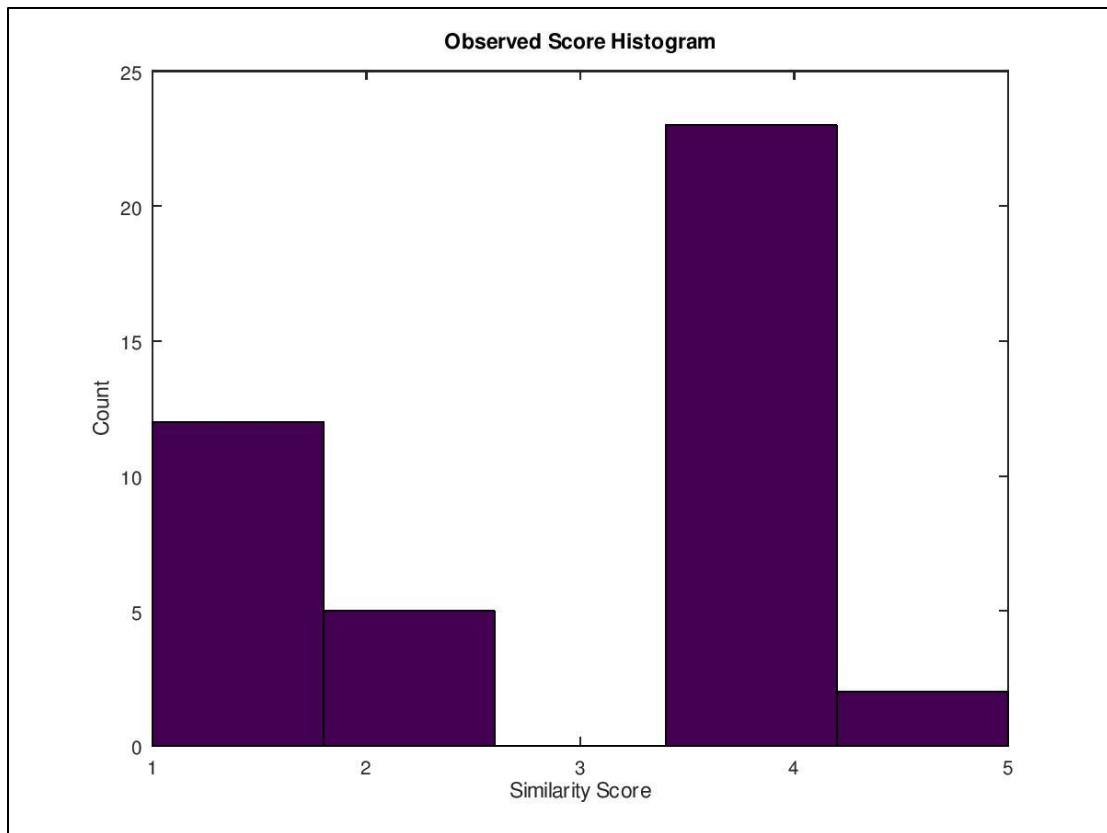


Figure 5-5. Histogram of scores from the 5 point scale for the 42 cores as they corresponded to their sampling sites. Matches to the soil series were rare (5 points), though similar soils were the most common result (4 points). Some matching subgroups (3 points) were observed, but in these cases they were also similar soils so they were given scores of 4 points. Scores of 1 point were generally where parent materials were markedly different.

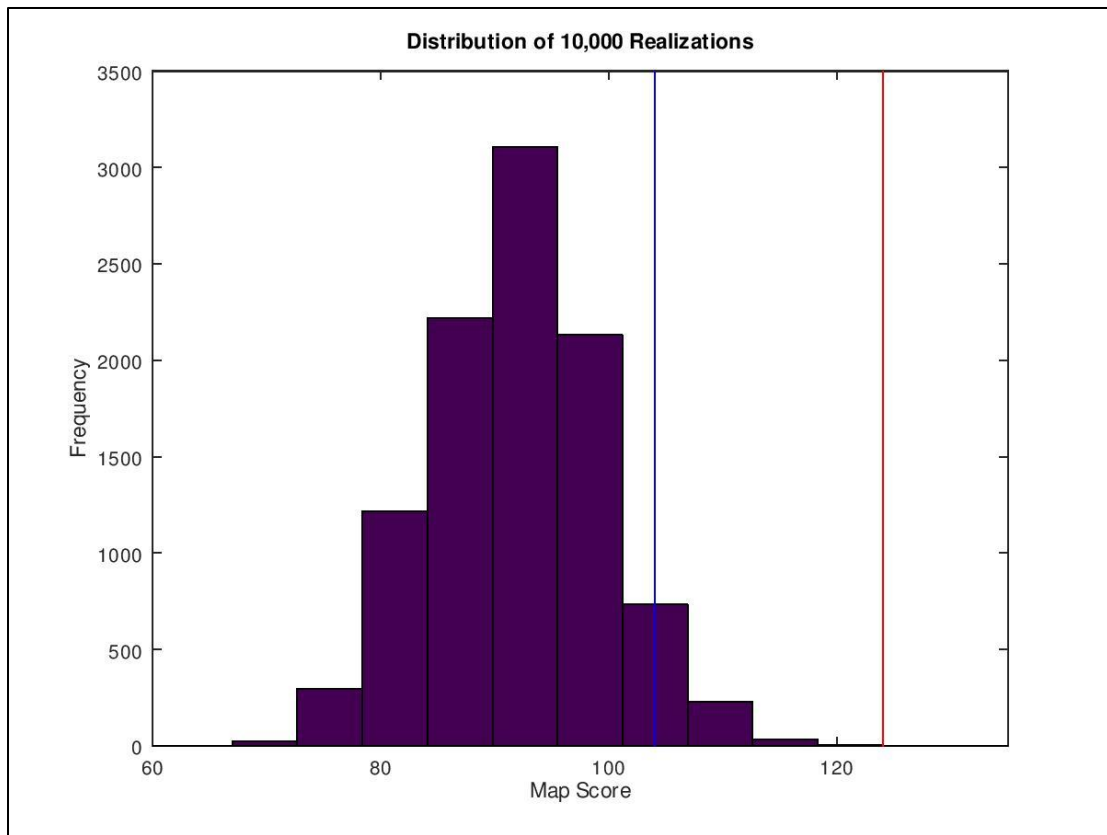


Figure 5-6. Results of resampling (bootstrapping) soil pedons across West River and summing the scores to generate 10,000 map scores for random distributions of those pedons. The blue line is the 95<sup>th</sup> percentile for these data, 103. The red line is the observed map score for the observed (real) distribution of soil cores in West River, 124.

#### 5.4.4 Limitations

As can be seen from the taxonomic diversity observed in Rhode River (Table 5-3), additional soil series can be developed to represent additional soil taxa found in these environments, though it is unclear if those taxa are abundant enough to justify their own consociation map units, or if they are already captured sufficiently as similar soils in the proposed consociations; as additional soil surveys are conducted in Chesapeake Bay the data will become available to address this issue. A major issue that arises here relates to Soil Taxonomy and what makes one soil similar to another. Similarity is determined in a complex way based on likely land-use interpretations, which have yet to be widely determined for subaqueous soils. Many potential subaqueous land-use interpretations have been suggested (Rabenhorst and Stolt, 2012) and a few have been developed for several regions (Balduff, 2007; Erich et al., 2010; Surabian, 2007), the topic is still quickly developing. This means that the concept of similar soils as applied in this study could produce different results through the same analysis if soil surveyors eventually decide that different soil characteristics are more important for grouping similar soils.

As an example, in this study Fluventic Sulfiwassents were generally considered to be similar to Grossic Hydrowassents. Both soils contain reduced sulfides and generate acid upon oxidation, but Grossic Hydrowassents maintain a pH above 4.0 in the upper meter, while Fluventic Sulfiwassents have horizons that drop to a pH of 4.0 or less within the upper 50 cm. The substantial difference in the classification of these two soils, placing them in different great groups, can sometimes be measured in tenths of a pH unit in one horizon. This may be the only

notable difference between these soils, which can both consist of finely textured Holocene mineral sediments, which are moderately to very fluid throughout the upper two meters. To further complicate matters, not all Fluventic Sulfiwassents were similar to Grossic Hydrowassents using this rationale. Most of the Fluventic Sulfiwassents sampled in West River were finely textured and moderately or very fluid, but some were sandy and nonfluid throughout most of the series control section. It is therefore not possible to create simple rules that define certain taxonomic subgroups as similar to the soil for which a consociation is named; the soil profiles must be considered individually. A revision to US Soil Taxonomy that would recognize sulfide-containing materials that acidify but remain above a pH of 4.0 could reduce the taxonomic distance between these two soils. This would allow taxonomy to more closely match land-use interpretations.

A rather different scenario can be reached if shellfish aquaculture is considered to be a more important land-use interpretation. Many shellfish are relatively tolerant of sulfide-containing soils, and oyster aquaculture significantly increases porewater sulfide around the organisms (Duball et al., 2019). Shellfish are commonly found with their shells stained black on the underside as a result of the presence of sulfide minerals. Some shellfish, especially oysters, require relatively hard bottom to survive. Some of their better habitats can be found on submerged wave-cut platforms and submerged wave-built terraces. Soils on these landforms are most commonly Typic Fluviwassents (Table 5-3), but can classify as Fluventic Sulfiwassents or Sulfic Fluviwassents based on the degree and distribution of acidification as a result of sulfide mineral oxidation. Yet, to an oyster, it makes little



difference. They sit on the firm sand or cultch at the top of a soil profile. Soil surveyors in a region that supports a large shellfish aquaculture industry might therefore consider these soils to be similar. Other soil surveyors, in a region where marine construction might be a more pertinent interpretation, might consider the presence of submerged upland soils in the profile to be more important (the approach taken in this study) and deem these soils to be dissimilar.

#### 5.4.5 Future refinement

As the prior two examples highlight, it may be unwise to mix taxonomic differences with other evaluations of soil similarity when considering scoring metrics such as the 5 point scale used in this study. While it can be used to evaluate a single conceptual model in similar settings, and perhaps to evaluate potential improvements to US Soil Taxonomy, it would be difficult to compare soil surveys completed in different settings. This is because the meaning of similar soils will change as expected major land uses change. Soils from different settings (e.g. a desert soil and an estuarine subaqueous soil) will produce different scores for different reasons, making the results incomparable and confounding attempts to develop generally applicable measures of the quality of a soil survey.

One proposed revision to the scoring scale is given in Table 5-5, which places emphasis on diagnostic horizons and materials. The table functions as a key, starting with the lowest possible score and moving to higher scores until the following case is false for the evaluation of a given soil description, at which point the last true score is assigned to the description. Dissimilarity is determined by the presence/absence of features with defined criteria that trained soil scientists are able to identify in their

regions. The importance of the series is retained at the 5 point level, and the issue of similar soils is removed with the new definition of the 3 and 4 point levels. At the 3 point level equal value is placed on missing predicted features and unexpected features; a pedon that was predicted to contain sapric materials (highly decomposed O horizons) but did not would receive a score of 3 points. However, if sapric materials were present but a lithologic discontinuity was also present, the pedon would still receive a score of 3 points. If the expected sapric materials were absent and a lithologic discontinuity were present, the pedon would only receive a score of 2 points. If the sapric materials were present and no lithologic discontinuity was present, but the sapric materials occurred outside of the allowable depth range for the predicted series, then the pedon would receive a score of 4 points. All expected features are present, no unexpected features are present, but due to slightly different placement of features in the profile the pedon does not quite meet the criteria to match the expected series. There is no direct dependence of this approach to regionally different valuations of important land-uses, only on identifiable soil features.

This proposed scoring scale can be applied consistently, across different environments and by different soil surveyors. It retains the value of more than a century of work that has been done to identify and define important soil features and to develop soil series. It does however depend on relevant characteristic horizons and materials having been defined in Soil Taxonomy. In subaqueous settings this process is in its infancy. For instance, a 50+ cm mantle of moderately to very fluid fine-

textured materials defines much of the deep areas of Rhode and West Rivers but has not been defined as a new epipedon.

Further, if this approach is to be widely applied then the relationships between closely related diagnostic horizons and features should be taken into account. This has already been done to some extent by excluding cambic horizons and ochric epipedons from unexpected features in the 1, 2, and 3 point categories. This means that if a submerged upland soil (similar to the Rhode River series) is expected to contain an argillic horizon but does not quite meet the criteria to have an argillic horizon, the score is not lowered further by the presence of a cambic horizon instead. The hypothetical soil could still receive a score of 4 points if that were the only difference. For such an approach to be generally applicable these sorts of exceptions would have to be determined for all possible diagnostic horizons and materials, such as the presence of durinodes instead of a duripan or the presence of hyposulfidic materials instead of hypersulfidic materials (Chapter 2). Once all such relationships are identified, the proposed revision could provide a generally applicable algorithmic approach to the evaluation of soil surveys and the conceptual models used to generate them.

Further, application of a revised scoring scale could enable the identification of areas where US Soil Taxonomy could be improved, and would enable testing of those improvements. A conceptual model could be evaluated using the previously described bootstrapping method (and the revised scale), and evaluated again based on the introduction of a new or revised diagnostic horizon or material. If the initial set of horizons and materials could not be used to reject a null hypothesis, but the revised

horizons and materials do produce a significant result, then the new horizons and materials may represent an improvement to US Soil Taxonomy. The pedological community in the United States is presently engaged in an evaluation of Soil Taxonomy (Stolt and Needelman, 2015), and quantitative approaches like this are needed to inform this endeavor.

Table 5-5. A proposed revision to the five point ordinal scale used to score observations (soil profiles) in this study (Table 5-1).

<b>Point Score</b>	<b>Criteria</b>
1	Observed soil possesses none of the diagnostic materials or horizons of the predicted series within 2 m of the soil surface. Unexpected diagnostic horizons or materials are present within 2 m of the soil surface (Cambic Horizon and Ochric Epipedon exempted).
2	One or more predicted diagnostic horizons or materials of the predicted series are absent from within 2 m of the soil surface AND Unexpected diagnostic horizons or materials are present within 2 m of the soil surface (Cambic Horizon and Ochric Epipedon exempted).
3	One or more predicted diagnostic horizons or materials of the predicted series are absent from within 2 m of the soil surface OR Unexpected diagnostic horizons or materials are present within 2 m of the soil surface (Cambic Horizon and Ochric Epipedon exempted).
4	All diagnostic horizons and/or materials of the predicted series are present within 2 m of the soil surface. No unexpected diagnostic horizons or materials are present within 2 m of the soil surface.
5	Observed soil matches the predicted series.

### 5.5 Conclusions

Pedological principals can be applied in the subaqueous environment. The subaqueous soils of Rhode River correlate well with their associated landforms, and these observations were used to develop an SSLP conceptual model that conveyed significant predictive power in surveying the subaqueous soils of West River. The shallow platforms that fringe these subestuaries are generally truncated submerged uplands, with sandy terraces on their seaward slopes. Coves and channels consist of deep, generally fine to very-fine textured, moderately to very fluid soils that are hyposulfidic or hypersulfidic materials (Chapter 2) and that become more coarsely textured closer to shore. Tidal creeks often contain buried tidal marshes near emergent tidal marshes, and even when they do not consist of organic soil materials, they do contain notable horizons, fine strata, or fragments of organic materials.

This model is expected to be applicable in other western shore subestuaries of Chesapeake Bay, though it will likely have to be modified to account for expected changes in the geology/mineralogy of these areas. The five point scale and bootstrapping statistical method presented here should, with minor modifications, be able to be applied in other landscapes not only to evaluate soil surveys and the conceptual models used to generate them, but also may be suitable to evaluate proposed changes to US Soil Taxonomy.

## Chapter 6: Conclusions

Pedological methods work in the subaqueous environment, enabling an understanding of the development of these environments over time, and allowing meaningful predictions of material distributions and properties to be made. The pedological scientific method used in this research builds on previous conceptual understandings of pedogenesis such as the model:

Factors of soil formation → Processes of soil formation → Soil properties  
(Arnold, 2005)

by adding an explicitly experimental step and subsequent evaluation. Clearer and more robust pedological research can be conducted via an experimental method:

Investigative sampling → SSLP Development → Hypothesis Map  
→ Experimental Survey.

Historical resources, particularly hydrographic surveys, should be a key component of future subaqueous soil surveys. Though bathymetric stability was discovered in Rhode River, different results may be uncovered in different geomorphic settings, and stability should not be assumed in all cases. Where sedimentation has been substantial and can be measured using these methods, it may be possible to infer erosion rates within the surrounding watershed, though where sedimentation rates are low the hydrographic comparison method is likely of limited use.

Hypersulfidic materials cannot be conclusively identified in the field, but informed predictions can be made based on morphological characteristics. Soils high

in organic matter such as buried O and A horizons, and adjacent mineral horizons, are the most likely to be hypersulfidic materials. Fluid muds, the “black mayonnaise” described by many who work with sediments or benthic organisms, does generate acidity but generally not enough to classify as hypersulfidic materials and to require the utmost care not to disturb. However, hypersulfidic materials do still occur in these materials, so adequate evaluation is still required before land-use decisions which would disturb the bottom are made.

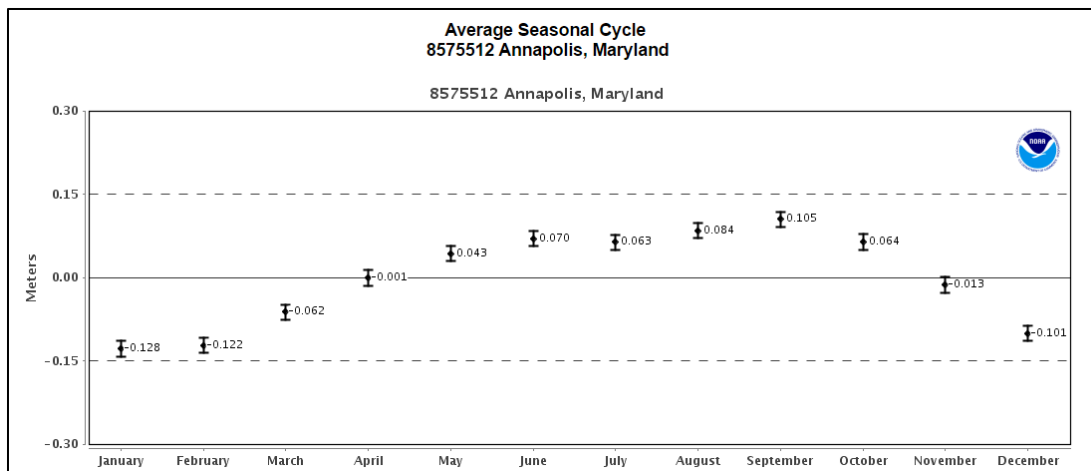
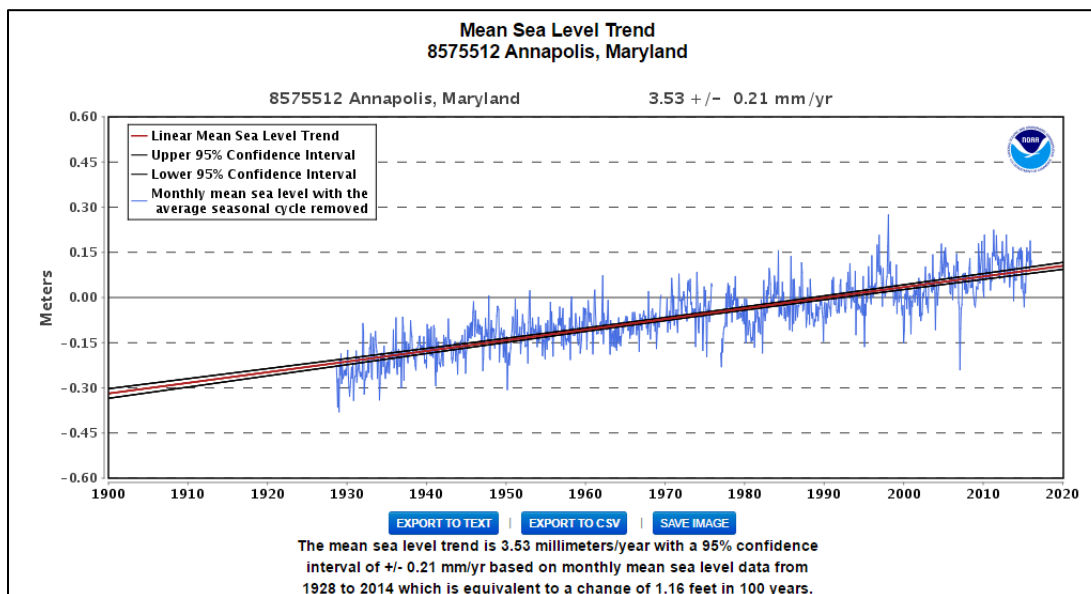
Inundation of upland soils triggers massive biogeochemical and physical shifts, although it also preserves a signature of prior exposure of soils to the atmosphere. After submergence and the establishment of reducing conditions, organic C built up in the A horizons of upland soils, as well as more available forms of Fe released from largely non-bioavailable forms via mineral weathering. This previously unavailable Fe was stored in A horizons as oxide minerals, easily available to microbial reduction and release to porewater and the overlying water column, resulting in the anomalous reactive Fe levels seen in inundated A horizons. In the presence of abundant sulfate, this abundance of available Fe causes a corresponding accumulation of sulfide minerals, which is seen to a slightly lesser extent in coastal freshwater environments as well. Soil structure and Fe oxides in the subsoil are sequestered from these changes, likely functioning as a reservoir of reactants that can continue to contribute to redox reactions long after submergence. As sea-level rise continues, what was observed in Gyldensteen Strand may occur across many of the world’s coasts at an accelerating rate.

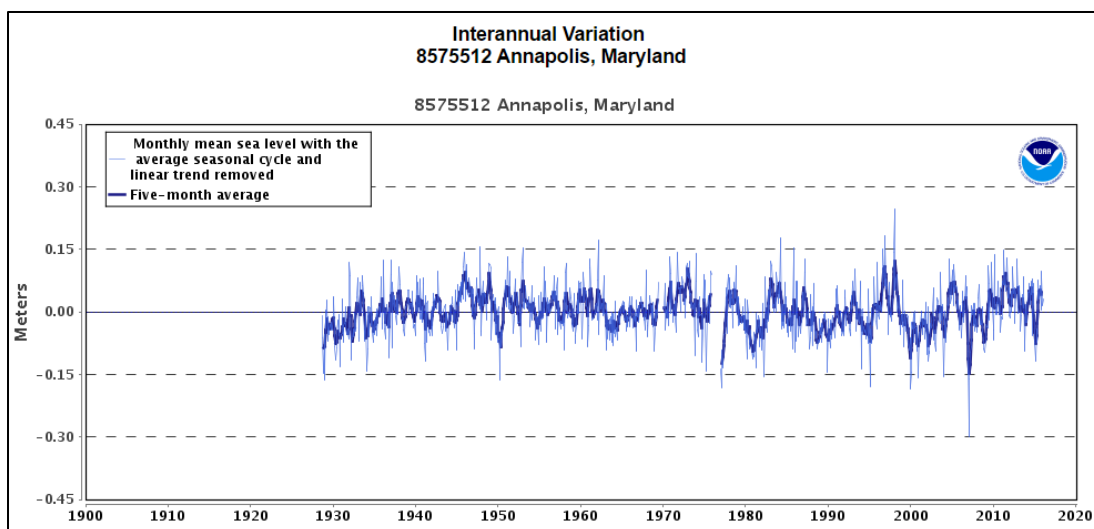


In Chesapeake Bay, subsoil features have persisted to some extent through geologic time, a conclusion supported by observations of similar features in submerged Danish subsoils. This, with other observations from Rhode River and an understanding of stable landform features, enables predictions in similar settings. The subaqueous soil-landscape conceptual model developed in Rhode River applied well in West River. This supports the approach of Investigative sampling → SSLP Development → Hypothesis Map → Experimental Survey to conduct robust pedological soil survey research that can be statistically evaluated. As the approach is further refined, it will continue to support soil survey activities, which will in turn support better natural resource management in subaqueous, and likely other, environments.

## Appendices

### Appendix A: Sea-level trends and variation from NOAA Tides and Currents





Appendix B: Rhode River pedons

Core	Lat	Long	Pedon ID	Taxonomic Subgroup	Landform
2015RR01	38.88293	-76.54795	S2015MD003001	Sapric Sulfiwassist	Submerged Tidal Marsh
2015RR02	38.88422	-76.54500	S2015MD003002	Grossic Hydrowassent	Estuarine tidal creek channel
2015RR03	38.87743	-76.55082	S2015MD003003	Grossic Hydrowassent	Estuarine tidal creek channel
2015RR05	38.88053	-76.53953	S2015MD003005	Sapric Sulfiwassist	Shoal
2015RR06	38.87732	-76.54150	S2015MD003006	Grossic Hydrowassent	Estuarine tidal creek channel
2015RR07	38.88010	-76.53902	S2015MD003007	Grossic Hydrowassent	Shoal
2015RR08	38.88113	-76.53658	S2015MD003008	Typic Fluviwassent	Submerged saddle
2015RR09	38.88363	-76.53682	S2015MD003009	Typic Fluviwassent	Submerged wave-cut platform
2015RR10	38.88620	-76.53745	S2015MD003010	Typic Fluviwassent	Submerged wave-cut platform
2015RR11	38.88463	-76.53113	S2015MD003011	Typic Fluviwassent	Shoal
2015RR12	38.88442	-76.53062	S2015MD003012	Typic Fluviwassent	Shoal
2015RR13	38.88758	-76.53313	S2015MD003013	upland	Island
2015RR14	38.88284	-76.53800	S2015MD003014	upland	Island
2015RR16	38.88396	-76.52422	S2015MD003015	Grossic Hydrowassent	Estuarine channel
2015RR17	38.88297	-76.52322	S2015MD003016	Typic Fluviwassent	Submerged wave-built terrace
2015RR18	38.88342	-76.52369	S2015MD003017	Aeric Fluviwassent	Submerged wave-built terrace
2015RR19	38.88524	-76.52367	S2015MD003018	Grossic Hydrowassent	Estuarine channel
2015RR21	38.88421	-76.52390	S2015MD003020	Grossic Hydrowassent	Estuarine channel
2015RR21.1	38.88228	-76.52352	S2015MD003021	Fluventic Psammowassent	Submerged wave-cut platform
2015RR22	38.87616	-76.52550	S2015MD003022	Typic Fluviwassent	Submerged wave-cut platform
2015RR23	38.87603	-76.52574	S2015MD003023	Typic Fluviwassent	Submerged wave-cut platform
2015RR24	38.87605	-76.52475	S2015MD003024	Grossic Hydrowassent	Mainland cove

2015RR25	38.87613	-76.52515	S2015MD003025	Typic Hydrowassent	Submerged wave-built terrace
2015RR26	38.87609	-76.52590	S2015MD003026	Typic Fluviwassent	Submerged wave-cut platform
2015RR27	38.87053	-76.51268	S2015MD003027	Sulfic Fluviwassent	Submerged wave-cut platform
2015RR28.1	38.87040	-76.51248	S2015MD003028	Fluventic Psammowassent	Submerged wave-built terrace
2015RR28	38.87069	-76.51417	S2015MD003029	Fluventic Sulfiwassent	Estuarine channel
2015RR29	38.89457	-76.52846	S2015MD003030	Grossic Hydrowassent	Estuarine tidal creek channel
2015RR30	38.89431	-76.52977	S2015MD003031	Aeric Fluviwassent	Estuarine tidal creek platform
2015RR31	38.89440	-76.52934	S2015MD003032	Grossic Hydrowassent	Estuarine tidal creek channel
2015RR33	38.89914	-76.52964	S2015MD003033	Haplic Sulfiwassent	Estuarine tidal creek platform
2015RR32	38.89923	-76.52996	S2015MD003034	Typic Fluviwassent	Estuarine tidal creek platform
2015RR34	38.89941	-76.52910	S2015MD003035	Grossic Hydrowassent	Estuarine tidal creek channel
2015RR37	38.88110	-76.51588	S2015MD003036	Typic Fluviwassent	Submerged wave-cut platform
2015RR40	38.88142	-76.51347	S2015MD003038	Grossic Hydrowassent	Estuarine tidal creek channel
2015RR39	38.88026	-76.51517	S2015MD003039	Sulfic Fluviwassent	Submerged wave-built terrace
2015RR41	38.88665	-76.51420	S2015MD003040	Aeric Fluviwassent	Estuarine tidal creek platform
2015RR43	38.88986	-76.53618	S2015MD003041	Typic Fluviwassent	Estuarine tidal creek platform
2015RR42	38.89001	-76.53656	S2015MD003042	Typic Haplowassent	Estuarine tidal creek platform
2015RR44	38.88898	-76.53533	S2015MD003043	Typic Fluviwassent	Estuarine channel
2015RR45	38.88809	-76.53406	S2015MD003044	Typic Fluviwassent	Submerged saddle
2015RR46	38.88760	-76.53365	S2015MD003045	Typic Fluviwassent	Submerged wave-built terrace
2015RR49	38.88333	-76.54744	S2015MD003046	Sulfic Hydrowassent	Estuarine tidal creek channel
2015RR50	38.88340	-76.54700	S2015MD003047	Grossic Hydrowassent	Estuarine tidal creek channel
2015RR51	38.88680	-76.53742	S2015MD003048	Grossic Hydrowassent	Estuarine channel

2015RR58	38.88213	-76.54695	S2015MD003049	Sapric Sulfiwassist	Submerged tidal marsh
2015RR59	38.88348	-76.53657	S2015MD003050	Grossic Hydrowassent	Submerged wave-built terrace
2015RR62	38.89128	-76.53139	S2015MD003051	Sulfic Psammowassent	Estuarine tidal creek platform
2015RR52	38.88660	-76.53740	S2015MD003052	Haplic Sulfiwassent	Submerged wave-built terrace
2015RR53	38.88216	-76.51941	S2015MD003053	Typic Fluviwassent	Submerged wave-built terrace
2015RR54	38.88222	-76.51918	S2015MD003054	Sulfic Psammowassent	Submerged wave-built terrace
2015RR55	38.88266	-76.51854	S2015MD003055	Sapric Haplowassist	Submerged wave-cut platform
2015RR56	38.88241	-76.51979	S2015MD003056	Grossic Hydrowassent	Estuarine Channel
2015RR57	38.89663	-76.53821	S2015MD003057	Fluentic Sulfiwassent	Estuarine tidal creek channel
2015RR59.1	38.88114	-76.52907	S2015MD003058	Aeric Fluviwassent	Submerged wave-cut platform
2015RR60	38.88256	-76.53007	S2015MD003060	Sulfic Hydrowassent	Estuarine channel
2015RR61	38.89296	-76.53337	S2015MD003061	Thapto-Histic Sulfiwassent	Estuarine tidal creek platform
2015RR63	38.89107	-76.53319	S2015MD003063	Grossic Hydrowassent	Estuarine tidal creek channel
2015RR64	38.89545	-76.52304	S2015MD003064	Sulfic Hydrowassent	Estuarine Tidal Creek Channel
2015RR65	38.86479	-76.51548	S2015MD003065	Grossic Hydrowassent	Estuarine channel
2015RR66	38.86410	-76.51811	S2015MD003066	Typic Fluviwassent	Submerged wave-cut platform
2015RR67	38.87607	-76.52202	S2015MD003067	Grossic Hydrowassent	Mainland cove
2015RR68	38.87613	-76.51802	S2015MD003068	Fluentic Psammowassent	Estuarine channel
2015RR69	38.88657	-76.52656	S2015MD003069	Aeric Haplowassent	Submerged wave-cut platform
2015RR70	38.88589	-76.52630	S2015MD003070	Grossic Hydrowassent	Submerged wave-built terrace
2015RR71	38.89670	-76.51715	S2015MD003071	Sapric Sulfiwassist	Submerged Tidal Marsh
2016RR03	38.88919	-76.54002	S2016MD003031	Grossic Hydrowassent	Mainland cove

2016RR04	38.87937	-76.51348	S2016MD003032	Grossic Hydrowassent	Mainland cove
2016RR05	38.88175	-76.51083	S2016MD003033	Grossic Hydrowassent	Mainland cove
2016RR06	38.87717	-76.55236	S2016MD003034	Grossic Hydrowassent	Estuarine tidal creek channel
2016RR09	38.87896	-76.52519	S2016MD003035	Sapric Sulfiwassist	Submerged wave-cut platform
2016RR14	38.87213	-76.51850	n/a	Sulfic Psammowassent	Submerged wave-cut platform
2016RR20	38.88008	-76.54295	n/a	Aeric Haplowassent	Estuarine tidal creek platform
2016RR21	38.88044	-76.54260	S2016MD003036	Grossic Hydrowassent	Estuarine tidal creek channel
2016RR24	38.87206	-76.51520	S2016MD003037	Grossic Hydrowassent	Estuarine channel
2016RR25	38.87531	-76.51865	S2016MD003038	Grossic Hydrowassent	Estuarine channel
2016RR31	38.87945	-76.51675	S2016MD003039	Grossic Hydrowassent	Estuarine channel
2016MC01	38.88002	-76.55392	S2016MD003040	Fluentic Sulfiwassent	Estuarine tidal creek channel
2016MC02	38.87976	-76.55352	S2016MD003041	Fluentic Sulfiwassent	Estuarine tidal creek channel
2016MC03	38.88335	-76.55406	S2016MD003042	Haplic Sulfiwassent	Estuarine tidal creek channel
2016MC04	38.88230	-76.55369	S2016MD003043	Typic Sulfiwassist	Estuarine tidal creek channel

Appendix C: Rhode River horizon data

Core and Horizon	Depth	Dist.	Color	Field Texture	3% H <sub>2</sub> O <sub>2</sub> Color Change	30% H <sub>2</sub> O <sub>2</sub> Peroxide Reaction	Fluidity	H <sub>2</sub> S Odor	Organic Fragment %	Shell %	Notes	%C	Initial pH	Oxidized pH
2015RR01														
Oese	0-68	c	10YR 2/2	mucky peat	No	sl	sf	st						
Oase1	68-128	c	7.5YR 2.5/2	muck	No	sl	sf	st						
Oase2	128-153	c	10YR 2/2	muck	No	sl	mf	st						
Oase3	153-200		10YR 2/1	muck	No	sl	mf	st						
2015RR02														
Ase1	0-32	c	5GY 2.5/0.5	C	Yes	m	vf			3				
Ase2	32-61	c	N 2.5/0	C	Yes	st	vf							
Cg1	61-120	g	5GY 4/0.5	SiC	No	sl	vf							
Cg2	120-168	d	5GY 3/0.5	SiC	No	sl	vf							
Cg3	168-200		5GY 3/0.5	SiC	Yes	sl	vf							
2015RR03														
A	0-27	c	10Y 3/0.5	CL	Yes	sl	mf							



2Cseg1	27-43	c	10Y 3/0.5	fSL	Yes	st	mf							
3Cseg2	43-85	c	5GY 3/0.5	CL	Yes	st	mf			1	30% N 2.5 krotovina with shell fragment s			
3Cseg3	85-131	g	10Y 3/0.5	SiC	Yes	st	mf							
3Cseg4	131- 200		10Y 3/1	SiC	Yes	sl	mf							
2015RR05														
Ase	0-9	a	5Y 4/1	S	No	st	nf							
Oese	9-29	c	10YR 2/2	mp	No	ne	sf	st						
Oase1	29-70	g	10YR 2/1	muck	No	ne	mf	st						
Oase2	70-114	c	10YR 2/1	muck	No	ne	mf	st						
Oase3	114- 131	c	10YR 2/1	muck	No	ne	mf				Common large roots			
A'se	131- 139	g	2.5Y 2.5/1	L	No	sl	mf							
Cseg1	139- 167	c	5GY 3/1	LS	Yes	sl	sf							
Cseg2	167- 185	c	5G 5/1	SL	Yes	st	sf							
Cseg3	185- 200		5G 4/2	SCL	Yes	st	nf							

2015RR06														
Ase	0-22	c	10Y 3/1	SiL	Yes	sl	vf			2	Live clams	3.35		
Cseg1	22-40	g	10Y 3/1	SiL	Yes	sl	vf							
Cseg2	40-67	c	10Y 3/1	SiL	Yes	sl	vf							
Cseg3	67-95	a	10Y 3/1	SiL	Yes	st	mf							
Aseb	95-112	c	7.5Y 2.5/1	L	Yes	st	mf							
Btsegb1	112- 151	d	2.5YR 6/2	SCL	Yes	st	nf				30% 5GY 7/1 depletion s, 30% 10 YR 4/6 concentr ations			
Btsegb2	151- 187		5GY 7/1	SCL	Yes	ve	nf				25% 5GY 4/1 depletion s, 5% 2.5YR 6/3 concentr ations			
2015RR07														
A	0-16	c	70% N 2.5, 30% 5Y 3/2	LS/S	No	sl	0							

Cg	16-33	g	5GY 3/1	L	No	sl	mf		1	1				
Cseg	33-64	g	5GY 3/1	SiL	No	sl	vf			1				
C'g1	64-88	g	5GY 2.5/1	L	No	sl	mf		4					
C'g2	88-109	g	10Y 3/1	CL	No	sl	mf							
2Ab	109- 127	g	60% 10Y 3/1, 40% 5GY3/1	LS	No	st	nf							
2Btsegb	127- 159		5G 3/2	SiCL	Yes	st	sf				7% 5YR 2.5/2 concentr ations			
2015RR08														
A1	0-8	c	10Y 2.5/1	LS	No	sl	nf			1	Gravels as relict peds			
A2	8-22	c	N 2.5/0	LS	Yes	st	nf				Gravels as relict peds			
Cseg1	22-43	g	10GY 2.5/1	SL	Yes	st	nf				Gravels as relict peds			
Cseg2	43-61	g	5G 2.5/1	fSL	Yes	vs	nf				Gravels as relict peds			
Aseb	61-78	g	10GY 2.5/1	fSL	Yes	st	nf				Gravels as relict peds			

BCb	78-109		10Y 2.5/1	SL	No	ne	nf				5% 5YR 5/8 concentrations, 1 mm thick cemented layer, trace cemented peds			
2015RR09														
A1	0-6	c	5G 3/1	S	No	sl	nf				7% relict peds			
A2	6-17	c	10GY 2.5/1	fSL	No	sl	nf		5					
Cg1	17-34	c	5GY 3/1	fSL	No	sl	nf							
Cg2	34-58	c	5GY 2.5/1	fSL	No	sl	nf		1					
Aseb1	58-71	c	N 3/0	fSL	No	st	sf		4					
Aseb2	71-76	a	5G 4/1	fSL	No	st	nf							
Bwb1	76-86	c	7.5YR 4/4	LS	No	st	nf							
Bwb2	86-97	a	2.5Y 5/3	SL	No	sl	nf				3% 2.5Y 7/6 jarosite concentrations, 13% 10GY 4/1			

											depletion s			
BCb	97-112		2.5Y 4/3	LS	No	ne	nf							
2015RR10														
Ase1	0-8	c	10Y 3/1	LfS	Yes	sl	nf	sl						
Ase2	8-16	c	10Y 2.5/1	fSL	Yes	sl	nf	sl		1				
Btg	16-29	c	5GY 4/1	SCL	Yes	sl	nf			1	2% 7.5YR 4/4 concentr ations			
BC1	29-50	g	5Y 3/2	fSL	Yes	st	nf				15% 7.5YR 4/4 concentr ations, 15% 5G 4/1 depletion s			

											9% 7.5YR 5/1 concentrations, 30% 10G 5/1 depletions			
BC2	50-92		2.5Y 4/4	fSL	Yes	st	nf							
2015RR11														
A	0-9	a	5GY 3/1	S	No	sl	nf				1			
C	9-11	a	5Y 5/3	Si	Yes	st	sf					Discontinuous horizon, 75% coverage		
A'	11-15	a	10Y 2.5/1	S	Yes	st	nf				3	Few large oyster shells		
C'	15-18	a	2.5Y 6/4	Si	No	sl	sf				3	Horizon appears to be bounded by 3 mm thick Fe cemented layers		

CB1	18-52	c	5Y 3/2	S	No	ne	nf				12% 2.5YR 3/6 concentrations, gravels as relict peds			
CB2	52-63		5Y 3/2	S	No	ne	nf				12% 2.5YR 2/6 concentrations			
2015RR12														
A	0-17	a	N 3/0	S	No	sl	nf				Beach stratification			
2CAg	17-34	a	10Y 4/1	LS	No	vs	nf				Beach stratification, 13% 10YR 6/8 relict peds			
3Cg1	34-80	g	5Y 5/2	fSL	No	vs	nf							
3Cg2	80-95	c	N 3/0	fSL	No	vs	nf							
3Cg3	95-112	c	N 2.5/0	fSL	No	vs	nf				20% 10YR 5/8 concentrations			

3Cg4	112-130		5Y 5/1	fSL	No	sl	nf					7% 10YR 6/6 concentrations			
2015RR13															
Oa	0-8		7.5YR 2.5/2	MP			nf								
A	8-22		10YR 2/2	fSL			nf								
AE	22-40		10YR 3/3	LfS			nf								
EB	40-55		10YR 4/4	LfS			nf								
Bt	55-85		10YR 4/4	SCL			nf								
BC	85-105		10YR 5/6	SL			nf								
2015RR14															
Oa	0-5		5YR 2.5/2	MP			nf								
A	5-10		10YR 4/3	SiL			nf								
E	10-24		2.5Y 6/4	SiL			nf								
Bt1	24-43		10YR 4/6	SiCL			nf								
Bt2	43-70		10YR 5/6	SiCL			nf					10YR 6/3 concentrations			



Bt3	70-101		10YR 5/6	SiCL			nf				10YR 7/2 concentrations			
2015RR16														
A	0-26	c	10Y 2.5/1	SiL	Yes	st	vf				Live clam			
Cgse1	26-81	g	10Y 4/1	SiCL	Yes	st	vf							
Cgse2	81-103	c	10Y 4/1	SiCL	No	st	vf							
Cgse3	103-141	a	5Y 4/1	L	No	sl	vf			7				
3Cg	141-152		7.5GY 5/1	L	No	sl	nf							
2015RR17														
Ase1	0-14	a	10YR 2/1	L	Yes	st	mf			6				
Ase2	14-26	a	5Y 2.5/1	SL	Yes	st	nf			75				
Ase3	26-41	c	5GY 2.5/1	SL	Yes	sl	mf			22				
Cgse1	41-67	c	5GY 3/1	SL	Yes	vs	mf			11				
Cgse2	67-78	c	5GY 3/0.5	LS	No	sl	nf			1				
Cgse3	78-101		10Y 3/0.5	L	No	vs			7	1				
2015RR18														
Ase1	0-15	c	/	shell			nf			90				

Ase2	15-30	a	10Y 4/1	L	No	vs	mf			55				
Ase3	30-38	a	5GY 3/1	fSL	No	sl	sf			5				
2Cg	38-52	c	5GY 5/1	SiL	No	ne	nf							
3Btb	52-58		2.5Y 5/4	SiCL	No	ne	nf				7.5YR 4/6 concentrations, 7.5YR 5/6 concentrations, 5Y 5/2 depletions			
2015RR19														
A	0-12	a	10Y 2.5/1	SiCL	Yes	st	vf							
Cgse1	12-90	g	5Y 3/0.5	SiCL	Yes	st	vf							
Cgse2	90-270	g	5GY 4/1	SiCL	Yes	vs	vf							
Cgse3	270-330	g	5GY 3.5/1	C	No	vs	vf							
Cgse4	330-350		5GY 4/1	C	No	vs	vf							
2015RR21														
Cg1	102-140		5GY 3/1	SiCL			vf			3				

Cg2	140-155		10Y 4/0.5	SL			vf							
2015RR21.1														
Ase	0-34	c	10Y 2.5/1	S	No	VS	NF			50			8.27	7.27
Cse1	34-65	g	10Y 2.5/1	S	No	VS	NF			3			8.34	7.38
Cse2	65-108	g	10Y 2.5/1	LS	No	VS	SL			0			8.2	7.31
Cse3	108-148		5GY 2.5/1	SL	No	VS	MF			6			8.08	7.36
2015RR22														
Ase1	0-6	c	10Y 2.5/1	fS	Yes	st	nf			2				
Ase2	6-29	c	5GY 3/1	fSL	No	st	nf		1	4				
2CBseg	29-41	c	5GY 4/1	fSL	No	st	sf				23% 10YR 4/4 concentrations			
2CBsegj1	41-62	a	10Y 5/0.1	SCL	No	st	nf				14% 5Y 6/4 jarosite concentrations, 30% 10YR 4/6 concentrations			

											35% 5Y 7/4 jarosite concentr ations, 2% 5YR 3/4 concentr ations			
2CBsegj2	62-78		5Y 4/2	L	No	st	nf							
2015RR23														
Ase	0-15	c	10Y 3/1	LS	No	SL	NF						7.21	6.16
											5% 10YR 3/4 concentr ations, 10% 2.5Y 7/6 jarosite concentr ations			
Btsejg	15-29		10Y 4/1	SCL	No	SL	NF						7.32	6.76
2015RR24														
Ase	0-11	c	10Y 2.5/1	SiL	Yes	st	vf							
Cgse1	11-52	g	10Y 3/1	SiL	Yes	st	vf							
Cgse2	52-115	g	10Y 3/1	SiCL	Yes	st	vf				Greener than horizon 2			
Cgse3	115- 183	g	5GY 4/1	SiL	Yes	sl	vf							

Cgse4	183-200		5GY 4/1	SiL	Yes	sl	vf			3				
2015RR25														
Ase	0-16		10Y 2.5/1	SiL	Yes	st	vf		1					
Cgse1	16-37		10Y 2.5/1	SiL	Yes	st	vf			1				
Cgse2	37-69		10Y 3/1	L	Yes	st	vf			1				
2Cgse3	69-92		5GY 3/1	fSL	No	sl	mf			1				
3Cg	92-100		10GY 5/1	SCL	No	vs	sf				1% 7.5YR 4/4 concentrations			
2015RR26														
Ase1	0-10		10Y 2.5/1	fSL	No	ve	sf			1				
Ase2	10-24		10Y 2.5/1	fSL	No	ve	nf			1				
2Bseg	24-39		2.5Y 4/1	SL	No	st	nf				3% 2.5Y 5/4 concentrations, 18% 10YR 6/8 concentrations			

											4% 5Y 7/4 jarosite concentrations, 6% 7.5YR 3/3 concentrations			
2Bgj	39-51		10YR 4/2	fSL	No	vs	nf							
											15% 5Y 7/4 jarosite concentrations, 4% 7.5YR 5/8 concentrations			
2Btj	51-69		2.5YR 4/3	fSL	No	vs	nf							
2Cseg	69-80		2.5Y 2.5/1	L	No	ve	nf				Unoxidized zone			
2015RR27														
Cg	0-20	c	2.5Y 4/1	CoS	No	vs	nf				3 Sand fraction is 15% glaucinite			
Cgse1	20-38	c	10Y 2.5/1	SL	Yes	vs	nf				Sand fraction is 10% glaucinite			

Cgse2	38-69	a	N 2/0	S	Yes	vs	nf					Sand fraction is 35% glauconite			
2Abse	69-83	c	5GY 2.5/0.5	L	Yes	se	vf		2	3		Sand fraction is 10% glauconite			
2C'gse1	83-112	g	N 2/0	SL	Yes	st	mf					Sand fraction is 45% glauconite			
2C'gse2	112-137	g	N 2/0	SL	Yes	st	mf								
2C'gse3	137-150		5GY 3/1	SL	Yes	st	mf								
2015RR28															
Cseg	0-34	c	5GY 2.5/1	SiCL	Yes	st	vf			1					
Ase	34-55	c	N 2/0	SiL	Yes	st	vf					45% glauconite in sand fraction			
C'seg1	55-83	g	5GY 2.5/1	SiCL	Yes	st	vf								
C'seg2	83-148	g	10Y 3/0.5	SiCL	Yes	st	vf			3					
C'seg3	148-230	g	5GY 4/1	SiC	No	se	vf								

C'seg4	230-250		5GY 4/1	SiL	No	vs	vf							
2015RR28.1														
Ase	0-7	c	5Y 4/1	S	No	VS	NF						7.71	6.38
Cse1	7-31	c	5Y 3/1	S	No	VS	NF				Krotovina		8.16	6.15
Cse2	31-45	c	10Y 2.5/1	CoS	Yes	VS	NF				Krotovina		8.46	6.7
Cse3	45-52	c	5Y 3/1	CoS	No	VS	NF				Krotovina		8.55	6.89
Cse4	52-76	g	5Y 3/1	S	No	VS	NF				Krotovina		8.43	6.72
Aseb	76-86	a	N 2.5/0	S	Yes	VS	NF			tr			8.36	7.28
Cseb1	86-102	a	5Y 3/1	CoS	No	VS	NF						8.15	7.58
Cseb2	102-107	c	5Y 3/1	CoS	Yes	VS	NF				Mixed gravels, many colors		8.88	7.33
2A'seb	107-132	g	N 2.5/0	SiL	Yes	SL	MF				Root channels, stains hands black		8.75	4.87
2C'seb	132-176		5GY 3/1	SiC	No	SL	SF			tr	Trace root channels		8.33	4.47
2015RR29														
Ase	0-35	c	5Y 2.5/1	SiL	Yes	sl	vf							



Cgse1	35-84	g	5GY 3/1	SiL	Yes	st	vf							
Cgse2	84-219	c	10Y 3/1	SiCL	Yes	st	vf				Sand fraction 33% glauconit e (field)			
Cgse3	219- 231	c	5GY 3/1	SiL	Yes	sl	vf							
Cgse4	231- 400		10Y 3/1	SiCL	No	st	vf			tr				
2015RR30														
Ase	0-16	c	10Y 2/1	SL	Yes	st	sf							
Cgse	16-32	a	5GY 2.5/1	LS	Yes	st	nf							
2BC1	32-50	c	5Y 4/3	SCL	No	st	nf				40% 5G 3/1 depletion s, 5% 5Y 3/4, 26% of sand fraction is glauconit e			

											10% 5YR 5/6 concentrations, 10% 7.5YR 5/8 concentrations, contains hard cemented nodules			
2BC2	50-69	g	5YR 3/2	LS	No	ve	nf							
2BC3	69-96		10YR 3/4	LS	No	ve	nf				10% 10Y 3/1 depletions, 1% 5Y 3/1, contains hard cemented nodules			
2015RR31														
Ase	0-26	c	10Y 2.5/1	SiL	Yes	sl	vf				1			
Cgse1	26-57	g	5GY 2.5/0.5	SiCL	Yes	st	vf							
Cgse2	57-97	c	10Y 3/1	SiL	Yes	st	vf							
Cgse3	97-161	g	10Y 3/0.5	SiCL	Yes	st	vf				1			
2Cgse1	161-190	g	5GY 3/1	SCL	Yes	st	NF							

2Cgse2	190-215		5GY 3/0.5	SL	No	st	NF		tr					
2015RR32														
Ase1	0-12	c	10Y 3/1	S	Yes	st	nf							
Ase2	12-26	c	5GY 3/1	S	Yes	st	nf							
2CBseg1	26-45	c	65% 5BG 3/1, 35% 5GY 3/1	CL	Yes	st/ve	nf							
2CBseg2	45-59		80% 5Y 4/2, 20% 5G 3/2	SCL	Yes	ve	nf				May be very close to UOZ, 3% bubbled			
2015RR33														
Ase	0-7	c	10Y 2.5/1	S	Yes	VS	NF			15			7.98	6.75
Cse1	7-42	g	5GY 2.5/1	LS	No	VS	NF		2	2			8.43	6.22
Cse2	42-78	g	5GY 2.5/1	SL	No	VS	SF		4	2	Sulfidic materials		8.78	3.78
Cse3	78-129	c	10GY 2.5/1	L	No	VS	MF		4	4	Sulfidic materials		7.91	3.56
Cse4	129-152		10GY 2.5/1	SL	No	VS	SL			0	Sulfidic materials		7.86	3.59

2015RR34														
Ase	0-32	c	5Y 2.5/0.5	SiL	Yes	st	vf	s						
Cgse1	32-56	c	5GY 2.5/1	SiL	Yes	st	vf							
Cgse2	56-71	a	5GY 2.5/1	SiL	Yes	st	vf							
Cgse3	71-85	g	5GY 2.5/0.5	SiL	Yes	st	vf							
Cgse4	85-100		10GY 3/1	SiCL	Yes	st	vf							
C'gse	477- 527		5GY 3/1	SiC	Yes	st	vf		1	3	Deep sample, skipped overlying material			
2015RR37														
Ase	0-7	c	5GY 3/1	fS	No	vs	nf							
Cgse1	7-33	c	5GY 4/1	fS	No	vs	nf							
Cgse2	33-54	g	10Y 4/1	L	Yes	vs	mf		7					
C/Oseg	54-116	c	5GY 4/0.5	CL	Yes	vs	mf	m	12					
C/Oseg	116- 141	c	5GY 3/1	CL	Yes	st	mf	sl petro chem ical	20	tr	Numerou s thin buried marsh surfaces			

C'gse3	141-167		5GY 3/1	CL	Yes	vs	mf		10					
2015RR39														
Ase	0-5	a	10Y 2.5/1	fS	Yes	SL	NF			0	2.5 Y 3/4 surface film		7.79	5.86
C	5-25	g	10Y 3/1	fS	No	VS	NF			2			8	5.83
Cg1	25-61	g	10Y 4/1	fS	No	VS	NF	sl		2			8.03	5.99
Cg2	61-88	g	10Y 4/1	LfS	No	VS	NF	sl		1	Sulfidic materials		7.95	4
C'1	88-135	c	10Y 3/1	L	No	VS	MF			1			7.46	4.69
C'2	135-145		10Y 3/1	L	No	VS	MF				Sulfidic materials		8	3.67
2015RR40														
Ase	0-21	g	5GY 3/1	SL	Yes	st	vf			3	Clam box	2.18		
Cgse1	21-62	c	5GY 4/1	SCL	Yes	st	vf							
Cgse2	62-88	g	5GY 4/1	SC	Yes	vs	vf							
Cg	88-124	g	5GY 4/1	SC	No	vs	vf							
C'gse3	124-200	g	5GY 4/1	C	No	sl	vf							
C'gse4	452-502		5GY 4/1	C	Yes	st	vf							
2015RR41														

Ase	0-25		10Y 2.5/1	S	Yes	sl	nf			10				
2Btseg1	25-40		10GY 4/1	SCL	No	st	nf				15% 10YR 4/6 concentr ations			
2Btseg2	40-72		10GY 3/1	SC	No	st	nf				45% 7.5YR 4/8 concentr ations			
2Btseg3	72-86		7.5YR 4/8	L	No	st	nf				45% 10GY 3/1 depletion s			
3BC1	86-95		2.5Y 4/4	LS	No	vs	nf							
3BC2	95-100		2.5Y 4/4	S	No	vs	nf							
3BC3	100- 120		10YR 4/4	LS	No	vs	nf				2.5YR and 10YR 6/2 relict peds, clay			
2015RR42														
Ase	0-19	c	5GY 2.5/1	S	No	SL	NF						7.9	4.8

2Btse1	19-38	g	10Y 3/2	SCL	Yes	ST	MF				3% 10YR 3/4 concentr ations, krotovina		7.62	4.22
2Btse2	38-58	c	10GY 3/1	SCL	No	ST	SF				10% 10YR 3/4 concentr ations		7.38	5.89
2Btse3	58-68		10GY 3/1	SC	No	VE	NF				30% 10YR 3/4 concentr ations		7.31	6.24
2015RR43														
Ase1	0-7		10Y 2.5/1	S	Yes	VS	NF	n					7.45	4.51
Ase2	7-17		10Y 2.5/1	S	Yes	VS	NF	n		40			8.28	7.31
Btse1	17-36		10Y 3/1	SCL	No	SL	SF	n			15% 2.5Y 4/3 concentr ations		7.82	4.86
Btse2	36-56		10GY 3/1	SCL	No	ST	NF	n			12% 2.5Y 4/3 concentr ations		7.43	6.44
2015RR44														
Ase	0-15	c	5GY 2.5/1	SiL	Yes	st	vf							

Cgse1	15-37	g	5GY 2.5/1	CL	Yes	st	vf							
Cgse2	37-52	a	5GY 3/1	SL	Yes	st								
2Bgse	52-75	g	10Y 4/1	LS	No	se	nf				17% 10YR 4/6 concentr ations, 17% 7.5 YR 3/4 concentr ations			
2Btgse	75-100		5GY 4.5/1	SC	No	se	nf				35% 10YR 4/6 concentr ations			
2015RR45														
Ase	0-5		5GY 3/1	S	Yes	st	nf			1				
2Bseg	5-21		5GY 5/2	CL	No	ve	nf				30% 10YR 5/8 concentr ations			
2015RR46														
Ase	0-4		2.5Y 2.5/1	S	Yes	st	nf				Horizons 3-9 are finely stratified, not ochric			



2BCse	4-12		2.5Y 5/6	S	No	vs	nf							
3CBgse	12-35		10Y 7/1	SiL	No	vs	nf				30% 7.5YR 5/8 concentr ations			
4Cgse1	35-54		10Y 7/1	L	No	vs	nf				5% 10YR 6/8 concentr ations			
4Cgse2	54-63		5Y 5/2	S	No	se	nf							
4Cg1	63-113		2.5Y 7/2	fS	No	ne	nf							
4Cg2	113- 133		2.5Y 6/2	fS	No	ne	nf							
4Cg3	133- 177		2.5Y 6/1	fS	No	ne	nf				15% 10YR 5/6 concentr ations			
4Cg4	177- 194		5Y 7/1	fS	No	ne	nf							
2015RR49														
Ase	0-22	c	10Y 3/1	SiL	Yes	st	vf	m				4.06		
Cgse1	22-76	a	10Y 4/1	SiCL	Yes	st	vf	m	4			4.75		
2Oase1	76-93	a	5YR 2.5/1	muck	No	vs	vf	st				41.5		
3C'seg2	93-98	a	5Y 4/1	SiL	No	se	vf	m				8.79		

4Oase2	98-132	g	7.5YR 2.5/2	muck	No	vs	vf	st				48.1		
4Oase3	132- 213	a	10YR 2/2	muck	No	vs	vf	st			larger fibers	48.9		
5C'seg3	213- 239	g	5GY 3.5/1	CL	Yes	ve	mf	sl				1.23		
5C'seg4	239- 250		10GY 4/1	SCL	Yes	se	nf	x	3			0.38		
2015RR50														
Ase	0-22	c	10Y 3/1	SiL	Yes	st	vf		1					
Cgse1	22-71	g	10Y 3/1	SiCL	Yes	st	vf				trace organic fragment s			
Cgse2	71-116	a	10Y 4/1	SiCL	Yes	st	vf							
2Oaseb1	116- 162	g	10YR 2/2	muck	No	ne	vf	sl						
2Oaseb2	162- 195	c	10YR 2/2	muck	No	ne	vf	sl			larger fragment s			
3C'gse	195- 200		10GY 4/1	SCL	No	sl	mf				same material as other horizon. 3% org frag			
2015RR51														
Ase	0-11	g	10Y 3/1	L	Yes	st	vf							

Cgse1	11-53	g	5GY 3/1	SiCL	Yes	st	vf			1				
Cgse2	53-91	g	5GY 4/1	fSL	No	vs	mf			1				
Cgse3	91-149	g	5GY 3/2	CL	No	vs	mf			4				
Cgse4	149- 180		5G 3/1	fSL	No	sl	sf							
2015RR52														
Ase	0-13	c	10Y 2.5/1	S	Yes	VS	NF			2	3% oxidized burrows		7.97	4.79
Cse	13-34	g	10Y 2.5/0.5	S	Yes	VS	NF			4			8.33	6.57
Aseb1	34-64	g	10Y 2.5/1	LS	No	SL	NF				Sulfidic materials		7.72	2.87
Aseb2	64-78		10Y 2.5/1	SL	No	VS	SF				Sulfidic materials		7.7	3.19
2015RR53														
Ase1	0-20	d	5GY 2.5/1	S	Yes	SL	NF			4			7.97	4.42
Ase2	20-40		5GY 2.5/1	LfS	Yes	VS	SF			4			8.58	4.8
Ase3	40-60		5GY 2.5/1	fSL	Yes	VS	SF			4			8.82	5.24
Ase4	60-80		5GY 2.5/1	L	Yes	SL	MF			4			9.08	4.98
2Cse1	80-100		5GY 3/1	SiL	No	ST	VF			4			8.75	6.18
2Cse2	100- 120		5GY 3/1	SiL	No	ST	VF			4			8.39	6.73

2Cse3	120-130		5GY 3/1	SiL	No	ST	VF			4			8.52	7.08
2015RR54														
Ag	0-24	a	50% 5Y 4/1, 50% 10Y 2.5/0.5	fS	Yes	vs	NF	n		0		0.08	7.64	5.57
Cg1	24-44	c	2.5Y 6/2	fS	No	ne	NF	n		15	Clam boxes	0.12	7.74	5.88
Cg2	44-120	g	90% 2.5Y 4/1, 10% 5Y 5/1	fS	No	vs	NF	n		0	Sulfidic materials	0.16	7.01	4.03
Cg3	120-153	c	10Y 4/1	fS	No	vs	NF	n		0	Sulfidic materials	0.16	8.15	3.83
Cg4	153-212	a	5GY 4/1	LfS	No	ne	NF	n		0	Sulfidic materials	0.27	8	3.7
Ab	212-218	a	10Y 3/1	LfS	No	vs	NF	n		0.1	Sulfidic materials	2.32	7.78	3.38
Cgse	218-239		10Y 4/1	fS	No	ne	NF	f		0	Sulfidic materials	0.22	7.78	3.69
2015RR55														
Ase	0-6	a	10Y 3/1	S	Yes	VS	NF	n		2			7.34	4.72
Oe	6-49	g	10YR 2/1	MP	No	NE	NF	n					7.11	5.93
Oa1	49-73	g	10YR 2/1	M	No	NE	VF	mod					7.1	5.95

Oa2	73-103	a	10YR 2/1	M	No	NE	VF	sl					6.77	5.84
2Cg	103- 121	va	5Y 4/1	fSL	No	VS	NF	n			Sulfidic materials		7.26	3.81
3Oab	121- 127		N 2.5/0	M	No	NE	VF	n			Slight petroche mical smell when rubbed		6.94	5.5
2015RR56														
Ase1	0-17	g	N 2.5/0	SiC	Yes	ST	MF			tr	vf copro		7.03	5.25
Ase2	17-56	d	10Y 3/1	SiC	Yes	ST	MF			tr	vf copro		7.99	5.59
Ase3	56-134		5GY 3/1	SiC	No	SL	MF			tr	f copro		8.22	6.98
2015RR57														
Ase	0-22	g	10Y 2.5/1	SiC	Yes	VE	MF			3			8.27	4.33
Cse1	22-46	c	10Y 2.5/1	SiC	Yes	VE	MF			3			8.49	6.26
Cse2	46-55	c	10Y 2.5/1	SiC	Yes	VE	MF			3	Sulfidic materials		8.44	4.05
Cse3	55-112	g	10Y 3/1	SiC	No	VE	MF			tr			8.09	4.73
2Cse4	112- 201	g	5GY 2.5/1	fSL	No	VE	SF			tr			7.87	4.28

2Cse5	201-241	c	5GY 2.5/1	fSL	No	VE	SF			3	Sulfidic materials , large wood fragment at 220	7.81	3.49
3BCg	241-268		5Y 4/2	SCL	No	VE	MF			0	20% 10YR 3/6 concentrations, 30% 10GY 4/1 depletions	7.73	6.35
2015RR58													
Oase1	0-17	c	7.5YR 2.5/2	muck	No	vs	vf	st					
Oase2	17-66	c	7.5YR 2.5/2	muck	No	vs	vf	st			Denser than overlying horizon		
2Oase3	66-86	c	10YR 2/2	muck	No	st		m					
2Oase4	86-112	c	10YR 2/1	muck	No	ve		m					
2Ase	112-120	c	2.5Y 3/1	fSL	No	ve		x					
3Cseg	120-150		5GY 5/1	fSL	No	ve		x					

2015RR59														
Ase	0-14	c	5GY 2.5/1	SiL	Yes	st	vf							
Cgse1	14-94	g	5GY 4/1	SiCL	Yes	st	vf							
Cgse2	94-159	g	5GY 4/1	CL	Yes	st	vf			16				
Cgse3	159- 184		5GY 4/0.5	SL	No	st	sf		5					
2015RR59.1														
Ase	0-9		5Y 2.5/0.5	L	Yes	ve	mf							
2Cgse1	9-21		2.5Y 2.5/0.5	L	No	ve								
2Cgse2	21-55		N 5/0	SiL	No	ve	nf				moderate angular blocky structure			
2Cse	55-164		7.5YR 4/3	SiL	No	ve	nf				strong angular blocky structure, few clay films			
2015RR60														
Ase1	0-22	g	10Y 2.5/1	SiC	Yes	VE	VF						7.57	4.31
Ase2	22-51	g	10Y 3/1	SiC	Yes	VE	VF						8.46	5.92

2Ase3	51-68	g	10Y 2.5/1	L	No	ST	MF			20			8.31	7.27
2Cse1	68-127	d	10Y 3/1	S	No	SL	NF				Sulfidic materials , Finely stratified		7.83	3.99
2Cse2	127- 167	c	5GY 2.5/1	LS	No	SL	SF				Sulfidic materials , Finely stratified		8.16	3.31
2Cse3	167- 219		5GY 2.5/1	LS	No	SL	SF				Finely stratified		8.34	6.27
2015RR61														
Ase	0-12	c	10Y 2.5/1	S	Yes	SL	NF						7.9	4.79
Oa1	12-30	g	10YR 2/1	Muck	No	NE	MF	mod					7.43	5.79
Oa2	30-37	c	10YR 2/1	Muck	No	VS	VF						7.45	4.45
A'se	37-46	c	10Y 2.5/1	SL	No	SL	MF				Sulfidic materials		7.18	2.77
BEse	46-61	g	10Y 5/1	SL	No	ST	SF				Sulfidic materials		6.96	3.88
Btse1	61-94	g	5GY 4/1	L	No	VE	MF				15% 10YR 4/4 concentr ations		6.94	4.21



Btse2	94-112		10GY 5/1	SCL	No	ST	SF				Sulfidic materials , 28% 10YR 4/6 concentr ations, 5% transport ed peds		6.58	3.29
2015RR62														
Ase	0-27	c	10Y 3/1	fS	Yes	VS	NF			tr	Sulfidic materials		8.2	3.94
Cgse	27-41	c	5Y 5/1	fS	No	VS	NF						5.59	5.57
Cg	41-88	a	5Y 5/2	LfS	No	NE	NF				27% 7.5YR 5/8 stratificat ions		4.58	4.79
2C	88-109	a	2.5Y 5/4	S	No	NE	NF				Beach stratificat ion		5.31	5.18
3C1	109- 131	d	10Y 3/2	S	No	NE	NF						5.04	5.01
3C2	131- 157		10Y 3/2	S	No	NE	NF				22% 10YR 3/6 concentr ations		5.14	5.19
2015RR63														
Ase	0-79	g	10Y 2.5/1	SiCL	Yes	ST	VF			2			7.8	4.95

Cse1	79-126	g	10Y 3/1	SiC	No	ST	MF			tr			8.53	5.6
Cse2	126- 214	d	10Y 3/1	SiC	No	ST	MF			tr	Sulfidic materials		8.46	3.98
Cse3	214- 268		5GY 3/1	SiC	No	ST	MF			tr	Sulfidic materials		8.4	3.9
2015RR64														
Ase1	0-27	g	N 2.5/0	SiL	Yes	VE	VF			tr	Coprogenous structure	3.6	8.3	4.43
Ase2	27-45	g	N 2.5/0	SiCL	Yes	VE	VF			tr		2.83	8.66	5.33
Cse1	45-87	g	5GY 2.5/0.5	SiC	Yes	VE	MF			3		2.35	8.02	5.67
Cse2	87-142	g	5GY 2.5/0.5	SiCL	Yes	VE	VF				Sulfidic materials	3.19	8.07	3.75
Cse3	142- 201	c	10Y 2.5/1	SiC	Yes	VE	MF				Sulfidic materials	3.4	8.06	3.5
Oaseb	201- 221	va	10YR 1/1	muck	No	VS	NF				Sulfidic materials	11.4	7.81	3.19
2Cse	221- 224	a	5Y 3/0.5	S	No	VS	NF				Sulfidic materials	0.47	7.73	2.86
3Aseb	224- 233	c	10YR 1/1	muckySL	No	VS	NF				Sulfidic materials	3.63	7.54	2.51
3Cseg	233- 257	c	5GY 4/2	S	No	VE	NF					0.22	7.81	4.29
4Btsegb	257- 269	g	5GY 4/2	SCL	No	VE	NF				15% 10YR 3/4 conc	0.11	8	6.59
4Btseb	269- 300		5G 3/2	C	No	EVE	NF				7% 10YR 3/4 conc	0.19	8.19	7.48

2015RR65														
Ase	0-31	d	5GY 2.5/1	SiCL	Yes	VE	VF			tr		1.5	7.46	5.04
Cse1	31-106	d	5GY 2.5/0.5	SiCL	Yes	VE	VF			tr		1.29	8.68	6.37
Cse2	106- 150		5GY 3/1	SiC	No	ST	VF			tr		1.59	7.99	7.08
2015RR66														
Ase1	0-16	c	10Y 3/1	S	No	SL	NF						8.06	7.04
Ase2	16-28	c	10Y 4/1	S	No	SL	NF			40	rounded quartz gravels		8.7	7.64
2Cseg	28-32	c	10G 4/1	C	No	VS					alluvial clay?		8.39	7.52
3BCseg1	32-65	g	10Y 4/1	LS	No	VS	NF				15% 10YR 5/3 concentr ations, 10% 10Y 5/1 depletion s		5.48	5.68
3BCseg2	65-72		10Y 6/1	SCL	No	VS	NF				33% 7.5YR 5/6 concentr ations, cemented gravels at top		5.32	5.31

2015RR67														
Ase	0-22	g	10Y 2.5/1	SiCL	Yes	VE	VF			4			7.98	5.77
Cse1	22-64	g	10Y 2.5/1	SiC	Yes	VE	MF						8.51	6.65
Cse2	64-88	g	10Y 3/1	SiC	Yes	VE	VF						8.46	6.5
Cse3	88-129	g	10Y 3/1	SiC	No	ST	VF						8.26	4.31
Cse4	129- 163		5GY 3/1	SiC	No	ST	VF						8.33	5.59
2015RR68														
Ase	0-26	a	5GY 2.5/1	S	Yes	ST	NF			3			6.76	5.97
Cse1	26-71	g	N 2.5/0	S	Yes	ST	NF			tr			7.66	5.3
Cse2	71-129	c	N 2.5/0	S	Yes	ST	NF			tr			8.46	5.69
Cse3	129- 174	g	N 2.5/0	CL	Yes	VE	MF			tr			7.85	4.93
Cse4	174- 196		5GY 3/1	CL	Yes	VE	SF			tr			7.92	5.75
2015RR69														
Ase	0-25	a	5GY 2.5/1	S	Yes	SL	NF			tr	Layer of clam shells at bottom of horizon	0.16	8.25	4.32

2Btseg	25-58	a	10Y 4/1	CL	No	ST	SF				2% 10YR 3/3 conc. As root channels	0.4	8.13	4.34
2BCseg	58-70	c	10GY 4/1	SCL	No	VE	NF				Sulfidic materials , 30% 10YR 3/3 conc	0.12	7.98	3.88
2BCse	70-78		2.5Y 4/3	SCL	No	VE	NF				45% 7.5YR 2.5/3 conc, 5% 10GY 4/1 depl.	0.1	7.5	4.26
2015RR70														
Ase	0-19	g	N 2.5/0	SiL	Yes	VE	VF			1			7.41	4.74
Cse1	19-42	g	10Y 2.5/0.5	SiL	Yes	ST	VF			1			8.23	6.09
Cse2	42-78	g	10Y 3/0.5	SiCL	Yes	SL	VF			1	Clam box		8.31	6.84
Cse3	78-141	g	5GY 2.5/1	SiC	No	SL	MF			1			8.1	7.14
Cse4	141- 177	a	5GY 2.5/1	CL	No	SL	VF			3			7.86	7.31
2BCseg1	177- 191	va	10GY 4/1	SCL	No	VS	MF						8.35	7.2
2BCseg2	191- 216	a	5G 4/2	SCL	No	VS	MF						8.56	7.31

2CBseg	216-225		10GY 5/1, 30% 10Y 5/1	SCL	No	VS	NF				20% 10YR 4/6 concentrations		8.22	8.02
2015RR71														
Ase	0-23	g	N 2.5/0	ML	Yes	VS	VF						6.84	5.04
Oase1	23-56	g	10YR 2/2	M	No	VS	NF	sl			Sulfidic materials		7.28	3.31
Oase2	56-94	g	10YR 2/1	M	No	VS	SF				Sulfidic materials		6.9	2.39
A'se	94-102	c	2.5Y 2.5/1	MS	No	VE	SF				Sulfidic materials		6.7	2.34
Cse	102-130	g	5GY 3/2	S	No	SL	NF				Sulfidic materials		6.64	3.34
2Btseg	130-155	g	5GY 4/2	C	No	ST	MF				17% 10YR 4/4 concentrations		6.52	4.69
2Btse	155-194	a	5GY 3/2	SC	No	SL	NF				3% 10YR 4/4 concentrations		6.53	4.85
2BCse	194-209		10YR 3/4	LS	No	VE	NF						6.37	5.21
2016RR03														
Ase	0-11	c	10Y 3/1	SiL							1 Live clam			

Cse1	11-55	g	10Y 2.5/1	SiCL						1				
Cse2	55-66	g	N 2.5/0	SiCL										
Cse3	66-77		10Y 3/1	SiCL										
2016RR04														
Ase	0-9	c	10Y 2.5/1	L			vf			1				
Cse1	9-26	g	10Y 2.5/1	SiCL			vf			1				
Cse2	26-54		10Y 3/1	SiCL			vf		1					
2016RR05														
Ase	0-8	g	10Y 2.5/1	SiL			vf			1				
Cse1	8-38	g	10Y 3/1	SiCL			vf							
Cse2	38-53		10Y 3/1	SiCL			mf			1				
2016RR06														
Ase	0-8	c	10Y 2.5/1	SiL			vf							
Cse1	8-25	c	10Y 2.5/1	SiL			vf			1	Denser than overlying horizon			
Cse2	25-47	c	10Y 3/1	SiCL			mf	sl	5					
Cse3	47-91	c	10Y 3/1	SiC			mf			3				

Cse4	91-104		N 2.5/0	SiC			vf		1					
2016RR09														
Ase	0-3	a	5GY 2.5/1	S	No	sl	nf							
Oese	3-43	c	7.5YR 2.5/1	MP	No	vs	mf							
Oase	43-61	c	7.5YR 2.5/1	M	No	vs	mf							
ABseg	61-78	d	10Y 4/1	CL	Yes	st	mf		30					
Btseg	78-100		10Y 4/1	SiCL	No	st	sf		15					
2016RR14														
Ase1	0-25		10GY 2.5/1	LS	Yes	ve	nf							
Ase2	25-48		10B 2.5/1	SL	Yes	ve	nf				Inferred to be sulfidic because of violent hydrogen peroxide reaction			
Cseg1	48-83		10Y 2.5/1	coLS	No		nf							
Cseg2	83-96		10B 2.5/1	LS	Yes		nf				Clam box, 6.5 cm long			
Cseg3 & Aseb1	96-130			S			nf				Several fine buried A lenses			



Cseg4 & Aseb2	130-165			SL			nf				Five buried A lenses			
2016RR20														
Ase	0-23		5Y 2.5/1	SL	Yes	sl	mf	sl						
2Bseg	23-28		60% 10GY 3/1, 30% 10Y 7/1, 10% 2.5YR 6/2	SiCL	Yes	sl	nf				Reduction front into Marlboro Clay			
2Bt	28-51		90% 2.5YR 5/4, 5% 10YR 6/6, 5% 5Y 4/2	SiCL	No	ne	nf				Marlboro Clay, clay films, possibly slickensides but no obvious flutes, some glauconitic spots near base			
3Cse	51-52		2.5Y 6/8	LS	No	sl	nf				Aquia Formation, ironstone at contact			

2016RR21														
Ase1	0-15	a	10Y 2.5/1	SiL	Yes	st	vf				Extremel y fluid			
Ase2	15-25	c	10Y 2.5/1	SiL	Yes	st	vf			1				
Cse1	25-63	g	10Y 3/1	SiL	Yes	st	vf			1				
Cse2	63-120	g	5GY 2.5/1	fSL	Yes	st	mf			1				
Cse3	120- 140		10Y 2.5/1	fSL	Yes	sl	mf			4				
2016RR24														
Ase	0-35	d	10Y 2.5/1	SiCL			vf				Weak coprogen ous structure			
Cgse1	35-77	d	5GY 2.5/1	SiCL			vf				Weak coprogen ous structure			
Cgse2	77-100		10Y 4/1	SiC			vf		tr		Weak coprogen ous structure			
2016RR25														

											Thin 2.5Y 4/3 surface film, 1 live clam, weak copro structure			
Ase	0-19	c	10Y 2.5/1	SiCL			vf			3				
Case	19-55	g	5GY 4/2	SiC			vf				Weak coprogen ous structure			
Cse	55-109		5GY 4/2	SiC			mf							
2016RR31														
Ase	0-19	c	10Y 2.5/1	SiCL	Yes	sl	vf			tr	Live clam			
Cse	19-61	c	10Y 3/1	SiC	Yes	sl	mf			tr				
Cgse1	61-119	g	10Y 4/1	SiC	Yes	sl	mf		tr					
Cgse2	119- 200		10Y 4/1	SiC	Yes	sl	mf				Somewh at denser			
2016MC01														
Ase	0-7	a	N 2.5/0	SiL	Yes	st	vf	st	20		wood fragment s, twigs			
Oese	7-17	c	10Y 3/1	mp	Yes	st	mf	st						

A'se	17-48	g	10Y 4/1	SiL	No	st	mf	m						
Cse	48-98		10Y 4/1	SiCL	No	sl	mf				One lens 3 cm thick of SL starting at 52 cm			
2016MC02														
Ase1	0-10	a	N 2.5/0	L	Yes	st	vf		20		S smell when core opened, dissipate d			
2Ase2	10-34	g	10Y 3/1	SiL	Yes	sl	vf		20					
2Ase3	34-72	c	10Y 3/1	SiL	No	sl	vf		15					
2Cseg	72-100		10Y 4/1	CL	No	sl	mf		5					
2016MC03														
Ase1	0-9	a	N 2.5/0	L	Yes	st	vf		15					
2Ase2	9-18	c	10Y 3/1	mSiL	Yes	st	mf	m	30					
3Cgse/4Cgse	18-81		10Y/5G 4/3/1/1	CL/S	No/No	st/sl	sl/nf				CL very dense and sticky but does not shine			

2016MC04														
Ase	0-2	a	N 2.5/0	L	Yes	st	vf							
Oese	2-24	a	5Y 3/2	mucky peat	Yes	st	mf	m						
Oase	24-45	a	5Y 3/2	muck	Yes	sl	vf	m			extremel y low density and fluid, could not do fiber content			
Cgse	45-102		5Y 4/2	mucky SiC	No	sl	mf	m	20					

*Appendix D: Rhode River particle size analysis*

Pedon	Horizon	% Sand	% Silt	% Clay	% vc sand	% c sand	% m sand	% f sand	% vf sand	Texture Class
2015 RR3	A	43.8	26.1	30.1	0.4	2.3	12.2	20.6	8.3	CL
2015 RR3	2Cg1	71.8	14.3	14.0	1.0	2.4	7.6	50.6	10.1	fSL
2015 RR3	3Cg2	26.4	35.0	38.6	1.5	1.5	2.4	12.7	8.2	CL
2015 RR3	3Cg3+3Cg4	8.5	41.9	49.6	1.5	1.6	1.6	1.9	1.8	SIC
2015 RR2	surface	7.1	51.2	41.7	2.3	1.8	1.3	0.5	1.2	SIC
2015 RR2	A1+A2	3.3	35.2	61.5	0.4	0.7	0.8	0.9	0.6	C
2015 RR2	Cg1	6.2	44.2	49.5	0.7	0.7	1.0	2.1	1.7	SIC
2015 RR2	Cg2	8.0	42.9	49.0	0.9	0.8	0.9	2.5	2.9	SIC
2015 RR2	Cg3	9.8	40.8	49.3	0.5	0.7	1.0	2.9	4.7	SIC
2015 RR5	Ase	96.9	1.3	1.8	4.0	15.5	54.8	21.8	0.8	S
2015 RR5	A'se	87.0	8.4	4.6	13.7	10.6	36.8	23.1	2.7	LS
2015 RR5	Cseg1	83.7	10.4	5.9	1.4	9.2	42.9	26.6	3.5	LS
2015 RR5	Cseg2	77.2	13.6	9.2	1.0	10.2	36.0	26.1	3.9	SL
2015 RR5	Cseg3	68.8	10.3	20.9	2.4	11.9	35.0	16.5	2.9	SCL
2015 RR6	Ase	9.9	49.2	41.0	2.8	1.1	2.1	2.1	1.6	SIC
2015 RR6	Cseg1	7.7	43.3	49.0	2.2	1.3	1.3	1.4	1.1	SIC
2015 RR6	Cseg2	8.2	48.3	43.5	3.2	1.2	1.3	1.4	1.0	SIC
2015 RR6	Cseg3	26.4	41.7	31.8	1.7	2.6	8.5	7.5	5.4	CL
2015 RR6	Aseb	59.6	24.7	15.7	1.4	5.3	28.0	18.7	5.8	SL
2015 RR6	Btsegb1	33.6	26.6	39.8	2.3	6.9	13.3	7.6	3.0	CL
2015 RR6	Btsegb2	52.2	17.7	30.1	0.6	10.9	31.6	7.5	1.3	SCL
2015 RR11	1	94.8	2.2	3.0	6.0	9.1	50.8	26.8	2.0	S

2015 RR11	2	27.5	24.0	48.5	2.0	2.4	8.7	12.6	1.7	C
2015 RR11	3	90.3	4.4	5.2	6.7	4.7	28.5	48.0	2.4	S
2015 RR11	4	58.4	10.0	31.6	5.3	5.9	21.2	23.6	2.4	SCL
2015 RR11	5	94.0	3.3	2.7	5.0	25.5	46.6	15.6	1.4	coS
2015 RR11	6	87.6	5.4	7.0	6.0	17.5	44.6	17.5	1.9	LS
2015 RR12	A	92.6	3.7	3.7	2.2	10.7	40.3	32.0	7.4	S
2015 RR12	2CAg	82.7	8.5	8.8	1.9	12.9	26.5	31.1	10.2	LS
2015 RR12	2CAg	3.2	55.9	40.9	0.0	0.2	0.6	1.3	1.1	SIC
2015 RR12	3Cg1	81.9	9.7	8.4	1.1	1.3	5.3	53.1	21.1	LfS
2015 RR12	3Cg2	87.2	6.6	6.2	1.0	0.9	5.8	66.8	12.7	LfS
2015 RR12	3Cg3	82.8	8.0	9.2	2.8	3.7	23.6	42.5	10.2	LS
2015 RR12	3Cg4	75.7	11.5	12.8	0.4	1.2	4.6	52.5	16.9	fSL
2015 RR13	A	81.8	10.0	8.2	0.5	9.8	27.5	35.1	8.8	LS
2015 RR13	AE	83.8	9.7	6.5	0.3	7.4	41.3	27.3	7.5	LS
2015 RR13	EB	82.8	10.4	6.8	0.2	6.6	29.1	37.3	9.6	LS
2015 RR13	Bt	68.9	6.7	24.5	0.3	9.6	26.8	23.9	8.2	SCL
2015 RR13	BC	70.0	7.6	22.4	0.1	7.4	30.6	27.4	4.4	SCL
2015 RR14	Bt1	27.6	34.2	38.2	0.0	0.7	1.9	13.9	11.0	CL
2015 RR14	Bt2	22.5	41.3	36.1	0.1	0.3	1.1	10.5	10.5	CL
2015 RR14	Bt3	19.6	47.8	32.6	0.0	0.5	1.2	8.8	9.1	SICL
2015 RR7	A	92.8	1.9	5.3	2.8	10.9	63.6	14.3	1.1	S
2015 RR7	Cg	78.1	8.1	13.7	2.0	11.1	23.6	39.8	1.8	fSL
2015 RR7	Cseg	67.1	14.5	18.4	2.0	8.5	35.4	17.7	3.6	SL
2015 RR7	C'g1	75.8	10.8	13.4	1.1	9.4	22.6	39.6	3.0	fSL
2015 RR7	C'g2	51.7	25.7	22.6	1.3	6.4	35.7	5.0	3.4	SCL
2015 RR7	2Ab	79.2	12.3	8.4	0.3	11.7	38.4	26.1	2.7	LS
2015 RR7	2Btsegb	64.8	7.0	28.3	0.7	14.1	40.7	8.1	1.1	SCL

2015 RR8	silty A1, A2	32.3	40.3	27.4	10.5	7.3	7.4	4.8	2.2	CL
2015 RR8	A	90.6	3.6	5.8	4.1	8.5	38.9	36.3	2.9	S
2015 RR8	A2	88.3	4.7	6.9	2.1	8.4	48.8	25.2	3.8	LS
2015 RR8	Cseg1	83.3	6.0	10.7	1.5	7.6	29.1	41.5	3.7	LS
2015 RR8	Cseg2	80.9	6.4	12.7	3.2	6.1	32.6	35.5	3.5	fSL
2015 RR8	Aseb	77.2	8.3	14.5	6.9	15.5	29.7	22.6	2.5	SL
2015 RR8	BCb	82.9	5.2	11.9	2.3	7.7	37.3	32.3	3.3	LS
2015 RR31	Ase	7.8	52.4	39.8	2.1	1.7	1.6	1.4	1.0	SICL
2015 RR31	Cgse1	3.6	46.2	50.2	0.1	0.7	1.1	1.0	0.7	SIC
2015 RR31	Cgse2	6.8	48.9	44.3	0.1	0.7	2.4	3.0	0.6	SIC
2015 RR31	Cgse3	30.4	35.3	34.3	0.2	1.5	8.9	16.2	3.6	CL
2015 RR31	2Cgse4	70.7	11.8	17.5	0.1	2.7	48.4	17.6	2.0	SL
2015 RR31	2Cgse5	75.7	8.6	15.8	0.2	4.3	63.1	7.3	0.7	SL
2015 RR44	Cgse1	57.6	21.0	21.4	0.5	9.8	32.9	12.2	2.2	SCL
2015 RR44	Cgse2	82.0	10.1	7.9	1.6	23.8	43.9	10.6	2.1	LcoS
2015 RR44	2Bgse	83.4	2.8	13.8	0.5	14.2	42.5	22.8	3.4	SL
2015 RR44	2Btgse	69.4	9.8	20.8	0.4	21.6	40.6	6.0	0.8	SCL
2015 RR34	Cgse1	5.0	43.5	51.5	2.3	1.1	0.5	0.6	0.5	SIC
2015 RR34	Cgse2+Cgse3	8.7	44.9	46.5	4.6	1.4	1.2	0.9	0.6	SIC
2015 RR34	Cgse4	4.8	47.3	47.9	1.0	0.9	1.1	1.2	0.6	SIC
2015 RR34	C'se	16.5	38.3	45.2	3.3	2.3	2.5	6.6	1.8	C
2015 RR45	Ase	94.1	2.2	3.7	2.0	16.9	40.9	31.6	2.7	S
2015 RR45	2Bgse	61.3	16.3	22.5	0.3	2.7	18.2	31.7	8.4	SCL
2015 RR18	Ase2	74.3	13.1	12.6	6.1	9.2	10.7	38.2	10.0	fSL
2015 RR18	Ase3	80.6	9.9	9.6	1.0	3.2	22.8	44.8	8.8	LS
2015 RR18	2Cg	42.8	35.3	21.9	1.0	10.6	18.9	10.5	1.8	L
2015 RR42	Ase	95.3	3.3	1.4	1.6	14.7	53.4	22.9	2.7	S



2015 RR71	Cse	92.0	4.4	3.6	0.7	20.5	46.9	21.9	2.0	S
2015 RR71	2Btse	59.0	5.6	35.4	2.6	20.4	29.7	5.5	0.8	SC
2015 RR71	2Btseg	58.4	5.9	35.7	0.4	11.8	25.8	15.2	5.2	SC
2015 RR71	2BCse	58.5	6.6	34.9	1.0	4.5	42.3	9.8	0.9	SCL
2015 RR42	2Btse1	67.9	16.4	15.7	0.4	14.2	33.5	17.0	2.7	SL
2015 RR42	2Btse2	63.2	7.9	28.9	0.6	11.8	34.1	15.0	1.6	SCL
2015 RR42	2Btse3	63.1	7.7	29.2	0.2	13.5	31.3	16.5	1.6	SCL
2015 RR61	Bese	65.1	25.3	9.6	0.3	8.2	22.1	28.8	5.6	SL
2015 RR61	Btse1	52.9	19.7	27.4	1.6	8.5	17.5	22.5	2.9	SCL
2015 RR61	Btse2	50.9	20.1	29.0	4.7	18.1	16.5	10.6	1.0	SCL
2015 RR62	Ase	90.9	4.1	5.0	1.0	5.0	30.6	52.7	1.6	fS
2015 RR62	Cg	80.5	9.3	10.2	0.1	1.0	9.6	60.5	9.3	LfS
2015 RR62	Cgse	85.9	5.8	8.3	0.1	0.6	9.0	68.7	7.5	LfS
2015 RR62	3Cb1	65.4	6.9	27.7	2.6	16.0	31.7	14.0	1.2	SCL
2015 RR62	3Cb2	62.9	5.5	31.6	0.3	18.7	30.1	12.6	1.1	SCL
2015 RR64	Ase1	63.4	22.7	13.9	0.0	0.0	0.0	0.0	0.0	SL
2015 RR64	<i>Cse1</i>	<i>44.7</i>	<i>33.9</i>	<i>21.4</i>	<i>0.0</i>	<i>0.0</i>	<i>0.0</i>	<i>0.0</i>	<i>0.0</i>	<i>L</i>
2015 RR64	Cse2	61.7	24.0	14.3	0.0	0.0	0.0	0.0	0.0	SL
2015 RR64	<i>Cse3</i>	<i>62.6</i>	<i>23.7</i>	<i>13.7</i>	<i>0.0</i>	<i>0.0</i>	<i>0.0</i>	<i>0.0</i>	<i>0.0</i>	<i>SL</i>
2015 RR64	3Cseg	84.3	8.3	7.4	1.8	18.9	37.7	21.7	4.1	LS
2015 RR64	4Btseb	50.1	8.4	41.5	2.7	4.8	14.1	26.9	1.6	SC
2015 RR64	Ase2	4.5	68.3	27.2	0.1	1.0	1.5	1.2	0.8	SICL
2015 RR64	<i>Cse1</i>	<i>5.7</i>	<i>66.1</i>	<i>28.1</i>	<i>0.4</i>	<i>0.8</i>	<i>1.4</i>	<i>2.1</i>	<i>1.0</i>	<i>SICL</i>
2015 RR64	<i>Cse3</i>	<i>21.4</i>	<i>50.5</i>	<i>28.1</i>	<i>0.1</i>	<i>2.3</i>	<i>8.1</i>	<i>8.7</i>	<i>2.2</i>	<i>CL</i>
2015 RR64	3Aseb	68.2	13.5	18.3	0.7	13.4	25.7	26.7	1.7	SL
2015 RR64	4Btsebg	80.1	6.4	13.5	1.0	15.5	40.3	19.8	3.4	SL
2015 RR57	Ase	46.3	36.9	16.8	0.0	0.0	0.0	0.0	0.0	L

2015 RR57	Cse1	12.4	50.3	37.3	0.0	0.0	0.0	0.0	0.0	SICL
2015 RR57	Cse3	27.5	42.2	30.2	0.0	0.0	0.0	0.0	0.0	CL
2015 RR57	2Cse4	81.2	10.7	8.1	0.6	7.5	38.7	30.7	3.8	LS
2015 RR57	2Cse5	84.4	8.6	7.1	1.4	33.7	31.9	15.7	1.6	LcoS
2015 RR57	3BCg	61.4	8.1	30.5	3.7	10.5	37.7	8.1	1.4	SCL
2015 RR69	Ase	97.9	0.4	1.7	0.6	7.5	73.1	15.5	1.2	S
2015 RR69	Btseg	56.1	15.5	28.4	0.8	4.0	15.5	30.4	5.5	SCL

Appendix E: Rhode River bulk density data

Pedon	Horizon	BD (g/cc)
2015RR21.1	Ase	1.44
2015RR21.1	Cse1	1.44
2015RR21.1	Cse2	1.19
2015RR21.1	Cse3	0.97
2015RR23	Ase	1.58
2015RR23	Btsejg	1.64
2015RR28.1	Cse1	1.66
2015RR28.1	Cse4	1.75
2015RR28.1	2A'seb	1.18
2015RR28.1	2C'seb	1.26
2015RR33	Cse1	1.26
2015RR33	Cse2	1.02
2015RR33	Cse3	0.72
2015RR33	Cse4	1.19
2015RR39	C	1.49
2015RR39	Cg1	1.62
2015RR39	Cg2	1.26
2015RR39	C'1	1.19
2015RR42	Ase	1.32
2015RR42	2Btse1	1.61
2015RR42	2Btse2	1.40
2015RR42	2Btse3	1.56
2015RR43	Ase1	1.24
2015RR43	Ase2	1.27
2015RR43	Btse1	1.43
2015RR43	Btse2	1.65
2015RR52	Ase	1.62
2015RR52	Cse	1.51
2015RR52	Aseb1	1.38
2015RR52	Aseb2	1.25
2015RR55	Oe	0.10
2015RR55	Oa1	0.14
2015RR55	Oa2	0.34
2015RR55	2Cg	1.60
2015RR57	Ase	0.40
2015RR57	Cse1	0.45
2015RR57	Cse3	0.45
2015RR57	2Cse4	1.29
2015RR57	2Cse5	1.36
2015RR57	3BCg	1.48
2015RR61	Oa1	0.10
2015RR61	BEse	1.76
2015RR61	Btse1	1.58
2015RR61	Btse2	1.57

2015RR62	Ase	1.55
2015RR62	Cgse	1.49
2015RR62	Cg	1.56
2015RR62	3C1	1.49
2015RR62	3C2	1.50
2015RR64	Ase1	0.45
2015RR64	Cse1	0.36
2015RR64	Cse2	0.21
2015RR64	Cse3	0.47
2015RR64	Oaseb	0.32
2015RR64	3Cseg	1.67
2015RR64	4Btseb	1.48
2015RR66	Ase1	1.62
2015RR66	3BCseg1	1.51
2015RR68	Ase	1.37
2015RR68	Cse1	1.48
2015RR68	Cse2	1.31
2015RR68	Cse3	0.98
2015RR68	Cse4	0.86
2015RR69	Ase	1.57
2015RR69	2Btseg	1.59
2015RR71	Ase	0.27
2015RR71	Oase1	0.14
2015RR71	Oase2	0.16
2015RR71	Cse	1.60
2015RR71	2Btseg	1.21
2015RR71	2Btse	1.49
2015RR71	2BCse	1.41

#### Summary statistics for bulk density by material type

Type	Count	Mean	SD	SE
Buried A	3	1.27	0.10	0.06
Fluid mud	12	0.57	0.30	0.09
Organic	7	0.18	0.10	0.04
Holocene sandy	30	1.42	0.20	0.04
Tertiary	20	1.51	0.13	0.03

*Appendix F: Gyldensteen Strand sample morphology*

Sample	Site	Layer	Bottom (cm)	Color	3%rxn	30%rxn	Fluidity	Structure	Redox
GF04-01	GF	A	15	2.5Y 2.5/1	y	sl	nf	sg	
GF04-02	GF	A	31	2.5Y 2.5/1	y	sl	nf	m	
GF04-03	GF	A	41	2.5Y 2.5/1	y	sl	nf	m	10% 2.5Y 4/1
GF04-04	GF	C	77	10YR 5/1	n	ne	nf	sg	
GF04-05	GF	C	93	2.5Y 4/1	n	vs	nf	sg	
GF04-06	GF	C	100	10Y 4/1	n	vs	nf	m	15% 7.5YR 4/4
GI08-01	GI	A	10	10YR 2/1	y	st	sf	m	
GI08-02	GI	A	33	10YR 3/2	y	st	nf	1sbk	
GI08-03	GI	C	46	2.5Y 4/1	n	sl	nf	sg	
GI08-04	GI	C	55	10YR 3/1	n	sl	nf	m	
GI08-05	GI	C	66	2.5Y 4/2	n	sl	nf	sg	
GI08-06	GI	C	78	2.5Y 3/2	n	ne	nf	sg	
GF03-01	GF	A	7	2.5Y 4/1	y	st	sf	m	
GF03-02	GF	A	41	2.5Y 4/1	y	st	sf	m	
GF03-03	GF	B	61	5Y 4/1	y	sl	nf	1sbk	25% 7.5YR 3/3
GF03-04	GF	B	74	5Y 4/1	n	vs	nf	sg	
GF03-05	GF	B	110	10YR 5/3	n	st	nf	m	15% 5Y 6/1
GF03-06	GF	B	165	10YR 6/3	n	st	nf	m	3% 10YR 5/6, 40% 5Y 6/1
GF03-07	GF	B	215	2.5Y 5/3	n	vs	sf	m	4% 10YR 4/6
GF08-01	GF	A	10	5Y 2.5/1	y	st	sf	m	
GF08-02	GF	A	40	5Y 2.5/1	y	st	nf	m	
GF08-03	GF	B	87	10YR 5/3	n	sl	nf	m	30% 5Y 6/1, 5% 10YR 4/4

GF08-04	GF	B	122	10YR 5/3	n	st	nf	1sbk	15% 5Y 6/1, 6% 7.5Y 5/4
GF08-05	GF	C	150	10YR 5/2	n	ve	sf	1sbk	5% 5Y 6/1
GF08-06	GF	C	168	10YR 5/2	n	ve	mf	m	7% 5Y 6/1
GA01-01	GA	A	26	7.5YR 2.5/2	n	sl	nf	2gr	
GA01-02	GA	B	59	7.5YR 4/4	n	st	nf	2sbk	12% 7.5YR 3/3, 24% 10YR 5/2.5
GA01-03	GA	B	83	10YR 5/3	n	vs	nf	1sbk	8% 7.5YR 4/3, 30% 10YR 5/2
GA01-04	GA	B	108	10YR 5/3	n	vs	nf	1sbk	15% 7.5Y R 4/4, 40% 10YR 5/2
GA01-05	GA	B	130	10YR 5/2.5	n	sl	nf	1sbk	12% 7.5YR 5/4, 10% 10YR 6/2
GA01-06	GA	B	156	2.5Y 6/2	n	vs	sf	m	
GA01-07	GA	C	192	2.5Y 6/2	n	vs	sf	m	10% 10YR 4/3
GA01-08	GA	C	205	10YR 5/2	n	ne	sf	m	1% 5YR 4/4
GA01-09	GA	C	266	10YR 5/2	n	vs	mf	m	
GA02-01	GA	A	14	10YR 2/2	n	sl	nf	2sbk	
GA02-02	GA	A	24	10YR 2/2	n	sl	nf	2gr	
GA02-03	GA	B	36	10YR 2/2	n	sl	nf	1sbk	
GA02-04	GA	B	66	10YR 3/4	n	sl	nf	2sbk	30% 7.5YR 4/6, 5% 10YR 2/1 (soft, OM?), 5% 2.5Y 6/3
GA02-05	GA	B	107	2.5Y 4/3	n	sl	nf	2sbk	5% 10YR 2/1, 20% 7.5YR 4/3
GA02-06	GA	B	140	10YR 4/3	n	st	nf	2sbk	10% 7.5YR 4/6
GA02-07	GA	C	167	2.5Y 6/2	n	vs	sf	m	3% 10YR 4/4

GA02-08	GA	C	230	2.5Y 6/2	n	vs	mf	m	
GA02-09	GA	C	274	2.5Y 5/3	n	vs	sf	m	
GI11-01	GI	A	11	10Y 2.5/1	y	sl	mf	m	5% 10YR 3/4
GI11-02	GI	A	41	5Y 2.5/2	y	sl	sf	m	
GI11-03	GI	A	65	5Y 2.5/2	y	sl	nf	1sbk	
GI11-04	GI	B	83	5Y 3/2	n	vs	nf	1sbk	15% 10YR 3/3
GI11-05	GI	B	97	10YR 4/2	n	vs	nf	2sbk	5% 10YR 3/3, 30% 2.5Y 4/1
GI11-06	GI	C	124	5Y 2.5/2	n	vs	sf	1sbk	
GI11-07	GI	C	140	5Y 2.5/2	y	vs	mf	m	
GF07-01	GF	A	10	2.5Y 4/1	y	st	sf	m	
GF07-02	GF	A	32	5Y 4/2	y	st	sf	m	
GF07-03	GF	B	50	5Y 3/2	y	st	nf	1sbk	5% 7.5YR 3/2, 5% 5Y 4/1
GF07-04	GF	B	57	5Y 2.5/1	y	sl	nf	sg	
GF07-05	GF	B	90	7.5YR 5/3	n	st	nf	m	3% 5YR 3/4, 3% 5Y 5/1
GF07-06	GF	B	141	7.5YR 5/3	n	vs	sf	m	3% 5YR 3/4 (finer than above), 3% 5Y 5/1
GF07-07	GF	B	176	7.5YR 5/2	n	sl	sf	m	5% 7.5YR 3/4, 3% 5Y 5/1
GF07-08	GF	C	186	5Y 4/1	n	sl	nf	sg	2% 10YR 5/2
GF07-09	GF	C	193	5Y 4/2	n	ne	nf	sg	
GO18-01	GO	A	5	10Y 2.5/1	y	sl	sf	sg	
GO18-02	GO	C	18	10Y 5/0.5	n	st	sf	m	
GO18-03	GO	C	45	5Y 5/2	n	st	nf	m/1sbk	1% 7.5YR 4/4
GO18-04	GO	C	72	2.5Y 5/2	n	st	nf	m	1% 7.5YR 4/4, nodule, finer inside
GO18-05	GO	C	98	2.5Y 5/2	n	vs	nf	sg	
GO18-06	GO	C	112	5Y 5/2	n	st	nf	m	

GO12vc-01	GO	A	4	5Y 2.5/2	y	vs	NF	SG	
GO12vc-02	GO	A	24	5Y 3/1	y	vs	NF	SG	
GO12vc-03	GO	A	28	2.5Y 5/1	n	vs	NF	SG	
GO12vc-04	GO	C	54	2.5Y 3/2	n	vs	NF	SG	
GO12vc-05	GO	C	85	2.5Y 3/1	n	vs	NF	SG	
GO12vc-06	GO	C	97	2.5Y 3/2	n	vs	MF	M	
GO12vc-07	GO	C	112	5Y 4/1	n	ne	NF	SG	
GO12vc-08	GO	C	142	5Y 3/2	n	vs	SF	M	
GO12vc-09	GO	C	172	5Y 2.5/2	n	vs	SF	M	
GI04-01	GI	A	13	5Y 2.5/1	y	sl	mf	m	2% 10YR 3/4
GI04-02	GI	A	32	5Y 4/1	y	vs	nf	m	2% 10YR 3/4
GI04-03	GI	A	54	5Y 4/1	y	vs	nf	sg	
GI04-04	GI	A	72	5Y 4/1	y	vs	nf	sg	
GI04-05	GI	B	84	2.5Y 4/4	n	vs	nf	sg	3% 7.5YR 4/4
GI04-06	GI	B	98	2.5Y 6/3	n	sl	nf	m	20% 7.5YR 5/6, 10% 2.5Y 7/1
GI04-07	GI	B	122	2.5Y 6/3	n	sl	nf	m	20% 7.5YR 5/6, 10% 2.5Y 7/1
GI04-08	GI	B	138	2.5Y 6/3	n	sl	nf	m	20% 7.5YR 5/6, 10% 2.5Y 7/1
GI04-09	GI	C	162	5Y 5/1	n	sl	nf	m	trace 2.5YR 4/4 nodules
GI04-10	GI	C	170	5Y 5/1	n	sl	nf	m	trace 2.5YR 4/4 nodules
GO20-01	GO	A	15	5Y 2.5/1	y	sl	NF	SG	
GO20-02	GO	C	29	10Y 5/1	n	sl	MF	M	
GO20-03	GO	C	54	10Y 5/1	n	sl	MF	M	
GO20-04	GO	C	65	10Y 5/1	n	sl	MF	M	
GI17-01	GI	A	6	10Y 2.5/1	y	sl	NF		



GI17-02	GI	A	18	N 3	y	sl	SF		2% 10YR 4/3
GI17-03	GI	B	41	5GY 5/1	n	sl	SF		10% 2.5Y 5/4
GI17-04	GI	B	72	2.5Y 5/2	n	sl	SF		30% 10Y 5/1, 20% 2.5Y 5/4
GI17-05	GI	C	95	10Y 5/1	n	sl	SF		10% 2.5Y 5/4
GI17-06	GI	C	120	10Y 5/1	n	sl	SF		25% 2.5Y 5/4
GO22-01	GO	A	5	5Y 3/1	y	st	NF	SG	
GO22-02	GO	C	20	5Y 6/1	n	sl	SF	M	
GO22-03	GO	C	38	5Y 5/1	n	sl	NF	M	
GO22-04	GO	C	58	5Y 5/2	n	sl	NF	M	
GI27-01	GI	A	16	10Y 2.5/1	y	st	mf	m	3% 7.5YR 4/4 worm channel
GI27-02	GI	A	42	10Y 3/1	y	st	mf	1sbk	
GI27-03	GI	B	75	10YR 5/3	n	sl	nf	2sbk	5% 7.5YR 3/4, 30% 5Y 6/4
GI27-04	GI	B	120	5Y 5/2	n	sl	nf	2sbk	5% 7.5YR 3/3, 10% 7.5YR 4/4
GI27-05	GI	B	160	5Y 5/2	n	st	sf	1sbk	5% 7.5YR 3/4
GI27-06	GI	C	170	5Y 5/1	n	sl	nf	sg	
GI27-07	GI	C	198	5Y 5/2	n	sl	sf	m	10% 7.5YR 4/3
GI27-08	GI	C	210	5Y 5/2	n	st	nf	m	3% 10YR 4/3
GI15-01	GI	A	22	5Y 3/1	y	sl	MF	M	3% 10YR 4/3
GI15-02	GI	A	37	5Y 3/1	y	sl	SF	1SBK	
GI15-03	GI	B	86	2.5Y 5/3	n	vs	SF	M	10% 10YR 4/6
GI15-04	GI	B	96	2.5Y 5/3	n	vs	NF	SG	
GI15-05	GI	B	138	2.5Y 5/3	n	vs	NF	2SBK	5% 7.5YR 4/3
GI15-06	GI	B	184	2.5Y 5/3	n	sl	NF	1SBK	5% 7.5YR 4/3
GI15-07	GI	B	233	2.5Y 4/3	n	sl	NF	2SBK	2% 7.5YR 4/3
GI15-08	GI	B	273	2.5Y 5/4	n	sl	NF	1SBK	10% 7.5YR 4/3

GI28-01	GI	A	19	N 2.5	Y	st	MF	M	2% 7.5YR 4/4
GI28-02	GI	A	38	10Y 4/1	Y	vs	NF	SG	
GI28-03	GI	B	54	10YR 4/3	n	sl	SF	M	3% 7.5YR 4/4, 3% 10Y 5/1
GI28-04	GI	B	75	10YR 4/4	n	ne	NF	2SBK	40% 10Y 4/1
GI28-05	GI	A	83	10YR 2/1	n	sl	NF		
GI28-06	GI	C	90	10Y 6/1	n	st	NF	1SBK	7% 7.5YR 4/6
GI22-01	GI	A	15	10Y 2.5/1	y	st	MF	M	15% 10YR 3/3
GI22-02	GI	A	35	10Y 2.5/1	y	st	MF	M	
GI22-03	GI	B	66	5Y 6/1	n	sl	SF	SG	20% 7.5YR 3/4
GI22-04	GI	B	78	5Y 5/2	n	st	SF	M	10% 7.5YR 3/4
GI22-05	GI	B	127	5Y 5/2	n	st	NF	1SBK	7% 7.5YR 3/3 root channels
GI03-01	GI	A	8	2.5Y 2.5/1	y	sl	mf	sg	3% 10YR 4/4 worm channels?
GI03-02	GI	A	29	2.5Y 2.5/1	y	sl	sf	m	
GI03-03	GI	C	43	2.5Y 4/1	n	vs	sf	m	5% 10YR 3/4
GI03-04	GI	C	69	2.5Y 4/1	n	vs	nf	sg	
GI03-05	GI	B	82	10YR 4/3	n	sl	nf	sg	7% 7.5YR 5/4, 16% 2.5Y 3/2
GI03-06	GI	B	105	10Y 4/4	n	st	sf	m	
GF02-01	GF	A	6	5Y 2.5/1	y	st	nf	sg	
GF02-02	GF	A	24	5Y 2.5/1	y	st	nf	m	
GF02-03	GF	A	42	5Y 2.5/1	y	st	nf	sg	
GF02-04	GF	A	65	5Y 6/1	n	vs	nf	sg	
GF02-05	GF	B	91	5Y 3/2	n	vs	nf	m	2% 10YR 4/4
GF02-06	GF	C	107	2.5Y 3/1	n	vs	nf	m	
GF02-07	GF	C	119	2.5Y 3/1	n	vs	mf	m	
GI05-01	GI	A	8	10Y 2.5/1	y	vs	mf	m	10% 10Y 4/3, 5% 5Y 4/2

GI05-02	GI	A	29	10Y 2.5/1	y	vs	sf	m	
GI05-03	GI	A	60	5Y 2.5/2	y	vs	sf	m	
GI05-04	GI	B	85	2.5Y 4/2	n	vs	nf	sg	15% 10YR 3/3
GI05-05	GI	C	113	5Y 2.5/2	n	vs	sf	1sbk	
GI05-06	GI	C	141	5Y 3/2	n	vs	sf	1sbk	1% 7.5YR 3/3
GO12-01	GO	A	8	10Y 2.5/1	y	vs	nf	sg	
GO12-02	GO	A	27	5Y 3/2	y	vs	nf	sg	
GO12-03	GO	C	35	5Y 3/2	y	vs	nf	sg	
GO12-04	GO	C	64	2.5Y 3/2	n	vs	nf	sg	
GF05-01	GF	A	10	5Y 2.5/1	y	st	nf	sg	
GF05-02	GF	A	34	2.5Y 2.5/1	y	st	nf	sg	
GF05-03	GF	B	51	10YR 4/4	n	vs	nf	1sbk	20% 7.5YR 4/6, 7% 2.5Y 5/2
GF05-04	GF	B	69	10YR 4/3	n	vs	nf	sg	20% 2.5Y 6/3
GF05-05	GF	C	71	2.5Y 4/2	n	sl	nf	sg	1% 2.5YR 4/6 (trans ped?)
GF05-06	GF	C	90	2.5Y 5/2	n	st	sf	m	
GF05-07	GF	C	102	2.5Y 5/2	n	sl	nf	sg	
GF05-08	GF	C	125	2.5Y 5/1	n	st	sf	m	
GI14-01	GI	A	10	5Y 2.5/1	y	sl	MF	M	10% 7.5YR 3/3
GI14-02	GI	A	28	10Y 2.5/1	y	sl	SF	M/1SBK	
GI14-03	GI	A	42	10Y 3/1	y	vs	SF	M	5% 10YR 3/3
GI14-04	GI	B	72	2.5Y 4/3	n	vs	NF	SG	10% 7.5YR 3/3
GI14-05	GI	B	82	5Y 3/2	n	vs	SF	1SBK	5% 7.5YR 3/3
GI14-06	GI	B	115	2.5Y 4/3	n	sl	SF	1SBK	20% 7.5YR 3/3, 20% 2.5Y 4/2
GI14-07	GI	B	137	2.5Y 4/4	n	ne	NF	SG	10% 10YR 4/4
GI14-08	GI	C	153	2.5Y 4/3	n	vs	NF	SG	
GI14-09	GI	C	174	5Y 6/1	n	st	SF	M	
GI01-01	GI	A	5	10Y 2.5/1	y	sl	sf	1sbk	

GI01-02	GI	A	13	5Y 2.5/1	y	sl	mf	1sbk	
GI01-03	GI	B	32	5Y 4/3	n	vs	nf	1sbk	10% 7.5YR 4/6, 30% 10YR 5/1, 2% 2.5Y 7/4
GI01-04	GI	B	59	2.5Y 5/2	n	ne	nf	1sbk	15% 7.5YR 4/6
GI01-05	GI	B	103	2.5Y 5/3	n	ne	nf	sg	5% 10YR 4/6
GI01-06	GI	C	130	2.5Y 5/2	n	ne	nf	sg	
GI01-07	GI	C	148	2.5Y 5/2	n	ne	nf	sg	
GI27-01	GI	A	3	10Y 2.5/1	y	vs	mf	m	15% 7.5YR 4/4
GI27-02	GI	A	12	N 2.5	y	sl	sf	m	2% 7.5YR 4/4
GI27-03	GI	A	33	N 2.5	y	sl	mf	m	1% 7.5YR 4/4
GI27-04	GI	A	46	10Y 4/1	y	st	nf	1sbk	
GI27-05	GI	B	76	10Y 5/1	n	sl	nf	1sbk	25% 2.5Y 5/4, 5% 7.5YR 4/4
GI27-06	GI	B	112	10Y 5/1	n	sl	nf	1sbk	25% 2.5Y 5/4, 5% 7.5YR 4/4
GI27-07	GI	C	157	10Y 5/1	n	vs	nf	sg	
GI27-08	GI	C	193	10Y 5/1	n	vs	mf	m	5% 2.5Y 5/4
GI30-01	GI	A	21	10YR 4/1	Y	vs	NF		
GI30-02	GI	B	42	10YR 4/1	n	vs	NF	SBK	
GI30-03	GI	B	56	10YR 5/2	n	ne	NF	SBK	20% 10YR 5/6, 15% 10YR 6/1
GI30-04	GI	B	75	10YR 6/3	n	ne	NF		10% 10YR 5/6, 15% 10YR 6/2
GI30-05	GI	B	82	10YR 5/3	n	ne	NF		10% 10YR 5/6, 20% 10YR 5/1
GI07-01	GI	A	7	10YR 2/1	y	sl	mf	m	
GI07-02	GI	A	26	2.5Y 2.5/1	y	st	sf	1gr	

GI07-03	GI	B	46	5Y 5/1	n	st	nf	m	30% 10YR 5/4, trace 7.5YR 3/3 channels
GI07-04	GI	B	70	10YR 5/3	n	st	sf	m	30% 10YR 5/2
GI07-05	GI	C	77	10YR 5/3	n	st	sf	m	
GI26-01	GI	A	36	10YR 2/1	Y	vs	NF		
GI26-02	GI	B	55	10YR 4/4	n	vs	NF		30% 2.5Y 6/1, 15% 10YR 4/3
GI26-03	GI	B	105	10YR 6/1	n	vs	NF		20% 10YR 5/6
GI24-01	GI	A	29	N 2.5	y	vs	NF	SG	
GI24-02	GI	A	54	2.5Y 4/1	y	ne	SF	SG/1SB K	25% 10YR 4/3
GI24-03	GI	B	77	10YR 5/2	n	sl	NF	2SBK	15% 5Y 6/1, 15% 10YR 5/4
GI24-04	GI	B	128	2.5Y 5/2	n	sl	NF	1SBK	7% 7.5YR 5/6, 4% 5YR 4/3
GF06-01	GF	A	10	5Y 3/1	y	sl	sf	m	
GF06-02	GF	A	32	5Y 3/1	y	sl	sf	m	
GF06-03	GF	B	48	5Y 3/1	n	sl	sf	1sbk	15% 10YR 3/3
GF06-04	GF	B	77	2.5Y 4/1	n	sl	nf	2sbk	20% 7.5YR 3/3
GF06-05	GF	B	99	2.5Y 3/3	n	vs	nf	2sbk	
GF06-06	GF	B	117	5Y 3/2	n	vs	nf	1sbk	25% 7.5YR 3/2
GI23-01	GI	A	6	2.5Y 2.5/1	Y	sl	MF	SG	
GI23-02	GI	A	30	2.5Y 2.5/1	Y	sl	SF	M	
GI23-03	GI	B	120	10YR 6/2	n	sl	NF	M	10% 5Y 6/1, 3% 10YR 5/3
GI23-04	GI	B	202	2.5Y 5/2	n	sl	NF	M	25% 10YR 5/3

*Appendix G: Gyldensteen Strand sample chemistry*

Sample	Site	Layer	dS/m	pH	%Fe2+	%Fe3+	Bulk Density (g/cc)	AVS% (dry)	CRS% (dry)	TRIS% (dry)	%Total-Fe (dry)	%BD-Fe (dry)	Organic C %	Carbonate C %
GF04-01	GF	A	0.18	6.87	0.03575	0.01596	1.41	0.00076	0.00913	0.00989				
GF04-02	GF	A	0.18	7.02	0.03121	0.01194	1.45	0.00091	0.00654	0.00745				
GF04-03	GF	A	0.19	7.01	0.02748	0.01074	1.53	0.00047	0.00919	0.00966				
GF04-04	GF	C	0.18	7.02	0.01460	0.00608	1.35	0.00001	0.00161	0.00162				
GF04-05	GF	C	0.19	6.98	0.01256	0.00495	1.61	0.00000	0.00525	0.00525				
GF04-06	GF	C	0.22	7.35	0.01637	0.00618	1.75	0.00000	0.20062	0.20062				
GI08-01	GI	A		6.94	0.15081	0.01046	0.89	0.02950	0.05920	0.08870				
GI08-02	GI	A		6.72	0.11022	0.03814	0.75	0.00332	0.02471	0.02803				
GI08-03	GI	C		6.98	0.00449	0.00229	1.38	0.00000	0.01003	0.01003				
GI08-04	GI	C		7.29	0.00980	0.00408	1.17	0.00002	0.03604	0.03606				
GI08-05	GI	C		7.27	0.00397	0.00056	1.36	0.00012	0.05206	0.05218				
GI08-06	GI	C		7.37	0.00338	0.00045	1.42	0.00013	0.01288	0.01301				
GF03-01	GF	A	0.29	7.12	0.06318	0.01195	1.62	0.00101	0.00733	0.00834	0.60	0.05	0.85	1.74
GF03-02	GF	A	0.23	7.18	0.05186	0.01666	1.80	0.00036	0.00237	0.00274	0.56	0.05	0.73	1.39
GF03-03	GF	B	0.19	7.23	0.04193	0.04739	1.53	0.00002	0.00063	0.00065	0.82	0.18	0.87	0.65
GF03-04	GF	B	0.21	7.15	0.02070	0.00093	1.55	0.00008	0.00068	0.00076	0.26	0.04	0.41	2.12
GF03-05	GF	B	0.23	7.82	0.00550	0.00708	1.86	0.00003	0.00022	0.00025	0.79	0.02	0.12	3.17

GF03-06	GF	B	0.15	8.23	0.00434	0.00504	1.95	0.00001	0.00022	0.00023	0.55	0.01	0.11	3.69
GF03-07	GF	B	0.25	9.36	0.00811	0.00087	2.05	0.00005	0.00018	0.00024	0.72	0.03	0.08	3.49
GF08-01	GF	A	0.29	7.19	0.14764	0.01231	1.72	0.00773	0.00667	0.01440	0.90	0.11	1.59	0.25
GF08-02	GF	A	0.25	7.24	0.09766	0.01502	1.75	0.00404	0.00835	0.01239	0.96	0.11	1.42	0.43
GF08-03	GF	B	0.18	7.64	0.00923	0.00677	1.87	0.00002	0.00223	0.00225	0.95	0.07	0.15	3.69
GF08-04	GF	B	0.16	7.75	0.00520	0.00829	1.92	0.00003	0.00051	0.00053	0.89	0.10	0.14	5.00
GF08-05	GF	C	0.14	7.88	0.00532	0.00841	1.96	0.00003	0.00014	0.00017	0.75	0.02	0.12	4.19
GF08-06	GF	C	0.16	7.86	0.00250	0.00798	1.92	0.00003	0.00006	0.00010	0.75	0.03	0.19	3.75
GA01-01	GA	A	0.04	6.3	0.00348	0.01792	1.67	0.00000	0.00019	0.00019	0.78	0.13	1.31	0.18
GA01-02	GA	B	0.05	6.62	0.00442	0.02127	1.70	0.00002	0.00044	0.00046	2.14	0.34	0.28	0.04
GA01-03	GA	B	0.05	7.06	0.00160	0.00700	1.83	0.00000	0.00012	0.00012	1.68	0.21	0.28	0.00
GA01-04	GA	B	0.07	7.31	0.00323	0.00938	1.74	0.00000	0.00007	0.00007	1.59	0.22	0.30	0.04
GA01-05	GA	B	0.11	8.09	0.00511	0.00471	1.86	0.00001	0.00022	0.00023	0.71	0.04	0.12	2.85
GA01-06	GA	B	0.12	8.05	0.00338	0.00815	1.87	0.00001	0.00304	0.00305	0.69	0.03	0.16	3.45

GA01-07	GA	C	0.13	8.01	0.00245	0.00715	1.91	0.00002	0.00200	0.00202	0.58	0.03	0.10	3.02
GA01-08	GA	C	0.14	7.56	0.00474	0.00934	1.84	0.00002	0.00052	0.00053	0.42	0.02	0.08	1.97
GA01-09	GA	C	0.13	7.91	0.00377	0.00507	1.96	0.00000	0.00004	0.00004	0.79	0.04	0.08	3.89
GA02-01	GA	A		5.6	0.00291	0.01510	1.67	0.00001	0.00029	0.00031	0.42	0.06	1.62	0.31
GA02-02	GA	A		5.61	0.00336	0.01698	1.67	0.00000	0.00032	0.00032	0.40	0.06	1.85	0.16
GA02-03	GA	B		5.92	0.00391	0.02004	1.69	0.00002	0.00054	0.00056	0.47	0.06	1.46	0.00
GA02-04	GA	B		6.52	0.00526	0.02598	1.92	0.00001	0.00051	0.00053	2.12	0.34	0.74	0.00
GA02-05	GA	B		6.97	0.00287	0.01790	1.97	0.00002	0.00010	0.00011	0.92	0.13	0.19	0.00
GA02-06	GA	B		7.77	0.00321	0.00913	1.99	0.00001	0.00009	0.00010	0.72	0.04	0.13	2.53
GA02-07	GA	C		7.54	0.00437	0.00943	2.01	0.00001	0.00742	0.00743	0.62	0.03	0.10	3.17
GA02-08	GA	C		7.33	0.00476	0.00738	1.90	0.00001	0.00114	0.00115	0.77	0.02	0.10	3.35
GA02-09	GA	C		7.46	0.00633	0.00630	2.07	0.00001	0.00018	0.00020	0.90	0.07	0.09	3.70
GI11-01	GI	A	2.94	7.16	0.06433	0.00852	1.35	0.04205	0.02688	0.06893	0.62	0.06	1.33	0.18
GI11-02	GI	A	2.46	7.05	0.07266	0.00974	1.49	0.01154	0.01429	0.02584	0.53	0.04	1.57	0.00
GI11-03	GI	A	2.13	6.98	0.07495	0.01545	1.52	0.00337	0.01085	0.01422	0.56	0.05	1.15	0.56
GI11-04	GI	B	1.85	7.04	0.05501	0.02681	1.34	0.00012	0.00360	0.00372	0.71	0.08	1.43	0.99



GI11-05	GI	B	2.08	6.93	0.03901	0.07128	1.18	0.00004	0.02222	0.02226	1.14	0.21	2.22	0.90
GI11-06	GI	C	1.60	7.01	0.07796	0.01813	0.92	0.00003	0.00219	0.00223	1.32	0.10	2.72	0.71
GI11-07	GI	C	1.69	6.93	0.04418	0.00193	0.96	0.00031	0.64992	0.65022	1.41	0.03	1.87	2.33
GF07-01	GF	A		6.97	0.08360	0.01215	1.66	0.00349	0.01983	0.02332	0.84	0.11	0.72	3.64
GF07-02	GF	A		7.05	0.09965	0.01274	1.74	0.00163	0.01152	0.01315	0.89	0.10	0.94	2.40
GF07-03	GF	B		7.07	0.03801	0.01187	1.69	0.00032	0.00188	0.00220	0.89	0.28	0.69	0.43
GF07-04	GF	B		7.12	0.03269	0.01124	1.63	0.00153	0.00490	0.00643	0.37	0.09	1.31	0.36
GF07-05	GF	B		7.53	0.00668	0.00873	1.83	0.00002	0.00228	0.00230	0.98	0.06	0.20	4.53
GF07-06	GF	B		7.51	0.00934	0.02179	1.84	0.00005	0.00099	0.00104	1.04	0.10	0.24	2.53
GF07-07	GF	B		7.49	0.01219	0.00745	1.90	0.00000	0.00689	0.00690	1.04	0.05	0.21	2.25
GF07-08	GF	C		7.75	0.01420	0.00731	1.49	0.00003	0.02876	0.02880	0.54	0.04	0.09	1.26
GF07-09	GF	C		8.2	0.00759	0.00418	1.45	0.00005	0.01138	0.01143	0.31	0.02	0.04	1.08
GO18-01	GO	A	2.16	7.76	0.00626	0.00099	1.66	0.00139	0.01835	0.01974	0.15	0.00	0.29	0.16
GO18-02	GO	C	1.39	9.01	0.02012	0.00236	1.92	0.00008	0.00037	0.00045	0.82	0.00	0.13	2.60
GO18-03	GO	C	1.09	8.81	0.00995	0.00315	1.96	0.00002	0.00108	0.00110	0.88	0.04	0.08	3.62

GO18-04	GO	C	1.49	8.65	0.02516	0.00412	1.90	0.00004	0.00154	0.00158	1.28	0.09	0.07	4.38
GO18-05	GO	C	1.73	8.37	0.02185	0.00544	1.75	0.00003	0.00095	0.00098	0.56	0.03	0.21	2.87
GO18-06	GO	C	1.64	8.73	0.02147	0.00652	1.90	0.00001	0.00041	0.00042	0.76	0.05	0.07	4.04
GO12vc-01	GO	A	1.47	7.64	0.00394	0.00180	1.51	0.00043	0.01840	0.01883	0.13	0.00	0.13	0.05
GO12vc-02	GO	A	1.62	7.72	0.00268	0.00160	1.49	0.00013	0.01897	0.01909	0.12	0.00	0.17	0.03
GO12vc-03	GO	A		7.83	0.00151	0.00027	1.59	0.00005	0.01960	0.01965	0.08	0.00	0.32	0.76
GO12vc-04	GO	C	2.33	7.7	0.00193	0.00028	1.40	0.00005	0.04004	0.04009	0.14	0.00	0.51	0.00
GO12vc-05	GO	C	2.31	8.07	0.00241	0.00011	1.42	0.00012	0.05522	0.05535	0.20	0.00	0.48	0.01
GO12vc-06	GO	C	2.37	8.02	0.00752	0.00000	1.27	0.00010	0.12461	0.12471	0.33	0.00	1.09	0.29
GO12vc-07	GO	C	1.61	8.24	0.00461	0.00026	1.41	0.00001	0.07172	0.07173	0.24	0.00	0.33	0.14
GO12vc-08	GO	C	2.37	7.61	0.00973	0.00000	1.12	0.00011	0.00019	0.00030	0.44	0.00	1.43	0.38
GO12vc-09	GO	C	1.75	7.85	0.01638	0.00090	0.98	0.00069	0.00036	0.00105	0.63	0.01	1.90	0.38
GI04-01	GI	A	2.48	7.58	0.06334	0.00897	1.59	0.02214	0.01992	0.04206	0.77	0.06	1.16	1.14
GI04-02	GI	A	1.76	7.35	0.03032	0.00380	1.74	0.00541	0.00441	0.00983	0.40	0.03	0.52	0.36
GI04-03	GI	A	1.66	7.7	0.00723	0.00254	1.61	0.00033	0.00238	0.00271	0.17	0.01	0.47	2.39
GI04-04	GI	A	2.01	7.57	0.00775	0.00190	1.60	0.00101	0.00160	0.00262	0.14	0.01	0.31	0.46

GI04-05	GI	B	0.98	7.4	0.01096	0.02012	1.90	0.00002	0.00151	0.00153	0.78	0.06	0.14	1.79
GI04-06	GI	B	0.53	7.61	0.00489	0.03556	1.96	0.00004	0.00233	0.00237	0.68	0.04	0.07	2.88
GI04-07	GI	B	0.40	7.42	0.00587	0.02216	1.91	0.00000	0.00174	0.00175	0.89	0.06	0.09	3.44
GI04-08	GI	B	0.44	7.43	0.00930	0.01449	1.92	0.00001	0.01205	0.01207	0.80	0.08	0.19	2.78
GI04-09	GI	C	0.28	8.04	0.03778	0.00220	1.96	0.00082	0.01092	0.01174	0.95	0.02	0.09	3.47
GI04-10	GI	C	0.32	8.36	0.02844	0.00397	1.98	0.00040	0.00899	0.00939	0.81	0.02	0.11	3.71
GO20-01	GO	A		7.98	0.00878	0.00085	1.74	0.00141	0.02484	0.02625				
GO20-02	GO	C		8.54	0.03020	0.00192	1.65	0.00018	0.07264	0.07282				
GO20-03	GO	C		8.18	0.03199	0.00183	1.64	0.00015	0.00022	0.00037				
GO20-04	GO	C		8.3	0.02456	0.00098	1.69	0.00014	0.00027	0.00041				
GI17-01	GI	A		7.64	0.04729	0.00442	0.82	0.03296	0.01621	0.04917	0.49	0.03	7.41	0.00
GI17-02	GI	A		7.65	0.06069	0.00183	1.56	0.00986	0.01916	0.02903	0.67	0.03	0.54	2.90
GI17-03	GI	B		7.13	0.04977	0.00476	1.70	0.00338	0.01042	0.01380	0.73	0.03	0.11	3.49
GI17-04	GI	B		7.14	0.02423	0.00367	1.85	0.00010	0.00143	0.00153	0.82	0.04	0.11	5.84

GI17-05	GI	C		7.38	0.03538	0.00230	1.91	0.00126	0.03949	0.04075	1.63	0.17	0.18	3.42
GI17-06	GI	C		8.03	0.03160	0.00513	1.69	0.00005	0.00047	0.00052	0.75	0.06	0.06	3.57
GO22-01	GO	A		7.5	0.00760	0.00099	1.74	0.00136	0.02029	0.02165	0.20	0.00	0.32	0.28
GO22-02	GO	C		8.57	0.02104	0.00284	1.90	0.00008	0.24287	0.24295	0.92	0.01	0.06	3.34
GO22-03	GO	C		8.32	0.02273	0.00336	1.92	0.00007	0.00733	0.00740	0.89	0.06	0.18	4.10
GO22-04	GO	C		7.85	0.01939	0.00382	1.89	0.00004	0.00094	0.00097	0.86	0.06	0.19	4.12
GI27-01	GI	A		7.3	0.10579	0.00701	1.62	0.02892	0.02232	0.05123	1.05	0.07		
GI27-02	GI	A		7.09	0.08956	0.00645	1.54	0.02184	0.00289	0.02474	0.96	0.10		
GI27-03	GI	B		6.97	0.00553	0.00669	1.90	0.00005	0.00182	0.00188	0.87	0.10		
GI27-04	GI	B		6.76	0.00545	0.01947	1.82	0.00004	0.00269	0.00273	0.89	0.08		
GI27-05	GI	B		6.91	0.00642	0.01377	1.83	0.00002	0.00374	0.00377	0.86	0.05		
GI27-06	GI	C		7.23	0.00820	0.00978	1.85	0.00003	0.00318	0.00321	0.45	0.04		
GI27-07	GI	C		7.02	0.00418	0.01201	1.91	0.00002	0.00052	0.00053	0.55	0.02		
GI27-08	GI	C		7.23	0.01879	0.00477	1.99	0.00003	0.00063	0.00066	0.72	0.06		
GI15-01	GI	A		7.22	0.04099	0.00607	1.71	0.00715	0.00386	0.01100	0.73	0.03	0.86	1.85
GI15-02	GI	A		7.18	0.04030	0.00413	1.73	0.01076	0.00494	0.01570	0.64	0.03	0.81	1.77

GI15-03	GI	B		7.06	0.00322	0.00751	1.86	0.00002	0.00066	0.00069	0.90	0.07	0.17	3.23
GI15-04	GI	B		7.04	0.00306	0.00615	1.94	0.00003	0.00028	0.00031	0.68	0.05	0.16	2.69
GI15-05	GI	B		7.22	0.00208	0.00456	1.92	0.00003	0.00043	0.00046	0.88	0.07	0.18	3.56
GI15-06	GI	B		7.25	0.00350	0.00475	1.93	0.00001	0.00055	0.00056	0.84	0.06	0.18	3.30
GI15-07	GI	B		7.39	0.00249	0.00541	1.85	0.00004	0.00035	0.00039	0.93	0.08	0.23	3.11
GI15-08	GI	B		7.65	0.00360	0.00507	1.86	0.00002	0.00043	0.00045	0.82	0.08	0.17	3.51
GI28-01	GI	A		7.27	0.06606	0.00515	1.43	0.01126	0.01350	0.02476				
GI28-02	GI	A		7.02	0.02535	0.00248	1.47	0.00224	0.00376	0.00600				
GI28-03	GI	B		6.75	0.03080	0.03012	1.16	0.00004	0.00543	0.00547				
GI28-04	GI	B		6.47	0.16998	0.13529	0.73	0.00003	0.06138	0.06141				
GI28-05	GI	A		5.59	0.28367	0.04358	0.63	0.00276	0.06712	0.06988				
GI28-06	GI	C		6.64	0.01184	0.02731	1.45	0.00002	0.03036	0.03038				
GI22-01	GI	A		7.57	0.06959	0.00781	1.62	0.01057	0.03460	0.04517	0.60	0.07	1.25	0.48
GI22-02	GI	A		7.36	0.05753	0.01000	1.63	0.02267	0.04656	0.06923	0.64	0.09	1.74	0.67
GI22-03	GI	B		7.1	0.03698	0.01705	1.55	0.00003	0.00460	0.00463	0.72	0.16	0.64	0.99
GI22-04	GI	B		7.04	0.00834	0.01553	1.76	0.00002	0.02369	0.02371	1.08	0.17	0.81	2.32

GI22-05	GI	B		6.99	0.00496	0.00987	1.89	0.00002	0.00214	0.00216	0.86	0.07	0.22	3.63
GI03-01	GI	A		7.61	0.05156	0.00819	1.51	0.02395	0.00326	0.02722				
GI03-02	GI	A		7.24	0.04571	0.00621	1.58	0.00249	0.00508	0.00757				
GI03-03	GI	C		6.98	0.05683	0.04214	1.33	0.00006	0.00651	0.00657				
GI03-04	GI	C		6.82	0.00918	0.00773	1.40	0.00005	0.00043	0.00048				
GI03-05	GI	B		6.9	0.01802	0.04217	1.52	0.00002	0.03325	0.03328				
GI03-06	GI	B		7.72	0.06614	0.00369	1.63	0.00058	0.00499	0.00557				
GF02-01	GF	A		6.88	0.03760	0.00592	1.26	0.02297	0.01082	0.03379				
GF02-02	GF	A		6.98	0.03488	0.00821	1.52	0.00088	0.00456	0.00544				
GF02-03	GF	A		7.01	0.03744	0.00732	1.57	0.00031	0.01326	0.01357				
GF02-04	GF	A		7.07	0.00875	0.00299	1.41	0.00100	0.00170	0.00270				
GF02-05	GF	B		7.14	0.06104	0.07601	0.94	0.00026	0.01173	0.01199				
GF02-06	GF	C		7.48	0.03015	0.00210	0.84	0.00029	0.00195	0.00224				
GF02-07	GF	C		7.49	0.02102	0.00184	0.81	0.00043	0.00118	0.00161				
GI05-01	GI	A		7.35	0.05110	0.00417	1.33	0.01663	0.02423	0.04087				
GI05-02	GI	A		7.22	0.06329	0.00375	1.47	0.01438	0.04216	0.05654				
GI05-03	GI	A		6.82	0.04107	0.01093	1.46	0.00035	0.02430	0.02465				
GI05-04	GI	B		6.65	0.03123	0.02102	1.36	0.00000	0.02081	0.02081				

GI05-05	GI	C		7.1	0.03999	0.04270	0.97	0.00001	0.01718	0.01719				
GI05-06	GI	C		7.19	0.04368	0.08120	0.93	0.00002	0.01551	0.01553				
GO12-01	GO	A		7.59	0.01181	0.00139	1.51	0.00213	0.01782	0.01995				
GO12-02	GO	A		7.87	0.00834	0.00115	1.47	0.00031	0.01717	0.01748				
GO12-03	GO	C		7.95	0.00344	0.00149	1.53	0.00010	0.02316	0.02326				
GO12-04	GO	C		7.88	0.00307	0.00036	1.45	0.00008	0.03468	0.03476				
GF05-01	GF	A		6.9	0.05672	0.01022	1.45	0.00201	0.00493	0.00694				
GF05-02	GF	A		7.06	0.05655	0.01277	1.56	0.00136	0.00206	0.00342				
GF05-03	GF	B		7.43	0.00658	0.04188	1.57	0.00002	0.00028	0.00030				
GF05-04	GF	B		7.48	0.01349	0.04795	1.70	0.00001	0.01059	0.01060				
GF05-05	GF	C		7.63	0.02826	0.04127	1.82	0.00000	0.03748	0.03748				
GF05-06	GF	C		7.68	0.01040	0.01144	1.92	0.00000	0.02139	0.02139				
GF05-07	GF	C		7.58	0.01584	0.02534	2.01	0.00000	0.00387	0.00387				
GF05-08	GF	C		8.22	0.00355	0.00091	2.01	0.00001	0.10238	0.10239				
GI14-01	GI	A		7.4	0.07242	0.00897	1.57	0.01111	0.00881	0.01992				
GI14-02	GI	A		7.32	0.07481	0.01061	1.67	0.00253	0.01250	0.01503				
GI14-03	GI	A		6.98	0.07978	0.01871	1.44	0.00089	0.00847	0.00936				
GI14-04	GI	B		7.09	0.01555	0.05363	1.81	0.00002	0.00069	0.00071				
GI14-05	GI	B		7.02	0.05235	0.04973	1.25	0.00002	0.00294	0.00296				

GI14-06	GI	B		6.99	0.01695	0.05411	1.82	0.00002	0.00515	0.00517				
GI14-07	GI	B		7.05	0.00888	0.05732	1.61	0.00001	0.00670	0.00671				
GI14-08	GI	C		7.31	0.01406	0.03117	1.67	0.00001	0.06580	0.06581				
GI14-09	GI	C		8.13	0.00012	0.00137	1.91	0.00014	0.07290	0.07303				
GI01-01	GI	A		6.81	0.06178	0.00741	1.74	0.02035	0.00609	0.02644				
GI01-02	GI	A		6.84	0.06431	0.00721	1.74	0.00649	0.00851	0.01500				
GI01-03	GI	B		7.17	0.01185	0.02556	1.82	0.00012	0.00122	0.00135				
GI01-04	GI	B		7.04	0.00340	0.02035	1.66	0.00000	0.00077	0.00078				
GI01-05	GI	B		7.22	0.00239	0.01660	1.60	0.00000	0.00074	0.00074				
GI01-06	GI	C		7.41	0.00535	0.00729	1.59	0.00000	0.00228	0.00228				
GI01-07	GI	C		7.31	0.00690	0.00622	1.56	0.00002	0.00200	0.00202				
GI27-01	GI	A		7.56	0.04886	0.01344	1.66	0.01828	0.00794	0.02622			0.85	0.51
GI27-02	GI	A		7.44	0.07643	0.01103	1.61	0.02098	0.00849	0.02947			0.77	0.70
GI27-03	GI	A		7.56	0.06542	0.01243	1.71	0.02156	0.00969	0.03125			1.05	0.89
GI27-04	GI	A		7.51	0.05392	0.01061	1.78	0.00270	0.00261	0.00531			0.73	0.88
GI27-05	GI	B		7.8	0.03053	0.00462	1.94	0.00056	0.00175	0.00231			0.21	3.02



GI27-06	GI	B		7.67	0.01913	0.00374	1.96	0.00000	0.00116	0.00116			0.21	2.74
GI27-07	GI	C		7.29	0.00890	0.01174	1.92	0.00001	0.00115	0.00116			0.18	2.80
GI27-08	GI	C		7.42	0.00144	0.00006	1.96	0.00001	0.00599	0.00600			0.19	3.00
GI30-01	GI	A		7.11	0.05151	0.00260	1.77	0.02736	0.00773	0.03509				
GI30-02	GI	B		6.94	0.04496	0.00667	1.89	0.00260	0.00234	0.00494				
GI30-03	GI	B		7.09	0.01147	0.00578	1.97	0.00004	0.00106	0.00110				
GI30-04	GI	B		7.21	0.00655	0.00862	1.88	0.00001	0.00048	0.00049				
GI30-05	GI	B		7.22	0.00781	0.00876	1.91	0.00002	0.00080	0.00082				
GI07-01	GI	A		7.2	0.03938	0.00598	1.70	0.01262	0.00772	0.02034				
GI07-02	GI	A		7.09	0.02910	0.00566	1.77	0.00277	0.00792	0.01070				
GI07-03	GI	B		7.19	0.01513	0.00830	1.90	0.00001	0.00926	0.00927				
GI07-04	GI	B		7.27	0.00667	0.00540	1.90	0.00000	0.00085	0.00085				
GI07-05	GI	C		7.44	0.00439	0.00502	1.98	0.00002	0.00103	0.00104				
GI26-01	GI	A		7.16	0.05506	0.00346	1.54	0.03837	0.01771	0.05608				
GI26-02	GI	B		7.44	0.03063	0.00602	1.78	0.00002	0.00783	0.00785				

GI26-03	GI	B		7.33	0.00637	0.00533	1.92	0.00002	0.00137	0.00139				
GI24-01	GI	A		7.29	0.05788	0.00479	1.65	0.01492	0.01469	0.02960				
GI24-02	GI	A		7.11	0.01649	0.00400	1.57	0.00180	0.00547	0.00728				
GI24-03	GI	B		7.05	0.00886	0.01782	1.83	0.00001	0.00722	0.00723				
GI24-04	GI	B		7.14	0.00525	0.01707	1.91	0.00006	0.01026	0.01032				
GF06-01	GF	A		7.04	0.09254	0.01677	1.30	0.00569	0.00884	0.01453				
GF06-02	GF	A		7.02	0.10339	0.00793	1.40	0.00125	0.01095	0.01220				
GF06-03	GF	B		6.95	0.05142	0.02916	1.44	0.00150	0.00667	0.00817				
GF06-04	GF	B		7.32	0.04065	0.06410	1.23	0.00003	0.00253	0.00256				
GF06-05	GF	B		7.12	0.04168	0.08804	1.00	0.00001	0.00904	0.00905				
GF06-06	GF	B		7	0.07204	0.12182	0.88	0.00001	0.12089	0.12090				
GI23-01	GI	A		7.39	0.05124	0.00413	1.53	0.01863	0.01048	0.02911				
GI23-02	GI	A		7.54	0.06710	0.00558	1.78	0.01158	0.00755	0.01913				
GI23-03	GI	B		7.24	0.00000	0.00000	1.97	0.00002	0.00049	0.00051				
GI23-04	GI	B		7.35	0.00345	0.00550	1.94	0.00002	0.00050	0.00051				

*Appendix H: West River pedon classifications*

Sample code	Taxonomic Subgroup	Closest Series	Lat	Long
259	Typic Psammowassent	Rhode River	38.86239	-76.52081
260	Sulfic Fluviwassent	Sand Point	38.86141	-76.52045
261	Fluventic Psammowassent	Dutchman Point	38.86049	-76.52049
262	Haplic Sulfiwassent	Sand Point	38.85997	-76.52033
263	Grossic Hydrowassent	Contees Wharf	38.85923	-76.52035
264	Sulfic Hydrowassent	Sellman	38.85778	-76.52035
265	Sulfic Hydrowassent	Sellman	38.85554	-76.52004
266	Haplic Sulfiwassent	Sand Point	38.85355	-76.51997
268	Typic Fluviwassent	Sand Point	38.85118	-76.51988
269	Typic Fluviwassent	Sand Point	38.85033	-76.51962
270	Typic Haplowassent	Rhode River	38.85151	-76.52468
271	Aeric Haplowassent	Rhode River	38.85202	-76.52459
272	Aeric Haplowassent	Rhode River	38.85314	-76.52449
273	Grossic Hydrowassent	Contees Wharf	38.85412	-76.52579
275	Fluventic Sulfiwassent	Sand Point	38.85562	-76.53206
276	Aeric Haplowassent	Rhode River	38.85556	-76.53413
277	Typic Haplowassent	Rhode River	38.85550	-76.53608
278	Aeric Fluviwassent	Rhode River	38.85547	-76.53703
279	Typic Fluviwassent	Sand Point	38.84986	-76.53599
279.5	Fluventic Sulfiwassent	Sand Point	38.84984	-76.52700
280	Grossic Hydrowassent	Sand Point	38.84974	-76.52953
283	Grossic Hydrowassent	Sellman	38.84982	-76.53086
284	Sulfic Hydrowassent	Contees Wharf	38.84978	-76.53205
285	Grossic Hydrowassent	Contees Wharf	38.84980	-76.53322
286	Sulfic Hydrowassent	Contees Wharf	38.84981	-76.53412
287	Typic Psammowassent	Dutchman Point	38.84981	-76.53460
288	Sulfic Psammowassent	Dutchman Point	38.84977	-76.53522
289	Haplic Sulfiwassent	Sand Point	38.84979	-76.53606
290	Fluventic Sulfiwassent	Muddy Creek	38.82541	-76.52371
292	Sulfic Hydrowassent	Muddy Creek	38.82549	-76.52410
293	Fluventic Sulfiwassent	Contees Wharf	38.82563	-76.52487
294	Sulfic Hydrowassent	Sellman	38.82602	-76.52635

295	Grossic Hydrowassent	Sellman	38.82917	-76.52897
303	Grossic Hydrowassent	Muddy Creek	38.82749	-76.54370
305	Fluentic Sulfiwassent	Muddy Creek	38.82754	-76.54419
306	Fluentic Sulfiwassent	Contees Wharf	38.82754	-76.54474
307	Fluentic Sulfiwassent	Contees Wharf	38.82757	-76.54595
308	Fluentic Sulfiwassent	Sellman	38.83044	-76.54681
309	Grossic Hydrowassent	Contees Wharf	38.85888	-76.54326
312	Grossic Hydrowassent	Contees Wharf	38.85944	-76.54205
313	Fluentic Sulfiwassent	Contees Wharf	38.85993	-76.54073
314	Fluentic Sulfiwassent	Contees Wharf	38.86036	-76.53977

Appendix I: West River horizon data

Pedon Code	Bottom Depth	Horizon	Dist.	Color	Field Texture	Fluidity	H2O2 3%	H2O2 30%	Odor	pH	Oxidized pH	Fragments	Redox
259	7	Aseg	a	10Y 2.5/1	S	NF	N	ST	N	7.67	8	Trace gravels and shell	
259	14	2CBg1	c	10Y 3/1	S	NF	N	VS	N	7.31	6.91		
259	26	2CBg2	b	5Y 4/1	S	NF	N	NR	N	5.21	4.69		
260	27	Aseg1	g	N 2.5	S	NF	N	SL	N	7.04	7.36	1% shell	
260	51	Aseg2	c	10Y 2.5/1	coS	NF	N	VS	N	6.64	7.47	1% shell	
260	102	2Cseg2	c	10Y 2.5/1	L	MF	N	VS	SL	6.19	3.48	trace organic	
260	119	3Cseg2	c	N 2.5	coS	NF	N	VS	N	4.71	3.27		
260	165	3Cseg3	c	N 2.5	LS	NF	N	VS	N	7.19	7.5	15% shell	
260	170	4Cseg4	b	10Y 2.5/1	L	SF	N	VS	N	5.2	3.09	2% organic, trace shell, trace gravels as translocated peds	
261	15	Aseg1	a	10Y 2.5/1	S	NF	N	VS	N	7.09	7.58		
261	41	Aseg2	g	10Y 2.5/1	S	NF	N	VS	N	6.92	7.22	trace shell	
261	82	Cseg1	g	10Y 2.5/1	LS	NF	N	VS	N	6.93	8.03	2% shell	
261	111	Cseg2	c	N 2.5	LfS	SF	N	VS	N	7.47	7.37		

261	184	Cseg3	g	N 2.5	LS	SF	N	VS	N	7.4	6.91	trace shell	
261	225	Cseg4	a	10Y 2.5/1	L	MF	N	VS	N	7.57	7.87	trace shell	
261	248	2Cseg5	b	10Y 2.5/1	SiL	SF	N	VS	SL	7.16	6.83	trace organic	
262	18	Cseg1	c	10Y 2.5/1	fS	NF	N	SL	N	7.26	7.91	trace shell	
262	32	Cseg2	a	10Y 2.5/1	fS	NF	N	SL	N	7.06	7.12	trace shell	
262	61	Asegb1	g	N 2.5	LfS	NF	Y	SL	N	6.76	5.8	trace shell	
262	118	Asegb2	d	N 2.5	SL	SF	Y	SL	N	6.58	4.97	1% shell	
262	204	C'seg1	a	10Y 3/1	SiC	MF	N	VS	N	6.84	5.09		
262	223	2C'seg2	c	10Y 3/1	LS	NF	N	VS	N	5.15	3.29		
262	266	3C'seg3	b	5GY 4/1	CL	SF	Y	SL	N	6.67	4.96	Trace organic fragments, sapric	
263	12	Aseg1	c	10Y 2.5/1	SiL	VF	Y	ST	N	6.15	5.89		
263	33	Aseg2	c	N 2.5	SiCL	VF	Y	ST	N	6.37	5.71	trace shell fragments	
263	75	Cseg1	g	10Y 4/1	SiCL	MF	N	SL	SL	6.26	5.3		
263	95	Cseg2	c	10Y 3/1	L	MF	N	SL	N	7.01	7.78	10% shells	
263	105	Cseg3	a	10Y 3/1	S	NF	N	SL	N	7.06	7.9	10% shells	
263	114	2Asegb	c	10Y 2.5/1	SL	SF	Y	SL	N	5.72	3.53	trace organic fragments	5% 10GY 4/1
263	136	2BAseg	c	10Y 4/1	SL	SF	N	SL	N	6.73	5.93	3% root fragments	

263	181	2Btseg	b	10Y 3/1	SCL	NF	Y	SL	N	7.15	7.1	2% root fragments	5% 10YR 4/4
264	19	Aseg1	g	10Y 2.5/1	SiCL	MF	Y	ST	N	4.98	5.24	trace clam shell fragments	
264	36	Aseg2	g	10Y 2.5/1	SiCL	MF	Y	ST	SL	6.57	6.33		
264	70	Cseg1	g	10Y 3/1	SiC	MF	N	ST	SL	5.29	4.63		
264	103	Cseg2	b	10Y 3/1	SiC	MF	N	SL	M	4.76	3.59		
265	34	Aseg	c	10Y 2.5/1	SiCL	VF	Y	ST	N	5.05	4.93	trace shells	
265	68	Cseg1	g	10Y 3/1	SiC	MF	Y	ST	SL	5.51	4.79	trace shells	
265	103	Cseg2	b	5GY 3/1	SiC	MF	N	ST	SL	4.4	3.76		
266	16	Aseg	c	N 2.5	L	VF	Y	SL	N	5.89	5.41	trace shell	
266	29	Cseg1	c	10Y 4/1	SL	SF	N	VS	N	6.8	7.73	5% shell	
266	52	Cseg2	a	10Y 4/1	LS	NF	N	VS	N	4.84	3.31		
266	72	Asegb1	c	N 2.5	LS	NF	N	SL	N	4.31	3.07		
266	88	Asegb2	b	10Y 2.5/1	SL	SF	N	SL	N	4.97	3.12	5% translocated peds	
268	18	Aseg1	c	10Y 2.5/1	S	NF	Y	SL	N	6.53	6.75	trace shells, 1 cm live clams	
268	31	Aseg2	c	10Y 2.5/1	SL	SF	Y	SL	SL	6.84	7.67	5% shell	
268	47	2Cseg1	a	5GY 2.5/1	L	MF	Y	VS	SL	6.72	4.55	trace shell fragments	

268	80	2Cseg2	g	10Y 4/1	SiCL	MF	N	VS	SL	7.12	4.86	trace shells and organic fragments	
268	119	2Cseg3	g	10Y 3/1	SiCL	MF	N	VS	SL	6.94	5.05		
268	165	2Cseg4	g	5GY 4/1	SiC	MF	N	VS	N	7.24	5.89	trace organic fragments	
268	217	2Cseg5	g	10Y 4/1	SiC	MF	N	VS	N	7.13	5.57	trace wood and shell fragments	
268	267	2Cseg6	d	5GY 4/1	SiC	MF	N	VS	N	6.95	5.23	trace wood and shell fragments	
268	288	2Cseg7	b	5GY 3/1	C	MF	N	VS	N	6.95	4.57	trace wood fragments	
269	23	Aseg1	c	N 2.5	S	NF	Y	SL	N	7.03	6.46	trace shells	
269	38	Aseg2	g	10Y 2.5/1	LfS	NF	Y	SL	N	7.13	6.21		
269	65	2Cseg1	g	10Y 3/1	CL	MF	Y	SL	SL	7.05	6.05	trace organic fragments	
269	122	2Cseg2	g	10Y 3/1	SiCL	MF	Y	SL	N	7.01	5.13	trace organics and shells	



269	162	2Cseg3	g	10Y 4/1	SiCL	MF	N	VS	N	6.49	3.98	trace wood and shell fragments	
269	181	2Cseg4	c	10Y 3/1	CL	MF	N	VS	N	6.57	4.08	5% shell, trace wood fragments	
269	189	2Cseg5	b	10Y 3/1	CL	MF	N	VS	N	6.13	3.44	2% wood fragments	
270	6	Btseg	a	5GY 4/1	SCL	NF	N	SL	N	7.56	7.97	trace shells at surface	15% 10YR 3/4
270	16	Btsej	b	5Y 3/1	SCL	NF	N	SL	N	5.31	4.65		20% 7.5YR 4/6, 10% 2.5Y 6/4
271	6	BAtse	c	10YR 2/2	L	NF	N	VE	N	7.04	7.61	trace shell and gravel	30% 5GY 2.5/1, 10% each 10YR 3/3, 7.5YR 3/4, 7.5YR 2.5/2, 2.5Y 5/3
271	13	Btse	b	2.5Y 4/3	CL	NF	N	SL	N	5.5	4.64		25% 5GY 2.5/1, 25% 5YR 3/4

272	4	Aseg	c	N 2.5	LS	SF	Y	SL	n	7.96	7.9	10% ribbed mussels, attached to 30% gravel as cemented peds	
272	13	2CBg	c	5Y 4/2	LS	NF	N	VS	n	5.33	4.34		
272	20	2CB	b	2.5Y 5/3	LS	NF	N	NR	n	6.5	5.87		
273	7	Ase	c	5Y 3/2	L	VF	Y	ST	N	4.81	4.95		
273	33	Aseg	g	10Y 3/1	L	VF	Y	ST	N	4.64	4.31	Live soft shell clam	
273	66	Cseg1	g	10Y 2.5/1	SiL	MF	Y	ST	N	4.74	4.46	5% clam shells	
273	78	Cseg2	b	10Y 2.5/1	SiL	MF	N	ST	N	5.44	4.52	10% clam shells	
275	14	Aseg1	c	10Y 2.5/1	L	VF	Y	SL	N	6.93	5.86	10% shell	
275	24	Aseg2	c	10Y 3/1	SL	VF	Y	VS	N	7.66	7.4	10% shell	
275	73	Cg1	g	10Y 3/1	SL	SF	N	VS	N	5.96	3.99	5% shell	
275	115	Cg2	g	10Y 3/1	LS	NF	N	VS	N	5.91	4.27	2% wood, trace shell	
275	133	Agb	c	10Y 2.5/1	LS	NF	N	VS	N	6.45	4.59	10% shell	
275	153	C'g	c	10Y 2.5/1	LS	NF	N	VS	N	4.81	3.78	trace gravel and wood	
275	165	2Btjg	b	10Y 3/1	CL	NF	N	VS	N	7.92	8.28		2% 2.5Y 6/4, 1% 10YR 4/6

276	8	Aseg	a	10Y 2.5/1	S	NF	y	ST	n	7.41	7.85	trace shells	
276	16	2Btseg	b	10GY 4/1	CL	NF	n	SL	n	7.37	7.42		40% 2.5Y 4/4 concentrations
277	3	Aseg	a	10Y 2.5/1	LS	SF	Y	ST	n	7.83	7.88	50% gravels as translocated peds, loose platform material; trace shell fragments	
277	17	2CBtjgb	b	5Y 4/2	CL	NF	N	VS	n	5.21	4.23		7% 7.5YR 3/4, 2% 2.5Y 6/4
278	3	Aseg	a	N 2.5	grSL	NF	N	ST	N	7.35	7.68	30% relict peds	
278	26	2Btsejg	b	N 5	CL	NF	N	VS	N	6.68	6.34		20% 2.5Y 6/6, 7% 7.5YR 5/6
279	22	Aseg	a	N 2.5	S	NF	Y	SL	N	6.99	6.78		
279	87	Cseg1	g	10Y 2.5/1	SL	MF	N	VS	N	6.5	4.8	trace shell	
279	147	2Cseg2	g	10Y 4/1	SiL	MF	N	VS	SL	7.13	4.92	trace shell and organic	
279	182	2Cseg3	b	10Y 4/1	SiCL	MF	Y	VS	N	6.82	4.04	trace shell	
279.5	17	Aseg1	c	N 2.5	SL	SF	Y	SL	N	6.06	5.18	trace shell	

279.5	37	Aseg2	c	10Y 2.5/1	L	MF	Y	SL	N	5.99	5.01		
279.5	61	Cseg1	c	10Y 3/1	CL	MF	N	VS	SL	5.12	3.65	One large oyster shell	
279.5	74	Cseg2	g	10Y 3/1	L	NF	N	VS	SL	5.54	3.14	trace organic	
279.5	91	2Cg	g	10Y 3/1	S	NF	N	NR	SL	4.31	3.23	trace organic	
279.5	143	3C'seg	b	10Y 2.5/1	L	MF	N	VS	M	4.77	3.44	15% woody organic	
280	20	Aseg	a	10Y 2.5/1	S	NF	y	ST	n	7.39	7.56	trace shell fragments	25% 2.5Y 4/3 krotovina?
280	41	2Cseg	g	5GY 2.5/1	SiL	MF	y	SL	n	6.24	4.85		
280	64	2ACseg	g	N 3	SiCL	MF	y	ST	n	6.45	4.21		
280	103	2Aseg1	g	N 2.5	SiC	MF	y	ST	n	6.87	5.25		
280	148	2Aseg2	g	N 2.5	SiC	MF	y	ST	n	6.84	5.55		
280	199	2C'seg	g	10Y 3/1	SiC	MF	y	SL	n	6.32	4.27	trace shell fragments	
280	221	3Cg1	c	10Y 4/1	S	NF	n	SL	n	6.15	4.31	2% shell	
280	248	3Cg2	c	10Y 3/1	fS	NF	n	VS	n	4.51	3.24	4% wood	
280	266	3Cg3	a	10Y 3/1	S	NF	n	VS	n	4.13	3.2	2% wood	
280	275	4CBt	b	10Y 3/1	SL	NF	n	VS	n	6.06	4.12		
283	15	Aseg1	c	N 2.5	SL	SF	Y	ST	N	6.6	6.32	trace shell	
283	51	Aseg2	d	N 2.5	SiC	VF	Y	SL	N	6.56	5.13	trace shell	
283	113	Cseg1	d	5GY 3/1	SiC	MF	Y	VS	N	6.44	4.82		

283	152	Cseg2	g	5G 4/1	SiC	MF	N	VS	N	6.14	4.46	trace shell, one large oyster shell	
283	179	Cseg3	a	5GY 4/1	CL	MF	N	VS	N	6.54	4.56	trace shell	
283	192	2Btsegb	b	5GY 6/1	C	NF	N	ST	N	7.34	7.51		
284	6	Aseg1	c	10Y 2.5/1	L	VF	Y	ST	N	4.02	3.83	Live clam	
284	40	Aseg2	g	10Y 3/1	L	VF	Y	ST	N	5.22	4.57		
284	66	Cseg1	g	10Y 2.5/1	SiCL	MF	Y	ST	N	5.06	4.34	Trace shell fragments	
284	121	Cseg2	g	10Y 2.5/1	SiCL	MF	N	ST	SL	4.52	3.87		
284	200	Cseg3	b	10Y 3/1	SiCL	MF	N	ST	N	4.44	3.89	Blocky structure, trace wood fragments	
285	9	Aseg1	c	10Y 2.5/1	SiL	VF	Y	ST	N	3.6	3.37		
285	48	Aseg2	g	N 2.5	SiL	VF	Y	ST	N	5.09	4.56	Trace shell fragments	
285	79	Cseg1	g	10Y 2.5/1	SiL	MF	Y	ST	N	5.08	4.71	Trace shell fragments	

285	106	Cseg2	b	10Y 2.5/1	SiCL	MF	Y	ST	N	5.53	4.48	3% gravels (slag?), angular sandstone at 98 cm	
286	8	Aseg1	c	10Y 2.5/1	L	VF	Y	ST	N	4.03	4.18		
286	33	Aseg2	g	10Y 2.5/1	L	VF	Y	ST	N	4.01	3.99		
286	63	Cseg1	g	10Y 2.5/1	L	MF	Y	ST	N	5.09	4.74		
286	97	Cseg2	b	10Y 2.5/1	L	MF	Y	ST	N	4.97	4.16	clam box	
287	9	Aseg1	c	10Y 2.5/1	S	NF	N	SL	N	7.58	7.57	trace shell	
287	43	Aseg2	c	5GY 2.5/1	S	NF	N	SL	N	7.46	7.46	trace shell, 4 cm live razor clam dead at 38 cm	
287	88	Cseg1	g	10GY 2.5/1	S	NF	Y	SL	N	6.78	4.7		
287	134	Cseg2	c	10GY 2.5/1	S	NF	N	SL	N	6.01	4.11	2% shell	
287	154	Cseg3	c	5GY 2.5/1	S	NF	N	SL	N	6.8	6.08	10% gravels	
287	188	Cseg4	g	10GY 2.5/1	S	NF	N	SL	N	7.8	7.54	trace gravels	
287	202	Cseg5	b	10GY 2.5/1	LS	NF	N	SL	N	7.9	7.69		
288	19	Aseg	c	10Y 2.5/1	S	NF	N	ST	N	7.99	7.66	trace shells	

288	44	Cseg1	c	5GY 2.5/1	S	NF	N	ST	N	7.18	5.32	trace translocated peds	
288	89	Cseg2	g	10Y 3/1	S	NF	N	SL	N	7.69	7.09	3% shells	
288	154	Asegb	g	N 2.5	S	NF	N	VS	SL	7.2	4.33	2% shells	
288	188	C'seg1	g	5GY 2.5/1	LfS	SF	N	VS	SL	7.33	3.8	trace shells	
288	219	C'seg2	c	5GY 2.5/1	SL	SF	N	VS	SL	7.77	5.52	trace organic	
288	230	C'seg3	b	5GY 3/1	SL	SF	N	VS	SL	7.34	4.58		
289	20	Aseg	c	10Y 2.5/1	S	NF	Y	VE	N	7.71	7.49	trace shells	
289	57	Cseg1	g	5GY 2.5/1	SL	NF	N	SL	N	6.81	3.73	trace shells	
289	107	Cseg2	g	10GY 2.5/1	SL	MF	N	SL	M	6.97	3.2	trace wood fragments	
289	142	Cseg3	g	5GY 4/1	SiL	MF	Y	SL	SL	7.42	4.42	trace shells and organic fragments	
289	182	Cseg4	d	5GY 3/1	SiL	MF	Y	SL	N	7.41	5.88	trace shells and organic fragments	
289	219	Cseg5	d	10Y 3/1	SiCL	MF	Y	SL	N	6.62	4.41	trace shells and organic fragments	
289	260	Cseg6	b	10Y 4/1	SiCL	MF	Y	SL	N	6.61	4.68	5% shells	

290	16	Aseg	c	10Y 2.5/1	L	VF	Y	SL	N	5.71	4.61	trace shell	
290	37	Cseg	a	10Y 2.5/2	L	MF	N	SL	N	5.03	3.35	trace wood	
290	42	2Aseb	a	10YR 2/2	mucky SiL	MF	N	VS	M	5.7	4.75		
290	46	2Oaseb	c	10YR 2/1	Muck	MF	N	VS	M	5.69	3.46		
290	62	2A'seb	c	5Y 2.5/1	L	MF	N	VS	SL	6.23	3.84	10% organic fragments	
290	82	2ABsegb	a	5Y 4/1	SL	SF	N	VS	SL	6.06	2.91	2% organic fragments	
290	130	2Bwsegb	c	10Y 5/1	SL	SF	N	VS	N	6.77	5.96		
290	152	3Btsegb	b	10GY 6/1	C	NF	N	ST	N	6.64	5.89		
292	18	Aseg1	c	N 2.5	SiL	VF	Y	SL	N	6.46	5.36	trace shell	
292	36	Aseg2	c	10Y 2.5/1	SiCL	VF	Y	VS	SL	6.25	4.74	trace shell	
292	76	Cseg1	g	10Y 4/1	SiCL	MF	Y	VS	SL	6.18	3.46	trace wood and organic	
292	101	Cseg2	g	10Y 3/1	SiL	MF	N	VS	SL	5.4	3.14	10% wood and organic	
292	131	Asegb	a	10Y 2.5/1	SiL	MF	N	VS	SL	5.28	3.28	30% organic	
292	138	Oaseb	a	10YR 2/1	Muck	MF	N	VS	N	5.65	3.48		
292	149	C'seg1	c	10Y 4/1	CL	MF	N	SL	N	4.86	2.88	trace organic	



292	164	C'seg2	b	10Y 4/1	CL	MF	N	SL	N	5.46	3.39	trace organic	
293	7	Aseg1	c	N 2.5	SiL	VF	Y	ST	N	2.99	3.27		
293	28	Aseg2	g	10Y 2.5/1	SiL	VF	Y	ST	SL	3.33	3.23	trace organic fragments	
293	64	Cseg	g	10Y 2.5/1	SiL	MF	N	ST	M	3.63	3.25	3% organic fragments	
293	124	Cse	g	2.5Y 2.5/1	L	MF	N	SL	M	3.1	3.16	5% organic fragments, weak blocky structure	
293	145	2Aseb1	g	2.5Y 2.5/1	L	MF	N	SL	SL	3.19	2.42	5% organic fragments	
293	169	2Aseb2	b	2.5Y 2.5/1	L	MF	N	SL	N	2.95	2.4	7% organic fragments, larger than above, blacker color	
294	21	Aseg	c	N 2.5	SiL	VF	Y	SL	N	5.94	4.86		
294	64	Cseg1	g	10Y 3/1	SiCL	VF	N	SL	N	6.23	6.18	trace shell	

294	114	Cseg2	g	10Y 3/1	SiCL	VF	N	VS	SL	5.71	3.59	1% organic, as finely distributed roots or fibers	
294	170	Cseg3	b	10Y 3/1	SiCL	MF	N	VS	SL	5.69	3.13	1% organic	
295	18	Aseg1	c	10Y 2.5/1	SiCL	VF	y	SL	n	6.42	5.76	trace shells	
295	52	Aseg2	g	10Y 2.5/1	SiCL	VF	y	SL	n	6.71	5.7	trace shells	
295	86	Cseg1	g	10Y 3/1	SiCL	MF	n	VS	n	6.70	5.45	trace shells	
295	125	Cseg2	g	10Y 4/1	SiCL	MF	n	VS	SL	6.85	4.72	trace shells, trace organic fragments	
295	149	Cseg3	g	10Y 3/1	SiCL	MF	n	VS	SL	6.70	3.66	trace shell fragments	
295	197	Cseg4	d	10Y 4/1	SiCL	MF	n	VS	SL	6.87	3.18	trace shell and organic fragments	
295	229	Cseg5	d	10Y 3/1	SiC	MF	n	VS	SL	6.70	3.06	trace shell and organic fragments	

295	262	Cseg6	d	5GY 3/1	SiC	MF	n	VS	n	6.57	3.2	1% organic fragments	
295	299	Asegb	a	5GY 3/1	SiC	MF	n	VS	n	5.85	3.03	1% organic fragments	
295	304	2Aseb	b	5Y 2.5/1	SiL	SF	n	VS	n	5.79	4.02	trace organic fragments	
303	5	Aseg	c	N 2.5	L	VF	Y	ST	ST	5.88	4.59	10% organic fragments	
303	21	Ase	c	5Y 2.5/1	SiL	VF	Y	ST	ST	6.22	4.36	7% organic fragments	
303	69	Cse	a	5Y 2.5/1	SiCL	VF	N	SL	M	6.39	4.75	3% organic	
303	84	Aseb	c	2.5Y 2.5/1	SiCL	VF	N	SL	M	6.36	4.17	15% organic	
303	113	Cse1	c	5Y 2.5/1	SiCL	VF	N	VS	M	6.40	5.01	10% organic, wood fragments at 90 cm	
303	134	Cse2	g	5Y 2.5/1	SiCL	MF	N	VS	M	6.34	4.11	7% organic	
303	149	Cse3	a	5Y 2.5/1	SiCL	MF	N	VS	M	6.22	4.56	20% organic	
303	157	Oaseb	b	10YR 2/1	Muck	VF	N	VS	M	6.25	4.22		
305	13	Aseg1	a	N 2.5	SiL	VF	Y		SL	3.25	3.25		

305	24	Aseg2	c	10Y 2.5/1	SiL	VF	Y		M	3.24	3.1	3% organic fragments	
305	41	Cseg1	c	10Y 3/1	SiL	MF	N		M	3.74	3.29	7% wood fragments	
305	119	Cseg2	a	10Y 2.5/1	SiL	MF	N		M	3.75	3.49	10% wood fragments	
305	141	2Oseb1	g	10YR 2/1	Muck	SF	N		ST	5.64	5.18		
305	173	2Oseb2	b	10YR 2/1	Muck	SF	N		ST	6.63	6.2		
306	14	Aseg1	a	N 2.5	SiL	VF			SL	3.38	3.3	trace organic fragments	
306	30	Aseg2	c	10Y 2.5/1	SiL	VF			N	3.64	3.98	trace organic fragments	
306	56	Cseg1	g	10Y 3/1	SiCL	MF			SL	3.28	3.16	trace organic fragments	
306	106	Cseg2	d	10Y 2.5/1	SiCL	VF			ST	3.74	3.33	3% organic fragments, trace shell	
306	156	Cseg3	d	10Y 2.5/1	SiCL	MF			M	4.05	3.57	7% organic fragments	

306	202	Cseg4	b	10Y 2.5/1	SiCL	MF			ST	3.3	3.03	7% organic fragments, larger and woody	
307	11	Aseg1	c	N 2.5/0	SiL	VF	Y		N	3.11	3.01	3% clam shell, trace organics	
307	43	Aseg2	g	10Y 2.5/1	SiL	VF	Y		M	4.2	3.42	trace organics, trace shell	
307	136	Cseg1	d	10Y 3/1	SiCL	VF	N		M	3.47	3.31	3% organics, 3% shell	
307	201	Cseg2	b	10Y 2.5/1	SiCL	MF	N		SL	3.67	3.18	5% organics	
308	25	Aseg1	g	N 2.5	SiCL	VF	Y		N	3.45	3.31		
308	53	Aseg2	c	10Y 2.5/1	SiCL	VF	Y		N	3.88	3.48	trace shell	
308	152	Cseg1	d	5GY 3/1	SiCL	VF	N		SL	3.75	3.01	5% organic, trace shell	
308	201	Cseg2	b	5GY 3/1	SiC	MF	N		SL	4.15	3.32	Shelly layer from 190- 198	
309	8	Aseg	c	N 2.5	SiL	VF	Y	SL	N	6.28	4.14	2% organic	
309	44	Cseg1	c	10Y 2.5/1	SiL	VF	N	VS	ST	6.77	4.45	3% organic	

309	94	Cseg2	d	10Y 3/1	SiC	MF	N	VS	M	7.04	5.62	trace organic and shell	
309	155	Cseg3	b	10Y 3/4	SiC	MF	N	VS	SL	6.79	4.19	trace shell	
312	12	Aseg1	c	N 2.5	SiL	VF	Y	ST	N	6.91	5.69	trace organic fragments	
312	44	Aseg2	c	10Y 2.5/1	SiL	VF	Y	ST	N	6.77	5.1	2% organic fragments, trace shells	
312	84	Cseg1	g	10Y 3/1	SiCL	MF	N	SL	SL	7.48	6.42	2% shells	
312	150	Cseg2	g	10Y 4/1	SiC	MF	N	SL	N	7.18	4.84	trace shell fragments	
312	180	Cseg3	b	10Y 4/1	SiC	MF	N	VS	N	6.84	3.49	trace shell and organic fragments	
313	11	Aseg1	c	10Y 2.5/1	L	VF	Y	ST	N	3.16	3.45		
313	36	Aseg2	c	10Y 2.5/1	SiL	VF	Y	ST	N	4.05	3.84	4% intact clam shells	
313	60	Aseg3	g	10Y 2.5/1	L	VF	Y	ST	SL	3.99	3.48		
313	138	Cseg1	g	10Y 3/1	SL	MF	N	SL	SL	4.29	3.36	4% organic fragments	
313	181	Cseg2	g	10Y 3/1	L	MF	N	SL	SL	4.37	3.37	4% leaf fragments	

313	201	Cseg3	b	10Y 4/1	SiL	MF	N	VS	SL	3.87	3.45		
314	25	Aseg1	g	10Y 2.5/1	L	VF	Y	ST	N	4	3.58		
314	70	Aseg2	g	10Y 2.5/1	SiL	MF	Y	ST	SL	4.52	3.73	trace shell and organic fragments	
314	99	Aseg3	g	10Y 2.5/1	SiCL	MF	Y	ST	N	5.39	4.32		
314	124	Cseg1	g	10Y 2.5/1	SiCL	MF	N	ST	N	4.31	3.57	trace wood and shell fragments	
314	159	Cseg2	g	10Y 3/1	SiCL	MF	N	ST	N	4.69	3.67		
314	205	Cseg3	b	10Y 4/1	CL	MF	N	SL	N	4.05	3.41		

*Appendix J: West River particle size analyses*

Pedon	Horizon	%	%	%	Sand Separates					Texture
		Sand	Silt	Clay	% vc	% c	% m	% f	% vf	Class
259	Aseg	97.0	0.1	2.9	1.6	13.8	37.9	41.0	2.7	S
259	2CBg1	91.6	3.2	5.2	1.6	17.9	41.4	26.4	4.3	S
259	2CBg2	93.0	2.6	4.5	1.0	17.9	41.0	27.4	5.6	S
260	Aseg1	96.0	0.8	3.2	0.5	11.2	43.5	39.7	1.0	S
260	Aseg2	95.3	2.7	2.0	3.6	25.8	47.2	16.9	1.8	coS
260	Cseg1	77.4	15.9	6.7	2.6	7.2	19.7	31.8	16.1	LS
260	Cseg2	94.7	0.8	4.5	8.4	45.4	26.5	12.1	2.3	coS
260	Cseg3	90.8	3.4	5.8	2.0	14.0	44.3	24.2	6.4	S
260	Cseg4	74.1	15.4	10.5	3.7	4.0	19.8	34.0	12.6	fSL
261	Aseg1	96.8	0.9	2.3	0.2	5.5	33.8	55.4	1.9	fS
261	Aseg2	97.7	0.0	2.3	0.2	9.3	48.3	38.6	1.3	S
261	Cseg1	95.1	0.8	4.1	3.1	18.3	51.8	19.9	2.0	S
261	Cseg2	93.5	1.4	5.2	3.6	4.5	12.9	68.5	4.0	fS
261	Cseg3	94.0	1.5	4.5	3.5	8.0	26.7	52.7	3.0	fS
261	Cseg4	83.2	8.0	8.8	5.8	6.6	21.7	44.7	4.5	LS
261	Cseg5	34.4	60.5	5.1	4.3	2.0	3.3	17.0	7.9	SIL
262	Cseg1	96.9	-0.8	3.9	4.5	3.6	32.2	54.5	2.1	fS
262	Cseg2	96.7	-0.5	3.9	5.2	3.9	20.9	64.0	2.8	fS
262	Asegb1	88.0	4.2	7.7	0.3	12.0	5.5	66.1	4.1	LfS
262	Asegb1	76.0	10.7	13.3	0.2	0.4	2.7	63.1	9.7	fSL
262	2Cseg2	88.4	3.0	8.6	0.3	6.6	36.2	35.3	10.0	LS
262	3Cseg3	49.1	23.9	27.0	0.5	0.9	2.8	21.9	23.0	SCL
263	Aseg1	33.7	37.2	29.1	0.4	0.9	1.2	13.3	17.8	CL
263	Cseg3	90.7	3.4	5.9	0.4	15.3	42.0	28.4	4.6	S
263	2Asegb	65.5	20.7	13.8	0.7	6.3	18.2	32.3	8.0	fSL
263	2BASeg	60.4	27.1	12.5	0.8	3.8	13.0	34.9	7.9	fSL
266	Aseg	69.3	17.4	13.3	0.1	0.4	3.2	45.2	20.4	fSL
266	Cseg1	81.5	11.9	6.6	9.3	5.3	14.8	45.8	6.2	LS
266	Cseg2	87.9	5.7	6.5	1.5	6.2	16.1	58.1	6.0	LfS
268	Cseg1	74.7	17.5	7.9	2.0	1.6	2.1	40.2	28.8	fSL
268	Cseg2	34.7	54.1	11.2	6.0	2.9	1.9	5.9	18.0	SIL
268	Cseg3	21.6	67.8	10.6	4.3	2.6	2.4	8.3	4.1	SIL
268	Cseg4	16.0	69.3	14.7	3.6	2.3	1.7	3.2	5.2	SIL
268	Cseg5	24.1	60.9	15.0	9.1	4.4	2.8	3.6	4.1	SIL
268	Cseg6	21.8	63.2	15.0	2.6	3.5	3.4	8.0	4.3	SIL
268	Cseg7	33.3	50.3	16.4	5.9	2.7	3.9	10.6	10.2	SIL
269	Cseg1	44.7	40.0	15.3	1.7	1.3	1.6	26.5	13.6	L
269	Cseg2	27.2	54.7	18.0	6.4	1.9	1.8	6.2	10.9	SIL
269	Cseg3	39.6	45.2	15.2	13.8	14.2	4.3	4.4	2.8	L
269	Cseg4	49.1	38.0	12.9	6.9	3.8	10.3	21.4	6.8	L
269	Cseg5	69.9	19.6	10.5	4.1	4.9	19.5	32.5	8.9	fSL
270	Btseg	83.3	6.3	10.4	5.3	14.5	25.8	31.4	6.3	LS



270	Btsejg	77.0	12.0	11.0	4.1	10.9	27.2	28.9	5.8	SL
271	BAtse	80.6	8.5	10.9	1.8	12.6	26.4	33.7	6.1	fSL
271	Btse	77.0	8.3	14.7	0.8	9.0	21.4	40.1	5.7	fSL
272	2CBg	90.3	6.2	3.5	1.6	16.9	35.2	30.9	5.7	S
272	2CB	89.8	6.1	4.1	1.4	14.6	36.6	31.1	6.2	S
275	Cg1	85.9	8.8	5.3	0.6	1.8	31.3	42.2	10.1	LS
275	Cg2	87.4	7.1	5.5	0.7	7.9	43.6	26.8	8.4	LS
275	C'g	89.8	5.8	4.4	3.9	20.3	28.9	28.9	7.7	S
275	2Btgj	74.4	9.8	15.8	1.4	11.2	31.8	25.5	4.6	SL
276	2Btseg	75.3	10.1	14.6	1.0	12.8	28.5	20.8	12.2	SL
277	2CBtjgb	54.7	25.1	20.2	8.7	7.6	14.5	13.0	10.9	SCL
278	2Btsejg	32.3	35.8	31.9	4.9	2.9	5.2	7.8	11.5	CL
279	Cseg1	77.8	12.4	9.7	1.6	2.6	4.6	49.2	19.8	fSL
279	Cseg2	49.8	32.9	17.3	3.2	0.9	2.0	23.4	20.3	L
280	2Cseg	35.7	47.3	17.0	0.8	0.7	1.0	18.1	15.0	L
280	2C'seg	22.3	62.6	15.1	14.0	2.0	2.2	2.2	1.8	SIL
280	3Cg1	89.0	6.5	4.5	0.3	2.0	52.6	30.1	4.0	S
280	3Cg2	92.0	3.8	4.2	0.6	2.8	53.7	28.0	6.9	S
280	3Cg3	87.1	8.6	4.3	0.7	3.3	28.3	45.6	9.2	LS
280	4CBt	68.9	22.2	8.9	1.4	3.6	30.3	28.2	5.5	SL
283	Cseg3	74.1	18.2	7.7	20.2	4.0	11.2	33.6	5.0	fSL
283	2Btsegb	28.0	44.0	28.0	0.6	1.4	2.2	13.7	10.1	CL
287	Cseg1	96.5	-0.8	4.4	5.7	2.9	52.6	34.1	1.2	S
287	Cseg2	88.1	5.3	6.5	3.0	2.3	11.5	67.1	4.2	LfS
287	Cseg3	94.9	-0.2	5.3	5.5	7.8	32.1	47.8	1.8	S
287	Cseg4	94.5	8.0	-2.4	0.2	0.5	15.0	76.0	2.8	fS
287	Cseg4	89.1	3.9	7.0	5.1	1.7	50.5	30.0	1.8	S
287	Cseg5	90.2	4.9	4.9	4.2	2.5	41.1	40.5	1.9	S
288	Cseg1	95.0	1.1	3.9	4.0	3.1	43.8	42.7	1.3	S
288	Cseg2	93.9	1.9	4.3	2.7	4.6	54.5	30.8	1.2	S
288	C'seg1	83.1	7.2	9.6	6.5	3.2	17.3	47.5	8.6	LS
288	C'seg2	81.2	8.8	10.0	3.8	2.1	4.7	62.7	7.8	LfS
288	Cseg3	69.4	16.3	14.3	2.8	1.6	2.0	48.6	14.4	fSL
289	Cseg1	80.0	11.7	8.4	3.0	2.4	6.7	59.6	8.3	LfS
289	Cseg2	73.0	16.9	10.1	4.0	2.1	3.4	49.6	14.0	fSL
289	Cseg3	43.7	38.0	18.3	3.8	1.7	2.7	21.1	14.4	L
289	Cseg4	36.6	43.1	20.3	2.4	1.1	1.3	14.3	17.6	L
289	Cseg5	28.2	53.6	18.2	3.9	1.6	1.9	11.6	9.1	SIL
289	Cseg6	24.1	58.8	17.1	5.6	2.3	1.8	2.8	11.6	SIL
290	Cseg	66.0	28.7	5.3	11.7	7.6	16.3	23.6	6.9	SL
290	2Bwseb	57.6	28.1	14.3	0.0	0.9	8.4	30.1	18.2	fSL
290	3Btseb	21.2	30.2	48.6	2.5	2.8	4.5	7.7	3.6	C

Appendix K: Proposed and tentative OSDs for Chesapeake Bay subestuaries

LOCATION RHODE RIVER MD

Tentative Series

BMW/DCS/RBT

10/2017

## **RHODE RIVER SERIES**

MLRA(s): 149A

Soil Survey Regional Office (SSRO) Responsible: Raleigh, North Carolina

Depth Class: Very deep

Drainage Class: Subaqueous (permanently submersed / continuously inundated)

Saturated Hydraulic Conductivity: Moderately high to high

Parent Material: coarse-loamy estuarine deposits over glauconitic coarse-loamy  
fluviomarine deposits

Slope: 0 to 3 percent

Mean Annual Air Temperature: 57 degrees F. (14 degrees C)

Mean Annual Water Temperature: 57 degrees F. (14 degrees C)

**TAXONOMIC CLASS:** Coarse-loamy, glauconitic, nonacid, mesic Aeric

Fluviwassents

**TYPICAL PEDON:** Rhode River fine sandy loam on an east facing submerged  
wave-cut platform with a 1 percent slope under 0.2 m of estuarine water. (Colors are

for moist soil unless otherwise stated).

**Ase1** -- 0 to 10 cm; greenish black (10Y 2.5/1) fine sandy loam; single grain; slightly fluid; 1 percent shell fragments; slightly alkaline, not sulfidic materials; no reaction with 3% hydrogen peroxide, violently effervescent with 30% hydrogen peroxide, clear boundary.

**Ase2** -- 10 to 24 cm; greenish black (10Y 2.5/1) fine sandy loam; single grain; nonfluid; 1 percent shell fragments; slightly alkaline, not sulfidic materials; no reaction with 3% hydrogen peroxide, violently effervescent with 30% hydrogen peroxide, clear boundary. (12 to 24 centimeters thick)

**2Bseg** -- 24 to 51 cm; dark gray (2.5Y 4/1) sandy loam; massive; nonfluid; 3% light olive brown (2.5Y 5/4) iron concentrations, 18% brownish yellow (10YR 6/8) iron concentrations; slightly alkaline, not sulfidic materials; no reaction with 3% hydrogen peroxide, strongly effervescent with 30% hydrogen peroxide, clear boundary.

**2Bjg** -- 51 to 76 cm; dark grayish brown (10YR 4/2) fine sandy loam; massive; nonfluid; 4% pale yellow (5Y 7/4) jarosite concentrations, 6% dark brown (7.5YR 3/3) iron concentrations; slightly alkaline, not sulfidic materials; no reaction with 3% hydrogen peroxide, very slightly effervescent with 30% hydrogen peroxide, abrupt boundary.

**2Btj** -- 76 to 123 cm; reddish brown (2.5YR 4/3) fine sandy loam; massive; nonfluid; 15% pale yellow (5Y 7/4) jarosite concentrations, 4% strong brown (7.5YR 5/8) iron concentrations; strongly acid, not sulfidic materials; no reaction with 3% hydrogen peroxide, very slightly effervescent with 30% hydrogen peroxide, abrupt boundary.

**2Cseg** -- 123 to 180 cm; black (2.5Y 2.5/1) loam; massive; nonfluid; strongly acid; no reaction with 3% hydrogen peroxide, violently effervescent with 30% hydrogen peroxide.

**TYPE LOCATION:** Anne Arundel County, Maryland; approximately 1,361 feet southwest of Locust Point and approximately 2,309 feet northwest of Sand Point in the Rhode River. USGS South River quadrangle; latitude 38 degrees, 52 minutes, 33.92 seconds N; longitude 76 degrees, 31 minutes, 33.22 seconds W, WGS 1984; Major Land Resource Area 149A.

**RANGE IN CHARACTERISTICS:**

Depth to Bedrock: Greater than 200 centimeters

Depth to Seasonal High Water Table: Permanently submersed

Depth to Lithologic Discontinuity: 12 to 52 centimeters

Depth to hyper-sulfidic materials: greater than 100 centimeters (if present)

Depth to hypo-sulfidic materials: less than 100 centimeters

Manner of Failure / Fluidity Class: Nonfluid to slightly fluid throughout

Shell Fragments: 0 to 10 percent, by volume, throughout

Soil reaction: Strongly acid to moderately alkaline; oxidized reaction: Very strongly acid to slightly alkaline

Salinity: Between 7 to 15 ppt throughout the profile.

### **RANGE OF INDIVIDUAL HORIZONS:**

Ase or A horizon:

Color— hue of 2.5Y to 5G, value of 2.5 and 3, chroma of 0 or 1

Texture (fine-earth fraction) – sand, loamy sand, loamy fine sand, fine sandy loam, or silt loam.

Cseg or CBseg horizon:

Color— hue of 10Y to 5G, value of 2.5, 3, 4, 7, chroma of 1

Texture (fine-earth fraction) – loamy sand, loamy coarse sand, fine sandy loam, silt loam, loam, sandy clay loam.

2Bseg or 2Btseg horizon:

Color— hue of 2.5Y to 10GY, value of 3 to 5, chroma of 1 or 2.

Texture (fine-earth fraction) – sandy loam, fine sandy loam, silt loam or sandy clay loam.

2Bjg or 2Btj horizon:

Color – hue of 5Y, 10Y, 5GY, 5G, or 5BG value of 3 to 5, chroma of 1 or 2.

Texture – loam, clay loam, or sandy clay loam.

Jarosite and iron concentrations are not always present in each soil profile.

2Cseg horizon:

Color – hue of 2.5Y or 5Y, value of 2.5 to 7, and chroma of 1 or 2.

Texture – loam, sandy loam, or fine sand.

**COMPETING SERIES:** None.

**GEOGRAPHIC SETTING:**

Landscape: Coastal Plain sub-estuaries

Landform: Submerged wave-cut platforms, saddles, and shoals

Parent Material: Coarse-loamy estuarine deposits over glauconitic fluviomarine deposits (paleosols)

Slope: 0 to 3 percent

Mean Annual Air Temperature: 52 to 59 degrees F. (11 to 15 degrees C.)

Mean Annual Water Temperature: 52 to 58 degrees F. (11 to 14 degrees C.)

Bathymetry: 0 to 300 centimeters below mean sea level

Water Regime: Tidal, 0 to 27 centimeter tidal range (0 to 1 foot)

**GEOGRAPHICALLY ASSOCIATED SOILS:**

Contees Wharf soils—are fine-silty and do not have contact with pre-Holocene materials within 100 centimeters of the soil surface.

Dutchman Point soils—are sandy throughout and do not have contact with pre-Holocene materials within 100 centimeters of the soil surface.

Fox Creek soils—have thick organic soil horizons.

Sand Point soils—are sandy, have sulfidic materials within 100 cm of the soil surface and are on wave-built terraces and platforms.

Sellman soils—are fine textured also do not have contact with pre-Holocene materials within 100 centimeters of the soil surface.

#### **DRAINAGE AND SATURATED HYDRAULIC CONDUCTIVITY:**

Drainage Class: Subaqueous drainage

Saturated Hydraulic Conductivity: Moderately high to high

Soil Moisture Regime: Peraquic

Soil is permanently submerged with salt or brackish water with a range of 7 to 15 ppt

#### **USE AND VEGETATION:**

Major Uses: Most areas of this soil are used for recreational fishing, swimming, and boating. Commercial uses include shell fishing and aquaculture.

Dominant Vegetation: Benthic fauna such as clams, blue crabs, and oysters are associated with this soil. Eelgrass (*Zostera marina*), sea lettuce (*Ulva* sp.), and horned pondweed (*Zannichellia palustris*) may occur on these soils.

**DISTRIBUTION AND EXTENT:** Western shore sub-estuaries of Chesapeake Bay (Maryland). MLRA 149A. This series is of small extent.

**SOIL SURVEY REGIONAL OFFICE (SSRO) RESPONSIBLE:** Raleigh, North Carolina.

**SERIES ESTABLISHED:** Anne Arundel County, Maryland, 2018.

**REMARKS:** This subaqueous series is named for the Rhode River sub-estuary of Chesapeake Bay and were areas formerly included with water.

Diagnostic horizons and other diagnostic soil characteristics recognized in this pedon are:

Ochric epipedon—the zone from 0 to 24 centimeters (Ase1 and Ase2 horizons)

Peraquic feature—the zone from 0 to 180 centimeters is permanently saturated

Lithologic Discontinuity—pre-Holocene contact (Tertiary aged marine deposits of the Aquia and Nanjemoy formations), the zone from 24 to 180 centimeters (2Bseg, 2Bjg, 2Btj, and 2Cseg horizons)

Argillic Horizon—the zone from 76 to 123 centimeters (2Btj horizon) featured developed before permanent submergence

**ADDITIONAL DATA:**

NASIS Data Map Unit ID: 800960

NASIS OSD Site and Pedon ID: 2015MD003026



Support pedons used to develop this series include S2015MD003066 and S2015MD003061 (sampled by the University of Maryland).

---

National Cooperative Soil Survey

U.S.A.

LOCATION DUTCHMAN POINT MD

Proposed Series

BMW

10/2017

## DUTCHMAN POINT SERIES

MLRA(s): 149A

Soil Survey Regional Office (SSRO) Responsible: Raleigh, North Carolina

Depth Class: Very deep

Drainage Class: Subaqueous (permanently submersed / continuously inundated)

Saturated Hydraulic Conductivity: Moderately high to high and low to very low in the lithologic discontinuity

Parent Material: Sandy estuarine deposits over fine-silty glauconitic fluviomarine deposits

Slope: 0 to 2 percent

Mean Annual Air Temperature: 57 degrees F. (14 degrees C)

Mean Annual Water Temperature: 57 degrees F. (14 degrees C)

**TAXONOMIC CLASS:** Glauconitic, mesic Fluventic Psammowassents

**TYPICAL PEDON:** Dutchman Point sand on a west facing submerged wave-built terrace with less than 1 percent slope under 0.9 m of estuarine water. (Colors are for moist soil unless otherwise stated).

**Ase** -- 0 to 7 cm; dark gray (5Y 4/1) sand; single grain; nonfluid; slightly alkaline (pH 7.7), slightly acid (pH 6.4) after 16 weeks; no color reaction with 3% hydrogen peroxide, very slightly effervescent with 30% hydrogen peroxide; clear boundary.

**Cse1** -- 7 to 31 cm; very dark gray (5Y 3/1) sand; single grain; nonfluid; moderately alkaline (pH 8.2), slightly acid (pH 6.2) after 16 weeks; no color reaction with 3% hydrogen peroxide, very slightly effervescent with 30% hydrogen peroxide; krotovina present; clear boundary.

**Cse2** -- 31 to 45 cm; greenish black (10Y 2.5/1) coarse sand; single grain; nonfluid; strongly alkaline (pH 8.5), neutral (pH 6.7) after 16 weeks; color reaction with 3% hydrogen peroxide, very slightly effervescent with 30% hydrogen peroxide; krotovina present; clear boundary.

**Cse3** -- 45 to 52 cm; very dark gray (5Y 3/1) coarse sand; 20% mixed gravels; single grain; nonfluid; strongly alkaline (pH 8.6), neutral (pH 6.9) after 16 weeks; no color reaction with 3% hydrogen peroxide, very slightly effervescent with 30% hydrogen peroxide; krotovina present; clear boundary.

**Cse4** -- 52 to 76 cm; very dark gray (5Y 3/1) sand; single grain; nonfluid; moderately alkaline (pH 8.4), neutral (pH 6.7) after 16 weeks; no color reaction with 3%

hydrogen peroxide, very slightly effervescent with 30% hydrogen peroxide; krotovina present; gradual boundary.

**Aseb1** -- 76 to 86 cm; black (N 2.5) sand; single grain; nonfluid; moderately alkaline (pH 8.4), neutral (pH 7.3) after 16 weeks; color reaction with 3% hydrogen peroxide, very slightly effervescent with 30% hydrogen peroxide; trace shell fragments; abrupt boundary.

**C'se1** -- 86 to 102 cm; very dark gray (5Y 3/1) coarse sand; single grain; nonfluid; moderately alkaline (pH 8.2), slightly alkaline (pH 7.6) after 16 weeks; no color reaction with 3% hydrogen peroxide, very slightly effervescent with 30% hydrogen peroxide; abrupt boundary.

**C'se2** -- 102 to 107 cm; very dark gray (5Y 3/1) very gravelly coarse sand; 50% mixed gravels; single grain; nonfluid; strongly alkaline (pH 8.9), neutral (pH 7.3) after 16 weeks; color reaction with 3% hydrogen peroxide, very slightly effervescent with 30% hydrogen peroxide; clear boundary.

**2Aseb2** -- 107 to 132 cm; black (N 2.5) silt loam; black root channels present that stain hands black; trace preserved roots present; massive; moderately fluid; strongly alkaline (pH 8.8), very strongly acid (pH 4.9) after 16 weeks; color reaction with 3% hydrogen peroxide, slightly effervescent with 30% hydrogen peroxide; gradual boundary.

**2Cse** -- 132 to 200 cm; very dark greenish gray (5GY 3/1) silty clay; trace preserved roots, root channels, and shell fragments present; massive; slightly fluid; moderately alkaline (pH 8.3), very strongly acid (pH 4.5) after 16 weeks; no color reaction with 3% hydrogen peroxide, slightly effervescent with 30% hydrogen peroxide.

**TYPE LOCATION:** Anne Arundel County, Maryland; approximately 882 feet northwest of Dutchman Point and approximately 2,200 feet southeast of Sand Point in the Rhode River. USGS Deale topographic quadrangle; latitude 38 degrees, 52 minutes, 13.43 seconds N; 76 degrees, 30 minutes, 44.92 seconds W; WGS 1984.

**RANGE IN CHARACTERISTICS:**

Depth to Bedrock: Greater than 200 centimeters

Depth to Seasonal High Water Table: Permanently submersed

Depth to Lithologic Discontinuity: Greater than 80 centimeters.

Depth to hyper-sulfidic materials: greater than 100 centimeters if present

Depth to hypo-sulfidic materials: 0 to 100 centimeters and generally throughout

Manner of Failure / Fluidity Class: Nonfluid in the upper 100 centimeters and slightly to moderately fluid below 100 centimeters.

Shell Fragments: 0 to 10 percent, by volume, throughout

Soil reaction: Neutral to strongly alkaline; oxidized reaction: neutral to very strongly acid

Salinity: Between 7 to 15 ppt throughout the profile.

Buried A horizons may be present in these soils.

**RANGE OF INDIVIDUAL HORIZONS:**

Ase or Aseg horizon:

Color— hue of 5Y, 10Y, and 5GY, value of 2.5 to 4, and chroma of 1

Texture (fine-earth fraction) - sand

Cse or Cseg horizons:

Color— hue of 5Y, 10Y, 5GY, and Neutral, value of 2.5, 3, and 5, and chroma of 0 and 1

Texture (fine-earth fraction) – coarse sand, sand, loamy sand, and loamy fine sand

Aseb horizon (if present):

Color— hue of Neutral, value of 2.5, and chroma of 0

Texture (fine-earth fraction)—sand

C'se horizon (if present):

Color— hue of 5Y, value of 3, and chroma of 1

Texture (fine-earth fraction): sand and coarse sand

2Aseb horizon (if present):

Color— hue of Neutral and 2.5Y, value of 2.5 and 3, chroma of 1

Texture (fine-earth fraction)—silt loam and sandy loam

2Cse or 2Cseg horizon:

Color— hue of Neutral, 10Y, and 5GY, value of 2.5 and 3, chroma of 1

Texture—sandy loam, sandy clay loam, silty clay, and clay loam

**COMPETING SERIES:** None.

**GEOGRAPHIC SETTING:**

Landscape: Northern Coastal Plain estuaries

Landform: Submerged wave-built terraces, wave-cut platforms, shoals, and estuarine tidal creek platforms

Parent Material: Sandy estuarine deposits over fine-silty glauconitic fluviomarine deposits

Slope: 0 to 2 percent

Mean Annual Air Temperature: 57 degrees F. (14 degrees C)

Mean Annual Water Temperature: 57 degrees F. (14 degrees C)

Bathymetry: 0 to 2.5 meters below mean sea level

Water Regime: Tidal, 0 to 1 foot (0 to 0.3 meters) tidal range

Water Salinity Range: 7 to 15 ppt

**GEOGRAPHICALLY ASSOCIATED SOILS:**

Rhode River soils (proposed) - These soils have a coarse-loamy particle size class and have a lithologic discontinuity contact with buried pre-Holocene upland soil materials.

Sand Point soils (proposed) - These soils are not sandy throughout the upper 100 centimeters and contain sulfidic materials within 10 centimeters of the soil surface.

#### **DRAINAGE AND SATURATED HYDRAULIC CONDUCTIVITY:**

Drainage Class: Subaqueous and peraquic soil moisture regime

Saturated Hydraulic Conductivity: Moderately high to high and low to very low in the lithologic discontinuity

Soil is permanently submerged / continuously inundated with brackish water. These soils have potential to have sulfidic materials within the soil profile putting these soils at risk for potential acid sulfate soil formation if they are dredged and exposed to the air.

#### **USE AND VEGETATION:**

Major Uses: Areas of this soil are used for recreational fishing, swimming, boating, and dock and marina construction. Commercial uses include shell fishing and aquaculture. Benthic fauna such as clams, blue crabs, and oysters are associated with this soil. Eelgrass (*Zostera marina*), sea lettuce (*Ulva* sp.), and horned pondweed (*Zannichellia palustris*) may occur on these soils.

#### **DISTRIBUTION AND EXTENT:**



Nothern Atlantic Coastal Plain estuaries of the western portion of Chesapeake Bay.

MLRA 149A. This series is of small extent.

**MLRA SOIL SURVEY REGIONAL OFFICE (MO) RESPONSIBLE:** Raleigh,  
North Carolina.

**SERIES ESTABLISHED:** Anne Arundel County, Maryland, 2018.

**REMARKS:** This subaqueous series is named for Dutchman Point, located at the  
mouth of the Rhode River subestuary of Chesapeake Bay.

Diagnostic horizons and features recognized in this pedon include:

Ochric epipedon— 0 to 7 centimeters

Peraquic conditions— 0 to 200 centimeters (permanently saturated)

Lithologic Discontinuity— 107 to 200 centimeters

**ADDITIONAL DATA:**

NASIS user site and Pedon ID: S2015MD003028

---

National Cooperative Soil Survey

U.S.A.

LOCATION SAND POINT MD

Tentative Series

BMW/DCS/RBT

6/2018

## **SAND POINT SERIES**

MLRA(s): 149A

Soil Survey Regional Office (SSRO) Responsible: Raleigh, North Carolina

Depth Class: Very deep

Drainage Class: Subaqueous (permanently submersed / continuously inundated)

Saturated Hydraulic Conductivity: Very high to moderately high in the substratum

Parent Material: sandy estuarine deposits over glauconitic coarse-loamy fluviomarine deposits

Slope: 0 to 25 percent

Mean Annual Air Temperature: 57 degrees F. (14 degrees C)

Mean Annual Water Temperature: 57 degrees F. (14 degrees C)

**TAXONOMIC CLASS:** Sandy, glauconitic, mesic Sulfic Fluviassents

**TYPICAL PEDON:** Sand Point fine sand on a southeast facing, 1 percent slope on a submerged wave-built terrace under 1.5 m of estuarine water. (Colors are for moist soil).

**Ase** -- 0 to 5 cm; greenish black (10Y 2.5/1) fine sand; dark olive brown (2.5Y 3/4) surface film; single grain; nonfluid; slightly alkaline (pH 7.8), moderately acid (pH 5.9) after 16 weeks; color reaction with 3% hydrogen peroxide, slightly effervescent with 30% hydrogen peroxide; abrupt boundary.

**Cseg1** -- 5 to 25 cm; very dark greenish gray (10Y 3/1) fine sand; single grain; nonfluid; 2 percent shell fragments; moderately alkaline (pH 8.0), moderately acid (pH 5.8) after 16 weeks; no reaction with 3% hydrogen peroxide, very slightly effervescent with 30% hydrogen peroxide; gradual boundary.

**Cseg2** -- 25 to 61 cm; dark greenish gray (10Y 4/1) fine sand; single grain; nonfluid; 2 percent shell fragments; slight hydrogen sulfide odor; moderately alkaline (pH 8.0), moderately acid (pH 6.0) after 16 weeks; no reaction with 3% hydrogen peroxide, very slightly effervescent with 30% hydrogen peroxide; gradual boundary.

**Cseg3** -- 61 to 88 cm; dark greenish gray (10Y 4/1) loamy fine sand; massive; nonfluid; 1 percent shell fragments; slight hydrogen sulfide odor; moderately alkaline (pH 8.0), extremely acid (pH 4.0) after 16 weeks; no reaction with 3% hydrogen peroxide, very slightly effervescent with 30% hydrogen peroxide; gradual boundary.

**2Cseg1** -- 88 to 135 cm; very dark greenish gray (10Y 3/1) loam; massive; moderately fluid; 1 percent shell fragments; slightly alkaline (pH 7.5), very strongly

acid (pH 4.7) after 16 weeks; no reaction with 3% hydrogen peroxide, very slightly effervescent with 30% hydrogen peroxide; clear boundary.

**2Cseg2** -- 135 to 200 cm; very dark greenish gray (10Y 3/1) loam; massive; moderately fluid; moderately alkaline (pH 8.0), extremely acid (pH 3.7) after 16 weeks; no reaction with 3% hydrogen peroxide, very slightly effervescent with 30% hydrogen peroxide.

**TYPE LOCATION:** Anne Arundel County, Maryland; Rhode River; approximately 795 feet southeast of the end of Cadle Creek Road and 890 feet northwest of the road intersections of Cliff Drive and Cherrystone Drive in the Beverly Beach community in the Rhode River. USGS 7.5 minute South River quadrangle; latitude 38 degrees, 52 minutes, 48.94 seconds N and longitude 76 degrees, 30 minutes, 54.60 seconds W, WGS 1984; Major Land Resource Area 149A.

**RANGE IN CHARACTERISTICS:**

Depth to Bedrock: Greater than 200 centimeters

Depth to Seasonal High Water Table: Permanently submersed

Depth to Lithologic Discontinuity: 64 to 100 centimeters

Depth to hyper-sulfidic materials: 50 to 100 centimeters

Depth to hypo-sulfidic materials: 0 to 100 centimeters

Manner of Failure / Fluidity Class: Nonfluid to slightly fluid in the sands and moderately fluid in the lithologic discontinuity

Shell Fragments: 0 to 10 percent, by volume, throughout

Soil reaction: Strongly acid to moderately alkaline; oxidized reaction: Extremely acid to moderately acid

Salinity: Between 7 to 15 ppt throughout the profile.

**RANGE OF INDIVIDUAL HORIZONS:**

Ase horizon:

Color—hue of 10Y, 5Y or 5GY value of 2 to 4, and chroma of 1

Texture—fine sand, sand, loamy sand

Cseg or Cse horizon:

Color—hue of 10Y, N, 2.5Y or 5GY value of 2.5 to 6, chroma of 1 or 2

Texture—fine sand, loamy fine sand, sand, or coarse sand

2Cseg horizon:

Color—hue of 10Y, N, 5GY or 2.5Y, value of 2.5 to 5, chroma of 1

Texture—loam, sandy loam, sandy clay loam, or silty clay loam

**COMPETING SERIES:** None.

**GEOGRAPHIC SETTING:**

Landscape: Coastal Plain sub-estuaries

Landform: Submerged wave-built terraces, shoals, and estuarine tidal creek platforms

Parent Material: Sandy estuarine deposits over glauconitic fluviomarine deposits (paleosols)

Slope: 0 to 25 percent

Mean Annual Air Temperature: 52 to 59 degrees F. (11 to 15 degrees C.)

Mean Annual Water Temperature: 52 to 58 degrees F. (11 to 14 degrees C.)

Bathymetry: 0 to 300 centimeters below mean sea level

Water Regime: Tidal, 0 to 27 centimeter tidal range (0 to 1 foot)

#### **GEOGRAPHICALLY ASSOCIATED SOILS:**

Contees Wharf soils—are fine-silty and do not have contact with pre-Holocene materials within 100 centimeters of the soil surface.

Dutchman Point soils—are sandy throughout and do not have a contact with pre-Holocene materials within 100 centimeters of the soil surface.

Rhode River soils—are coarse-loamy, are on wave-cut platforms, and do not have sulfidic materials within 100 centimeters of the soil surface.

Sellman soils--are fine textured and are moderately to very fluid throughout the upper 100 centimeters

#### **DRAINAGE AND SATURATED HYDRAULIC CONDUCTIVITY:**

Drainage Class: Subaqueous drainage

Saturated Hydraulic Conductivity: Very high to moderately high in the substratum

Soil Moisture Regime: Peraquic

Soil is permanently submerged with salt or brackish water with a range of 7 to 15 ppt

**USE AND VEGETATION:**

Major Uses: Most areas of this soil are used for recreational fishing, swimming, and boating. Commercial uses include shell fishing and aquaculture.

Dominant Vegetation: Benthic fauna such as clams, blue crabs, and oysters are associated with this soil. Eelgrass (*Zostera marina*), sea lettuce (*Ulva* sp.), and horned pondweed (*Zannichellia palustris*) may occur on these soils

**DISTRIBUTION AND EXTENT:** Western shore sub-estuaries of Chesapeake Bay (Maryland). MLRA 149A. This series is of small extent.

**SOIL SURVEY REGIONAL OFFICE (SSRO) RESPONSIBLE:** Raleigh, North Carolina.

**SERIES ESTABLISHED:** Anne Arundel County, Maryland, 2018.

**REMARKS:** This subaqueous series is named for Sand Point, a feature within the Rhode River sub-estuary of Chesapeake Bay and were areas formerly included with water.

Diagnostic horizons and other diagnostic soil characteristics recognized in this pedon are:

Ochric epipedon—the zone from 0 to 5 centimeters (Ase horizon)

Peraquic feature—the zone from 0 to 200 centimeters is permanently saturated

Lithologic Discontinuity—pre-Holocene contact (Tertiary aged marine deposits of the Aquia and Nanjemoy formations), the zone from 88 to 200 centimeters (2Cseg1 and 2Cseg2 horizons).

**ADDITIONAL DATA:**

NASIS Data Mapunit ID: 800964

NASIS OSD Site and Pedon ID: S2015MD003039

---

National Cooperative Soil Survey

U.S.A.



LOCATION CONTEES WHARF MD

Tentative Series

BMW/DCS/RBT

06/2018

## CONTEES WHARF SERIES

MLRA(s): 149A

Soil Survey Regional Office (SSRO) Responsible: Raleigh, North Carolina

Depth Class: Very deep

Drainage Class: Subaqueous (permanently submersed / continuously inundated)

Saturated Hydraulic Conductivity: Low to moderately low

Parent Material: Fine-silty, glauconitic estuarine deposits

Slope: 0 to 3 percent

Mean Annual Air Temperature: 57 degrees F. (14 degrees C)

Mean Annual Water Temperature: 57 degrees F. (14 degrees C)

**TAXONOMIC CLASS:** Fine-silty, mixed, nonacid, mesic Sulfic Hydrowassents

**TYPICAL PEDON:** Contees Wharf silty clay loam on a south flowing estuarine tidal creek channel with less than 1 percent slope under 2.0 m of estuarine water.

(Colors are for moist soil unless otherwise stated).

**Ase** -- 0 to 79 cm; greenish black (10Y 2.5/1) silty clay loam; massive; very fluid; 2

percent shell fragments; slightly alkaline (pH 7.8), very strongly acid (pH 5.0) after 16 weeks; color reaction with 3% hydrogen peroxide, strongly effervescent with 30% hydrogen peroxide; gradual boundary.

**Cse1** -- 79 to 126 cm; very dark greenish gray (10Y 3/1) silty clay; massive; moderately fluid; trace shell fragments; strongly alkaline (pH 8.5), moderately acid (pH 5.6) after 16 weeks; no color reaction with 3% hydrogen peroxide, strongly effervescent with 30% hydrogen peroxide; gradual boundary.

**Cse2** -- 126 to 214 cm; very dark greenish gray (10Y 3/1) silty clay; massive; moderately fluid; trace shell fragments; strongly alkaline (pH 8.5), extremely acid (pH 4.0) after 16 weeks; no color reaction with 3% hydrogen peroxide, strongly effervescent with 30% hydrogen peroxide; diffuse boundary.

**Cse3** -- 214 to 268 cm; very dark greenish gray (5GY 3/1) silty clay; massive; moderately fluid; trace shell fragments; moderately alkaline (pH 8.4), extremely acid (pH 3.9) after 16 weeks; no reaction with 3% hydrogen peroxide, strongly effervescent with 30% hydrogen peroxide.

**TYPE LOCATION:** Anne Arundel County, Maryland; Sellman Creek in Rhode River, approximately 1,200 feet north of Flat Island and approximately 1,200 feet northwest of Camp Letts. USGS South River topographic quadrangle; latitude 38 degrees, 53 minutes, 27.85 seconds N. and longitude 76 degrees, 31 minutes, 59.48

seconds W., WGS 1984; Major Land Resource Area 149A.

**RANGE IN CHARACTERISTICS:**

Depth to bedrock: Greater than 200 centimeters

Depth to seasonal high water table: Permanently submersed

Depth to hyper-sulfidic materials (incubated pH  $\leq$  4.0): Greater than 100 centimeters

Depth to hypo-sulfidic materials: 0 to 50 centimeters

Manner of Failure / Fluidity Class: moderately to very fluid throughout

Shell Fragments: 0 to 10 percent, by volume, throughout

Soil reaction: Neutral to strongly alkaline; oxidized reaction: moderately acid to very strongly acid and extremely acid below 100 centimeters

Salinity range is 7 to 15 (ppt).

**RANGE OF INDIVIDUAL HORIZONS:**

Ase horizon:

Color – hue 10Y, value of 2.5, and chroma of 1

Texture – silty clay loam, silt loam, or loam

Consistence – very fluid to moderately fluid

Cse horizon:

Color – hue of 10Y or 5GY, value of 3, and chroma of 1

Texture – silty clay, silty clay loam, silt loam or loam

Consistence – very fluid to moderately fluid

**COMPETING SERIES:** None.

**GEOGRAPHIC SETTING:**

Landscape: Northern Coastal Plain estuaries

Landform: Estuarine channels, estuarine tidal creek channels, and mainland coves

Parent Material: Fine-silty, glauconitic estuarine deposits

Slope: 0 to 3 percent

Mean Annual Air Temperature: 50 to 59 degrees F. (10 to 15 degrees C.)

Mean Annual Water Temperature: 52 to 58 degrees F. (11 to 14 degrees C.)

Water Depth Range: 0 to 14.8 feet (0 to 4.5 meters)

Water Regime: Tidal, 0 to 1 foot (0 to 0.3 meters) tidal range

Water Salinity Range: 7 to 15 ppt

**GEOGRAPHICALLY ASSOCIATED SOILS:**

Muddy Creek soils (proposed)—occur on similar landforms but have buried organic horizons between 100 and 200 centimeters

Rhode River soils—occur on wave-cut platforms, are coarse-loamy throughout and have a pre-Holocene contact within 100 cm of the soil surface

Sellman soils (proposed)—occur on similar landforms but have a fine particle size family class.

Tingles soils—contain sulfidic materials within 50 cm of the soil surface and occur in MLRA 153D in coastal bays and lagoons with higher salinity ranges.

**DRAINAGE AND SATURATED HYDRAULIC CONDUCTIVITY:**

Drainage Class: Subaqueous drainage

Saturated Hydraulic Conductivity: Low to moderately low

Soil Moisture Regime: Peraquic

Soil is permanently submerged / continuously inundated with brackish water. The presence of hypo-sulfidic materials within 50 cm of the soil surface puts these soils at risk for potential acid sulfate soil formation if they are dredged and exposed to the air.

**USE AND VEGETATION:**

Major Uses: Areas of this soil are used for recreational fishing, swimming, and boating. Commercial uses include shell fishing and aquaculture.

Dominant Vegetation: Benthic fauna such as clams, blue crabs, and oysters are associated with this soil. Eelgrass (*Zostera marina*), sea lettuce (*Ulva* sp.), and horned pondweed (*Zannichellia palustris*) may occur on these soils.

**DISTRIBUTION AND EXTENT:** Northern Atlantic Coastal Plain sub-estuaries of the western portion of Chesapeake Bay. This series is of small extent.

**SOIL SURVEY REGIONAL OFFICE (SSRO) RESPONSIBLE:** Raleigh, North Carolina.

**SERIES ESTABLISHED:** Anne Arundel County, Maryland, 2018.

**REMARKS:** This subaqueous series is named for Contees Wharf in the Rhode River sub-estuary of Chesapeake Bay and areas of mapping were formerly included with water.

Diagnostic horizons and other diagnostic soil characteristics recognized in this pedon are:

Ochric epipedon—the zone from 0 to 79 centimeters (Ase horizon)

Peraquic feature—the zone from 0 to 268 centimeters is permanently saturated

Hypo-sulfidic materials—the zone from 0 to 268 centimeters

Hyper-sulfidic materials—the zone from 126 to 268 centimeters

**ADDITIONAL DATA:**

Data Map Unit ID: 800954

NASIS user site and pedon ID: S2015MD003063.

---

National Cooperative Soil Survey

U.S.A.

LOCATION SELLMAN MD

Proposed Series

BMW

6/2018

## **SELLMAN SERIES**

MLRA(s): 149A

Soil Survey Regional Office (SSRO) Responsible: Raleigh, North Carolina

Depth Class: Very deep

Drainage Class: Subaqueous (permanently submersed / continuously inundated)

Saturated Hydraulic Conductivity: Low to moderately low

Parent Material: Fine, glauconitic estuarine deposits

Slope: 0 to 3 percent

Mean Annual Air Temperature: 57 degrees F. (14 degrees C.)

Mean Annual Water Temperature: 57 degrees F. (14 degrees C)

**TAXONOMIC CLASS:** Fine, mixed, nonacid, mesic Sulfic Hydrowassents

**TYPICAL PEDON:** Sellman silty clay loam on a south flowing estuarine channel with less than 1 percent slope under 3.3 m of estuarine water. (Colors are for moist soil unless otherwise stated).

**Ase** -- 0 to 22 cm; greenish black (10Y 2.5/1) silty clay loam; massive; very fluid; 4

percent shell fragments; moderately alkaline (pH 8.0), moderately acid (pH 5.8) after 16 weeks; color reaction with 3% hydrogen peroxide, violently effervescent with 30% hydrogen peroxide, gradual boundary.

**Cse1** -- 22 to 64 cm; greenish black (10Y 2.5/1) silty clay; massive; moderately fluid; strongly alkaline (pH 8.5), neutral (pH 6.6) after 16 weeks; color reaction with 3% hydrogen peroxide, violently effervescent with 30% hydrogen peroxide, gradual boundary.

**Cse2** -- 64 to 88 cm; very dark greenish gray (10Y 3/1) silty clay; massive; very fluid; strongly alkaline (pH 8.5), slightly acid (pH 6.5) after 16 weeks; color reaction with 3% hydrogen peroxide, violently effervescent with 30% hydrogen peroxide, gradual boundary.

**Cse3** -- 88 to 129 cm; very dark greenish gray (10Y 3/1) silty clay; massive; very fluid; moderately alkaline (pH 8.3), extremely acid (pH 4.3) after 16 weeks; no reaction with 3% hydrogen peroxide, strongly effervescent with 30% hydrogen peroxide, gradual boundary.

**Cse4** -- 129 to 163 cm; very dark greenish gray (5GY 3/1) silty clay; massive; very fluid; moderately alkaline (pH 8.3), moderately acid (pH 5.6) after 16 weeks; no reaction with 3% hydrogen peroxide, strongly effervescent with 30% hydrogen peroxide.



**TYPE LOCATION:** Anne Arundel County, Maryland; Rhode River, approximately 1,770 feet south of Locust Point and 1,305 feet north of Sand Point. USGS South River topographic quadrangle; latitude 38 degrees, 52 minutes, 33.83 seconds N. and longitude 76 degrees, 31 minutes, 19.28 seconds W., WGS 1984; Major Land Resource Area 149A.

**RANGE IN CHARACTERISTICS:**

Depth to bedrock: Greater than 200 centimeters.

Depth to seasonal high water table: Permanently submersed

Shell Fragments: 0 to 2 percent, by volume, throughout

Soil reaction: Neutral to strongly alkaline; oxidized reaction: extremely acid to neutral

Depth to hyper-sulfidic materials (incubated  $\text{pH} \leq 4.0$ ): Greater than 100 centimeters

Depth to hypo-sulfidic materials: 0 to 50 centimeters

Manner of Failure / Fluidity Class: moderately to very fluid throughout

Salinity range is 7 to 15 (ppt).

Tidal range is 27 cm.

Water depth is 0 to 450 cm.

Occasionally horizons may qualify as sulfidic materials.

**Range of Individual Horizons:**

Ase horizon:

Color – hue 10Y or 5GY, value of 2.5 or 3, and chroma 0 to 1.

Texture – silty clay loam through loam

Consistence – very fluid

Cse horizon:

Color – hue 10Y or 5GY, value of 2.5 or 3, and chroma of 0 to 1.

Texture – silty clay, silty clay loam, or clay loam

Consistence – moderately fluid to very fluid

**COMPETING SERIES:** None

**GEOGRAPHIC SETTING:**

Landscape: Northern Coastal Plain estuaries

Landform: Estuarine channels, estuarine tidal creek channels, and mainland coves

Parent Material: Fine, glauconitic estuarine deposits

Slope: 0 to 3 percent

Mean Annual Air Temperature: 50 to 57 degrees F. (10 to 14 degrees C.)

Mean Annual Water Temperature: 52 to 58 degrees F. (11 to 14 degrees C.)

Water Depth Range: 0 to 14.8 feet (0 to 4.5 meters)

Water Regime: Tidal, 0 to 1 foot (0 to 0.3 meters) tidal range

Water Salinity Range: 7 to 15 ppt

**GEOGRAPHICALLY ASSOCIATED SOILS:**

Coards soils—contain sulfidic materials within 50 cm of the soil surface and occur in MLRA 153D in coastal bays and lagoons with higher salinity ranges.

Contees Wharf soils (proposed)—occur on similar landforms but have a fine-silty particle size family class.

Rhode River soils (proposed)—occur on wave-cut platforms, saddles and shoals and have pre-Holocene materials within 100 cm of the soil surface.

Sand Point soils (proposed)--have sandy surface horizons and hyper-sulfidic materials within 100 centimeters of the soil surface.

**DRAINAGE AND SATURATED HYDRAULIC CONDUCTIVITY:**

Drainage Class: Subaqueous and peraquic soil moisture regime

Saturated Hydraulic Conductivity: Low to moderately low

Soil is permanently submerged / continuously inundated with brackish water. The presence of hypo-sulfidic materials within 50 cm of the soil surface puts these soils at risk for potential acid sulfate soil formation if they are dredged and exposed to the air.

**USE AND VEGETATION:**

Major Uses: Areas of this soil are used for recreational fishing, swimming, and boating. Commercial uses include shell fishing and aquaculture.

Dominant Vegetation: Benthic fauna such as clams, blue crabs, and oysters are associated with this soil. Eelgrass (*Zostera marina*), sea lettuce (*Ulva* sp.), and horned

pondweed (*Zannichellia palustris*) may occur on these soils.

**DISTRIBUTION AND EXTENT:** Northern Atlantic Coastal Plain estuaries of the western portion of Chesapeake Bay. MLRA 149A. This series is of small extent.

**SOIL SURVEY REGIONAL OFFICE (SSRO) RESPONSIBLE:** Raleigh, North Carolina.

**SERIES ESTABLISHED:** Anne Arundel County, Maryland, 2018.

**REMARKS:** This subaqueous series is named for Sellman Creek, which is a tributary to the Rhode River sub-estuary of Chesapeake Bay. Areas of Sellman soils were formerly included with water.

Diagnostic horizons and other diagnostic soil characteristics recognized in this pedon are:

Ochric epipedon—the zone from 0 to 22 centimeters (Ase horizon)

Peraquic feature—the zone from 0 to 163 centimeters is permanently saturated

Hypo-sulfidic materials—the zone from 0 to 163 centimeters

**ADDITIONAL DATA:**

NASIS Data Map Unit ID: 800963

NASIS user site and pedon ID: S2015MD003067.

---

National Cooperative Soil Survey

U.S.A.

LOCATION FOX CREEK MD

Tentative Series

BMW/DCS/RBT

06/2018

## FOX CREEK SERIES

MLRA(s): 149A

Soil Survey Regional Office (SSRO) Responsible: Raleigh, North Carolina

Depth Class: Very deep

Drainage Class: Subaqueous (permanently submersed / continuously inundated)

Saturated Hydraulic Conductivity: Moderately high to very high

Parent Material: herbaceous organic materials over glauconitic fluviomarine deposits

Slope: 0 to 3 percent

Mean Annual Air Temperature: 57 degrees F. (14 degrees C)

Mean Annual Water Temperature: 57 degrees F. (14 degrees C)

**TAXONOMIC CLASS:** Euic, mesic Sapric Sulfiwassists

**TYPICAL PEDON:** Fox Creek mucky loam on a southwest flowing submerged tidal marsh with less than 1 percent slope under 0.9 m of estuarine water. (Colors are for moist soil unless otherwise stated).

**Ase** -- 0 to 23 cm; black (N 2.5) mucky loam; massive; very fluid; neutral (pH 6.8),

very strongly acid (pH 5.0) after 16 weeks; color reaction with 3% hydrogen peroxide, very slightly effervescent with 30% hydrogen peroxide, gradual boundary.

**Oase1** -- 23 to 56 cm; very dark brown (10YR 2/2) muck; nonfluid; neutral (pH 7.3), ultra acid (pH 3.3) after 16 weeks; 3% unrubbed fibers, 0% rubbed fibers; no reaction with 3% hydrogen peroxide, very slightly effervescent with 30% hydrogen peroxide, gradual boundary.

**Oase2** -- 56 to 94 cm; black (10YR 2/1) muck; slightly fluid; neutral (pH 6.9), ultra acid (pH 2.4) after 16 weeks; 10% unrubbed fibers, 7% rubbed fibers; no reaction with 3% hydrogen peroxide, very slightly effervescent with 30% hydrogen peroxide, gradual boundary.

**A'se** -- 94 to 102 cm; very dark greenish gray (2.5Y 2.5/1) mucky sand; massive; slightly fluid; neutral (pH 6.7), ultra acid (pH 2.3) after 16 weeks; no reaction with 3% hydrogen peroxide, violently effervescent with 30% hydrogen peroxide, clear boundary.

**Cse** -- 102 to 130 cm; very dark grayish green (5GY 3/2) sand; massive; nonfluid; neutral (pH 6.6), ultra acid (pH 3.3) after 16 weeks; no reaction with 3% hydrogen peroxide, slightly effervescent with 30% hydrogen peroxide, gradual boundary.

**2Btseg** -- 130 to 155 cm; dark grayish green (5GY 4/2) sandy clay; massive; moderately fluid; slightly acid (pH 6.5), very strongly acid (pH 4.7) after 16 weeks; no reaction with 3% hydrogen peroxide, strongly effervescent with 30% hydrogen peroxide; 17% dark yellowish brown (10YR 4/4) iron concentrations, gradual boundary.

**2Btse** -- 155 to 194 cm; very dark grayish green (5GY 3/2) sandy clay; massive; nonfluid; slightly acid (pH 6.5), very strongly acid (pH 4.8) after 16 weeks; no reaction with 3% hydrogen peroxide, slightly effervescent with 30% hydrogen peroxide; 3% dark yellowish brown (10YR 4/4) iron concentrations, abrupt boundary.

**2BCse** -- 194 to 209 cm; dark yellowish brown (10YR 3/4) sandy clay loam; massive; nonfluid; slightly acid (pH 6.4), strongly acid (pH 5.2) after 16 weeks; no reaction with 3% hydrogen peroxide, violently effervescent with 30% hydrogen peroxide.

**TYPE LOCATION:** Anne Arundel County, Maryland; easternmost end of Whitmarsh Creek and approximately 1,182 feet north of the intersection of Whitmarsh Cove Court and Carrs Wharf Road and approximately 1,191 feet west of Rt. 214, Central Avenue; latitude 38 degrees, 53 minutes, 48.12 seconds N. longitude 76 degrees, 31 minutes, 1.76 seconds W; WGS 1984; Major Land Resource Area 149A.

**RANGE IN CHARACTERISTICS:**



Depth to Bedrock: Greater than 200 centimeters

Depth to Seasonal High Water Table: Permanently submersed

Depth to Lithologic Discontinuity: Between 100 and 130 centimeters

Depth to hyper-sulfidic materials: less than 50 centimeters

Depth to hypo-sulfidic materials: less than 50 centimeters

Organic soil materials: 40 centimeters or greater and within 40 centimeters of the soil surface.

Manner of Failure / Fluidity Class: Nonfluid to moderately fluid throughout mineral horizons

Shell Fragments: 0 to 2 percent, by volume, throughout

Soil Reaction: Neutral to slightly acid; oxidized reaction: strongly acid to ultra acid

Salinity range is 7 to 15 (ppt).

#### **RANGE OF INDIVIDUAL HORIZONS:**

Ase horizons (if present):

Color— hue of 5Y, 5GY, or Neutral, value of 2.5 or 4, chroma of 0 or 1

Texture (fine earth fraction) — sand or loam (and their mucky equivalents)

Consistence— nonfluid or very fluid

Oase or Oese horizons:

Color— hue of 7.5YR, 10YR, or 5Y, value of 2, 2.5, 3, chroma of 1 or 2

Texture— muck or mucky peat

A'se or 2Ase horizon (if present):

Color— hue of 2.5Y, value of 2.5 or 3, chroma of 1

Texture (fine earth fraction) — sand, loamy sand, or fine sandy loam

Consistence— slightly fluid or moderately fluid

Cseg or 2Cseg horizon:

Color— hue of 5Y or 5GY, value of 3 to 5, chroma of 1 or 2

Texture (fine earth fraction) — sand, loamy sand, sandy loam, or sandy clay loam

Consistence— nonfluid or slightly fluid

2Btseg or 2Btse horizon (if present):

Color— hue of 10Y or 5GY, value of 3 and 4, chroma of 1 or 2

Texture (fine earth fraction) — sandy clay, clay, or silty clay loam

Consistence— nonfluid to moderately fluid

The A, C, and B horizons are not always present in the upper 200 cm.

### **COMPETING SERIES:**

Tumagan soils—found in more saline waters of coastal bays and lagoons within the

Northern Tidewater Area. Does not have buried argillic horizons within 200 cm.

### **GEOGRAPHIC SETTING:**

Landscape: Northern Coastal Plain estuaries

Landform: Permanently submerged tidal marshes and submerged wave-cut platforms

Parent Material: herbaceous organic materials over glauconitic fluviomarine deposits

Slope: 0 to 3 percent

Mean Annual Air Temperature: 50 to 59 degrees F. (10 to 15 degrees C.)

Mean Annual Water Temperature: 52 to 58 degrees F. (11 to 14 degrees C.)

Water Depth Range: 0 to 3.3 feet (0 to 1 meters)

Water Regime: Tidal, 0 to 1 foot (0 to 0.3 meters) tidal range

Water Salinity Range: 7 to 15 ppt

#### **GEOGRAPHICALLY ASSOCIATED SOILS:**

Contees Wharf soils—occur in estuarine tidal stream landforms, have a fine-silty family class, and do not contain organic horizons within the upper 200 cm.

Muddy Creek soils— occur on estuarine tidal stream channels, have a fine-silty family class, and do not have organic horizons 40 centimeters thick within 40 centimeters of the soil surface

Sellman soils— occur on mainland cove and estuarine tidal stream channels, have a fine family class, and do not contain organic horizons within upper 200 cm.

#### **DRAINAGE AND SATURATED HYDRAULIC CONDUCTIVITY:**

Drainage Class: Subaqueous drainage

Saturated Hydraulic Conductivity: Moderately high to very high

Soil Moisture Regime: Peraquic

Soil is permanently submerged / continuously inundated with brackish water. The presence of hyper-sulfidic materials within 50 cm of the soil surface puts these soils at risk for potential acid sulfate soil formation if they are dredged and exposed to the air.

**USE AND VEGETATION:**

Major Uses: Areas of this soil are used for recreational fishing and boating. These are nearshore areas that may be developed as marinas or with private docks.

Dominant Vegetation: Benthic fauna such as clams, blue crabs, and oysters are associated with this soil. Eelgrass (*Zostera marina*), sea lettuce (*Ulva* sp.), and horned pondweed (*Zannichellia palustris*) may occur on these soils.

**DISTRIBUTION AND EXTENT:** Northern Atlantic Coastal Plain sub-estuaries of the western portion of Chesapeake Bay. This series is of small extent.

**SOIL SURVEY REGIONAL OFFICE (SSRO) RESPONSIBLE:** Raleigh, North Carolina.

**SERIES ESTABLISHED:** Anne Arundel County, Maryland, 2018.

**REMARKS:** This subaqueous series is named for Fox Creek, which is a tributary to the Rhode River sub estuary of Chesapeake Bay. Areas of mapping were formerly included with water.

Diagnostic Horizons and other diagnostic soil characteristics recognized in this pedon are:

Ochric Epipedon—the zone from 0 to 102 centimeters (Ase, Oase1, Oase2, A'se horizons)

Peraquic feature—the zone from 0 to 209 centimeters, which is permanently saturated

Sapric soil materials—the zone from 23 to 94 centimeters (Oase1 and Oase2 horizons)

Sulfidic materials—the zone from 23 to 130 centimeters, oxidized pH values less than 4.0 after 16 weeks.

Agrillic horizon—the zone from 130 to 194 centimeters (2Btseg and 2Btse horizons)

Lithologic discontinuity—the zone from 130 to 209 centimeters (2Btseg, 2Btse, and 2BCse horizons)

**ADDITIONAL DATA:**

Data Map Unit ID: 800958

NASIS used site and Pedon ID: S2015MD003071

---

National Cooperative Soil Survey

U.S.A.

LOCATION MUDDY CREEK MD

Tentative Series

BMW/DCS/RBT

06/2018

## MUDDY CREEK SERIES

MLRA(s): 149A

Soil Survey Regional Office (SSRO) Responsible: Raleigh, North Carolina

Depth Class: Very deep

Drainage Class: Subaqueous (permanently submersed / continuously inundated)

Saturated Hydraulic Conductivity: Low to moderately low

Parent Material: Fine-silty estuarine deposits over herbaceous organic material

Slope: 0 to 3 percent

Mean Annual Air Temperature: 57 degrees F. (14 degrees C)

Mean Annual Water Temperature: 57 degrees F. (14 degrees C)

**TAXONOMIC CLASS:** Fine-silty, mixed, nonacid, mesic Sulfic Hydrowassents

**TYPICAL PEDON:** Muddy Creek silt loam on a sheltered, east facing, submerged tidal marsh with less than 1 percent slope under 1.5 m of estuarine water. (Colors are for moist soil).

**Ase** -- 0 to 22 cm; very dark greenish gray (10Y 3/1) silt loam; massive; very fluid; 1

percent organic fragments; slightly alkaline (pH 7.7), very strongly acid (pH 5.0) after 16 weeks; color reaction with 3% hydrogen peroxide, strongly effervescent with 30% hydrogen peroxide, clear boundary.

**Cseg1** -- 22 to 71 cm; very dark greenish gray (10Y 3/1) silty clay loam; massive; very fluid; moderately alkaline (pH 8.0), very strongly acid (pH 5.0) after 16 weeks; color reaction with 3% hydrogen peroxide, strongly effervescent with 30% hydrogen peroxide, gradual boundary.

**Cseg2** – 71 to 116 cm; dark greenish gray (10Y 4/1) silty clay loam; massive; very fluid; moderately alkaline (pH 8.0), ultra acid (pH 3.2) after 16 weeks; color reaction with 3% hydrogen peroxide, strongly effervescent with 30% hydrogen peroxide, abrupt boundary.

**2Oaseb1** – 116 to 162 cm; very dark brown (10YR 2/2) muck; very fluid; very strongly acid (pH 4.5), ultra acid (pH 3.0) after 16 weeks; no reaction with 3% hydrogen peroxide, non-effervescent with 30% hydrogen peroxide; slight hydrogen sulfide odor; 60% unrubbed fibers, 5% rubbed fibers; gradual boundary.

**2Oaseb2** – 162 to 195 cm; very dark brown (10YR 2/2) muck; very fluid; very strongly acid (pH 4.5), ultra acid (pH 3.0) after 16 weeks; no reaction with 3% hydrogen peroxide, non-effervescent with 30% hydrogen peroxide; slight hydrogen sulfide odor; 75% unrubbed fibers, 20% rubbed fibers; gradual boundary.

**3Cseg** – 195 to 200 cm; dark greenish gray (10GY 4/1) sandy clay loam; massive; moderately fluid; very strongly acid (pH 4.5), ultra acid (pH 3.0) after 16 weeks; no color reaction with 3% hydrogen peroxide, slightly effervescent with 30% hydrogen peroxide.

**TYPE LOCATION:** Anne Arundel County, Maryland; Fox Creek in Rhode River, approximately 2,347 feet southwest of Contees Wharf Road where it meets the Rhode River, and approximately 2,777 feet west northwest of Big Island. USGS South River topographic quadrangle; latitude 38 degrees, 53 minutes, 0.24 seconds N. and longitude 76 degrees, 32 minutes, 49.20 seconds W; WGS 1984; Major Land Resource Area 149A.

**RANGE IN CHARACTERISTICS:**

Depth to bedrock: Greater than 200 centimeters

Depth to seasonal high water table: Permanently submersed

Shell Fragments: 0 to 5 percent, by volume, throughout

Soil reaction: Very strongly acid to moderately alkaline; oxidized reaction: very strongly acid to ultra acid

Depth to hyper-sulfidic materials (incubated pH  $\leq$  4.0): Between 50 and 100 centimeters

Depth to hypo-sulfidic materials: 0 to 50 centimeters

Manner of Failure / Fluidity Class: moderately to very fluid throughout



Salinity range is 7 to 15 (ppt).

**RANGE OF INDIVIDUAL HORIZON CHARACTERISTICS:**

Ase horizon:

Color— hue of 10Y, value of 2.5 and 3, chroma of 1

Texture (fine earth fraction) — silt loam and silty clay

Consistence — moderately fluid and very fluid

Cseg horizons:

Color— hue of 10Y, value of 2.5 to 4, chroma of 1

Texture (fine earth fraction) – silty clay loam, silty clay, clay loam

Consistence – moderately fluid and very fluid

2Oaseb horizons:

Color— hue of 10YR to 5YR, value of 2 and 2.5, chroma of 1 and 2

Texture (fine earth fraction) – muck

3Cseg horizons (if present):

Color— hue of 5GY and 10GY, value of 4, chroma of 1

Texture (fine earth fraction) — sandy clay loam and clay loam

Consistence— moderately fluid and non-fluid

**COMPETING SERIES:** None.

**GEOGRAPHIC SETTING:**

Landscape: Northern Coastal Plain estuaries

Landform: Submerged tidal marshes and estuarine tidal stream channels

Parent Material: Fine-silty estuarine deposits over herbaceous organic material

Slope: 0 to 3 percent

Mean Annual Air Temperature: 50 to 59 degrees F. (10 to 15 degrees C.)

Mean Annual Water Temperature: 52 to 58 degrees F. (11 to 14 degrees C.)

Water Depth Range: 0 to 5 feet (0 to 1.5 meters)

Water Regime: Tidal, 0 to 1 foot (0 to 0.3 meters) tidal range

Water Salinity Range: 7 to 15 ppt

**GEOGRAPHICALLY ASSOCIATED SOILS:**

Fox Creek soils – have organic soil materials greater than 40 centimeters thick near the soil surface and occur on submerged tidal marsh landforms.

Contees Wharf soils — occur on similar landforms but do not have buried organic horizons between 100 and 200 centimeters.

**DRAINAGE AND SATURATED HYDRAULIC CONDUCTIVITY:**

Drainage Class: Subaqueous drainage

Saturated Hydraulic Conductivity: Moderately low to high

Soil Moisture Regime: Peraquic

Soil is permanently submerged / continuously inundated with brackish water. The presence of hypo-sulfidic materials within 50 cm of the soil surface puts these soils at risk for potential acid sulfate soil formation if they are dredged and exposed to the air.

**USE AND VEGETATION:**

Major Uses: Areas of this soil are used for recreational fishing and boating.

Commercial uses include shell fishing and aquaculture.

Dominant Vegetation: Benthic fauna such as clams, blue crabs, and oysters are associated with this soil. Eelgrass (*Zostera marina*), sea lettuce (*Ulva* sp.), and horned pondweed (*Zannichellia palustris*) may occur on these soils.

**DISTRIBUTION AND EXTENT:** Northern Atlantic Coastal Plain sub-estuaries of the western portion of Chesapeake Bay. This series is of small extent.

**SOIL SURVEY REGIONAL OFFICE (SSRO) RESPONSIBLE:** Raleigh, North Carolina.

**SERIES ESTABLISHED:** Anne Arundel County, Maryland, 2018.

**REMARKS:** This subaqueous series is named for Muddy Creek, which is a tributary to the Rhode River sub-estuary of Chesapeake Bay. Areas of mapping were formerly included with water.

Diagnostic Horizons and other diagnostic soil characteristics recognized in this pedon are:

Ochric Epipedon—the zone from 0 to 22 centimeters (Ase horizon)

Peraquic feature—the zone from 0 to 200 centimeters which is permanently saturated

Sapric soil materials—the zone from 116 to 195 centimeters (2Oaseb1 and 2Oaseb2 horizons)

Hypo-sulfidic materials—the zone from 0 to 200 centimeters

Hyper-sulfidic materials—the zone from 71 to 200 centimeters, oxidized pH values less than 4.0 after 16 weeks.

Lithologic discontinuity—the zones from 116 to 195 (2Oaseb horizons) and 195 to 200 centimeters (3Cseg horizon)

**ADDITIONAL DATA:**

Data Map Unit ID: 800959

NASIS used site and pedon ID: 2015MD003047

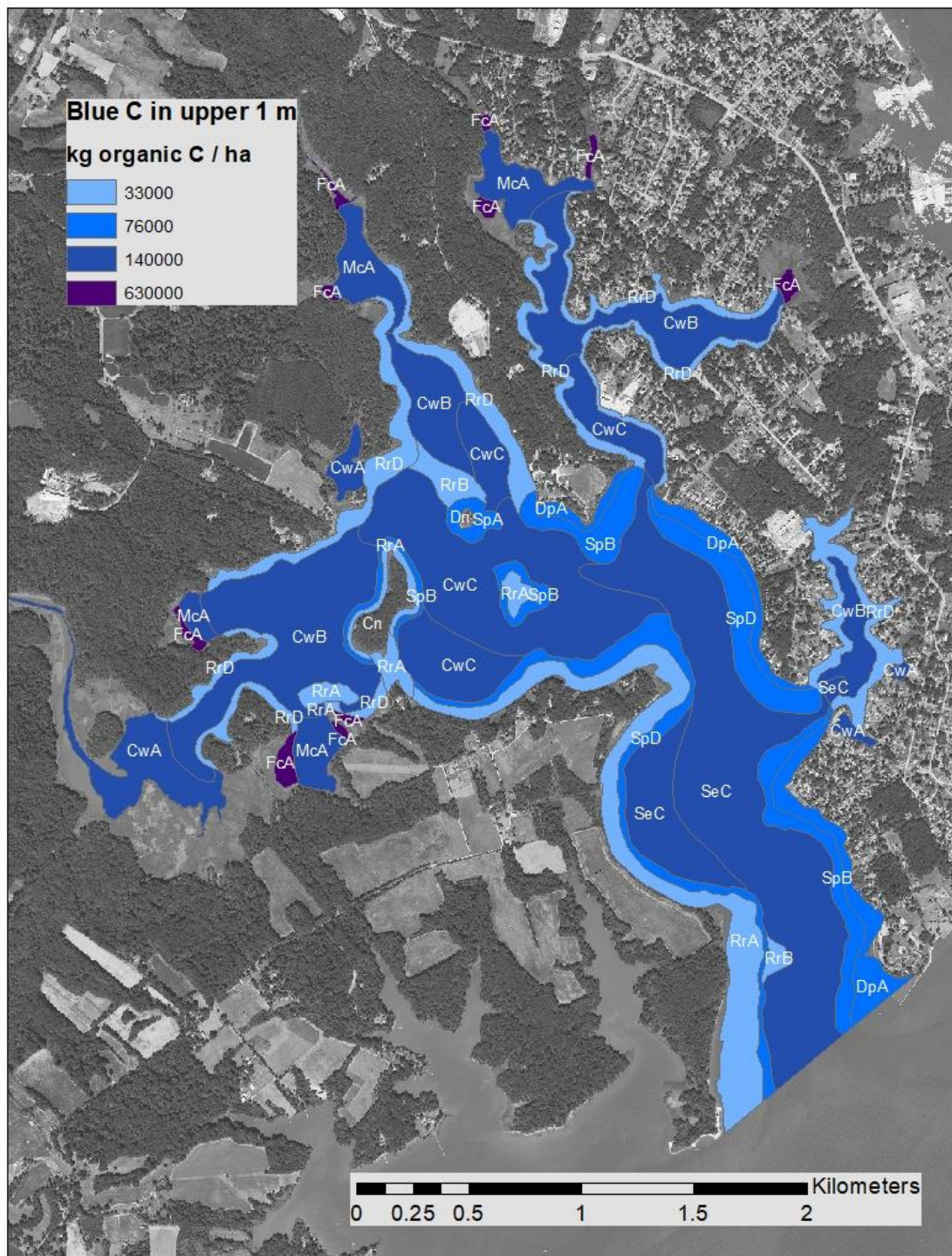
---

National Cooperative Soil Survey

U.S.A.

Appendix L: Blue carbon map

By using the soil organic C contents (Table 3-1) and bulk densities (Appendix E) reported for different materials types, C contents of those soil materials can be calculated on a per volume basis. Applying these values to the profile descriptions in Appendix K (to a depth of 1 m), and applying these values across the soil map in Figure 5-3, the C map below was generated. Though C concentrations are highest in Fox Creek map units, the extent of Contees Wharf and Sellman map units result in them being larger C reservoirs.



## Bibliography

- Ahern, C.R., McElnea, A.E., Sullivan, L.A., 2004. Acid Sulfate Soils Laboratory Methods Guidelines. Queensland Department of Natural Resources, Mines and Energy, Indooroopilly, Queensland, Australia.
- Anne Arundel County Department of Public Works, LimnoTech, Versar, 2016. West and Rhode Watersheds Assessment Comprehensive Summary Report. Anne Arundel County Department of Public Works, Bureau of Engineering, Watershed protection and Restoration Program.
- Antisari, L.V., De Nobili, M., Ferronato, C., Natale, M., Pellegrini, E., Vianello, G., 2016. Hydromorphic to subaqueous soils transitions in the central Grado lagoon (Northern Adriatic Sea, Italy). *Estuarine Coastal and Shelf Science* 173, 39-48.
- Anton, A., Hendriks, I.E., Marbà, N., Krause-Jensen, D., Garcias-Bonet, N., Duarte, C.M., 2018. Iron Deficiency in Seagrasses and Macroalgae in the Red Sea Is Unrelated to Latitude and Physiological Performance. *Frontiers in Marine Science* 5, 74.
- Arkesteyn, G.J.M.W., 1980. Pyrite oxidation in acid sulphate soils: Role of microorganisms. *Plant and Soil* 54(1), 119-134.
- Arnold, R.W., 2005. The paradigm of pedology: How we learn what we learn. *Eurasian Soil Science* 38(12), 1286-1289.
- Austin, N.C., 1972. Descriptive Report to Accompany H-9280. US National Ocean Service.
- Austin, N.C., Baker, R.L., 1972. H-09280, Maryland, Chesapeake Bay, Rhode River. National Ocean Survey, scale 1:5,000.
- Bache, A.D., 1856. General Instructions in Regard to the Hydrographic Work of the Coast Survey. United States Coast Survey.

- Bakken, J., Stolt, M.H., 2018. Mapping Freshwater Subaqueous Soil Resources: Examples from Southern New England. *Soil Science Society of America Journal* 82(2), 403-412.
- Balduff, D.M., 2007. Pedogenesis, inventory, and utilization of subaqueous soils in Chincoteague Bay, Maryland. Dissertation Thesis, University of Maryland, College Park.
- Barrera-Bassols, N., Zinck, J.A., van Ranst, E., 2009. Participatory soil survey: experience in working with a Mesoamerican indigenous community. *Soil Use and Management* 25(1), 43-56.
- Bell, R., Green, M., Hume, T., Gorman, R., 2000. What regulates sedimentation in estuaries? *Water & Atmosphere* 8(4), 13-16.
- Bernal, B., Megonigal, J.P., Mozdzer, T.J., 2017. An invasive wetland grass primes deep soil carbon pools. *Global Change Biology* 23(5), 2104-2116.
- Berner, R.A., 1970. Sedimentary pyrite formation. *American Journal of Science* 268(1), 1-23.
- Berner, R.A., 1985. Sulfate reduction, organic-matter decomposition and pyrite formation. *Philosophical Transactions of the Royal Society A: Mathematical Physical and Engineering Sciences* 315(1531), 25-38.
- Bicki, T.J., Tandarich, J.P., 1989. The Roots of Pedology: A Response to “Pedology, a Field or Laboratory Science” by R. B. Daniels. *Soil Science Society of America Journal* 53, 1920-1921.
- Biddle, J.F., 1953. Bladensburg: An Early Trade Center. *Records of the Columbia Historical Society, Washington, D.C.* 53/56, 309-326.
- Bolan, N.S., Hedley, M.J., White, R.E., 1991. Processes of soil acidification during nitrogen cycling with emphasis on legume based pastures. *Plant and Soil* 134(1), 53-63.
- Boman, A., Åström, M., Frojdo, S., 2008. Sulfur dynamics in boreal acid sulfate soils rich in metastable iron sulfide-The role of artificial drainage. *Chemical Geology* 255(1-2), 68-77.



- Bond, J.A., 1933. Descriptive Report to Accompany Hydrographic Sheet No. 3, Chesapeake Bay, West and Rhode Rivers - Western Shore Chesapeake Bay, Franklin Point to Saunders Point. US Coast and Geodetic Survey.
- Bond, J.A., Sturmer, D.E., 1933a. H-05432, Vicinity of West and Rhode Rivers, Chesapeake Bay, Maryland. US Coast and Geodetic Survey, scale 1:10,000.
- Bond, J.A., Sturmer, D.E., 1933b. Hydrographic Survey No. 5432, Vicinity of West and Rhode Rivers, Chesapeake Bay, Maryland. U.S. Coast and Geodetic Survey, scale 1:10,000.
- Bradley, M.P., Stolt, M.H., 2002. Evaluating methods to create a base map for a subaqueous soil inventory. *Soil Science* 167(3), 222-228.
- Breitenbucher, R., Wisotzky, F., Eisenberg, V., Siebert, B., 2009. Concrete Attack in Iron Disulphidic Soils. *Beton- Und Stahlbetonbau* 104(5), 289-301.
- Brevik, E.C., Cerdà, A., Mataix-Solera, J., Pereg, L., Quinton, J.N., Six, J., Van Oost, K., 2015. The interdisciplinary nature of <i>SOIL</i>. *SOIL* 1(1), 117-129.
- Center for Naval Analysis, 2007. National security and the threat of climate change. The CNA Corporation.
- Certini, G., Corti, G., Ugolini, F.C., De Siena, C., 2002. Rock weathering promoted by embryonic soils in surface cavities. *European Journal of Soil Science* 53(1), 139-146.
- Charlton, R., 2008. Fundamentals of fluvial geomorphology. Routledge, London ; New York.
- Childs, C., 2004. Interpolating Surfaces in ArcGIS Spatial Analyst. *ArcUser* July-September, 32-35.
- Claff, S.R., Sullivan, L.A., Burton, E.D., Bush, R.T., 2010. A sequential extraction procedure for acid sulfate soils: Partitioning of iron. *Geoderma* 155(3-4), 224-230.

- Cleaves, E.T., Edwards Jr., J., Glaser, J.D., 1968. Geologic map of Maryland. Maryland Geological Survey, Baltimore, Maryland, scale 1:250,000.
- Cline, J.D., 1969. Spectrophotometric Determination of Hydrogen Sulfide in Natural Waters. *Limnology and Oceanography* 14(3), 454-458.
- Cohen, K.M., Finney, S.C., Gibbard, P.L., Fan, J.X., 2013. The ICS International Chronostratigraphic Chart. *Episodes* 36(3), 199-204.
- Cory, R.L., Dresler, P.V., 1980. Water quality in Rhode River at Smithsonian Institution Pier near Annapolis, Maryland, January 1976 through December 1978. 79-109.
- Creeper, N., Fitzpatrick, R., Shand, P., 2012. A simplified incubation method using chip-trays as incubation vessels to identify sulphidic materials in acid sulphate soils. *Soil Use and Management* 28(3), 401-408.
- Creeper, N., Fitzpatrick, R., Shand, P., 2013. The occurrence of inland acid sulphate soils in the floodplain wetlands of the MurrayDarling Basin, Australia, identified using a simplified incubation method. *Soil Use and Management* 29(1), 130-139.
- Creeper, N.L., Shand, P., Hicks, W., Fitzpatrick, R.W., 2015. Porewater Geochemistry of Inland Acid Sulfate Soils with Sulfuric Horizons Following Postdrought Reflooding with Freshwater. *Journal of Environmental Quality* 44(3), 989-1000.
- Dahl, E., 1956. Ecological Salinity Boundaries in Poikilohaline Waters. *Oikos* 7(1), 1-21.
- Dalrymple, R.W., Choi, K., 2003. Sediment transport by tides. In: G.V. Middleton, M.J. Church, M. Coniglio, L.A. Hardie, F.J. Longstaffe (Eds.), *Encyclopedia of Sediments and Sedimentary Rocks*. Springer Netherlands, Dordrecht, pp. 606-609.
- Daniels, R.B., 1988. Pedology, a Field or Laboratory Science? *Soil Science Society of America Journal* 52, 1518-1519.

- Darmody, R.G., Fanning, D.S., Drummond, W.J., Foss, J.E., 1977. Determination of total sulfur in tidal marsh soils by X-ray spectroscopy. *Soil Science Society of America Journal* 41(4), 761-765.
- DeBow, J.D.B., 1853. *The Seventh Census of the United States: 1850*. Robert Armstrong, Public Printer.
- Demas, G.P., 1998. Subaqueous soils of Sinepuxent Bay, Maryland. Thesis (Ph D ) Thesis, University of Maryland, College Park, Md., 1998., xiii, 266 leaves pp.
- Demas, G.P., Rabenhorst, M.C., 1999. Subaqueous soils: Pedogenesis in a submersed environment. *Soil Science Society of America Journal* 63(5), 1250-1257.
- Demas, G.P., Rabenhorst, M.C., 2001. Factors of subaqueous soil formation: a system of quantitative pedology for submersed environments. *Geoderma* 102(3-4), 189-204.
- Demas, G.P., Rabenhorst, M.C., Stevenson, J.C., 1996. Subaqueous soils: A pedological approach to the study of shallow-water habitats. *Estuaries* 19(2A), 229-237.
- Demas, S.Y., Hall, A.M., Fanning, D.S., Rabenhorst, M.C., Dzantor, E.K., 2004. Acid sulfate soils in dredged materials from tidal Pocomoke Sound in Somerset County, MD, USA. *Australian Journal of Soil Research* 42(5-6), 537-545.
- Dent, D.L., Pons, L.J., 1995. A world perspective on acid sulfate soils. *Geoderma* 67(3-4), 263-276.
- Dittmann, S., Rolston, A., Bengner, S., Kupriyanova, E., 2009. Habitat requirements, distribution and colonisation of the tubeworm *Ficopomatus enigmaticus* in the Lower Lakes and Coorong.
- Downer, J.A., 2015. *Hallowed Ground, Sacred Place: The Slave Cemetery at George Washington's Mount Vernon and the Cultural Landscapes of the Enslaved*, George Washington University, 129 pp.

- Duarte, C.M., Merino, M., Gallegos, M., 1995. Evidence of iron-deficiency in seagrasses growing above carbonate sediments. *Limnology and Oceanography* 40(6), 1153-1158.
- Duball, C., Vaughan, K., Berkowitz, J.F., Rabenhorst, M.C., VanZomerem, C.M., 2020. Iron monosulfide identification: Field techniques to provide evidence of reducing conditions in soils. *Soil Science Society of America Journal* n/a(n/a).
- Duball, C.E., Amador, J.A., Salisbury, L.E., Stolt, M.H., 2019. Impacts of Oyster Aquaculture on Subaqueous Soils and Infauna. *Journal of Environmental Quality* 48, 1890-1898.
- Eaton, J.W., Bateman, D., Hauberg, S., Wehbring, R., 2018. GNU Octave version 4.4.1 manual: a high-level interactive language for numerical computations URL <https://www.gnu.org/software/octave/doc/v4.4.1/>.
- Edwards, R.L., Merrill, A.S., 1977. A reconstruction of the continental shelf areas of Eastern North America for the times 9,500 B.P. and 12,500 B.P. *Archaeology of Eastern North America* 5, 1-43.
- Erich, E., Drohan, P.J., 2012. Genesis of freshwater subaqueous soils following flooding of a subaerial landscape. *Geoderma* 179, 53-62.
- Erich, E., Drohan, P.J., Ellis, L.R., Collins, M.E., Payne, M., Surabian, D., 2010. Subaqueous soils: their genesis and importance in ecosystem management. *Soil Use and Management* 26(3), 245-252.
- Fairbanks, R.G., 1989. A 17,000-year glacio-eustatic sea-level record - Influence of glacial melting rates on the Younger Dryas event and deep-ocean circulation. *Nature* 342(6250), 637-642.
- Fanning, D.S., Burch, S.N., 2000. Coastal acid sulfate soils. In: R.I. Barnhisel, R.G. Darmody, W.L. Daniels (Eds.), *Reclamation of drastically disturbed lands*. American Society of Agronomy, Madison, WI, pp. 921-937.
- Fanning, D.S., Fanning, M.C.B., 1989. *Soil: morphology, genesis, and classification*. Wiley, New York.

- Fanning, D.S., Rabenhorst, M.C., 1990. Micromorphology of acid sulfate soils in Baltimore Harbor dredged materials. In: L.A. Douglas (Ed.), *Micromorphology: A basic and applied science*. Elsevier, Amsterdam, pp. 279-288.
- Fanning, D.S., Rabenhorst, M.C., 2008. Acid sulfate soil issues raised by the 2006 World Congress of Soil Science acid sulfate soils tour in the U.S. Mid-Atlantic region. In: C. Lin, S. Huang, Y. Li (Eds.), *Proceedings of the Joint Conference of the 6th International Acid Sulfate Soil Conference and the Acid Rock Drainage Symposium*. Guangdong Science and Technology Press, Guangzhou, China, pp. 48-52.
- Fanning, D.S., Rabenhorst, M.C., Balduff, D.M., Wagner, D.P., Orr, R.S., Zurheide, P.K., 2010. An acid sulfate perspective on landscape/seascape soil mineralogy in the US Mid-Atlantic region. *Geoderma* 154(3-4), 457-464.
- Fanning, D.S., Rabenhorst, M.C., Bigham, J.M., 1993. Colors of acid sulfate soils. In: J.M. Bigham, E.J. Ciolkosz (Eds.), *Soil Color*. SSSA Special Publications. SSSA, Madison, WI, pp. 91-108.
- Fanning, D.S., Rabenhorst, M.C., Burch, S.N., Islam, K.R., Tangren, S.A., 2002. Sulfides and Sulfates, *Soil Mineralogy with Environmental Applications*. SSSA Book Series. Soil Science Society of America, Madison, WI, pp. 229-260.
- Fanning, D.S., Rabenhorst, M.C., Fitzpatrick, R.W., 2017. Historical developments in the understanding of acid sulfate soils. *Geoderma* 308, 191-206.
- Fanning, D.S., Rabenhorst, M.C., May, L., Wagner, D.P., 1989. Oxidation state of iron in glauconite from oxidized vs reduced zones of soil-geological columns. *Clays and Clay Minerals* 37(1), 59-64.
- Feistel, R., Wielgosz, R., Bell, S.A., Camoes, M.F., Cooper, J.R., Dexter, P., Dickson, A.G., Fisticaro, P., Harvey, A.H., Heinonen, M., Hellmuth, O., Kretzschmar, H.J., Lovell-Smith, J.W., McDougall, T.J., Pawlowicz, R., Ridout, P., Seitz, S., Spitzer, P., Stoica, D., Wolf, H., 2016. Metrological challenges for measurements of key climatological observables: oceanic salinity and pH, and atmospheric humidity. Part 1: overview. *Metrologia* 53(1), R1-R11.

- Ferreira, C.M.H., Lopez-Rayó, S., Lucena, J.J., Soares, E.V., Soares, H., 2019. Evaluation of the Efficacy of Two New Biotechnological-Based Freeze-Dried Fertilizers for Sustainable Fe Deficiency Correction of Soybean Plants Grown in Calcareous Soils. *Frontiers in Plant Science* 10.
- Ferronato, C., Falsone, G., Natale, M., Zannoni, D., Buscaroli, A., Vianello, G., Antisari, L.V., 2016. Chemical and pedological features of subaqueous and hydromorphic soils along a hydrosequence within a coastal system (San Vitale Park, Northern Italy). *Geoderma* 265, 141-151.
- FGDC-MCSDS 2012. Coastal and Marine Ecological Classification Standard. (Federal Geographic Data Committee - Marine and Coastal Spatial Data Subcommittee).
- Flick, R.E., Knuuti, K., Gill, S.K., 2013. Matching Mean Sea Level Rise Projections to Local Elevation Datums. *Journal of Waterway Port Coastal and Ocean Engineering* 139(2), 142-146.
- Flower, G.L., 1903. H-02667, Chesapeake Bay West Shore, Franklin Pt. to Thomas Pt. US Coast and Geodetic Survey, scale 1:20,000.
- Folk, R.L., 1954. The distinction between grain size and mineral composition in sedimentary rock nomenclature. *Journal of Geology* 62(4), 344-359.
- Food and Agriculture Organization of the United Nations, 2015. World reference base for soil resources 2014. World soil resources reports,. Food and Agriculture Organization of the United Nations, Rome.
- Fossing, H., Jørgensen, B., 1998. Measurement of Bacterial Sulfate Reduction in Sediments: Evaluation of a Single-Step Chromium Reduction Method. *Biogeochemistry* 8(3), 205-222.
- Gaye, W., 2007. Jefferson authorizes the Survey of the Coast. Monticello, newsletter of the Thomas Jefferson Foundation, Inc. 18(2), 1-2.
- Gibson, W.M., Gill, S.K., 1999. Tides and water level requirements for NOS hydrographic surveys. *International Hydrographic Review* 76(2), 141-150.

- Gill, S.K., Hubbard, J.R., Scherer, W.D., Mts, 1998. Updating the National Tidal Datum Epoch for the United States. Ocean Community Conference'98: Celebrating 1998 International Year of the Ocean, Proceedings Vols 1 and 2.
- Glaser, J.D., 1971. Geology and Mineral Resources of Southern Maryland. Maryland Geological Survey, Report of Investigations No. 15.
- Glaser, J.D., 2002. Geologic Map of the South River Quadrangle, and Portions of the Annapolis Quadrangle, Anne Arundel County, Maryland. Maryland Geological Survey, Scale 1:24,000, Baltimore, MD.
- Gottschalk, L.C., 1945. Effects of Soil Erosion on Navigation in Upper Chesapeake Bay. *Geographical Review* 35(2), 219-238.
- Haering, K.C., Rabenhorst, M.C., Fanning, D.S., 1989. Sulfur speciation in some Chesapeake Bay tidal marsh soils. *Soil Science Society of America Journal* 53(2), 500-505.
- Hansen, J., Sato, M., Russell, G., Kharecha, P., 2013. Climate sensitivity, sea level and atmospheric carbon dioxide. *Philosophical Transactions of the Royal Society A: Mathematical, Physical and Engineering Sciences* 371(2001), 20120294.
- Harris, C., 2001. Archival fieldwork. *Geographical Review* 91(1-2), 328-334.
- Hartemink, A.E., 2016. The Definition of Soil Since the Early 1800s. In: D.L. Sparks (Ed.), *Advances in Agronomy*, Vol 137. *Advances in Agronomy*, pp. 73-126.
- Hartley, R.D., Buchan, H., 1979. High-performance liquid-chromatography of phenolic-acids and aldehydes derived from plants or from the decomposition of organic-matter in soil. *Journal of Chromatography* 180(1), 139-143.
- Hem, J.D., 1962. Restraints on dissolved ferrous iron imposed by bicarbonate redox potential, and pH, Chemistry of iron in natural water, Geological Survey water-supply paper 1459. US Government Printing Office, Washington, pp. 33-56.

- Hem, J.D., Cropper, W.H., 1962. Survey of ferrous-ferric chemical equilibria and redox potentials, Chemistry of iron in natural water, Geological Survey water-supply paper 1459. US Government Printing Office, Washington, pp. 1-32.
- Hess, K.W., 2003. Tidal Datums and Tide Coordination. *Journal of Coastal Research*, 33-43.
- Hicks, D.M., Terry, M.H., 1997. Determining Sand Volumes and Bathymetric Change on an Ebb-Tidal Delta. *Journal of Coastal Research* 13(2), 407-416.
- Hillel, D., 2004. Introduction to environmental soil physics. Elsevier Academic Press, Amsterdam ; Boston.
- Hilton, J., Lishman, J.P., Millington, A., 1986. A comparison of some rapid techniques for the measurement of density in soft sediments. *Sedimentology* 33(5), 777-781.
- Holmer, M., Ahrensberg, N., Jorgensen, N.P., 2003. Impacts of mussel dredging on sediment phosphorus dynamics in a eutrophic Danish fjord. *Chemistry and Ecology* 19(5), 343-361.
- Hudson, B.D., 1990. Concepts of Soil Mapping and Interpretation. *Soil Horizons* 31.
- Hudson, B.D., 1992. The Soil Survey as a Paradigm-Based Science. *Soil Science Society of America Journal* 56(3), 836-841.
- Hydrographic Surveys Division, 1878. General Instructions in Regard to the Inshore Hydrographic Work of the Coast Survey. Government Printing Office, Washington.
- Indorante, S.J., McLeese, R.L., Hammer, R.D., Thompson, B.W., Alexander, D.L., 1996. Positioning soil survey for the 21st century. *Journal of Soil and Water Conservation* 51(1), 21-28.
- IPCC, 2014. Summary for Policymakers. In: C.B. Field, V.R. Barros, D.J. Dokken, K.J. Mach, M.D. Mastrandrea, T.E. Bilir, M. Chatterjee, K.L. Ebi, Y.O. Estrada, R.C. Genova, B. Girma, E.S. Kissel, A.N. Levy, S. MacCracken, P.R. Mastrandrea, L.L. White (Eds.), *Climate Change 2014: Impacts, Adaptation, and Vulnerability. Part A: Global and Sectoral Aspects. Contribution of*



Working Group II to the Fifth Assessment Report of the Intergovernmental Panel on Climate Change. Cambridge University Press, Cambridge, United Kingdom, and New York, NY, USA, pp. 1-32.

- Isbell, R.F., National Committee on Soil and Terrain, 2016. The Australian soil classification. Australian soil and land survey handbooks series. Second edition. ed. CSIRO Publishing, Australia.
- Jackson, N.L., Nordstrom, K.F., Smith, D.R., 2002. Geomorphic - Biotic Interactions on Beach Foreshores In Estuaries. *Journal of Coastal Research*, 414-424.
- Jefferson, T., 1805. State of the Union Address.
- Jenny, H., 1941. Factors of soil formation; a system of quantitative pedology. McGraw-Hill publications in the agricultural sciences L J Cole, consulting ed. 1st ed. McGraw-Hill, New York, London,.
- Jensen, H.S., Thamdrup, B., 1993. Iron-bound phosphorus in marine sediments as measured by bicarbonate-dithionite extraction. *Hydrobiologia* 253, 47-59.
- Jespersen, J.L., Osher, L.J., 2007. Carbon storage in the soils of a mesotidal Gulf of Maine estuary. *Soil Science Society of America Journal* 71(2), 372-379.
- Jiang, L.Q., Carter, B.R., Feely, R.A., Lauvset, S.K., Olsen, A., 2019. Surface ocean pH and buffer capacity: past, present and future. *Scientific Reports* 9.
- Jordan, T.E., Correll, D.L., Whigham, D.F., 1983. Nutrient flux in the Rhode River - tidal exchange of nutrients by brackish marshes. *Estuarine Coastal and Shelf Science* 17(6), 651-667.
- Jordan, T.E., Pierce, J.W., Correll, D.L., 1986. Flux of particulate matter in the tidal marshes and subtidal shallows of the Rhode River estuary. *Estuaries* 9(4B), 310-319.
- Kolodziej, K., Lejano, R., Sassa, C., Maharjan, S., Ghaemghami, J., Plant, T., 2004. Mapping the industrial archeology of Boston. *URISA Journal* 16, 5-13.

- Koropchak, S.C., Daniels, W.L., Wick, A., Whittecar, G.R., Haus, N., 2016. Beneficial Use of Dredge Materials for Soil Reconstruction and Development of Dredge Screening Protocols. *Journal of Environmental Quality* 45(1), 62-73.
- Kraft, J.C., 1971. Sedimentary Facies Patterns and Geologic History of a Holocene Marine Transgression. *GSA Bulletin* 82(8), 2131-2158.
- Kraft, J.C., Belknap, D.F., 1986. Holocene Epoch coastal geomorphologies based on local relative sea-level data and stratigraphic interpretations of paralic sediments. *Journal of Coastal Research*, 53-59.
- Kristensen, E., Flindt, M.R., Thorsen, S.W., Holmer, M., Valdemarsen, T., 2016. Gyldensteen Strand - fra agerland til kystlagune. *Vand og Jord* 1, 36.
- Kristensen, E., Kristiansen, K.D., Jensen, M.H., 2003. Temporal behavior of manganese and iron in a sandy coastal sediment exposed to water column anoxia. *Estuaries* 26(3), 690-699.
- Kristensen, E., Penha-Lopes, G., Delefosse, M., Valdemarsen, T., Quintana, C.O., Banta, G.T., 2012. What is bioturbation? The need for a precise definition for fauna in aquatic sciences. *Marine Ecology Progress Series* 446, 285-302.
- Kristensen, E., Rabenhorst, M.C., 2015. Do marine rooted plants grow in sediment or soil? A critical appraisal on definitions, methodology and communication. *Earth-Science Reviews* 145(0), 1-8.
- Kristiansen, K.D., Kristensen, E., Jensen, M.H., 2002. The influence of water column hypoxia on the behaviour of manganese and iron in sandy coastal marine sediment. *Estuarine Coastal and Shelf Science* 55(4), 645-654.
- Lanesky, D.E., Logan, B.W., Brown, R.G., Hine, A.C., 1979. New Approach to Portable Vibracoring Underwater and on Land. *Journal of Sedimentary Petrology* 49(2), 654-657.
- Lee, S.P., Woolsey, M.B., Caldwell, W.M., Jones, C.A., Rolando, H., Fox, G.V., Smith, A.N., Aulick, R., Mahon, C., 1846. H-00188 Sounding Sheet, Chesapeake Bay, Thomas Point to Tilghman Island. U.S. Coast Survey, scale 1:20,000.

- Leventhal, J., Taylor, C., 1990. Comparison of methods to determine degree of pyritization. *Geochimica et Cosmochimica Acta* 54(9), 2621-2625.
- Lewis, E.L., 1980. The Practical Salinity Scale 1978 and its antecedents. *IEEE Journal of Oceanic Engineering* 5(1), 3-8.
- Lisitzin, A.P., Kennett, J.P., 1996. Oceanic sedimentation : lithology and geochemistry. American Geophysical Union, Washington, D.C.
- Loeppert, R.H., 1986. Reactions of iron and carbonates in calcareous soils. *Journal of Plant Nutrition* 9(3-7), 195-214.
- Long, D.D., Maxon, E.T., Kirk, N.M., Lewis, H.G., Hayes, F.A., Hall, E.C., Geib, H.V., Crabb, G.A., 1919. Soil survey of Oconee, Morgan, Greene, and Putnam Counties, Georgia. US Department of Agriculture.
- Lovley, D.R., 1993. Dissimilatory metal reduction. *Annual Review of Microbiology* 47, 263-290.
- Lovley, D.R., Phillips, E.J., 1987. Rapid assay for microbially reducible ferric iron in aquatic sediments. *Appl Environ Microbiol* 53(7), 1536-1540.
- Lowdermilk, W.C., 1948. Conquest of the land through seven thousand years. In: S.C.S. US Department of Agriculture, MP-32 (Ed.).
- Lu, H.Y., Qi, W.C., Liu, J., Bai, Y.C., Tang, B.P., Shao, H.B., 2018. Paddy periphyton: Potential roles for salt and nutrient management in degraded mudflats from coastal reclamation. *Land Degradation & Development* 29(9), 2932-2941.
- MacCrehan, W., Shea, D., 1995. Temporal Relationship of Thiols to Inorganic Sulfur Compounds in Anoxic Chesapeake Bay Sediment Porewater, *Geochemical Transformations of Sedimentary Sulfur*. ACS Symposium Series. American Chemical Society, pp. 294-310.
- MacGillis, A., Desmon, S., Gibson, G., 2003. Wrath of Isabel, *The Baltimore Sun*. September 19th.

- Mack, S.C., Berkowitz, J.F., Rabenhorst, M.C., 2018. Improving Hydric Soil Identification in Areas Containing Problematic Red Parent Materials: a Nationwide Collaborative Mapping Approach. *Wetlands*.
- Martin-Anton, M., Negro, V., del Campo, J.M., Lopez-Gutierrez, J.S., Esteban, M.D., 2016. Review of coastal Land Reclamation situation in the World. *Journal of Coastal Research*, 667-671.
- Massey, A.C., Paul, M.A., Gehrels, W.R., Charman, D.J., 2006. Autocompaction in Holocene coastal back-barrier sediments from south Devon, southwest England, UK. *Marine Geology* 226(3), 225-241.
- McVey, S., Schoeneberger, P.J., Turenne, J., Payne, M., Wysocki, D.A., Stolt, M., 2012. Subaqueous soils (SAS) description. In: P.J. Schoeneberger, D.A. Wysocki, E.C. Benham, Soil Survey Staff (Eds.), *Field Book for Describing and Sampling Soils*, Version 3.0. Natural Resources Conservation Service, National Soil Survey Center, Lincoln, NE.
- Megonigal, J.P., Rabenhorst, M., 2013. Reduction-Oxidation Potential and Oxygen. In: R.D. DeLaune, K.R. Reddy, C.J. Richardson, J.P. Megonigal (Eds.), *Methods in Biogeochemistry of Wetlands*. Soil Science Society of America Book Series, pp. 71-85.
- Millar, C.M., Aduomih, A.A.O., Still, B., Stolt, M.H., 2015. Estuarine Subaqueous Soil Organic Carbon Accounting: Sequestration and Storage. *Soil Science Society of America Journal* 79(2), 389-397.
- Miller, J.T., Drosdoff, M., Fuller, G.L., 1941. Soil survey of Hall County, Georgia. Series 1937. US Department of Agriculture.
- Muhrizal, S., Shamshuddin, J., Husni, M.H.A., Fauziah, I., 2003. Alleviation of aluminum toxicity in an acid sulfate soil in Malaysia using organic materials. *Communications in Soil Science and Plant Analysis* 34(19-20), 2993-3012.
- Neuendorf, K.K.E., Mehl, J.P., Jackson, J.A., American Geosciences Institute., 2011. *Glossary of geology*. 5th ed. American Geosciences Institute, Alexandria, Va.

- Neumann, D., 2012. Improving Access to NOAA's Hydrographic Survey Metadata Office of Coast Survey Continues to Add and Verify Survey Data to National Ocean Service Database. *Sea Technology* 53(3), 31-33.
- Nichols, M.M., Johnson, G.H., Peebles, P.C., 1991. Modern sediments and facies model for a microtidal Coastal-Plain estuary, the James estuary, Virginia. *Journal of Sedimentary Petrology* 61(6), 883-899.
- Nilsson, B., Gravesen, P., 2018. Karst Geology and Regional Hydrogeology in Denmark. In: W.B. White, J.S. Herman, E.K. Herman, M. Rutigliano (Eds.), *Karst Groundwater Contamination and Public Health: Beyond Case Studies*. *Advances in Karst Science*, pp. 289-298.
- Nunn, A.D., Clifton-Dey, D., Cowx, I.G., 2016. Managed realignment for habitat compensation: Use of a new intertidal habitat by fishes. *Ecological Engineering* 87, 71-79.
- OCM Partners, 2020. CoNED Topobathymetric Model for New Jersey and Delaware, 1880 to 2014. US Geological Survey.
- Orndorff, Z.W., 2001. Evaluation of sulfidic materials in Virginia highway corridors. PhD Dissertation Thesis, Virginia Polytechnic Institute and State University, 175 pp.
- Orndorff, Z.W., Daniels, W.L., Fanning, D.S., 2008. Reclamation of acid sulfate soils using lime-stabilized biosolids. *Journal of Environmental Quality* 37(4), 1447-1455.
- Otto, J.S., 1983. The Decline of Forest Farming in Southern Appalachia. *Journal of Forest History* 27(1), 18-27.
- Overland, J.E., Preisendorfer, R.W., 1982. A Significance Test for Principal Components Applied to a Cyclone Climatology. *Monthly Weather Review* 110(1), 1-4.
- Parker, B.B., 2003. The Difficulties in Measuring a Consistently Defined Shoreline—The Problem of Vertical Referencing. *Journal of Coastal Research*, 44-56.

- Pastore, M.A., Megonigal, J.P., Langley, J.A., 2017. Elevated CO<sub>2</sub> and nitrogen addition accelerate net carbon gain in a brackish marsh. *Biogeochemistry* 133(1), 73-87.
- Pedersen, A.B., 2010. The fight over Danish nature : Explaining policy network change and policy change. *Public Administration* 88(2), 346-363.
- Pethick, J., 2002. Estuarine and tidal wetland restoration in the United Kingdom: Policy versus practice. *Restoration Ecology* 10(3), 431-437.
- Piper, C.S., 1942. Organic matter, Soil and plant analysis. Interscience Publishers, Inc, New York, pp. 213.
- Pocknee, S., Sumner, M.E., 1997. Cation and nitrogen contents of organic matter determine its soil liming potential. *Soil Science Society of America Journal* 61(1), 86-92.
- Pomeroy, R.D., Cruse, H., 1969. Hydrogen sulfide odor threshold. *Journal of the American Water Works Association* 61(12), 667.
- Pons, L.J., 1973. Outline of the genesis, characteristics, classification and improvement of acid sulphate soils. In: H. Dost (Ed.), *Proceedings of the 1st International Symposium on Acid Sulphate Soils, 13-20 August 1972*. ILRI Publication 18, Wageningen, pp. 3-27.
- Pons, L.J., Vandermo, W.H., 1973. Soil genesis under dewatering regimes during 1000 years of polder development. *Soil Science* 116(3), 228-235.
- Prouhet, J.N., 2011. Quantifying Rates of Autocompaction in the Pearl River Marsh, Louisiana. Master's Thesis Thesis, University of Southern Mississippi.
- Rabenhorst, M., Post, J., 2018. Manganese Oxides for Environmental Assessment. *Soil Science Society of America Journal* 82(2), 509-518.
- Rabenhorst, M.C., 1990. Micromorphology of induced iron sulfide formation in a Chesapeake Bay (USA) tidal marsh In: L.A. Douglas (Ed.), *Soil Micromorphology: A Basic and Applied Science* Elsevier Science Publishers, Amsterdam, pp. 303-310.

- Rabenhorst, M.C., Balduff, D.M., Orr, R., Zurheide, P.K., Wessel, B.M., 2016a. IRIS (Indicator of Reduction In Soils) Technology for Assessing Sulfidization Processes in Subaqueous Soils. Poster, 8th International Acid Sulfate Soils Conference, College Park, MD.
- Rabenhorst, M.C., Burch, S.N., 2006. Synthetic iron oxides as an indicator of reduction in soils (IRIS). *Soil Science Society of America Journal* 70(4), 1227-1236.
- Rabenhorst, M.C., Fanning, D.S., 1989. Pyrite and trace-metals in glauconitic parent materials of Maryland. *Soil Science Society of America Journal* 53(6), 1791-1797.
- Rabenhorst, M.C., Megonigal, J.P., Keller, J., 2010. Synthetic Iron Oxides for Documenting Sulfide in Marsh Pore Water. *Soil Science Society of America Journal* 74, 1383-1388.
- Rabenhorst, M.C., Stolt, M., Lindbo, D., 2016b. Is there a case to be made for a "wet" soil order? Poster, Resilience Emerging from Scarcity and Abundance: Annual Meeting of the Soil Science Society of America, Phoenix, AZ.
- Rabenhorst, M.C., Stolt, M.H., 2012. Subaqueous Soils: Pedogenesis, Mapping, and Applications. *Hydropedology: Synergistic Integration of Soil Science and Hydrology*, 173-204.
- Rabenhorst, M.C., Valladares, T.M., 2005. Estimating the depth to sulfide-bearing materials in Upper Cretaceous sediments in landforms of the Maryland coastal plain. *Geoderma* 126(1–2), 101-116.
- Raiswell, R., Buckley, F., Berner, R.A., Anderson, T.F., 1988. Degree of pyritization of iron as a paleoenvironmental indicator of bottom-water oxygenation. *Journal of Sedimentary Petrology* 58(5), 812-819.
- Rickard, D., 1997. Kinetics of pyrite formation by the H<sub>2</sub>S oxidation of iron (II) monosulfide in aqueous solutions between 25 and 125 degrees C: The rate equation. *Geochimica Et Cosmochimica Acta* 61(1), 115-134.

- Rickard, D., Luther, G.W., 1997. Kinetics of pyrite formation by the H<sub>2</sub>S oxidation of iron(II) monosulfide in aqueous solutions between 25 and 125 degrees C: The mechanism. *Geochimica Et Cosmochimica Acta* 61(1), 135-147.
- Rickard, D., Morse, J.W., 2005. Acid volatile sulfide (AVS). *Marine Chemistry* 97(3-4), 141-197.
- Rickard, D.T., 2012. Sulfidic sediments and sedimentary rocks. *Developments in sedimentology*, Elsevier, Amsterdam.
- Robinson, W.O., 1927. The determination of organic matter in soils by means of hydrogen peroxide. *Journal of Agricultural Research* 34(4), 339-356.
- Rodriguez, M.B., Godeas, A., Lavado, R.S., 2008. Soil Acidity Changes in Bulk Soil and Maize Rhizosphere in Response to Nitrogen Fertilization. *Communications in Soil Science and Plant Analysis* 39(17-18), 2597-2607.
- Rogovska, N.P., Blackmer, A.M., Mallarino, A.P., 2007. Relationships between Soybean Yield, Soil pH, and Soil Carbonate Concentration. *Soil Science Society of America Journal* 71(4), 1251-1256.
- Roos, M., Åström, M., 2006. Gulf of Bothnia receives high concentrations of potentially toxic metals from acid sulphate soils. *Boreal Environment Research* 11(5), 383-388.
- Rude, G.T., 1928. Instructions for Tide Observations, Special Publication No. 139. US Government Printing Office, US Coast and Geodetic Survey.
- Sallenger, A.H., Goldsmith, V., Sutton, C.H., 1975. Bathymetric chart comparisons: A manual of methodology, error criteria and applications. Special report in applied marine science and ocean engineering (SRAMSOE), 66. Virginia Institute of Marine Science, Gloucester Point, Virginia.
- Salmon, S.U., Rate, A.W., Rengel, Z., Appleyard, S., Prommer, H., Hinz, C., 2014. Reactive transport controls on sandy acid sulfate soils and impacts on shallow groundwater quality. *Water Resources Research* 50(6), 4924-4952.
- Schertz, D.L., 1983. The basis for soil loss tolerances. *Journal of Soil and Water Conservation* 38(1), 10.



- Schlacher, T.A., Connolly, R.M., 2014. Effects of acid treatment on carbon and nitrogen stable isotope ratios in ecological samples: a review and synthesis. *Methods in Ecology and Evolution* 5(6), 541-550.
- Schoeneberger, P.J., Wysocki, D.A., Benham, E.C., Soil Survey Staff, 2012. Field book for describing and sampling soils, Version 3.0. Natural Resources Conservation Service, National Soil Survey Center, Lincoln, NE.
- Schwartz, M.L., 1982. The Encyclopedia of beaches and coastal environments. *Encyclopedia of earth sciences*. Hutchinson Ross Pub. Co., Stroudsburg, Pa.
- Scott, M., 2005. Mapping and characterization of the Marlboro Clay formation, University of Maryland College Park.
- Seasholes, N.S., 1988. On the use of historical maps. In: M.C. Beaudry (Ed.), *Documentary archaeology in the new world*. Cambridge University Press, Cambridge, pp. 92-118.
- Shalowitz, A.L., 1964. Shore and Sea Boundaries. *Shore and Sea Boundaries*, 2. U.S. Government Printing Office, U.S. Dept. of Commerce, Coast and Geodetic Survey, pub. 10-1.
- Shapiro, J., 1966. On the measurement of ferrous iron in natural waters. *Limnology and Oceanography* 11(2), 293-298.
- Simonson, R.W., 1959. Outline of a Generalized Theory of Soil Genesis<sup>1</sup>. *Soil Sci. Soc. Am. J.* (2), 152-156.
- Simón, M., García, I., 1999. Physico-chemical properties of the soil-saturation extracts: estimation from electrical conductivity. *Geoderma* 90(1), 99-109.
- Sjogaard, K.S., Treusch, A.H., Valdemarsen, T.B., 2017. Carbon degradation in agricultural soils flooded with seawater after managed coastal realignment. *Biogeosciences* 14(18), 4375-4389.
- Sjogaard, K.S., Valdemarsen, T.B., Treusch, A.H., 2018. Responses of an Agricultural Soil Microbiome to Flooding with Seawater after Managed Coastal Realignment. *Microorganisms* 6(1).

- Sjøgaard, K.S., Treusch, A.H., Valdemarsen, T.B., 2017. Carbon degradation in agricultural soils flooded with seawater after managed coastal realignment. *Biogeosciences* 14(18), 4375-4389.
- Smith, A.W.S., 1984. Tidal corrections in hydrographic surveying - Discussion. *Journal of Waterway Port Coastal and Ocean Engineering-Asce* 110(1), 126-127.
- Smith, G.F., Lyons, L., McManus, A., Insley, K., 1997. Maryland's Historic Oyster Bottom: A Geographic Representation of the Traditional Named Oyster Bars. Maryland Department of Natural Resources Fisheries Service, Cooperative Oxford Laboratory, Maryland.
- Soil Science Division Staff, 2017. Soil survey manual, USDA Handbook 18. Government Printing Office, Washington, D.C.
- Soil Survey Staff, 1975. Soil Taxonomy: A basic system of soil classification for making and interpreting soil surveys. Agriculture Handbook. 1st ed. Soil Conservation Service, U.S. Department of Agriculture, Washington, D.C.
- Soil Survey Staff, 1999. Soil Taxonomy: A basic system of soil classification for making and interpreting soil surveys. Agriculture Handbook. 2nd ed. Natural Resources Conservation Service, U.S. Department of Agriculture, Washington, D.C.
- Soil Survey Staff, 2014. Keys to Soil Taxonomy. 12th edition ed. USDA-Natural Resources Conservation Service, Washington, D.C.
- Soil Survey Staff, 2016. Web Soil Survey. Available at <http://websoilsurvey.nrcs.usda.gov/> (verified 28 Dec. 2016). USDA-NRCS.
- Stenak, M., 2005. Inddæmningerne på Nordfyn, De inddæmmede landskaber - en historisk geografi. Landbohistorisk Selskab, pp. 123-170.
- Still, B.M., Stolt, M.H., 2015. Subaqueous Soils and Coastal Acidification: A Hydropedology Perspective with Implications for Calcifying Organisms. *Soil Science Society of America Journal* 79(2), 407-416.

- Stolt, M., Bradley, M., Turenne, J., Payne, M., Scherer, E., Cicchetti, G., Shumchenia, E., Guarinello, M., King, J., Boothroyd, J., Oakley, B., Thornber, C., August, P., 2011. Mapping Shallow Coastal Ecosystems: A Case Study of a Rhode Island Lagoon. *Journal of Coastal Research*, 1-15.
- Stolt, M., Rabenhorst, M., Collins, M., Osher, L., Shaw, R., Fischer, S., Turenne, J., Keirstead, D., Hammer, G., McVey, S., Hurt, W., Schoeneberger, P., Ahrens, B., Casby-Horton, S., Ditzler, C., Anderson, S., Henderson, W., Smith, D., Gordon, C., 2005. Glossary of Terms for Subaqueous Soils, Landscapes, Landforms, and Parent Materials of Estuaries and Lagoons. Subaqueous Soils Subcommittee of the Standing Committee on NCSS Standards, National Cooperative Soil Survey Conference, Corpus Cristi, Texas, NRCS, Corpus Cristi, Texas.
- Stolt, M.H., Needelman, B.A., 2015. Fundamental Changes in Soil Taxonomy. *Soil Science Society of America Journal* 79(4), 1001-1007.
- Stookey, L.L., 1970. Ferrozine - a new spectrophotometric reagent for iron. *Analytical Chemistry* 42(7), 779-&.
- Straub, K.L., Benz, M., Schink, B., Widdel, F., 1996. Anaerobic, nitrate-dependent microbial oxidation of ferrous iron. *Applied and Environmental Microbiology* 62(4), 1458-1460.
- Stumpner, E.B., Kraus, T.E.C., Liang, Y.L., Bachand, S.M., Horwath, W.R., Bachand, P.A.M., 2018. Sediment accretion and carbon storage in constructed wetlands receiving water treated with metal-based coagulants. *Ecological Engineering* 111, 176-185.
- Surabian, D.A., 2007. Moorings: An Interpretation from the Coastal Zone Soil Survey of Little Narragansett Bay, Connecticut and Rhode Island. *Soil Horizons* 48.
- Teifke, R.H., 1973. Stratigraphic Units of the Lower Cretaceous through Miocene Series, Geologic Studies, Coastal Plain of Virginia, Bulletin 83. Virginia Division of Mineral Resources.
- Thorsen, S.W., Kristensen, E., Valdemarsen, T., Flindt, M.R., Quintana, C.O., Holmer, M., 2019. Fertilizer-derived N in opportunistic macroalgae after flooding of agricultural land. *Marine Ecology Progress Series* 616, 37-49.

- Trimble, S.W., 1969. Culturally accelerated sedimentation on the middle Georgia Piedmont. Master's Thesis Thesis, University of Georgia, Athens, GA.
- Trimble, S.W., 1998. Dating fluvial processes from historical data and artifacts. CATENA 31(4), 283-304.
- Turenne, J., 2014. Mapping Soils under Water. Soil Horizons 55.
- Tyler, R.H., Boyer, T.P., Minami, T., Zweng, M.M., Reagan, J.R., 2017. Electrical conductivity of the global ocean. Earth, Planets and Space 69(1), 156.
- U.S. Department of Agriculture, 2019. National Soil Survey Handbook, title 430-VI. Natural Resources Conservation Service.
- Uhl, J.H., Leyk, S., Chiang, Y.Y., Duan, W.W., Knoblock, C.A., 2018. Map Archive Mining: Visual-Analytical Approaches to Explore Large Historical Map Collections. Isprs International Journal of Geo-Information 7(4).
- Valdemarsen, T., Quintana, C.O., Thorsen, S.W., Kristensen, E., 2018. Benthic macrofauna bioturbation and early colonization in newly flooded coastal habitats. Plos One 13(4).
- Vepraskas, M.J., Craft, C.B., 2016. Wetland soils : genesis, hydrology, landscapes, and classification. Second edition. ed. CRC Press, Taylor & Francis Group, Boca Raton.
- Wagner, D.P., 1982. Acid sulfate weathering in upland soils of the Maryland Coastal Plain Dissertation Thesis, University of Maryland, 171 pp.
- Wallmann, K., Hennies, K., König, I., Petersen, W., Knauth, H.-D., 1993. New procedure for determining reactive Fe(III) and Fe(II) minerals in sediments. Limnology and Oceanography 38(8), 1803-1812.
- Weil, R.R., Brady, N.C., 2016. The nature and properties of soils. Fifteenth edition. ed. Pearson, Columbus.

- Wessel, B.M., Fiola, J.C., Rabenhorst, M.C., 2017a. Soil morphology, genesis, and monolith construction of an acid sulfate soil with silica-cementation in the US Mid-Atlantic Region. *Geoderma* 308, 260-269.
- Wessel, B.M., Galbraith, J.M., Stolt, M.H., Rabenhorst, M.C., Fanning, D.S., Levin, M.J., 2017b. Soil Taxonomy proposals for acid sulfate soils and subaqueous soils raised by the 8th International Acid Sulfate Soils Conference. *South African Journal of Plant and Soil*.
- Wessel, B.M., Levin, M.J., Fanning, D.S., Rabenhorst, M.C., 2016. Soil Taxonomy proposals for acid sulfate soils and subaqueous soils. In: C. van Huyssteen (Ed.), *Proceedings of the 5th International Soil Classification Congress*, Bloemfontein, South Africa, pp. 41.
- Wessel, B.M., Rabenhorst, M.C., 2017. Identification of sulfidic materials in the Rhode River subestuary of Chesapeake Bay. *Geoderma* 308(Supplement C), 215-225.
- Wessel, B.M., Rabenhorst, M.C., Yonkos, L.T., Hartzell, S.E., 2015. Do Chemically Contaminated Subaqueous Soils Present a Challenge for Classification? Poster, *Synergy in science: Partnering for solutions*, Annual Meeting of the Soil Science Society of America, Minneapolis, MN.
- Westrich, J.T., Berner, R.A., 1984. The role of sedimentary organic-matter in bacterial sulfate reduction - The G model tested. *Limnology and Oceanography* 29(2), 236-249.
- Wheeler, P.J., Peterson, J.A., Gordon-Brown, L.N., 2010. Channel Dredging Trials at Lakes Entrance, Australia: A GIS-Based Approach for Monitoring and Assessing Bathymetric Change. *Journal of Coastal Research* 26(6), 1085-1095.
- Williams, M.R., Wessel, B.M., Filoso, S., 2016. Sources of iron (Fe) and factors regulating the development of flocculate from Fe-oxidizing bacteria in regenerative streamwater conveyance structures. *Ecological Engineering* 95, 723-737.
- Wolfanger, L.A., 1931. Abandoned Land in a Region of Land Abandonment. *Economic Geography* 7(2), 166-176.

- Wolters, M., Garbutt, A., Bakker, J.P., 2005. Salt-marsh restoration: evaluating the success of de-embankments in north-west Europe. *Biological Conservation* 123(2), 249-268.
- Young, F.J., Hammer, R.D., Williams, F., 1997. Estimation of map unit composition from transect data. *Soil Science Society of America Journal* 61(3), 854-861.
- Zervas, C., 2009. Sea Level Variations of the United States 1854-2006. NOAA Technical Report NOS CO-OPS 053.
- Zuur, A.J., 1952. Drainage and reclamation of lakes and of the Zuiderzee. *Soil Science* 74(1), 75-89.
- Åström, M., Björklund, A., 1995. Impact of acid sulfate soils on stream water geochemistry in western Finland. *Journal of Geochemical Exploration* 55(1-3), 163-170.